UNIVERSITY OF CALIFORNIA

Los Angeles

Energy and Cost Optimization of

Reverse Osmosis Desalination

A dissertation submitted in partial satisfaction of the

requirements for the degree of Doctor of Philosophy

in Chemical Engineering

by

Aihua Zhu

2012

The dissertation of Aihua Zhu is approved.

_____

William Kaiser

_____
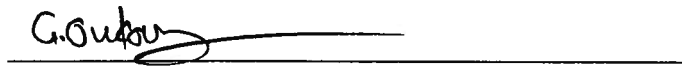
Gerassimos Orkoulas

_____

Yoram Cohen, Committee Co-Chair

_____
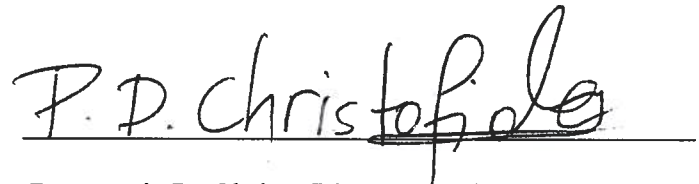
Panagiotis D. Christofides, Committee Co-Chair

University of California, Los Angeles

2012

ii

To my family.

TABLE OF CONTENTS

Contents

LIST OF TABLES

LIST OF FIGURES

xiii

ACKNOWEDGEMENTS

VITA

January 4, 1978	Born: Xiantao, China
1999	B.S. Biochemical Engineering Beijing University of Chemical Technology
2002	MS. Biochemical Engineering Beijing University of Chemical Technology

PUBLICATIONS AND PRESENTATIONS

1. **Zhu, A.,** Christofides, P. D. and Cohen, Y. Effect of Thermodynamic Restriction on Energy Cost Optimization of RO Membrane Water Desalination, Industrial & Engineering Chemistry Research, 2009, 48(13): 6010-6021.

2. **Zhu, A.,** Christofides, P. D. and Cohen, Y. Minimization of Energy Consumption for a Two-Pass Membrane Desalination: Effect of Energy Recovery, Membrane Rejection and Retentate Recycling, Journal of membrane science, 2009, 339(1-2): 126--137.

3. **Zhu, A.**, Christofides, P. D. and Cohen, Y. Energy Consumption Optimization of Reverse Osmosis Membrane Water Desalination Subject to Feed Salinity Fluctuation, Industrial & Engineering Chemistry Research, 2009, 48 (21): 9581-–9589.

4. **Zhu, A.,** Christofides, P. D. and Cohen, Y. On RO Membrane and Energy Costs and Associated Incentives for Future Enhancements of Membrane Permeability, Journal of membrane science, 2009, 344(1-2): 1--5.

5. **Zhu, A.,** Rahardianto, A., Christofides, P. D. and Cohen, Y. Reverse Osmosis Desalination with High Permeability Membranes - Cost Optimization and Research Needs, Desalination and Water Treatment, 15(2010)256-266.

6. **Zhu, A.,** P. D. Christofides and Y. Cohen, Effect of Stream Mixing on RO Energy Cost Minimization, Desalination, 261, 232-239, 2010.

7. Bartman, A., **A. Zhu,** P. D. Christofides and Y. Cohen, Minimizing Energy Consumption in Reverse Osmosis Membrane Desalination Using Optimization-Based Control, Journal of Process Control, 20, 1261-1269, 2010.

8. A. Zhu, P. D. Christofides, Y. Cohen, Reducing Energy Consumption in Reverse Osmosis Desalination: Cyclic or Multi-Stage Operation? AIChE Annual Meeting, Minneapolis, Minnesota, 2011

9. X. Pascual, H. Gu, A. Bartman, A., A., J. Giralt, R. Rallo, J. Ferrer-Giné, F. Giralt and Y. Cohen, Dynamic Data-Driven Models of Reverse Osmosis Desalination Systems, AIChE Annual Meeting, paper, Minneapolis, Minnesota, 2011

10. A. R. Bartman, H. Gu, L. Gao, A. Zhu, J. Thompson, B. McCool, A. Rahardianto, P. D. Christofides, Y. Cohen, Design, Operation and Control of Next-Generation Water Purification Systems Utilizing Reverse Osmosis Desalination: Commercial Scale System Design, Construction, and Field Testing, UCLA Chemical and Biomolecular Engineering Department Seminar Series, May 27, 2011, Los Angeles, CA

11. A. R. Bartman, A. Zhu, H. Gu, L. Gao, J. Thompson, A. Rahardianto, P. D. Christofides, Y. Cohen, Optimal Operation and Control of Reverse Osmosis Water

Desalination," Southern California Nonlinear Control Workshop, May 13, 2011, Riverside, CA

12. A. Zhu, B. McCool, A. Bartman, A. Rahardianto, P. D. Christofides, and Y. Cohen, Strategies for Reducing the Cost of RO Water Desalination, California - Neveda AWWA 2011 Spring Conference, March, Long Beach, CA

13. A. Zhu, P. D. Christofides, Y. Cohen, Reverse Osmosis Desalination: Thermodynamic Restriction and Process Economics, UCLA Technology Forum, Mar. 1, 2011, Los Angeles, CA

14. A. Zhu, P. D. Christofides, Y. Cohen, Stream Recycling and Mixing in Reverse Osmosis Desalination, AIChE Annual Meeting, paper, Salt Lake City, Utah, 2010

15. A. R. Bartman, A. Zhu, P. D. Christofides, Y. Cohen, Minimizing Energy Consumption in Reverse Osmosis Membrane Desalination Using Optimization-Based Control, AIChE Annual Meeting, Nov. 10, 2010, Salt Lake City, UT

16. X. Pascual, H. Gu, A. R. Bartman, A. Rahardianto, A. Zhu, J. Giralt, R. Rallo, and Y. Cohen, "Rapid Prototyping of Reverse Osmosis Processes Using Data-Driven Models", AIChE Annual Meeting, paper, Salt Lake City, Utah, 2010

17. A. R. Bartman, A. Zhu, P. D. Christofides and Y. Cohen, Minimizing Energy Consumption in Reverse Osmosis Membrane Desalination Using Optimization-based Control, Proceedings of the American Control Conference, Baltimore, Maryland, (2010), 3629-3635.

18. A. R. Bartman, A. Zhu, P. D. Christofides, Y. Cohen, Nonlinear Model-Based Control and Optimization in an Experimental Reverse Osmosis Desalination Process,

In Proceedings of the American Membrane Technology Association, accepted, San Diego, CA, 2010

19. A. R. Bartman, A. Zhu, P. D. Christofides, Y. Cohen, Optimal Operation and Control of Reverse Osmosis (RO) Desalination," Keynote Session Presentation, Canadian Society for Chemical Engineering (AIChE) Annual Meeting, Oct. 26th, 2010, Saskatoon, SK.

20. A. Zhu, P. D. Christofides, Y. Cohen, Reverse Osmosis Desalination: Thermodynamic Restriction and Process Economics, AMTA Annual Conference & Exposition, July 12-15, 2010, San Diego, CA

21. A. R. Bartman, A. Zhu, P. D. Christofides, Y. Cohen, Nonlinear Model-Based Control and Optimization in an Experimental Reverse Osmosis Desalination Process," AMTA Annual Meeting, Jul. 15, 2010, San Diego, CA

22. Zhu, A., Rahardianto, A., Christofides, P. D. and Cohen, Y. Minimization of RO Desalination Cost: Considerations of Membrane Permeability and Feed Salinity Variations, 2009 AIChE Annual Meeting, November 8-13, 2009, Nashville, Tennessee, USA.

23. A. R. Bartman, A. Zhu, P. D. Christofides, Y. Cohen, Modeling and Control of An Experimental Reverse Osmosis Water Desalination System," AIChE Annual Meeting, Nov. 11, 2009, Nashville, TN

24. Gu, H., Bartman, A., Zhu, A., Thompson, J., Lam, Y., Uchymiak, M., McCool, B. C., Rahardianto, Christofides, P. D., Cohen, Y and Kaiser, W. A Novel Approach and

System for Rapid Field Evaluation of Water Desalination, 2009 AIChE Annual Meeting, November 8-13, 2009, Nashville, Tennessee, USA.

25. Zhu, A., Christofides, P. D. and Cohen, Y. Energy Consumption Optimization of RO Membrane desalination Subject to Feed Salinity Fluctuation, Proceedings of IFAC International Symposium on Advanced Control of Chemical Processes, Istanbul, Turkey, 2009.

26. Zhu, A., Christofides, P. D. and Cohen, Y. Minimization of RO Desalination Cost: considerations of process configuration, energy and membrane costs, brine disposal and temporal feed salinity variations, 19th Annual Meeting of the North American Membrane Society, June 20-24, 2009, Charleston, South Carolina, USA. (Also presented in a Poster Session in the same meeting).

27. A. R. Bartman, A. Zhu, P. D. Christofides, Y. Cohen, Modeling and Control of an Experimental Reverse Osmosis Water Desalination System, North American Membrane Society Annual Meeting, Jun. 20, 2009, Charleston, SC

28. Zhu, A., Christofides, P. D. and Cohen, Y. Optimization of Energy Utilization of Reverse Osmosis Membrane Desalination and Smart Mini-Modular-Mobile Water System. Poster Presentation, 4th Annual UCLA Engineering Technology Forum, April 23, 2009, Los Angeles, California, USA.

29. Zhu, A., Christofides, P. D. and Cohen, Y. Energy Cost Optimization of Reverse Osmosis Membrane Desalination - Single Stage, Multi-Stage and Multi-Pass Configurations. 2009 CA-NV AWWA Spring Conference, April 6-9, 2009, Santa Clara, California, USA. (Also presented in a Poster Session in the same meeting).

30. Gu, H., Bartman, A., Zhu, A., Lam, Y., Uchymiak, M., Christofides, P. D., Cohen, Y and Kaiser, W. Smart Water Desalination Research Platform: Mini-Modular-Mobile (M3) Reverse Osmosis System. 2009 CA-NV AWWA Spring Conference, April 6-9, 2009, Santa Clara, California, USA. (Also presented in a Poster Session in the same meeting).

31. B. C. McCool, A. Rahardianto, A. Zhu, and Y. Cohen, Economic Analysis of High Recovery Brackish Water Desalination, AWWA, California-Nevada Section, 2009 Annual Spring Conference, Santa Clara, CA

32. Zhu, A., Christofides, P. D. and Cohen, Y. Optimizing Energy Usage in Membrane Desalination: Emerging Constraint of Thermodynamic restriction. Poster presentation, West Coast Water Technology Transfer Workshop, February 20, 2009, California Nano systemNanosystems Institute, Los Angeles, California, USA.

33. Gu, H., Bartman, A., Zhu, A., Lam, Y., Uchymiak, M., Christofides, P. D., Cohen, Y and Kaiser, W. Live demonstration of the advanced Mini-Modular-Mobile (M3) research, training and pilot plant platform, West Coast Water Technology Transfer Workshop, February 20, 2009, California Nanosystems Institute, Los Angeles, California, USA.

34. Zhu, A., Christofides, P. D. and Cohen, Y. Energy Cost Optimization of Current Highly Permeable Membrane Desalination. Poster presentation, Engineering for Life Enrichment: A mini-Symposium in conjunction with the National Academy of Engineering (NAE) Meeting, February 12, 2009, UCLA, Los Angeles, California, USA.

35. Zhu, A., Christofides, P. D. and Cohen, Y. Minimizing Energy Consumption in Membrane Process and the Thermodynamic Restriction. American Institute of Chemical Engineers, 2008 Annual Meeting (AIChE 2008), November 16-21, 2008, Philadelphia, USA.

36. Zhu, A., Christofides, P. D. and Cohen, Y. Energy Cost Optimization in RO Desalting and the Thermodynamic Restriction (keynote presentation). International Congress on Membranes and Membrane Processes (ICOM 2008), July 12-18, 2008, Honolulu, Hawaii, USA. (Also presented in a Poster Session in the same meeting).

37. Zhu, A., Christofides, P. D. and Cohen, Y. Fundamental analysis of RO desalting with respect to optimization of specific energy consumption. Poster presentation, 3rd Annual UCLA Engineering Technology Forum, May 27, 2008, Los Angeles, California, USA.

38. Zhu, A., Christofides, P. D. and Cohen, Y. Fundamental analysis and practical implications of RO process optimization with respect to energy minimization. 2008 CA-NV AWWA Spring Conference, April 21-24, 2008, Hollywood, California, USA. (Also presented in a Poster Session in the same meeting).

ABSTRACT OF THE DISSERTATION

Energy and Cost Optimization of

Reverse Osmosis Desalination

by

Aihua Zhu

Doctor of Philosophy in Chemical Engineering

Professor Panagiotis D. Christofides, Co-Chair

Professor Yoram Cohen, Co-Chair

The availability of surface and ground water sources for agricultural, industrial, and personal use is becoming increasingly constrained. In response, reverse osmosis (RO) water desalination has been touted as a potential technology for increasing the available water resources in many parts of the world. Different research ideas have been proposed to find the "ultimate" solution to decrease the cost of RO desalination, such as creating more permeable RO membranes, using two-pass nanofiltration (NF) membranes to replace single-pass RO membranes, closed-circuit discharge technology, forward osmosis and etc. Motivated by this, my PhD research focused on creating a framework, from first-principles, to allow for evaluating the cost effectiveness of various "new" ideas and identify the most promising ones and, based on which, minimize the overall cost of

RO water desalination with current generation of highly permeable membranes, which enables practical RO processes to be operated up to the thermodynamic limit.

The framework developed in my PhD research led to a conclusion that there is little economic incentive for developing higher permeability membranes if the objective is to lower the cost of water desalination, balancing the energy consumption, membrane expenditure, and concentrate management costs. Future reduction in RO water production cost can arise from a variety of other process improvements including, but not limited to improved fouling-resistant membranes, lower cost of feed pretreatment and brine management, advanced control schemes (e.g. to account for feed salinity fluctuation), process configuration optimization (e.g., multi-stage or multi-pass, mixing and recycling operation), as well as low cost renewable energy sources.

The designed framework is utilized to predict the optimum operating conditions of a single-stage cross-flow RO process, with/without energy recovery devices, under different feed and permeate flow requirement and feed water salinity fluctuation. The algorithms were implemented as the automated energy-optimal based control software in a first-generation pilot mini-mobile-modular (M3) system, equipped with online standard process monitors (i.e., pressure, flow rate, pH and conductivity, and tested both in the lab and in the field desalting the agricultural drainage water at the Panoche Drainage District of the San Joaquin Valley. The framework is also utilized for multi-stage (where the concentrate stream from the previous stage is desalted to increase the overall water recovery) and multi-pass (where the permeate stream from the previous pass is further desalted to meet the product water quality requirement) RO network structures to

evaluate their energy efficiency. The analysis revealed that a multi-stage RO process is more energy efficient than a single-stage RO process, but at the expense of more membrane area requirement. The present work also showed that the two-pass NF/RO process is less energy efficient than a single-pass RO process. Notwithstanding, such a process could be necessary if a single-pass RO process cannot achieve the salt rejection requirement. Different recycling and stream mixing options were also evaluated for their energy effectiveness under the framework and the close-circuit discharge operation, even less energy efficient than a single-stage process with full energy recovery, but is more energy efficient at water recoveries lower than a critical value than single-stage without energy recovery and is able to achieve the effect of energy recovery from the brine stream without incurring the capital cost of acquiring an energy recovery device. The close-circuit discharge technology can be even more cost-effective than multi-stage in low recovery (<35%, for example seawater desalination) where ERD and pump costs are high.

The energy optimal policy is also utilized in operating the smart compact modular second-generation RO (CoM2RO) with the integration of ultrafiltration (UF) pretreatment, which is gaining more market share in seawater pretreatment due to its compact size, relatively easy operation and less maintenance required. This system with its adaptive backwash has been tested with the cooling tower water at the UCLA co-generation plant and is currently being tested with seawater at a navy base for its future deployment as a shipboard desalination unit in the open ocean and coastal areas.

Chapter 1   Introduction

1.1.   Background

Freshwater scarcity and declining water quality are expected to worsen with rising population growth, as well as climate change [1-4]. In order to increase the per capita availability of freshwater supplies various approaches have been practiced including, but not limited to, water conservation, water recycling, increased water use efficiency and water desalination. Water desalination in particular has become a major component of the freshwater portfolio in a number of countries (e.g., Singapore, Australia, Israel and Spain) with water desalting by membrane reverse osmosis (RO) technology being the dominant desalination technology. RO membrane water desalination is now well established as a mature water desalination technology for production of potable water as well as for upgrading agricultural, municipal and industrial water for reuse applications [4-18]. Reverse osmosis is one of the primary means of desalination practiced today along with multi-stage flash (MSF), multiple effect distillation (MED), vapor compression, andelectrodialysis (ED) and ED reversal (EDR). Other desalination technologies have also been proposed in recent years including membrane distillation (MD) and forward osmosis. Of these technologies, reverse osmosis has been proven to be, in most cases, more energy efficient with the specific energy consumption (SEC) for permeate (potable water) production of ~2-4 kWh/m^3 depending on plant design, size and location [4,19].

Reverse osmosis (RO) is a process where external pressure is exerted on the saline water side of RO membrane. This semi-permeable membrane has much high selectivity of water over the dissolved salt in the saline water. As a result, the saline water is desalinated by RO membrane and the permeate water with little salt content is produced.

As shown in Figure 1-1, reverse osmosis process requires external pressure on the saline water side; while forward osmosis (FO) is a different membrane process which uses draw solutions with high osmotic pressure to extract water from a high salinity water resource under low pressure [4]. Water recovery and chemical recycling of the draw solution active ingredients are typically achieved by distillation as shown in Figure 1-2, thereby increasing the energy cost of the FO process. It is interesting to note that even for the highly celebrated FO process in which ammonium carbonate is used for the draw solution [20], heat energy is required for the separation of the draw solution active species (e.g., the ammonia and CO_2 from the solution and for the evaporation of large volumes of water). Indeed, recent work has shown [21], as summarized in Table 1-1, that the energy consumption of the FO-Distillation process is about four times greater than for the RO processes. The above conclusion is also supported by an analysis carried out in the present study as described in Appendix A. Attempts to reduce the cost of draw solution regeneration have been proposed to utilize magentic species to increase the osmotic pressure [22]; however, sufficient recovery of these species by suitable magnetic fields has not shown the level of required removal of draw solution active species nor a reduction in the costly regeneration energy.
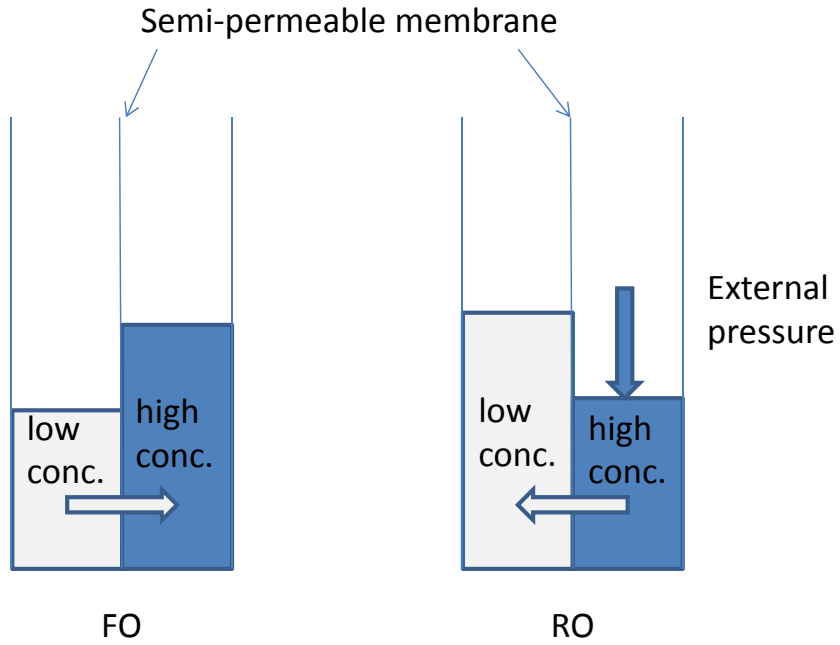
Figure 1-1. **Osmosis processes: forward osmosis (FO) and reverse osmosis (RO).**
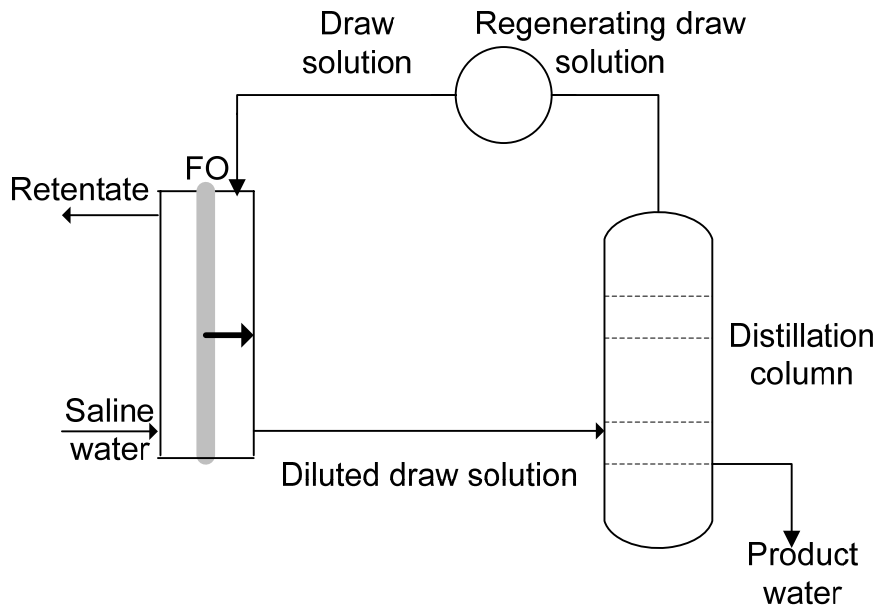
Source: [20]

Figure 1-2. **Forward osmosis followed by distillation and draw solution regeneration.**

Table 1-1.   Energy consumption in forward osmosis followed by distillation.

Operation	Estimated energy consumption (kWh/m^3 product)	Remarks
Pretreatment and concentrate disposal	1.7	Pumping, filtration, etc. similar to RO plant
Pumping water and draw solutions through the membranes	0.3	
Evaporator distillation energy consumption	3	Electricity charge of 13 kWh per ton exhaust steam
Cooling water at the distillation column	3	Pumping energy requirement
Cooling water for adsorbing draw solution gases	4	Pumping energy requirement
Vacuum pump for non-condensable gases removal	4	
Credit for cooling water saved in power station for steam supplied to distillation column	−3	Removal of heat from 250 kg of steam.
Total	13	±20% error estimate

Source: [21]

The introduction of highly permeable membranes in the mid 1990's with low salt passage [23] has generated considerable interest given their potential for reducing the RO energy consumption [23-26]. Water production cost in a typical RO desalination plant generally consists of the cost of energy consumption, equipment, membranes, brine management, labor, maintenance and financial charges. Typical RO desalination cost for seawater desalination is shown in Table 1-2 and energy consumption is a major portion of the total cost of water desalination [27-29] that can reach as high as ~44% of the total permeate production cost (Figure 1-3). As indicated in Table 1-2 and Figure 1-3, the energy cost for seawater RO desalination, is ~10–20 times greater than the minimum theoretical RO

energy cost to desalt seawater, which was reported to be $0.7 kwh / m^3$ (for seawater of 25

atmospheric pressure [30]). RO energy consumption per volume of produce permeate is

strongly affected by the level of water product recovery (i.e., permeate flow rate/feed

flow rate [31]) and energy recovery from the high pressure RO concentrate [31], in

addition to being impacted by the level by friction losses in the RO elements and

associated piping, pump efficiency, operating conditions (e.g., RO feed channel velocity

and feed-side pressure), and plant configuration in terms of membrane modules

arrangements.

Table 1-2.   Typical RO desalination cost.

Plant location	Type of water processed	Daily production capacity (m^3)	Average cost ($\$ / m^3$) (2005)
Madwar and Tarazi study	Waste	10,000	0.54
Ashkelon, Israel	Sea	273,973	0.61
Brownsville, USA	River	94,635	0.73
Corpus Christi, USA	Sea	94,635	1.01
Madwar and Tarazi study	Sea	10,000	1.18
Freeport, USA	River	37,854	1.20

Source: [32]

5
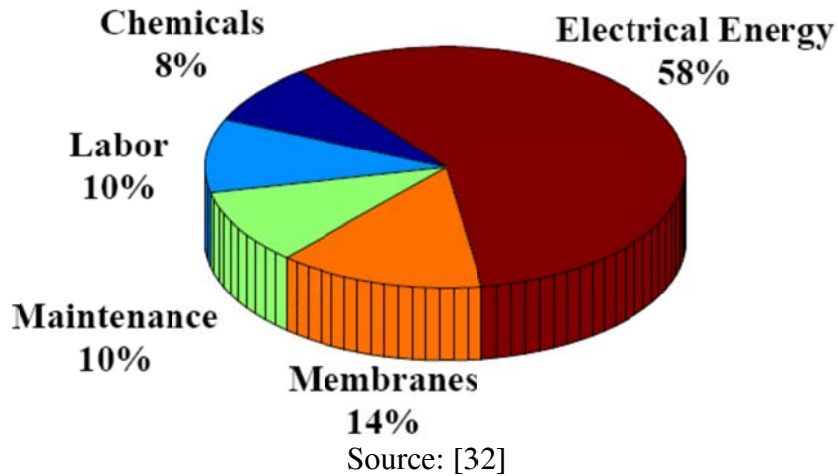
Figure 1-3.   Cost structure for reverse-osmosis desalination of seawater.

In contrast with seawater RO desalination, the major cost of RO inland brackish water desalting is the management of the desalination concentrate (i.e., residual concentrated byproduct from the recovery of fresh water from brackish water [3, 4, 33, 34]). At inland locations, concentrate disposal options are often limited and costly [35]. Thermally-driven evaporative and crystallization systems, the so-called zero-liquid-discharge (ZLD) technologies, are capable of eliminating liquid RO concentrate discharge, but are often prohibitively energy intensive for processing large feed volumes [35, 36]. Consequently, cost-effective inland brackish water desalting require RO operations at sufficiently high levels of product water recovery (90-95%) in order to minimize RO concentrate volumes. However, with increasing product water recovery, dissolved mineral salt concentrations (e.g., gypsum ($CaSO_4 \cdot 2H_2O$), $BaSO_4$, $SrSO_4$, $CaCO_3$, SiO_2, etc.) in the RO retentate stream may rise above their solubility limits. As a result, membrane scaling may occur, which can lead to membrane surface blockage and thus degradation of membrane performance (i.e., permeate flux decline and deteriorating

6

salt rejection) and translate into increased desalination cost [37]. Therefore, in order to enhance product water recovery, it is necessary to reduce the concentration of mineral scale precursors (e.g., calcium, barium, sulfate, etc.) below the membrane scaling threshold. The integration of RO desalting with chemical precipitation has been proposed as a promising approach for achieving this goal [37]. In this approach, a primary RO (PRO) step desalts the source water up to a water recovery level just below the membrane scaling threshold. A subsequent intermediate concentrate demineralization (ICD) step then serves to precipitate mineral salts in order to lower the concentrations of mineral scale precursors in the PRO concentrate stream. As a result, desalting of the demineralized PRO concentrate becomes feasible in a secondary RO (SRO) step, thereby enhancing the overall product water recovery from the brackish source water [37]. It is noted that when inland water desalination is operated at high recovery (above ~50%), the specific energy consumption (i.e., energy per volume of produced permeate) increases with recovery [38] and thus robust operational process control strategies are needed to ensure that the RO plant operates close to the minimum energy consumption level while avoiding the occurrence of mineral scaling.

The efficiency of RO operation is dictated by the feed water composition and salinity, feed water quality with respect to the source water fouling potential and temperature. Plant operation to minimize energy consumption must address temporal changes in source water characteristics in order to adjust the optimal level of product water recovery. For example, source water salinity may fluctuate due to seasonal rainfall events (for both near shore seawater intake and groundwater). There can also be seasonal

variations in water salinity as has been documented for groundwater in the central San Joaquin Valley, where total dissolved solids (TDS) content was reported to deviate by up to 52% from its annual average [39]. Clearly, sustained optimal RO plant operation requires real-time adjustment of operating conditions based on dynamic energy optimization methodology and robust process control.

1.2.   Problem statement

Previous studies on optimization of the specific energy consumption (SEC) have focused on evaluation of the SEC dependence on water recovery at one or several normalized feed and permeate flow rates. However, the global minimum SEC has not been identified along with SEC optimization via a generalized theoretical framework. Because the economic feasibility of membrane desalination is highly dependent on operational costs (with energy cost being the highest), the minimization of these costs is a critical step in the RO design process.

A fundamental approach is currently lacking for a rigorous first-principle cost-minimization of membrane desalination utilizing modern low-pressure highly permeability reverse osmosis (RO) and nanofiltration (NF) membranes. These membranes have enabled desalting operations at much lower pressures (Figure 1-4b) than previously possible (Figure 1-4a), approaching the limit of thermodynamic equilibrium (at the module exit) wherein the retentate osmotic pressure approaches the applied pressure. Consequently, it is imperative to develop rigorous integrated process and

thermodynamic models for optimizing desalination with respect to various process factors, such as feed water chemistry, operating conditions, membrane module properties, brine disposal cost, and the use of energy recovery devices. This includes optimizations of multi-stage and multi-pass membrane process configurations with respect to feed and product water qualities, operating conditions and modes (e.g., mixing and recycling), and water recovery levels. Ultimately, optimization models need to be incorporated into a robust membrane desalination design and process control to be able to design smart membrane desalination systems that are able to automatically adapt to changing feed water characteristics by adjusting process conditions to ensure operation at the highest efficiency.

Operating pressure $\quad \Delta P$

Osmotic pressure barrier

$\Delta \pi$

Axial distance along the membrane channel

Operating pressure $\quad \Delta P$

$\Delta \pi$ Osmotic pressure barrier

Axial distance along the membrane channel
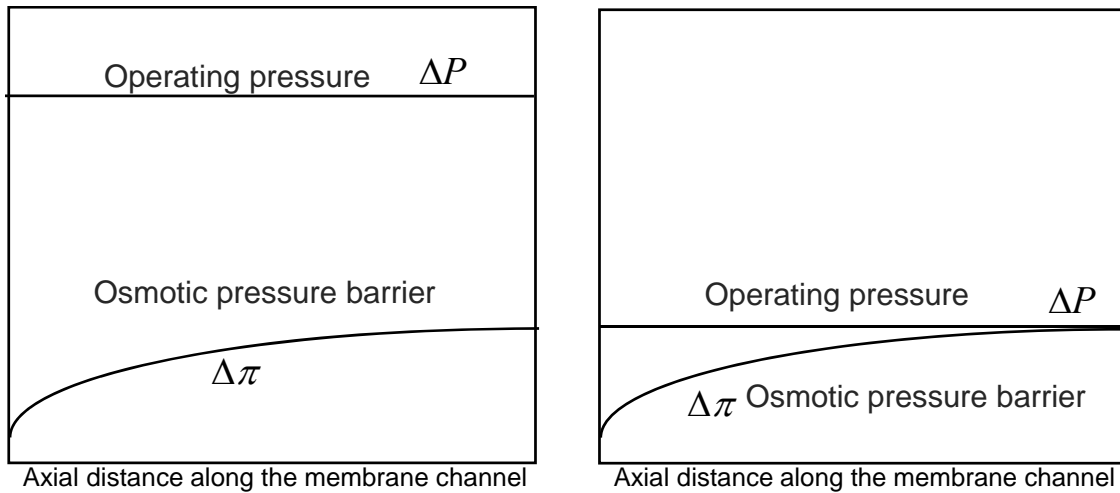
Figure 1-4.   **Schematics of the comparison of transmembrane pressure and osmotic pressure for (a) past (left) and (b) modern (right) RO/NF membranes.**

1.3. Objectives of the dissertation

This dissertation has as its primary goal the development of a theoretical framework for the optimization of reverse osmosis (RO) membrane desalination with respect to energy consumption, in addition to membrane, brine management, and pump costs. Within this framework, accomplishment of these broad goals is via optimization of RO system performance with respect to a number of factors including feed water salinity, operating conditions, membrane module area, RO module arrangement (e.g., single versus multiple stages or passes), and the use of energy recovery devices. The major objectives of the study are listed below.

1. Develop an a-priori model to predict the optimum operating conditions of RO desalting (e.g., pressure and water recovery), for given feed water quality, with respect to minimization of energy consumption.

2. Evaluate the energy efficiency of RO operation using single-stage and multiple-stage RO desalting, as well as multi passes when all of them operated up to the limit of the thermodynamic restriction.

3. Develop an optimization-based operation policy to account for the fluctuations of feed water properties (i.e., water quality and physicochemical properties) to ensure that the RO process is optimally operated.

4. Evaluate the energy cost effectiveness of different modes of RO feed, concentrate and permeate mixing and recycling operations in both steady-state and unsteady-state operation.

1.4. Approach and structure of the dissertation

The stated objectives were accomplished using a multi-pronged approach involving theoretical process analysis and an experimental investigation in support of the theoretical analysis. Rigorous analysis was used for characterizing process conditions, specifying process goals, and analyzing process performance. The premise of the present analysis of the economics of RO operation is that the current generation of high permeability RO membranes makes it feasible to carry out RO desalination up to the thermodynamic restriction limit.

Following a brief literature review, Chapter 3 establishes the framework for quantifying the energy consumption, membrane area requirements and brine disposal cost for RO operation up to the thermodynamic limit. This chapter studies a single-stage RO process and evaluates its various elements of water production cost (energy, membrane area and permeability, brine management, and frictional pressure drop) from the viewpoint of minimizing the overall cost of water production as well as considering the thermodynamic cross-flow constraint, utilization of energy recovery devices, and operational feed and permeate flow rate constraints.

Chapter 4 presents an analysis of the impact of increasing RO membrane permeability on the reduction of water desalination cost for RO desalting brackish water and seawater desalination operated up to the limit imposed by the thermodynamic restriction. At this limit, the ratio of membrane to energy cost can be expressed as a function of the water recovery level and a dimensionless cost parameter that accounts for feed water salinity, as well as the purchase cost of electrical energy and membrane area.

Chapter 5, following the results of Chapter 3 regarding the membrane module arrangement and building upon Chapter 4, extends the analysis of the single-stage RO process to a two-stage RO process to evaluate its cost effectiveness compared to a single-stage RO process. Chapter 5 quantifies the SEC, specific membrane cost (SMC) and specific pump cost (SPC) of both the single-stage and two-stage RO processes. A comparison is then made regarding the economic effectiveness of a single and two-stage RO processes as a function of feed salinity and product water recovery.

Chapter 6 presents a two-pass RO membrane configuration, based on the methodology developed in Chapter 4. In Chapter 6, the energy optimization of the two-pass membrane desalination process, at the limit imposed by the thermodynamic restriction is compared with a single-pass membrane desalting operation at the equivalent targeted overall salt rejection and permeate product recovery. The analysis also considers the effect of pump and energy recovery efficiencies and membrane salt rejection.

Chapter 7 addresses a practical problem of energy-optimal process operation in the presence of feed salinity fluctuation which is common in both seawater and brackish water desalination. The presented analysis is directed at predicting the energy savings that can be achieved with optimal process control relative to constant pressure operation.

Chapter 8 evaluates various approaches that have been proposed in the literature to reduce RO energy consumption with various modes of mixing/recycling operations between the feed, retentate and permeate streams to assess their potential effectiveness for single-stage, two-pass and two-stage RO desalination processes.

Chapter 9 develops a model to quantify the specific energy consumption (SEC) for a reverse osmosis (RO) desalting process under cyclic operation, i.e., full recycling of the retentate stream to mix with the fresh source water being fed into the RO module. The normalized SEC for this cyclic operation, with respect to the water recovery, is derived and compared with continuous single-stage and two-stage RO operation without recycling, in terms of overall cost consisting of energy consumption and pumping cost.

Finally, Chapter 10 provided a refined numerical simulation to evaluate the impact of concentration polarization and frictional pressure drop on the energy consumption optimization.

Chapter 2   Literature Review

2.1.   Optimization progress for single-stage RO desalination

Reverse osmosis (RO) membrane water desalination is now well established as a mature water desalination technology. However, there are intensive efforts to reduce the cost of RO water desalination in order to broaden the appeal and deployment of this technology [9,11,38,40-47]. The water production cost in a typical RO desalination plant generally consists of the cost of energy consumption, equipment, membranes, labor and maintenance and financial charges. Energy consumption is a major portion of the total cost of water desalination and can reach as high as about 45% of the total permeate production cost [27-29]. The energy cost per volume of produced permeate (i.e., the Specific Energy Consumption or SEC) is significant in RO operation due to the high pressure requirement (up to about 1000 psi for seawater and in the range of 100-600 psi for brackish water desalting). Considerable effort has been devoted to optimize the RO process dating back to the initial days of RO development in the early 1960's [8, 10, 25, 29, 39, 47-131].

Early research in the 1960's [65-67, 80] focused on unit cost optimization with respect to water recovery, energy recovery system efficiency, feed flow rate and the applied transmembrane pressure. Efforts to reduce the SEC also considered increasing the permeate flow rate, at a given applied pressure and feed flow rate, by either optimizing the membrane module with respect to its permeate flux [73, 114, 121, 132-136] and/or by using more permeable membranes [23-26]. For example, studies have shown that specific

permeate productivity of spiral wound RO and nanofiltration modules could be improved by optimizing module configuration (e.g., feed channel height, permeate channel height, and porosity [121]). The introduction of highly permeable membranes in the mid 1990's with low salt passage [23] has generated considerable interest given their potential for reducing the RO energy required to attain a given permeate [23-26].

It is important to recognize that previous studies that focused on optimization of the SEC have only evaluated the SEC dependence on water recovery at one or several normalized feed and permeate flow rates. Previous researchers have reported the minimum SEC for one or several flow rates or a range of product water recoveries [23-26, 65-67, 73, 80, 114, 121, 132-136]. However, the global minimum SEC has not been identified along with SEC optimization via a general theoretical framework. Motivated by the above considerations, the current study revisits the problem of RO energy cost optimization when highly permeable membranes are used, via a simple mathematical formalism, with respect to the applied pressure, water recovery, feed flow rate, and permeate flow rate and accounting explicitly for the limitation imposed by the minimal required applied pressure. Subsequently, the impact of using an energy recovery device, brine disposal cost, membrane hydraulic permeability and pressure drop within the membrane module are discussed for one-stage RO. Additionally, an analysis is presented of the energy efficiency of a two-stage RO relative to one-stage RO following the formalism proposed in the present study.

2.2. Energy recovery devices

In RO desalination, the feed stream is separated into low salinity (permeate stream) and high salinity (concentrate) stream. The concentrate stream is of high pressure due to the nature of the reverse osmosis operation. In order to reduce energy consumption per unit volume of permeate produced, energy recovery from the concentrate stream has been implemented using a variety of energy recovery devices (ERDs). The effect of an energy recovery device (ERD) on the SEC was first studied in the early 1960's [66, 67]. Avlonitis et al. [137] discussed four kinds of ERDs (i.e., Pelton wheel, Grundfos Pelton wheel, Turbo charger and Pressure exchanger) and reported that the pressure exchanger was the most efficient energy recovery device (>90%) and other types are usually less than 90% [137]. More recently, Manth et al. [27] proposed an energy recovery approach, in which a booster pump is coupled with a Pelton turbine (instead of a single-component high-pressure feed pump), or is used as an interstage booster for dual-stage brine conversion systems.
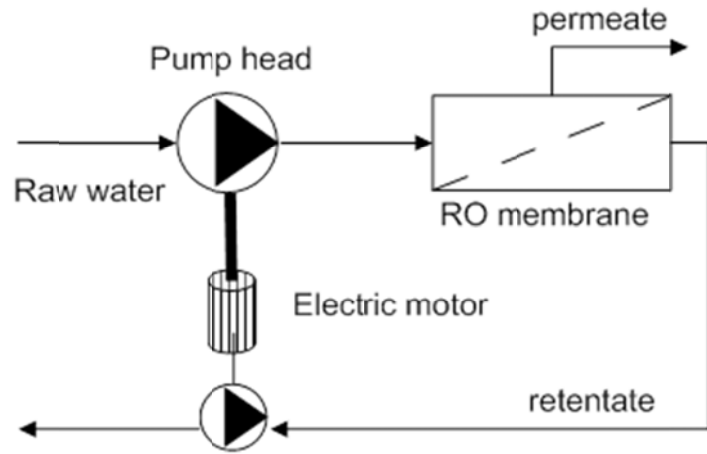
a. Pelton wheel energy recovery system
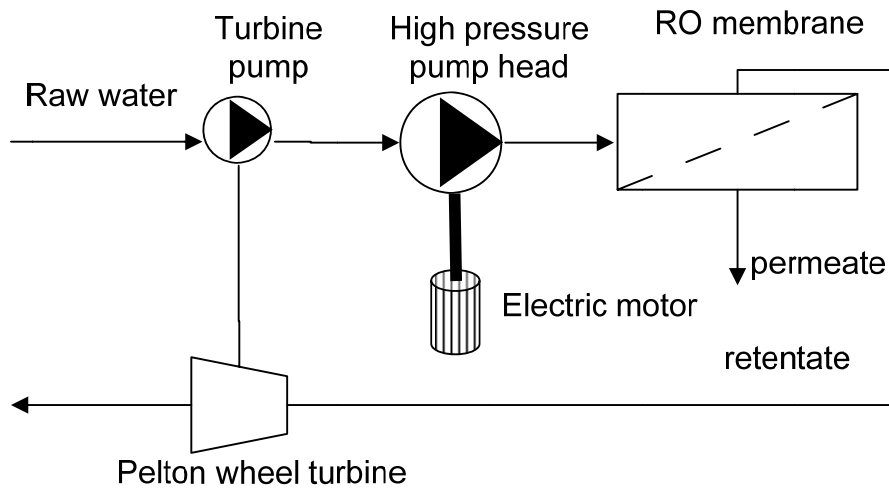
b. Grundfos Pelton wheel energy recovery system
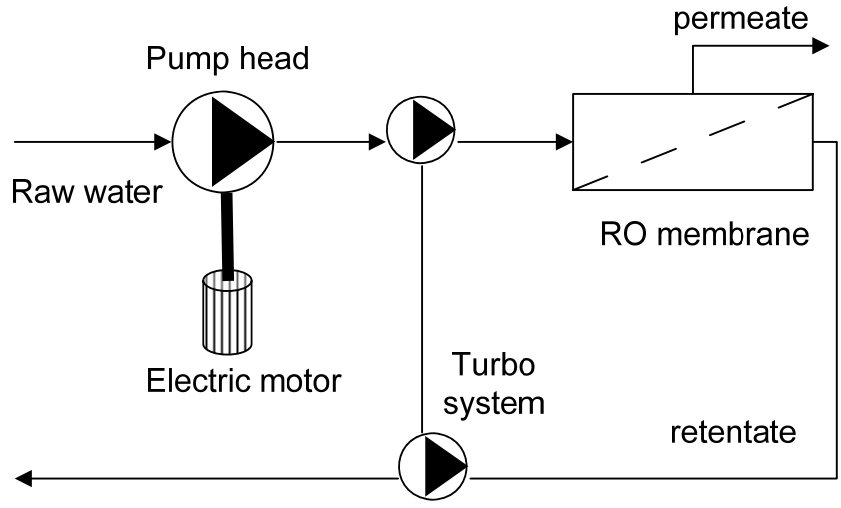
c. Turbo charger energy recovery system
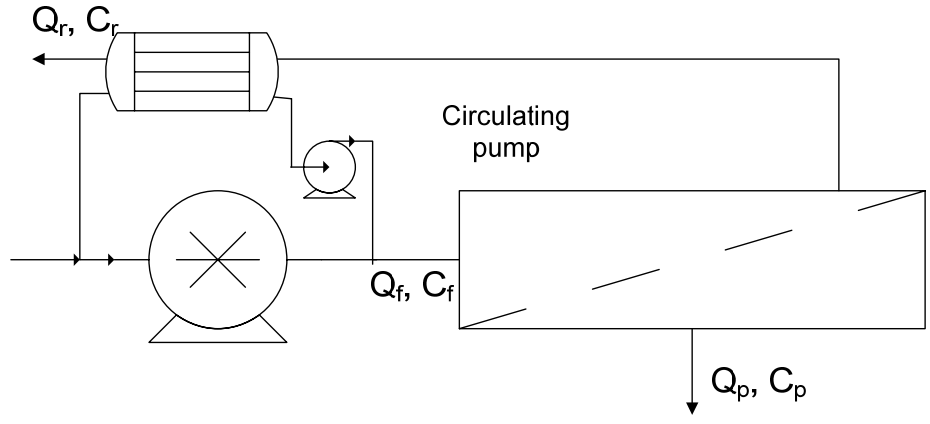
d. Pressure Exchanger energy recovery system

Figure 2-1.   Illustration of different energy recovery systems.

As a result of all the above technological improvements, the power consumption in seawater desalination, for example, decreased over the years and is reaching a plateau after 2004 (Figure 2-2). The minimum energy consumption is obtained from the integration of the following equation when the change of n_w is infinitely small [138]:

$$-d(\Delta G_{mix}) = -RT \ln a_w dn_w = \pi_s \overline{V}_w dn_w \qquad (1a)$$

where ΔG_{mix} is the free energy of mixing, which is equal to the energy of separation in magnitude but opposite in sign, R is the ideal gas constant, T is the absolute temperature, a_w is the activity of water, n_w is the number of moles of water, π_s is the osmotic pressure of the seawater, and $\overline{V}_w$ is the molar volume of water. The integration of the above equation implies that the applied pressure is always equal to the osmotic pressure of seawater as water recovery increases. As the salinity of seawater or desired water recovery increases, so does the minimum energy required for desalination. For example, the theoretical minimum energy of desalination for seawater at 35,000 parts per million (ppm) salt and at a recovery of 50% is 1.06 kWh/m^3 [20]. The actual energy consumption, however, is greater because desalination plants do not operate as a reversible thermodynamic process. Therefore, it is important to determine the various options for reducing the energy consumption and other operational involved in RO desalination which are the subject of the following sections.
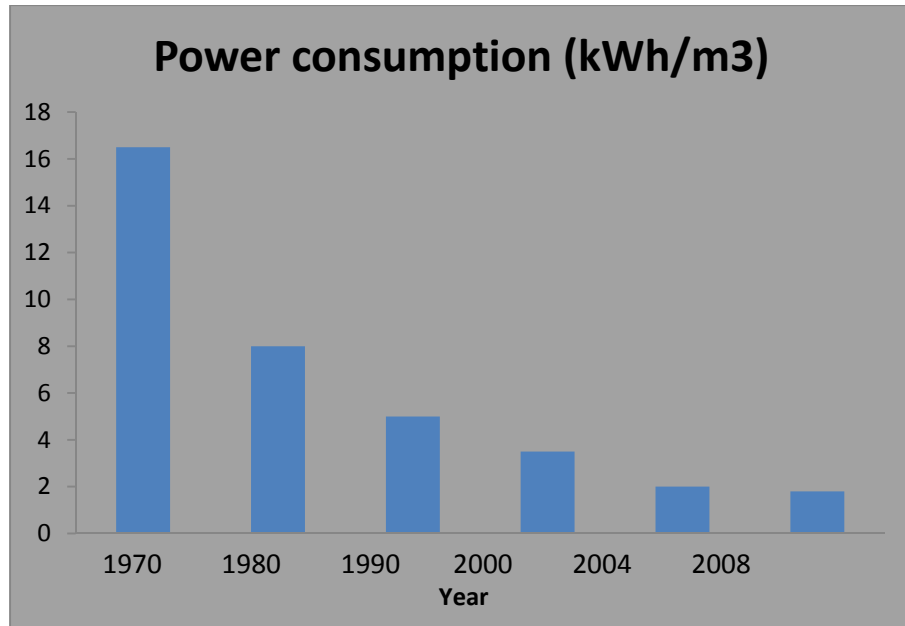
Figure 2-2. The change of power consumption in seawater reverse osmosis desalination plants from 1970s to 2008.

2.3. Thermodynamic restriction

Wilf [23] and later Spiegler [138] and Lachish [139] proposed that operation close to the minimum level of applied pressure (i.e., pressure approaching the concentrate osmotic pressure plus frictional pressure losses), would result in the lowest energy cost. Clearly, in the absence of pressure drop in the membrane module, the minimum required applied pressure when a highly permeable membrane is used would be very close to the osmotic pressure of the RO concentrate that would be reached at the membrane outlet [23, 140-142]. As illustrated in **Figure 2-3,** in order to achieve a given water recovery and utilize the entire membrane area, there is a minimum pressure that must be applied and this pressure must be greater than the osmotic pressure of the concentrate exiting the process, but this applied pressure can approach the osmotic pressure of the brine stream

when highly permeable membranes are used. It is noted, that the requirement of a minimum pressure, for the lowest energy cost, will apply even when one considers concentration polarization, albeit the required pressure will be based on the osmotic pressure at the membrane surface at module exit [140, 141].
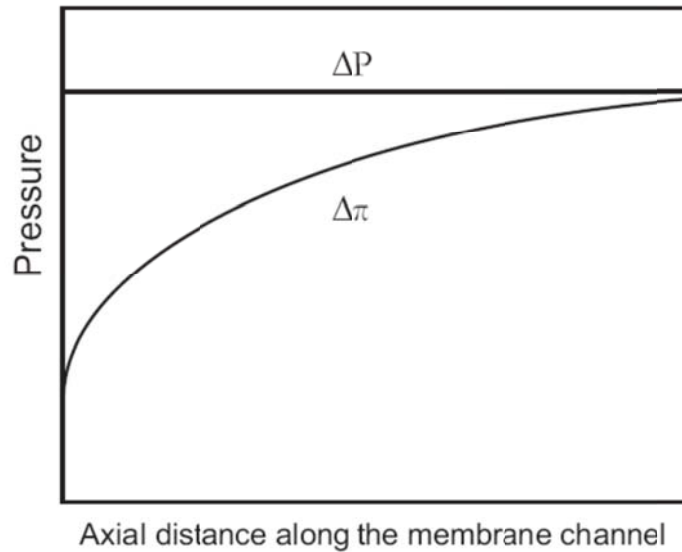
Figure 2-3. **Schematic illustration of the thermodynamic restriction for cross-flow RO desalting.**

For example, for typical low pressure RO membranes with permeability in the range of $L_p = 0.5 - 0.8 \times 10^{-10} m^3 / m^2 \cdot s \cdot Pa$ (pressure operability in the range of 2067-4134 kPa or 300-600 psi), desalting of brackish water of salinity in the range of 1000-2000 mg/L total dissolved solids (TDS) to water recovery level in the range of 50-75% would result in a concentrate stream having osmotic pressure of 1034-4134 kPa (or 150-600 psi). Given the high permeability of current brackish water membranes, it should be feasible to operate the RO process, at the above recovery levels, with the feed pressure set at or close to the exit brine osmotic pressure osmotic pressure, thereby enabling operation at the

minimum level of energy consumption. It is also noted that recent seawater RO desalination studies [143] by the Affordable Desalination Collaboration (ADC) reported 42.5% water recovery (at permeate flux of 2.83×10^{-6} $m^3 / m^2 \cdot s$ or 6 gfd) at feed-pressure of 4654 kPa (675 psi) that was only 15% higher than the osmotic pressure of the exit brine stream (4027 kPa or 584 psi).

Given that, with the present generation of high permeability RO membranes, it is feasible to operate the RO process over a wide range of practical water recoveries to the limit of the thermodynamic restriction, an important question arises as to the merit of developing membranes with yet higher permeabilities than currently available. The total energy cost for RO desalination is the product of the feed flow rate and the applied feed pressure irrespective of the rate of permeate productivity. Therefore, to the extent that a given assembly of high permeability membranes can provide the targeted overall permeate flow rate (while operating up to the thermodynamic limit), for a given feed flow rate (i.e., same recovery for a given feed flow rate), the energy cost would be independent of the type (i.e., permeability) of membrane used in the process. It is emphasized that the above statement would hold provided that, irrespective of the selected membrane, the RO process can be operated up to the limit of the thermodynamic restriction. However, the required membrane area, for a given feed flow rate at a selected target recovery, would decrease with increasing membrane permeability. Therefore, one would argue that once the capability for operating at the thermodynamic limit has been approached the benefit of higher permeability membranes is to lower the membrane cost for the process

(typically <10% of the overall water production cost relative to >30% for energy cost [47]).

2.4. Membrane module arrangements

Simplified process models to optimize the structure of RO membrane desalination plants have been proposed in the literature [90, 120, 125, 126, 129, 144-146]. Early studies have shown that the "Christmas tree" configuration developed in the early 1970's was suitable for the early generation of RO spiral-wound membranes. However, with the emergence of higher permeability membranes, it is unclear if such configuration of membrane modules is also optimal for ultra-low pressure RO modules [120]. It has been argued that the SEC can be lowered by utilizing a large number of RO membrane units in parallel so as to keep the flow and operating pressure low [145]. It has also been claimed that the SEC decreases upon increasing the number of membrane elements in a vessel [29].

In the mid 1990's researchers have suggested that a single-stage RO process would be more energy efficient [147] than a two-stage system. However, it has been also claimed that a two-stage RO process was more energy efficient than single-stage RO [8, 145]. The above conflicting views suggest that there is a need to carefully compare the energy efficiency of RO desalination by appropriately comparing single and multiple-stage RO on the basis of appropriately normalized feed flow rate and SEC taking into consideration the feed osmotic pressure, membrane permeability and membrane area. There is another relatively new configuration for seawater desalting, two-pass desalting,

which has not been extensively studied yet [58, 148, 149]. For example, Noronha *et al.* [[148] proposed an approach to optimizing the partial recoveries (i.e., for each pass) in a two-pass desalination process, without energy recovery for overall product water recovery in the range of 50%-70%. The above study showed that an optimal solution, with respect to the recoveries of each pass, can be obtained via a numerical algorithm, for specific plant configuration and membranes, however, it did not provide a comparison of energy consumption with a single-stage operation, but it was noted that energy consumption is higher for a two-pass process. In a later study, Cardona *et al.* [58] compared the SEC of a two-pass membrane desalination process, which they termed "double-stage", to a single-pass RO process, both without the use of an energy recovery device. Based on a specific case study using standard process model calculations based on bulk properties of the retentate stream, for a target salt rejection of 98.3% and 41.2% water recovery, it was concluded that the two-pass process has a potential for energy savings on the order of 13-15% for the specific case of less than 50% total water recovery. A recent report [149] on extensive pilot studies of a two-pass seawater NF desalination process by the Long Beach Water Department, suggested that the two-pass process would require about 20% less energy, when operating at 42% product water recovery, compared to a single pass RO membrane desalination process. The above two-pass NF desalination study did not report the use of energy recovery devices and did not present conclusive experimental data or theoretical reasoning for the claimed superiority of the two-pass process. Moreover, the relatively limited comparisons provided in the

24

literature have not addressed the limitations imposed by the thermodynamic crossflow restriction on the minimum achievable specific energy consumption.

Optimization of RO water production cost with respect to capital cost has also been addressed in order to explore means of reducing the total specific cost of water production [145, 147]. Such optimization studies have considered the costs associated with feed intake (primarily for seawater) and pretreatment, high pressure pumps, energy recovery system, and membrane replacement [147]. The problem of maximizing RO plant profit, considering energy cost, amortized membrane plant cost, cleaning and maintenance cost, and amortized cost of process pumps in the absence of energy recovery devices has also been addressed [145]. The majority of the existing studies have accepted the standard operating procedure whereby the applied pressures is set to be significantly higher than the minimum required pressure limit that would correspond to the lowest SEC. Moreover, a formal mathematical approach has not been presented to enable an unambiguous evaluation of the optimization of the RO water production cost with respect to the applied pressure, water recovery, pump efficiency, membrane cost and the use of energy recovery devices.

Table 2-1.   Contributions and shortcomings of important literatures.

Literature	Contributions	Shortcomings
[48]	Neural network model to predict permeate flow rate based on feed pressure, temperature and salt concentration. The network learned the input-output mappings with accuracy for interpolation cases, but not for extrapolation.	Need extensive experimental data to enable prediction of optimum operating condition
[137]	Reduction in the specific energy consumption for 4 different types of energy recovery devices and concluded that pressure exchangers are more efficient than other ERDs to recover the energy in the brine stream.	Optimization results were not provided
[143]	Developed a software package for Dow/FilmTec BW30-400 membrane to predict the water recovery and salt rejection for given feed flow rate and pressure under different arrangement in single-stage RO brackish water desalination. The configuration that all pressure vessels are arranged in parallel was found to yield the best results in terms of the production rate, product quality and overall pressure drop across the feed channel.	No optimization results with respect to specific energy consumption were provided.
[56, 136]	Developed a software package to predict the membrane performance of single-stage seawater reverse osmosis (SWRO) plants and concluded that the optimum water recovery for Dow Filmtec SW30HR380 membrane desalination is 45%.	Did not analyze the two-stage configuration and how that would affect the SEC and overall cost of seawater desalination.
[149]	Theoretically studied the effect of membrane properties and operating parameters on specific energy consumption following the same idea of quantifying the membrane cost and energy consumption for RO operation up to the thermodynamic restriction by the author of this dissertation.	Adopt arithmetic average for the feed-brine side osmotic pressure. Did not study the effect of adopting log-mean average. Only studied single-stage RO.
[8]	Analytically studied the energy consumption optimization	It assumed that the salt is fully mixed in each cross

26

	mathematically from differential mass balance and Darcy's law assuming 100% salt rejection for single-stage and two-stage from pure mathematic point of view. It concluded that pushing an RO system to the thermodynamic restriction will reduce the SEC and that the optimum water recovery is 50% for single-stage and two-stage is more energy efficient than a single-stage RO.	section along the flow channel, and therefore did not take into account of concentration polarization.
[39]	Based on the same approach in [8], the SEC was extended to multi-stages and studied the optimum number of stages in reverse osmosis and concluded that 3-5 stages will be optimal.	It assumed that the salt is fully mixed in each cross section along the flow channel.
[9]	Experimental study using Dow Filmtec XLE-2540 brackish water RO membrane and desalting between 30 and 80% water recovery implicitly indicated that the optimal water recovery for brackish water desalination to be 50%.	No ultimate conclusion regarding the optimal energy consumption is made. It is only a small pilot system and no ERD is used
[66]	One of the first papers addressed the optimization of single-stage RO processes by computer simulations. Used boundary layer flow and concentration empirical parameterized model to relate water production rate to the operating conditions, Reynolds number, and membrane area. Model showed that the optimization of the energy consumption with respect to several given feed flow rates.	It did not optimize the specific energy consumption with respect to the permeate flow rate.
[67]	Following the same boundary layer flow and concentration empirical parameterized model in [66], three-stage RO desalination optimization was conducted with and without flow-work exchanger and concluded that arrangement of RO modules needed to be investigated further and flow-work exchanger should receive serious consideration.	Membrane replacement cost difference due to the different operation conditions was not included.
[80]	Developed a mathematic model, based	It did not optimize the

	on empirical correlation for average mass transfer coefficient and membrane property (water permeability and salt permeability) dependence on fabricating temperature, to quantify the concentration polarization, of a system similar to the Coalinga Pilot Plant to maximize the product flux and determine the optimal arrangement of membrane assemblies with respect to fabrication temperature. It was concluded that the first-stage RO membrane should have higher water permeability than the second-stage if each stage has the same membrane area.	specific energy consumption for the system, it only optimize the product flux instead, which will not guarantee minimal specific energy consumption.
[10]	Compared the life cycle of different desalination technologies: thermal desalination (multi-stage flash and multi-effect evaporation), reverse osmosis and concluded that desalination based on RO provokes significantly lower environmental load than thermal desalination.	N/A
[11]	Utilized response surface methodology (RSM) to predict the salt rejection coefficient, specific permeate flux and RO energy consumption. The optimum operating conditions of minimal specific energy consumption was determined using the step adjusting gradient method.	The model requires experimental data to be trained for each new system and unsuitable for extrapolation and process design.
[13]	An exponential function, simulating the decline in the water permeability coefficient was introduced in a mixed-integer nonlinear programming (MINLP) to minimize the total annualized cost while optimizing the design and operation of the RO network. The results show that the fouling distribution between stages significantly affects the optimal design and operation of the RO process.	The study did not involve detailed dynamic modeling of membrane fouling. The mass transfer coefficient (used to quantify concentration polarization) was assumed to be independent of position along the membrane.
[135]	Differential mass balance approach is	Maximization of water

	combined with permeate flux equation and concentration polarization simulated by the film model. It is concluded that using a pressure exchanger device, it is possible to reduce energy consumption by up to 50%.	recovery was evaluated; however, it is noted that the minimum energy consumption is not necessarily at the maximum recovery.
[14]	A comprehensive review was presented of the main innovations and future trends in the design of seawater reverse osmosis desalination technology. It argues for desalination with renewable energy sources as an attractive combination in many regions with the possibility of reducing stress on existing water supplies.	N/A
[15]	Response surface methodology (RSM) and artificial neural networks (ANN) have been used to develop predictive models for simulation and optimization of reverse osmosis (RO) desalination process based on short-term experimental pilot plant data. The developed ANN model was valid over the whole range of feed salt concentration demonstrating its ability to overcome the limitation of the quadratic polynomial model obtained by RSM and to solve non-linear problems.	The model requires experimental data to be trained for each new system and unsuitable for extrapolation and process design.
[16, 17]	The optimum design problem was formulated as a mixed-integer non-linear programming (MINLP) problem, which minimizes the total annualized cost. The mathematical programming problem was solved with the general algebraic modeling system (GAMS) software to determine the optimal operational parameters. The optimal cleaning and membrane replacement schedule were predicted for a given fouling dynamics: water and salt permeability profile vs. operation time. .	Oversimplified the fouling mechanism.

[7]	RO operation optimizing energy consumption for seawater desalination was sought subject to hourly electricity price changes using standard global optimization tools. The results show significant electricity and production cost-saving potentials.	Oversimplified the concentration polarization effect using the empirical equation $C_{mem}/C_{retentate}=exp(0.7Y)$. It needs to compare with the mass transfer coefficient approach.
[19]	Approach to minimize the energy consumption in seawater desalination in the presence of membrane fouling, which was quantified by reduced membrane area available for permeate production. Depending on the fouling mechanism, boron rejection may be different even at the same fouling level.	The mass transfer coefficient to calculate CP via the film model was assumed constant along the flow channel. Also, the arithmetic average was used for the feed-brine side osmotic pressure
[5]	Quadratic correlation was used to compute the osmotic pressure as a function of temperature. Other aspects of the simulation are the same as [16] and [17]. It simulated the water recovery and permeate concentration for desalting using FilmTec SW30HR-380 spiral-wound membrane module for different values of feed flow rate, feed pressure and channel length.	Mass transfer coefficient used to estimate the level of concentration polarization, via the film model was taken to be invariant of axial position along the membrane. The simulated water recovery (<10%) is too low even for seawater desalination.
[6]	Developed a model based on first principle differential mass balance taking account of the concentration polarization, which is quantified by the film model assuming constant mass transfer coefficient. It predicted the local permeate flux and concentration.	A mass transfer coefficient for turbulent conditions was used and the pressure drop was not considered.

2.5. Summary

The economic feasibility of membrane desalination is highly dependent on operational costs (with energy cost being the highest). Therefore, minimization of these costs is a critical step in the RO design process. In this regard, current high permeability

RO membranes have enabled desalting operations at much lower pressures than previously possible, approaching the limit of thermodynamic restriction wherein the retentate osmotic pressure approaches the applied pressure. Consequently, it is imperative to develop rigorous integrated process and thermodynamic models for optimizing RO desalination with respect to various process factors, such as feed water chemistry, operating conditions, membrane module properties, brine disposal cost, and the use of energy recovery devices. This includes optimizations of multi-stage and multi-pass membrane process configurations with respect to feed and product water qualities, operating conditions, and water recovery levels. Ultimately, these optimization models need to be incorporated into a robust membrane desalination control system to be able to design smart membrane desalination systems that are able to automatically adapt to feed water fluctuations by adjusting process conditions to ensure operation at the highest efficiency.

Chapter 3   Single-stage RO Optimization

3.1.   Overview

Advances in highly permeable reverse osmosis (RO) membranes have enabled desalting operation in which it is practically feasible for the applied pressure to approach the osmotic pressure of the exit brine stream (Figure 3-1). Reduction of the overall cost of water production represents a major challenge and in the present work various elements of water production cost are evaluated from the viewpoint of optimization with respect to various costs (energy, membrane area and permeability, brine management, and pressure drop), as well as the important thermodynamic cross-flow constraint, utilization of energy recovery devices, and operational feed and permeate flow rate constraints. More specifically, in this chapter an approach to optimization of product water recovery at pressures that approach the osmotic pressure of the exit brine stream is presented via a number of simple RO process models which utilize highly permeable membranes.
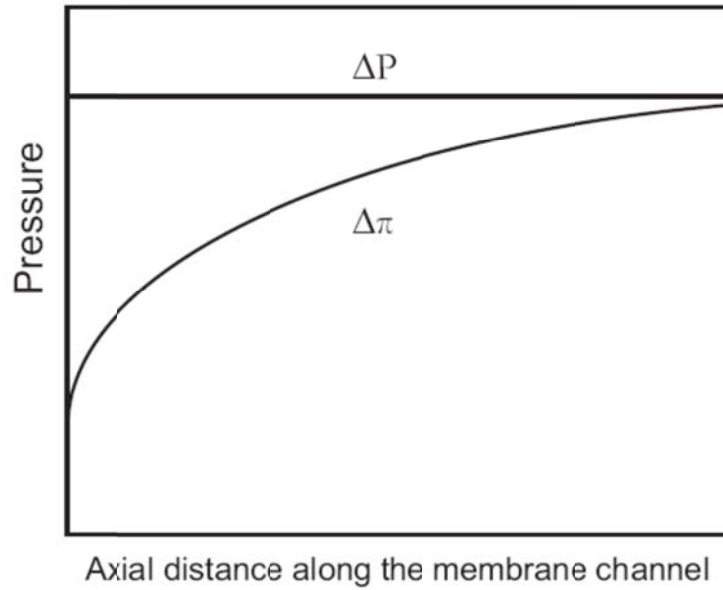
Figure 3-1. **Schematic illustration of the thermodynamic restriction for cross-flow RO desalting.**

3.2. Single-stage RO modeling

In order to illustrate the approach to energy cost optimization it is instructive to consider a membrane RO process without the deployment of an energy recovery device (ERD) as shown schematically in Figure 3-2.
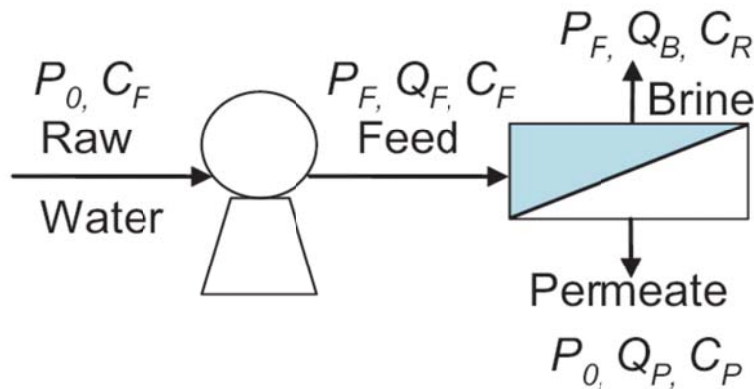
Figure 3-2. **Schematic of a simplified RO system.**

The energy cost associated with RO desalination is presented in the present analysis as the specific energy consumption (SEC) defined as the electrical energy needed to produce a cubic meter of permeate. Pump efficiency can be included in the following analysis in a straightforward fashion as presented later in Section 3.5.2. As a first step, however, in order to simplify the presentation of the approach, the required electrical energy is taken to be equal to the pump work, (i.e., assuming a pump efficiency of 100%). Accordingly, the SEC for the plant shown in Figure 3-2 is given by:

$$SEC = \frac{\dot{W}_{pump}}{Q_p} \qquad (3.1)$$

where Q_p is the permeate flow rate and $\dot{W}_{pump}$ is the rate of work done by the pump, given by:

$$\dot{W}_{pump} = \Delta P \times Q_f \qquad (3.2)$$

in which

$$\Delta P = P_f - P_0 \qquad (3.3)$$

where P_f is the water pressure at the entrance of the membrane module, P_0 is the pressure of the raw water which is assumed (for simplicity) to be the same as the permeate pressure, and Q_f is the volumetric feed flow rate. In order to simplify the analysis, we initially assume that the impact of the pressure drop (within the RO module) on locating the minimum SEC is negligible; this issue is addressed further in Section 3.5.1. It is acknowledged that, fouling and scaling will impact the selection of practical RO process operating conditions and feed pretreatment. The permeate product

water recovery for the RO process, Y, is an important measure of the process productivity, defined as:

$$Y = \frac{Q_p}{Q_f} \qquad (3.4)$$

and combining Eqs. (3.1), (3.2) and (3.4), the SEC can be rewritten as follows:

$$SEC = \frac{\Delta P}{Y} \qquad (3.5)$$

The permeate flow rate can be approximated by the classical reverse osmosis flux equation [150]:

$$Q_p = A_m L_p (\Delta P - \sigma \overline{\Delta \pi}) = A_m L_p (\overline{NDP}) \qquad (3.6)$$

where A_m is the active membrane area, L_p is the membrane hydraulic permeability, σ is the reflection coefficient (typically assumed to be about unity for high rejection RO membranes and in this study $\sigma = 1$), ΔP is the transmembrane pressure, $\overline{\Delta \pi}$ is the average osmotic pressure difference between the retentate and permeate stream along the membrane module, and $(\Delta P - \sigma \overline{\Delta \pi})$ is the average trans-membrane net driving pressure designated as $\overline{NDP}$. i8nIn many cases the osmotic pressure can be assumed to vary linearly with concentration (i.e., $\pi = f_{os} C$ where f_{os} is the osmotic pressure coefficient and C is the solution salt concentration [150]. In order to evaluate the above approximation, a series of osmotic pressure calculations were carried out for aqueous sodium chloride solutions using the OLI thermodynamic simulator [151]. The results shown in Figure 3-3 indicate a high degree of linearity (the R^2 is 0.9988) of osmotic pressure with salt concentration up to 70,000 mg/L. The average osmotic pressure

35

difference (up to the desired level of product water recovery), $\overline{\Delta\pi}$, along the membrane channel can be approximated as either an arithmetic or log-mean average along the membrane [152]:

$$\overline{\Delta\pi} = f_{os}C_f \frac{ln\left[\frac{1}{1-Y}\right]}{Y} \qquad (3.7a)$$

$$\overline{\Delta\pi} = \frac{f_{os}C_f}{2}\left(1+\frac{1}{1-Y}\right) \qquad (3.7b)$$

where C_f is the salt concentration of the feed to the membrane module. The effect of different osmotic pressure averaging is discussed in Section.3.4.3.
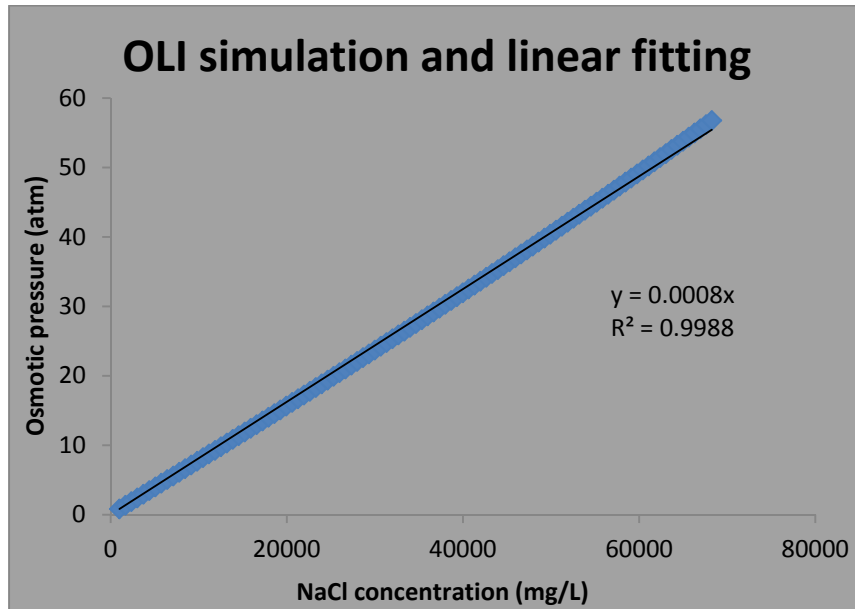
Figure 3-3. **Osmotic pressure vs. NaCl concentration (OLI simulation at 25°C).**

The osmotic pressures at the entrance and the exit of the membrane module, relative to the permeate stream, are approximated by:

$$\Delta \pi_{entrance} = f_{os} C_f - \pi_p \tag{3.8}$$

$$\Delta \pi_{exit} = f_{os} C_r - \pi_p \tag{3.9}$$

where C_r is the salt concentration of the exit brine (i.e., concentrate) stream and is the permeate osmotic pressure ($\pi_p = f_{os} C_p$, C_p is the permeate concentration). For sufficiently high rejection level, the osmotic pressure of the permeate stream can be taken to be negligible relative to the feed or concentrate streams and C_r can be approximated by:

$$C_r = \frac{C_f}{1-Y} \tag{3.10}$$

Combining Eqs. (3.8), (3.9) and (3.10), the osmotic pressure difference between the retentate and permeate stream at the exit of the module can be expressed as:

$$\Delta \pi_{exit} = \frac{R \pi_0}{1-Y} \tag{3.11}$$

where $\pi_0 = f_{os} C_f$ is the feed osmotic pressure and R is the salt rejection ($R = 1 - \frac{C_p}{C_f}$).

Equation (3.11) is a simple relationship that illustrates that the well-known inherent difficulty in reaching high recovery in RO desalting is due to the rapid rise in osmotic pressure with increased recovery.

3.2.2. Thermodynamic restriction of cross-flow RO operation

In the process of RO desalting, an external pressure is applied to overcome the osmotic pressure, and pure water is recovered from the feed solution through the use of a

semipermeable membrane. Assuming that the permeate pressure is the same as the raw water pressure, P_0, the applied pressure (ΔP) needed to obtain a water recovery of Y should be no less than the osmotic pressure difference at the exit region [23, 140, 141] (See **Figure 3-1**), which is given by Eq. (3.11). Therefore, in order to ensure permeate productivity along the entire RO module (or stage), the following lower bound is imposed on the applied pressure:

$$\Delta P \geq \Delta \pi_{exit} = \frac{R\pi_0}{1-Y} \tag{3.12}$$

Equation (3.12) the so-called thermodynamic restriction of cross-flow RO [140-142] and herein referred to as the "thermodynamic restriction". The equality on the right-hand-side of Eq. (3.12) is the condition at the "limit of thermodynamic restriction" at the exit of the membrane module and is attained at the limit of infinite membrane permeability for a finite membrane area. It is particularly important from a practical point of view when a highly-permeable membrane is used for water desalination at low pressures. It is emphasized that the constraint of Eq. (3.12) arises when one wants to ensure that the entire membrane area is utilized for permeate production.

3.2.3. Computation of Q_p close to the thermodynamic limit

Referring to the computation of the $\overline{NDP} = \Delta P - \overline{\Delta \pi}$, and in turn the water production rate Q_p, for operation near the limit of the "thermodynamic restriction", it is noted that given the approximation of $\overline{\Delta \pi}$ as given in Eqs. 3.7a and 3.7b, the following

approximation is used for the NDP, where salt rejection is assumed to be 100% (Eq. (3.6 as derived based on the logarithmic and arithmetic osmotic pressure averaging,)):

$$\overline{NDP} = \frac{\pi_0}{1-Y} - \pi_0 \frac{ln\left[\dfrac{1}{1-Y}\right]}{Y} \tag{3.13a}$$

$$\overline{NDP} = \frac{\pi_0}{1-Y} - \frac{\pi_0}{2}\left[1 + \frac{1}{1-Y}\right] \tag{3.13b}$$

The above expressions are reasonable approximations when the RO process is allowed to approach the pressure limit imposed by the thermodynamic restriction (Eq. (3.12)). It is noted that operation approaching this limit is possible only when highly permeable membranes are used in an RO process. To demonstrate this point, a differential mass balance of the salt across the membrane, employing the logarithmic osmotic pressure average, yields the following expression for the $\overline{NDP}$:

$$\overline{NDP} = \Delta P - \overline{\Delta\pi} = \frac{Q_p}{AL_p} = \frac{\Delta P}{1 + \dfrac{\pi_0}{\Delta P}\dfrac{1}{Y}ln\dfrac{1-(\pi_0/\Delta P)}{1-Y-(\pi_0/\Delta P)}} \tag{3.14}$$

where Y denotes the actual water recovery when the applied pressure is ΔP .. For operation at the limit of thermodynamic restriction (i.e., $\Delta P = \pi_0/(1-Y)$), it is clear from Eq. (3.14) that a highly permeable membrane (i.e., high L_P) and/or large surface area would be required. Given that the present analysis focuses on RO desalting made possible by highly permeable membranes, instead of using the pressure implicit *NDP* expression (Eq. (3.14)), it is reasonable to utilize, without loss of generality of the overall approach, the log-mean average (Eq. (3.13)). The implication of using different averaging approaches for the computation of $\overline{\Delta\pi}$ is discussed in Section 3.3.

3.3. Optimization for RO Operation at the Limit of Thermodynamic Restriction

The basic equations for the RO process presented in Section 3.2 form the basis for deriving the basic relationship between the minimum SEC for a single-stage RO process (without and with an ERD) with respect to the level of product water recovery. The derivation is similar to that of Uri Lachish [31]. It is presented here for completeness because the theoretically minimum SEC, for different water recoveries, is used as the constraint on the set of energy-optimal and feasible operating points as discussed in Section 3.4. The impacts of ERD, brine disposal cost, and membrane permeability on the optimal water recovery are then considered as well as the possible energy savings when using a two-stage RO process, relative to the increased membrane area requirement.

3.3.1. Energy Cost Optimization for a Single-stage RO without an Energy Recovery Device

The specific energy consumption (SEC) for the RO desalting process can be derived by combining Eqs. (3.1)–(3.4) and (3.12), to obtain:

$$SEC \geq \frac{R_t \pi_0}{Y_t(1-Y_t)} \tag{3.15}$$

where SEC is in pressure units. It is convenient to normalize the SEC, at the limit of thermodynamic restriction (i.e., operation up to the point in which the applied pressure equals the osmotic pressure difference between the concentrate and permeate at the exit of the membrane module), with respect to the feed osmotic pressure such that:

$$SEC_{tr,norm} = \frac{SEC_{tr}}{\pi_0} = \frac{R_t}{Y_t(1-Y_t)} \qquad (3.16)$$

and this dependence is plotted in Figure 3-4, showing that there is a global minimum. In order to obtain the analytical global minimum $SEC_{tr,norm}$, with respect to the water recovery, one can set $d(SEC_{tr,norm})/(dY)=0$ from which it can be shown that the minimum $SEC_{tr,norm}$ occurs at a fractional recovery of $Y=0.5$ (or 50%) where $(SEC_{tr,norm})_{min}=4$ (i.e., four times the feed osmotic pressure). The above condition, i.e., $(SEC_{tr,norm})_{min}=4$ at $Y=0.5$, represents the global minimum SEC (represented by the equality in Eq. 3.15). In order to achieve this global minimum energy consumption, the RO process should be operated at a water recovery of 50% with an applied pressure equivalent to $2\pi_0$ (i.e., double that the feed osmotic pressure).
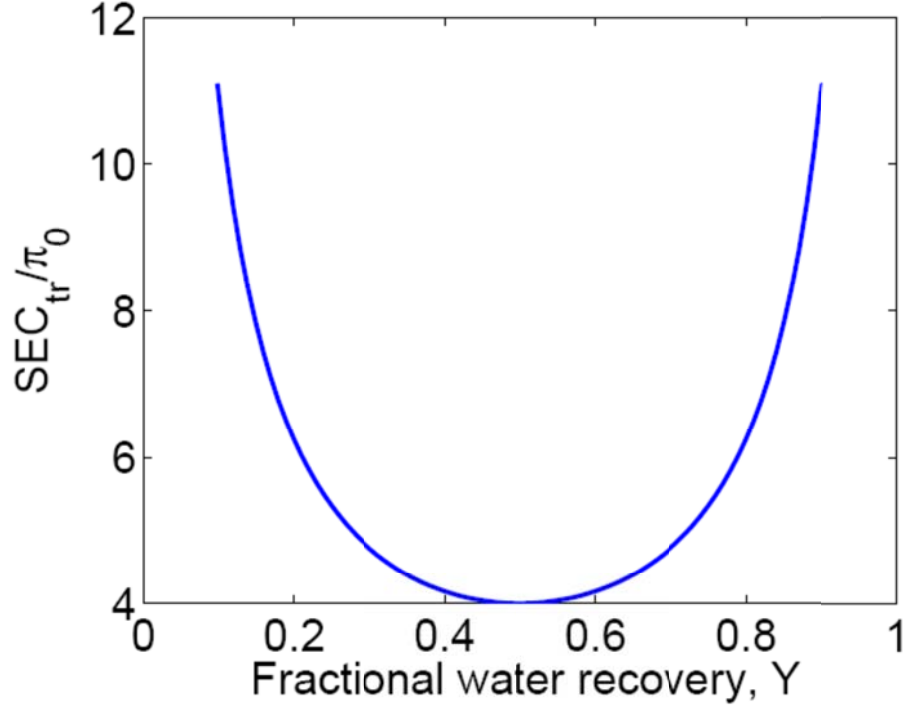
Figure 3-4. **Variation of the normalized SEC with water recovery for a single-stage RO at the limit of the thermodynamic restriction.**

As an example of the implications of the above analysis it is instructive to consider a single-stage seawater RO plant with the following feed salinity of $35,000 mg/L$ (and thus $\pi_0 = 25\,atm$) and membrane permeability of $L_p = 10^{-11} m^3/m^2 \cdot s \cdot Pa$ (which is high with respect to commercially available membranes). In this case, the global minimum energy cost is $4\pi_0 = 2.8 kWh/m^3$. The average permeate flux for single-stage seawater desalination, at the above optimal condition, can be computed from Eq. (3.6) as follows:

$$(FLUX)_{opt} = \frac{Q_p}{A_m} = L_p \times ((\Delta P)_{opt} - ln(\frac{1}{1-Y_{opt}})\frac{R_t \pi_0}{Y_{opt}}) = 0.6137 \times \pi_0 \times L_p = 13.5 GFD$$

where GFD denotes the permeate flow rate in $gallons/ft^2 \cdot day$, $Y_{opt} = 0.5$, and $(\Delta P)_{opt} = 2R_t\pi_0$. The permeate flow can be determined once the membrane area is established and the optimum feed flow rate can be calculated using Eq. (3.4). At the globally energy-optimal operating point, the applied pressure and feed flow rate which are input process variables and hence the output variables (brine and product flow rate) are fixed for an RO plant with given A_m and L_p. It is noted that, the above analysis is specific to a single-stage RO plant. Cost reduction that can be achieved by adopting multiple stage process configurations is discussed in the following chapter.

3.3.2. Impact of brine management cost on the thermodynamic restriction and the minimum SEC

Management of the RO concentrate (i.e., brine) stream can add to the overall cost of water production by RO desalting and in fact alter optimal energy cost and associated product water recovery. As an example of the possible influence of brine management (including disposal) on RO water product cost we assume a simple linear variation of the cost of brine management with the retentate stream. Accordingly, the specific brine management cost (SBC) per unit volume of produced permeate, normalized with respect to the feed osmotic pressure, is given by:

$$SBC_{norm} = \frac{b \times Q_b}{\pi_0 Q_p} = \frac{b}{\pi_0} \times \frac{1-Y}{Y} \tag{3.17}$$

where b is the concentrate (brine) management cost expressed on energy equivalent units per concentrate volume ($Pa \cdot m^3 / m^3$). Inspection of Eq. (3.17) suggests that a convenient

43

dimensionless brine management cost can be defined as, $b_{norm} = b/\pi_0$, where π_0 is the osmotic pressure of the feed water for salinity range of about $1,000 - 35,000 mg/L$ total dissolved solids, $b = b_A \beta / \varepsilon$ in which b_A is the concentrate management cost in units of $\$/m^3$ in the range of $0 - 20 cents/m^3$ and the ε and β are the energy price $0.05 - 0.15 \$/kWh$ and energy conversion factor, $(3.6*10^6 Pa \cdot m^3/kWh)$, respectively. Given the above, one can ascertain that b_{norm} is in the range of 0-100.

The combined normalized energy (Eq. (3.15)) and brine management costs (Eq. (3.17)) for a single-stage RO process is given by:

$$SEC_{norm} + SBC_{norm} \geq \frac{1}{Y(1-Y)} + b_{norm} \times \frac{(1-Y)}{Y} \qquad (3.18)$$

In which the equality in Eq. (3.18) signifies the cost when the pressure at the exit region equals the osmotic pressure of the concentrate stream As shown in Figure 3-5, the recovery level at the optimal (i.e., minimum) cost increases with increased brine management cost. In other words, the higher the brine management cost, for a given membrane cost, the greater the incentive for operating at a higher recovery level. The optimal product water recovery, Y_{opt}, can be obtained by differentiating Eq. (3.18) with respect to Y and setting the resulting expression to zero, resulting in the following expression:

$$Y_{opt} = \frac{\sqrt{1+b_{norm}}}{1+\sqrt{1+b_{norm}}} \qquad (3.19)$$

indicating that the optimal recovery, for a given membrane area, will increase with the concentrate management cost (see Figure 3-5), reducing to $Y_{opt}=0.5$ for the case of a vanishing brine management cost.
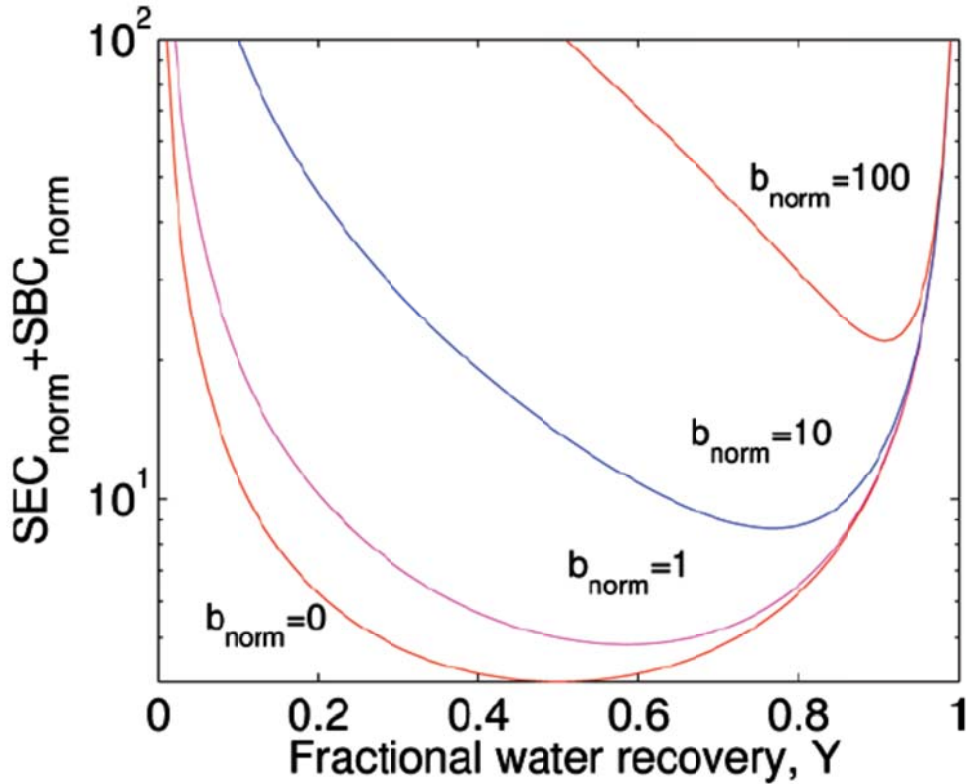
Figure 3-5.   **Variation of the summation of energy and brine management costs with product water recovery for a single-stage RO.**

3.4.   Optimization for RO operation above the limit imposed by the thermodynamic restriction

For a given RO plant, process conditions that would enable desalting at the global minimum energy utilization condition are fixed (see Section 3.2). However, the desired level of productivity or feed processing capacity may force deviation from the globally

optimal operation. Therefore, for an energy-optimal operating condition, product water recovery may have to be shifted to ensure optimal operation. Accordingly there is merit in exploring the SEC optimization, as constrained by the normalized feed or permeate flow rates, and the implications of the thermodynamic restriction of Eq. (3.12) on this optimization.

3.4.1. Optimization at a constrained permeate flow rate

For a given plant, when the desired level of permeate productivity cannot be accommodated by operating at global optimum, the permeate flow rate is a constraint that shifts the optimal water recovery (and thus, the corresponding feed flow rate). In this case, it is convenient to define a normalized permeate flow rate as follows:

$$Q_{p,norm} = \frac{Q_p}{A_m L_p \pi_0} = \frac{\Delta P - \overline{\Delta \pi}}{\pi_0} = \frac{\Delta P}{\pi_0} - \frac{\overline{\Delta \pi}}{\pi_0} \tag{3.20}$$

where the first term on the right-hand-side of Eq. (3.20) is $Y \cdot SEC_{norm}$ $Y \cdot SEC_{norm}$ and the second term can be expanded using Eq. (3.7) and thus the SEC_{norm} can be expressed as:

$$SEC_{norm} = \frac{SEC}{\pi_0} = \frac{Q_{p,norm}}{Y} + \frac{ln(\frac{1}{1-Y})}{Y^2} \tag{3.21}$$

where SEC_{norm} is a function of the water recovery and the normalized permeate flow rate. As shown in Figure 3-6, the minimum SEC_{norm} shifts to higher water recoveries and higher $(SEC_{norm})_{min}$ as plant productivity is pushed beyond the globally energy-optimal operating point, which has a water recovery of 50%.

46
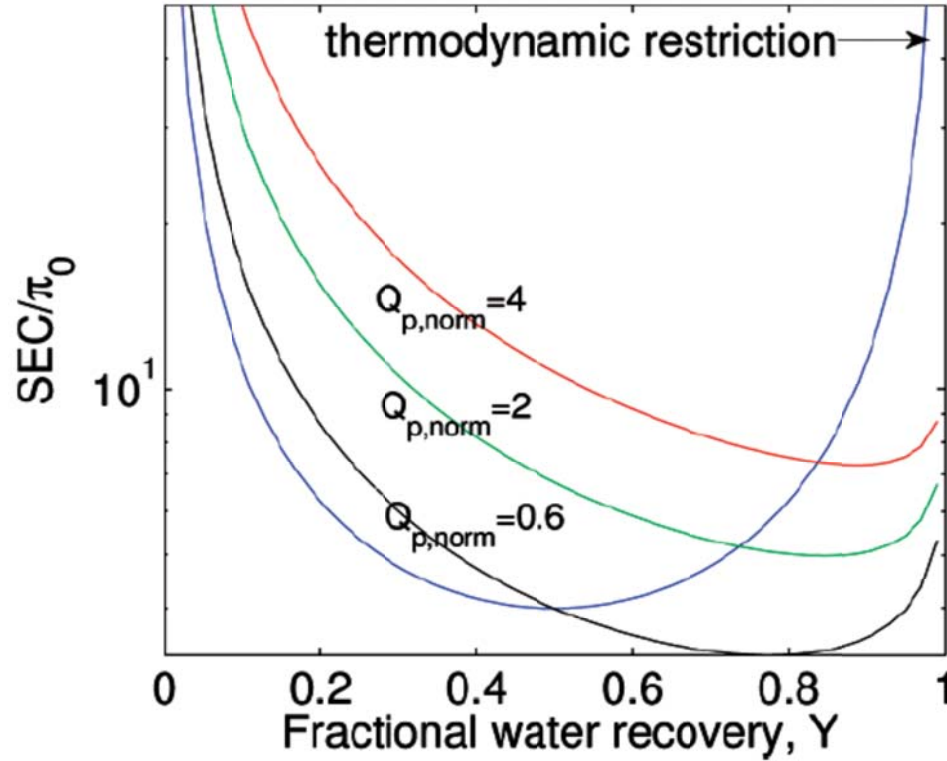
Figure 3-6. **Dependence of the normalized SEC (without ERD) on water recovery at different normalized permeate flow rates for single-stage RO.**

It is important to recognize that RO operation below the symmetric curve imposed by the thermodynamic restriction is not realizable. In fact, the lowest practically realizable SEC_{norm} values (i.e., the minima above the thermodynamic restriction or the points of intersection with this curve) for each $Q_{p,norm}$ are plotted in Figure 3-7 (a) with the corresponding optimal water recovery dependence on $Q_{p,norm}$ shown in Figure 3-7 (b).
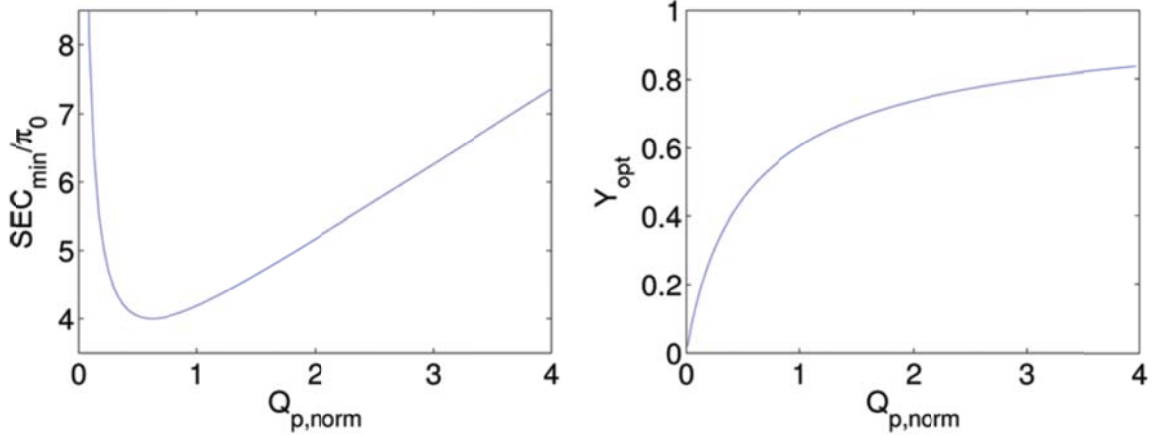
Figure 3-7. Normalized minimum SEC vs. normalized permeate flow rate; b) Dependence of the optimum water recovery on the normalized permeate flow rate.

The additional cost associated with brine management can be included by adding its associated normalized cost (Eq. (3.17)) to the SEC_{norm} (Eq. (3.21)) resulting in:

$$SEC_{norm} + SBC_{norm} = \frac{Q_{p,norm}}{Y} + \frac{ln\left[\dfrac{1}{1-Y}\right]}{Y^2} + b_{norm} \times \frac{1-Y}{Y} \tag{3.22}$$

where b_{norm} is the brine disposal penalty factor. The additional brine management cost shifts the optimal recovery, for a given b_{norm}, to higher water recovery values while raising the achievable minimum energy operating condition (Figure 3-8). Here it is also emphasized that, RO operation where the combined cost of $SEC_{norm} + SBC_{norm}$ is in the region below the curve representing the thermodynamic restriction (Figure 3-8) is not realizable. Thus, the lowest combined energy and brine management costs that can be achieved are either the minima in the region above the thermodynamic cross-flow restriction curve or at the intersection of this curve with the thermodynamic restriction curve.
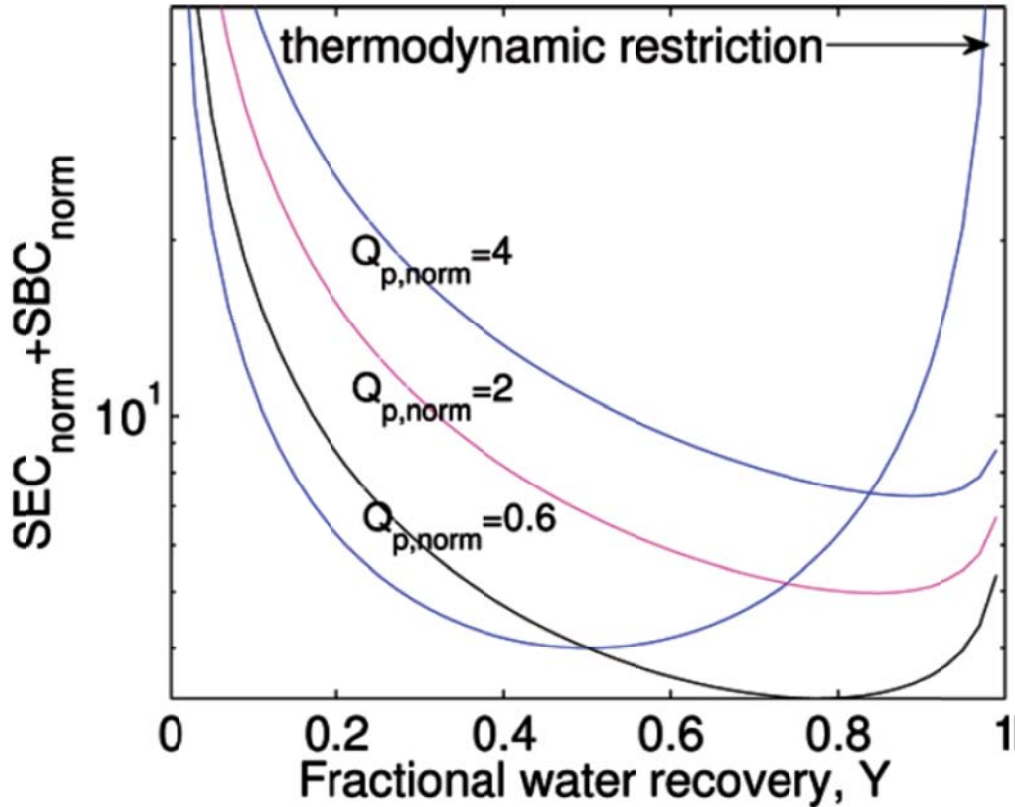
Figure 3-8. **Variation of summation of normalized energy cost without ERD and brine management cost vs. water recovery at different normalized permeate flow rates with brine disposal penalty factor equal to one.**

3.4.2. Optimization at a constrained feed flow rate

The feed flow rate may be constrained (e.g., due to restrictions on the available water source) for an RO plant. Therefore, the optimization objective is to determine the optimal water recovery and corresponding permeate flow rate under this constraint that would result in a minimal specific energy consumption. In a typical operation, the permeate flux can be expressed as $Q_p / A_m L_p = \Delta P - \overline{\Delta \pi}$ and since $Q_p = Q_f Y$ one can express Q_p, in a normalized form as:

$$Q_{f,norm} = \frac{Q_f}{A_m L_p \pi_0} = \frac{\Delta P - \overline{\Delta \pi}}{Y \pi_0} = \frac{\Delta P}{Y \pi_0} - \frac{\overline{\Delta \pi}}{Y \pi_0} \tag{3.23}$$

in which the first term on the right-hand-side of Eq. (3.23) is SEC_{norm} (see Eq. (3.5)) that

can thus be expressed as:

$$SEC_{norm} = \frac{SEC}{\pi_0} = Q_{f,norm} + \frac{ln(\frac{1}{1-Y})}{Y^2} \tag{3.24}$$

in which use was made of Eq. (3.7) as in the derivation of Eq. (3.24) and

$Q_{f,norm} = Q_{p,norm}/Y$. As a reference, the SEC_{norm} curve for operation at the limit of the

thermodynamic restriction is also shown in Figure 3-9. Operation below the above curve

(i.e., the thermodynamic restriction) is not realizable. Therefore, the locus of the lowest

permissible SEC_{norm} is given by the minima that exist above the thermodynamic

restriction curve and the intersections of this curve with the individual SEC_{norm} curves

with the resulting plot shown in Figure 3-10. The minimum SEC_{norm} with respect to

$Q_{f,norm}$ is obtained from Figure 3-9 and plotted in Figure 3-10 (a). Figure 3-10 (b)

presents the corresponding optimal water recovery at each normalized feed flow rate.

Accordingly, if $Q_{f,norm} > 2.4$, the optimal water recovery is 71.53%, which is determined

by solving $\partial(SEC_{norm})/\partial Y = 0$ with respect to Eq. (3.24) independently of the

thermodynamic restriction.
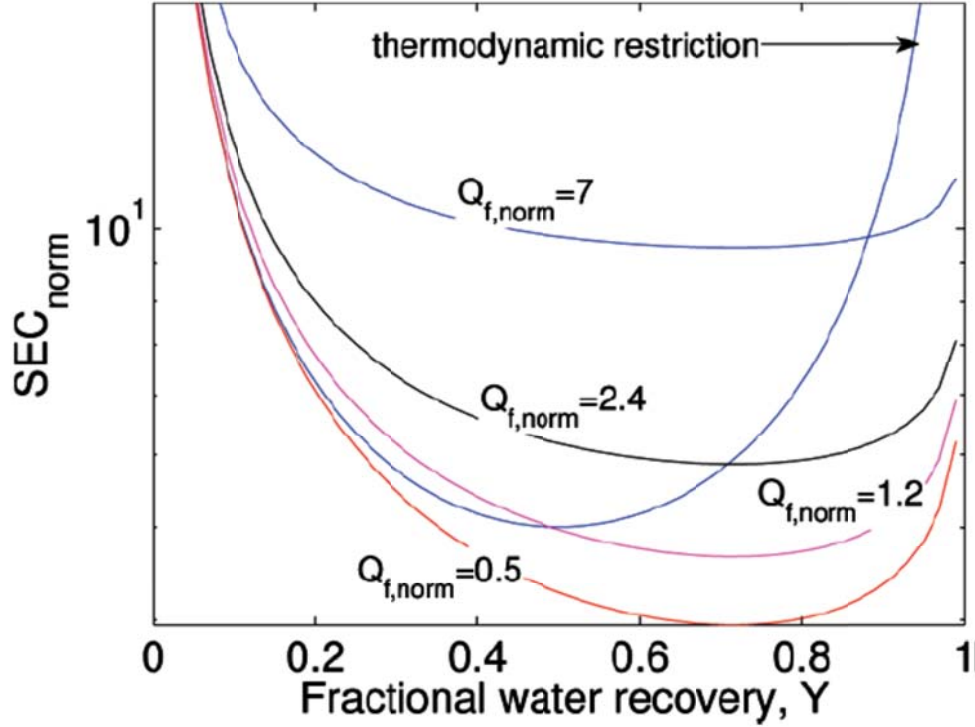
Figure 3-9.   **Dependence of SEC_{norm} on water recovery for different normalized feed flow rates for a single-stage RO without an ERD.**

Finally, it is important to note that the curves of different $Q_{f,norm}$ in Figure 3-9 can be interpreted as curves of different membrane permeability, L_p, for a fixed Q_f, A_m and π_0 (see Eq. (3.23)); in such an interpretation, we can see that as L_p increases ($Q_{f,norm}$ decreases), the SEC decreases but the benefit is limited at high recoveries owing to the effect of the thermodynamic restriction. Similar behavior is observed for different $Q_{p,norm}$ values in Figure 3-7.
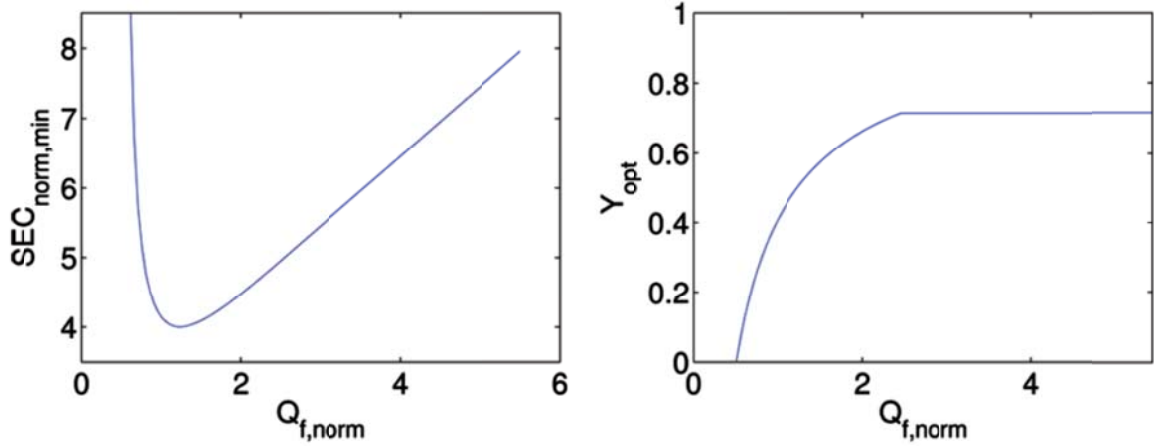
Figure 3-10. **a) Normalized minimum SEC vs. normalized feed flow rate; b) Optimum water recovery at each normalized feed flow rate.**

The optimal condition for operation subject to the feed flow constraint, when considering the additional cost of brine management, can be obtained from the sum of the normalized energy cost (Eq. (3.24)) and brine management cost (Eq. (3.24)) as follows:

$$SEC_{norm} + SBC_{norm} = Q_{f,norm} + \frac{ln(\frac{1}{1-Y})}{Y^2} + b_{norm} \times \frac{1-Y}{Y} \qquad (3.25)$$

As shown in Figure 3-11 (for the example of $b_{norm} = 1$), the minimum (or optimal) cost shifts to higher recoveries.
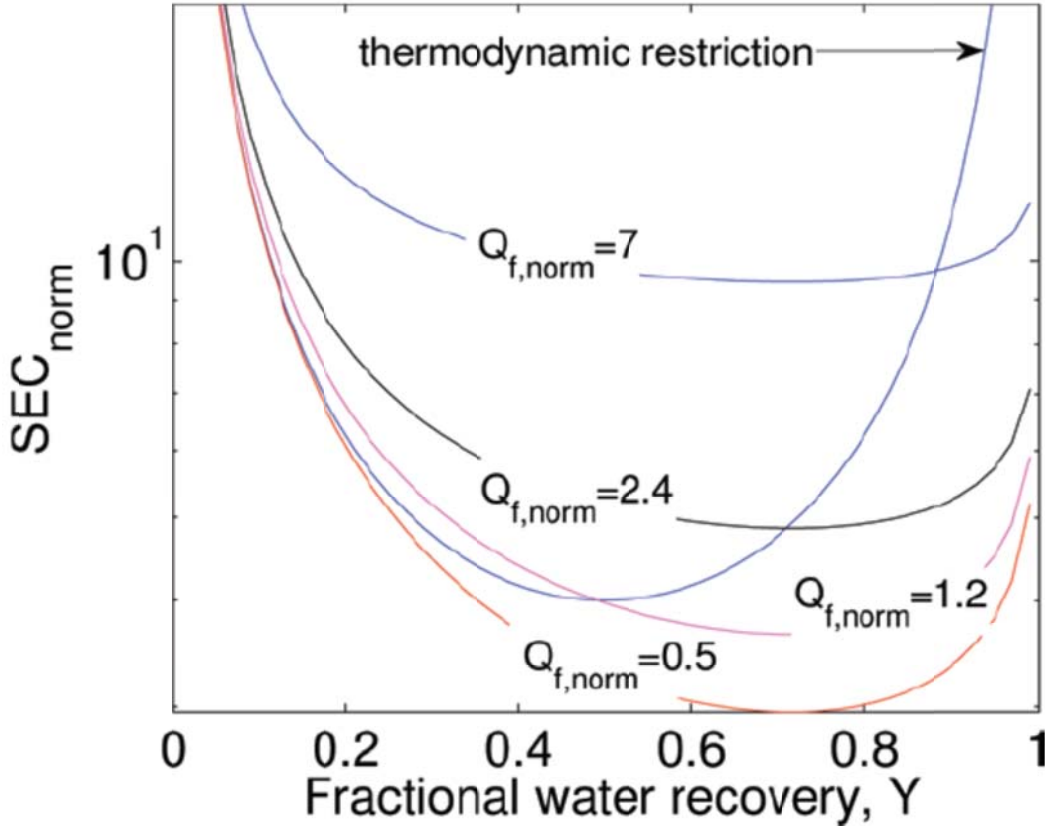
Figure 3-11. **Variation of summation of normalized energy cost without ERD and brine management cost vs. water recovery at different normalized feed flow rates with brine disposal penalty factor equal to one.**

The optimal recovery (i.e., at the point of minimum cost considering the brine management cost) is obtained from solving $\partial(SEC_{norm}+SBC_{norm})/\partial Y=0$, leading to

$$Y_{opt}=\frac{\sqrt{2(1+b_{norm})}}{1+\sqrt{2(1+b_{norm})}} \quad Y_{opt}=\frac{\sqrt{2(1+b_{norm})}}{1+\sqrt{2(1+b_{norm})}} \tag{3.26}$$

Eq. (3.26) reveals that when the brine management cost is neglected (i.e., $b_{norm}=0$), $Y_{opt}=71.53\%$. However, the inclusion of brine disposal cost shifts the optimal water recovery to higher values. It is important to recognize that the operating points for which

the combined cost, $SEC_{norm} + SBC_{norm}$, falls below the value dictated by the thermodynamic restriction are not realizable.

3.4.3. Effect of osmotic pressure averaging on SEC

The averaging of the osmotic pressure can have a quantitative effect on the identified optimal operating conditions, although the overall analysis approach used and the trends presented in the present work should remain independent of the averaging method. For example, if the arithmetic osmotic pressure average, $\overline{\Delta \pi} = \frac{1}{2}(f_{os}C_f + f_{os}C_r)$, is used instead of the log-mean average (Eq. (3.7)), the $SEC_{tr,norm}$ for the thermodynamic restriction remains the same as shown previously; however, there can be a shift in the optimum conditions as shown in Figure 3-12 for the case of SEC optimization subject to a feed flow constraint. This example shows that at low water recoveries, $Y < 0.4$, the log-mean and arithmetic osmotic pressure averages yield similar results, while at high water recoveries, the use of the log-mean average results in lower $(SEC_{norm})_{min}$ than the arithmetic average because the former predicts a greater average net driving pressure, and thus, a higher permeate flow for a given applied pressure.
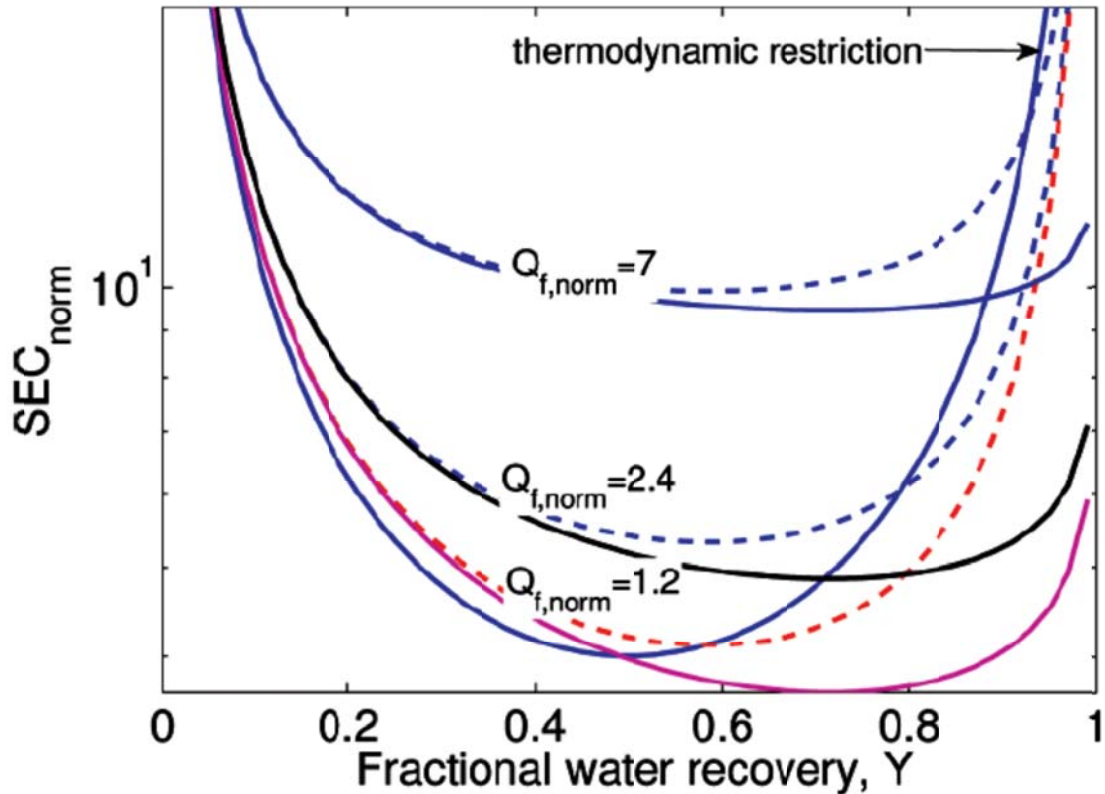
Figure 3-12. **Normalized SEC vs. water recovery at different normalized feed flow rates: without ERD. The results for the arithmetic and log-mean average osmotic pressures are depicted by the dashed and solid curves, respectively.**

3.5. Considerations of pressure drop and pump efficiency

3.5.1. Effect of pressure drop within the RO membrane module

The pressure drop in RO modules is typically small compared to the total applied pressure and its contribution to the required total applied pressure can be assessed by a simple order of magnitude analysis. Accounting for the frictional pressure drop, ΔP_f, the permeate flow rate is given by [90]:

$$Q_p = A_m L_p (\Delta P - \overline{\Delta \pi} - \frac{\overline{\Delta P_f}}{2})$$

(3.27)

Thus, the applied pressure ΔP is given by:

$$\Delta P = \overline{NDP} + \frac{\overline{\Delta P_f}}{2} + \overline{\Delta \pi}$$

(3.28)

where the average net driving pressure $\overline{NDP} = \dfrac{Q_p}{A_m L_p}$, and ΔP_f can be estimated

from [153]:

$$\Delta P_f = (\frac{1}{2} \rho \overline{u}^2)(\frac{24}{Re} - \frac{648}{35} \frac{Re_W}{Re})(1 - \frac{2 Re_W}{Re} \frac{x}{h})(\frac{x}{h})$$

(3.29)

where ρ is the solution density, x is the axial length, h is the half height of the channel,

$\overline{u}$ is the average axial velocity given as $\overline{u} = \dfrac{\overline{Q_f}}{2hW} = \dfrac{1}{2hW}(\dfrac{Q_f + Q_b}{2}) = \dfrac{Q_p}{4hW}(\dfrac{2}{Y} - 1)$

(where W is the channel width and Y is the fractional water recovery), Re is the axial

Reynolds number ($Re = 4h\overline{u}\rho/\mu$, where μ is the solution viscosity), and Re_W is the

permeate Reynolds number (defined as $Re_W = hv_w\rho/\mu$, where v_w is the permeate flow

velocity). Inspection of Eq. (3.29) shows that:

$$\Delta P_f < (\frac{1}{2} \rho \overline{u}^2)(\frac{24}{Re})(\frac{x}{h})$$

(3.30)

and can be rearranged as follows:

$$\frac{\Delta P_f}{\overline{NDP}} < \frac{3 \mu x^2 L_p (\frac{2}{Y} - 1)}{2h^3}$$

(3.31)

where the definitions of $\overline{u}$ and Re are used. Thus, the ratio of the frictional pressure loss

relative to the applied pressure can be estimated as follows:

56

$$\frac{\Delta P_f}{\Delta P} < \frac{\Delta P_f}{\overline{NDP}} < \frac{3\mu x^2 L_p(\frac{2}{\overline{Y}}-1)}{2h^3} \qquad (3.32)$$

A reasonable order of magnitude assessment of the various terms in Eq. (3.32) reveals

that $h \approx 0.001 - 0.01 m$, $\mu \approx 0.001 - 0.005 Pa.s$, $L_p \approx 10^{-11} - 10^{-10} m \cdot s^{-1} \cdot Pa^{-1}$, and $x \approx 0.1 - 1 m$.

For practical range of product water recovery of $Y \approx 0.3 - 0.95$, the right-hand-side of

equation Eq. (3.32) is at most of the order of $10^{-10} - 10^{-2}$. Therefore, one can conclude

that the effect of frictional pressure drop on determining the optimal operating condition

would be small but can be readily incorporated into the present formalism.

Given the above order of magnitude analysis of frictional losses, one can assess

the relative importance of the various pressure terms (Eq. (3.28)) as a function of product

water recovery. Accordingly, the fractional contribution of the different pressure terms on

the right-hand-side of Eq. (3.28) can be assessed as illustrated in Figure 3-13, for a

specific set of process conditions (at the limit of thermodynamic restriction, i.e., the

applied pressure equals the osmotic pressure difference at the exit region of the RO

membrane).
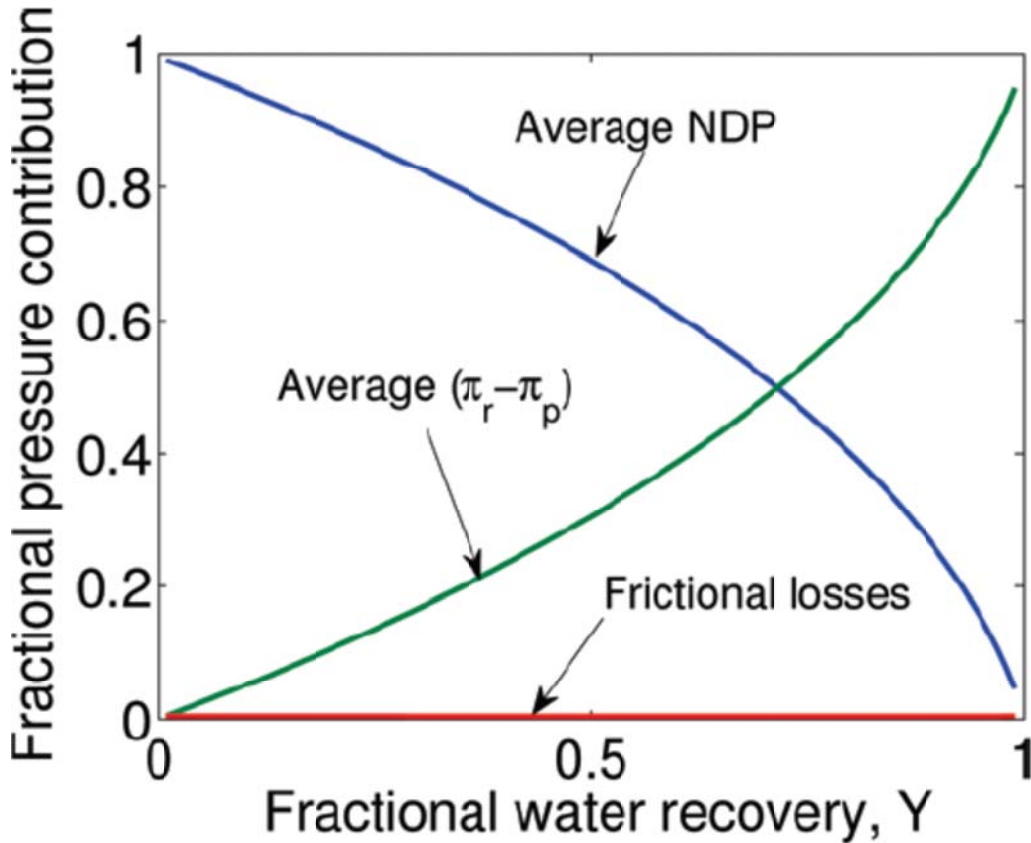
Figure 3-13. **Fractional contribution of the average $\overline{NDP}$, osmotic pressure and frictional pressure losses to the total applied pressure (Calculated for RO operation at the limit of the thermodynamic restriction. The log-mean average of osmotic pressure was utilized, with $h = 0.001\,m$, $\mu = 0.001\,Pa \cdot s$, $L_p = 10^{-9}\,m \cdot s^{-1} \cdot Pa^{-1}$, and $x = 1\,m$. $\pi_r = f_{os}C_r$ is the local osmotic pressure of the retentate and C_r is the local retentate concentration.).**

It is clear that the frictional losses are small ($<1\%$ of the total required pressure), the average osmotic pressure increases with recovery, while the required net driving pressure ($\overline{NDP}$) decreases with increased recovery. It is important to note that, as the required $\overline{NDP}$ increases (e.g., due to decreasing membrane permeability), the fractional contribution of osmotic pressure to the total applied pressure will decrease. As the $\overline{NDP}$

58

decreases, there is less incentive for improving membrane permeability since the cost for overcoming the osmotic pressure begins to dominate the energy cost. Conversely, a process that is found to operate at a high $\overline{NDP}$ will have a greater benefit from employing membranes of higher permeability.

3.5.2. Effect of pump efficiency on SEC

Pump efficiency can be easily included in the present analysis approach of the optimal SEC, as shown in this section, for the single-stage RO (Figure 3-2). Specifically, the normalized specific energy consumption at the limit of thermodynamic restriction accounting for pump efficiency, $SEC_{tr,norm}(\eta_{pump})$, can be expressed as:

$$SEC_{tr,norm}(\eta_{pump}) = \frac{SEC_{tr}(\eta_{pump}=1)}{\pi_0 \eta_{pump}} = \frac{1}{Y(1-Y)\eta_{pump}} \tag{3.33}$$

where η_{pump} is the pump efficiency which takes values in the interval $(0,1]$. For this case, the optimal water recovery remains at $Y_{opt} = 50\%$, and the corresponding normalized minimum SEC is $4/\eta_{pump}$.

3.5.3. Effect of energy recovery device on SEC for a single-stage RO process

In order to reduce the required energy for RO desalination, energy can be extracted from the high pressure retentate (or brine) stream using a variety of energy recovery schemes. A simple schematic representation of energy recovery is shown in Figure 3-14 for a simplified model RO process. P_e and P_p are the brine discharge and permeate pressure, respectively, which are assumed here to be equal to P_0.

59
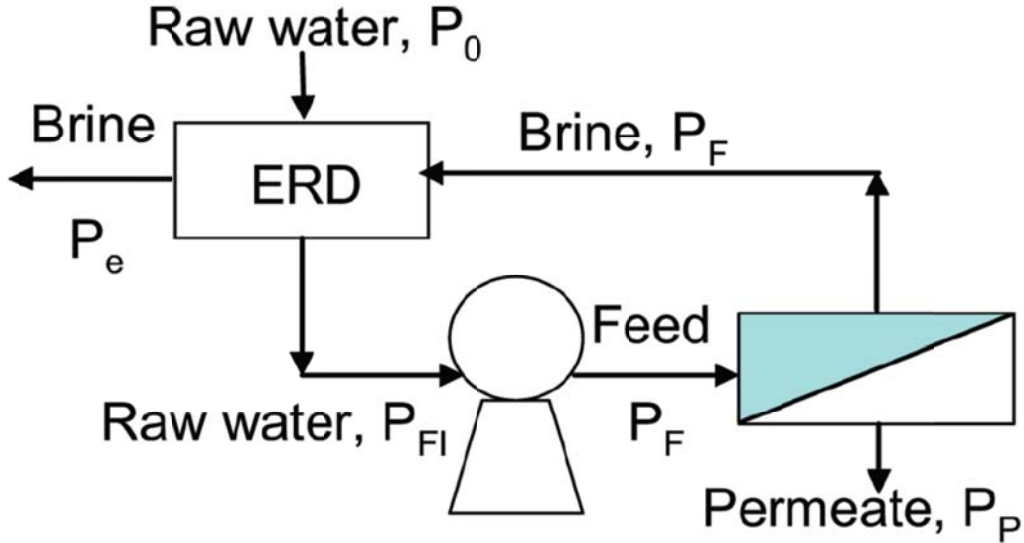
Figure 3-14. Simplified RO system with an energy recovery device (ERD).

The rate of work done by the pump on the raw water, at the presence of an ERD, is given by:

$$\dot{W}_{pump} = \Delta P \times (Q_f - \eta Q_b) \tag{3.34}$$

where $\Delta P Q_b$ is the maximum energy one can recover from the brine stream, $\Delta P = P_f - P_p$, Q_b is the brine flow rate, and η_p is the energy recovery efficiency of the ERD that refers to the ability of the ERD to recover pressure energy from the brine stream. Thus, the specific energy consumption for RO desalting, in the presence of an ERD, $SEC^{ERD}(Y, \Delta P, \eta)$, is given by:

$$SEC^{ERD}(Y, \Delta P, \eta) = \frac{\Delta P(Q_f - \eta Q_b)}{Q_p} = \frac{\Delta P(1 - \eta(1 - Y))}{Y} \tag{3.35}$$

The thermodynamic restriction for the single-stage RO process, in which an ERD is used, can be obtained by substituting Eq. (3.12) to Eq. (3.35). Accordingly, the normalized SEC for this configuration (Figure 3-14), $SEC_{tr,norm}^{ERD}$, is given by:

$$SEC_{tr,norm}^{ERD} = \frac{SEC_{tr}^{ERD}}{\pi_0} = \frac{(1-\eta(1-Y))}{Y(1-Y)} \tag{3.36}$$

Eq. (3.36) represents the equilibrium state for the exit brine stream (i.e., at the exit of the membrane module), which yields the minimum energy cost that can be achieved for a given recovery when using an ERD.
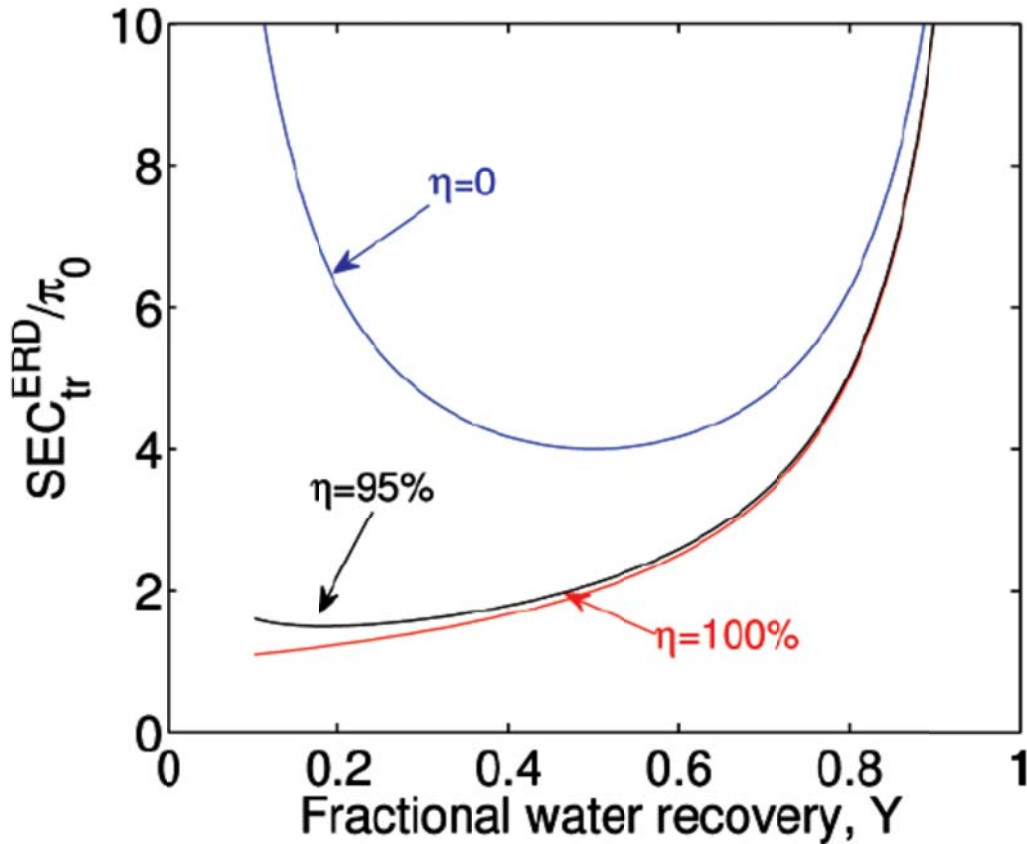
Figure 3-15. Variation of the normalized SEC with fractional product water recovery using an ERD in a single-stage RO (note: η represents the ERD efficiency).

The global minimum SEC (i.e., based on Eq. (3.36)), with respect to recovery, can be derived by setting $(\partial(SEC_{tr,norm}^{ERD}))/(\partial Y)=0$ and solving to obtain $Y_{opt}=\dfrac{\sqrt{1-\eta\,p}}{1+\sqrt{1-\eta\,p}}$

$Y_{opt}=\dfrac{\sqrt{1-\eta}}{1+\sqrt{1-\eta}}$ and $(SEC_{tr,norm}^{ERD})_{min}=(1+\sqrt{1-\eta})^2$. Clearly, as the fractional ERD efficiency (i.e., η) increases, Y_{opt} decreases (Figure 3-15), suggesting that with increased ERD efficiency, a lower water recovery operation would be most optimal to minimizing the SEC. Indeed, it is known in the practice of RO desalting that, a higher benefit of energy recovery is attained when operating at lower recoveries. Comparison with the case of a single-stage RO without an ERD (Figure 3-2) reveals that the presence of an ERD shifts the optimal water recovery (for attaining a minimum SEC) to lower than 50%.

3.6. Summary

The wide application of low pressure membrane modules, owing to the development of high permeability RO membranes, has enabled the applied pressure in RO processes to approach the osmotic pressure limit. Therefore, it is possible to optimize RO membrane processes with respect to product water recovery, with the goal of minimizing energy consumption, while considering constraints imposed by the thermodynamic cross-flow restriction and feed or permeate flow rate. In this chapter, an approach was presented for optimization of product water recovery in RO membrane desalination when highly permeable membranes are utilized was presented via a number of simple RO process models. The current results suggest that it is indeed feasible to

refine RO desalting so as to target the operation toward the condition of minimum energy consumption, while considering the constraint imposed by the osmotic pressure as specified by the thermodynamic cross-flow restriction. The impact of energy recovery devices, membrane permeability, brine management cost, pump efficiency, and frictional pressure drop can all be considered using the proposed approach as shown in a series of illustrations. Overall, as process costs above energy costs are added, the operational point for achieving minimum energy consumption shifts to higher recoveries.

Chapter 4   Research needs identification of RO optimization

4.1.   Overview

Reverse osmosis (RO) membrane desalination is now a mature process for the production of potable water from seawater and inland brackish water. Current generation RO membranes are of sufficiently high permeability to enable desalting at low pressures such that the operational feed pressures can now approach the thermodynamic osmotic pressure (**Figure 4-1**) of the produced concentrate (i.e., brine) stream [23]. In other words, it is technically feasible to operate the RO process up to the limit of the thermodynamic restriction [38]. It is noted that with the early low permeability membranes, the applied feed pressure had to be set at a significantly higher level relative to the osmotic pressure in order to achieve a reasonable permeate flux. In contrast, current high permeability membranes enable equivalent or higher permeate productivity at lower pressures, but with the achievable product water recovery now being limited by the concentrate osmotic pressure.
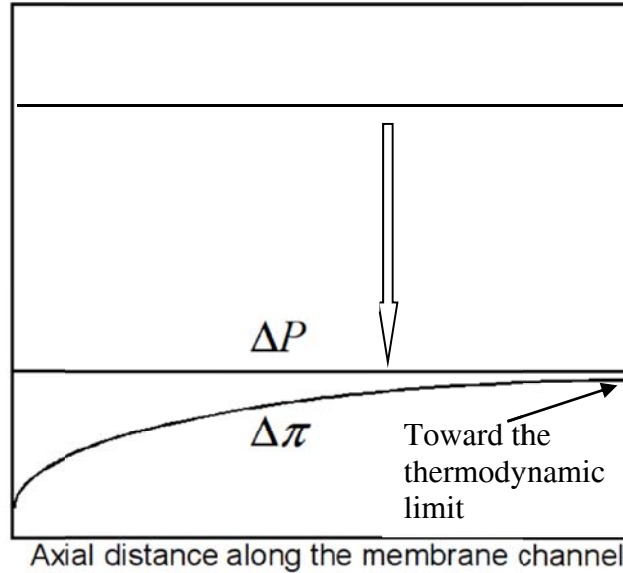
Figure 4-1. **Schematic illustration of the relationship between imposed feed pressure and feed-side osmotic pressure for low and high permeability RO membranes.**

Given that, with the present generation of high permeability RO membranes, it is feasible to operate the RO process over a wide range of practical water recoveries to the limit of the thermodynamic restriction as detailed in Chapter 2 Section 2.3, an important question arises as to the merit of developing membranes with yet higher permeability than currently available. RO desalting operation at lower pressures would result in lower energy consumption for a given product water recovery. The energy cost is the product of the feed flow rate and the applied feed pressure [38]. Therefore, to the extent that a given assembly of high permeability membranes can provide with the targeted overall permeate flow for a given feed flow rate (i.e., same recovery for a given feed flow rate), the energy cost would be independent of the type of membrane used in the process. Of course, this statement would hold provided that, irrespective of the selected membrane, the RO process can be operated up to the limit of the thermodynamic restriction.

However, the required membrane area, for a given feed flow rate at a selected target recovery, would decrease with increasing membrane permeability. Therefore, one would argue that once the capability for operating at the thermodynamic limit has been closely approached the benefit of higher permeability membranes is to lower the membrane cost for the process (typically <10% of the overall water production cost relative to >30% for energy cost [47]).

Given the emerging significance of RO desalination for generating new potable water resources, the present work addresses the question of the benefit of improving RO membrane permeability with respect to the cost of energy and the required membrane area for achieving a targeted product water recovery for a given feed. The analysis approach considers the implication of the thermodynamic restriction following Chapter 3.

4.2. Modeling and results

In order to illustrate the relative costs of required RO energy and membrane area, the simple example of a single-stage RO desalting is considered (**Figure 4-2**). Previous studies [43]have shown that, in order to ensure permeate productivity along the entire membrane module, the lower bound (or imposed thermodynamic limit) on the applied pressure $\Delta P \, (= P_f - P_0$, where P_f and P_0 being the water pressures at the entrance to the membrane module and raw feed water at the source, respectively) is the osmotic pressure difference between the retentate exit (brine) and permeate stream as expressed by the following "thermodynamic" restriction

66

$$\Delta P \geq \Delta \pi_{exit} = \frac{\pi_0 R}{1 - Y} \qquad (4.1)$$

in which the target recovery is $Y (= Q_p / Q_f$, where Q_p and Q_f are the permeate and feed flow rates, respectively) and R is the fractional salt rejection. It is noted that for desalting operation at the thermodynamic limit (i.e., $\Delta P = \Delta \pi_{exit}$) the exit osmotic pressure of the bulk solution is the same as at the membrane surface. The above can be rationalized by considering the simple film model for the concentration polarization modulus [154], $CP = C_m / C_b = \exp(J / k)$, where C_m and C_b are the salt concentrations at the membrane surface and the bulk, respectively, J is the permeate flux and k is the feed-side mass transfer coefficient. The above relations imply that the permeate flux will vanish as the thermodynamic restriction limit is reached at the membrane channel exit where CP=1 and thus C_m=C_b.
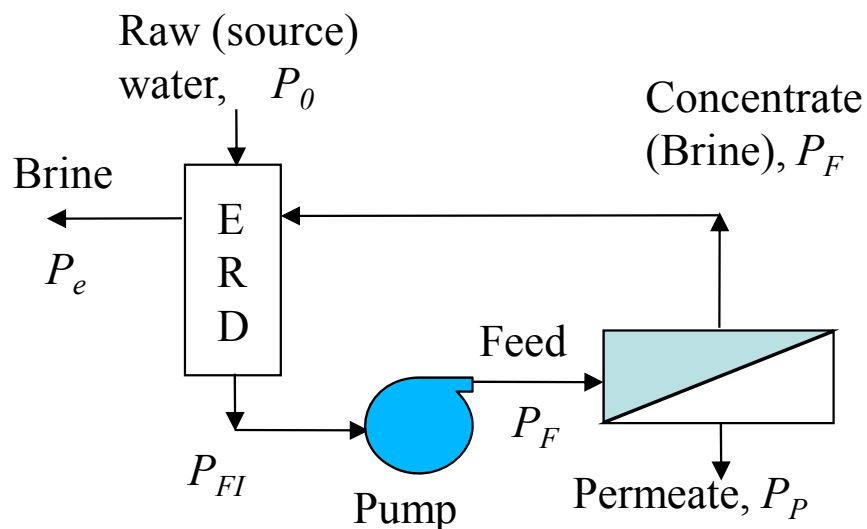
Figure 4-2. **Simplified schematic of RO system with an energy recovery device (ERD).**

4.2.2. Energy consumption for RO operation at the thermodynamic limit

As shown recently [43], the specific energy consumption (*SEC*), normalized with respect to the feed osmotic pressure ($SEC_{norm} = SEC / \pi_o$), is equal to or greater than the normalized energy consumption (SEC_{tr}^{norm}) for operation at the thermodynamic limit,

$$SEC_{tr}^{norm} = \frac{SEC_{tr}}{\pi_0} = \frac{\left(1 - \eta_E \left(1 - Y\right)\right) R}{\eta_p Y \left(1 - Y\right)} \tag{4.2}$$

where η_P is the pump efficiency, η_E is the efficiency of the energy recovery device (ERD), $\dot{W}_{pump}$ is the rate of pump work (i.e., $\dot{W}_{pump} = \Delta P \times (Q_f - \eta_E Q_b) / \eta_p$, where η_p is the pump efficiency and Q_b is the brine stream flow rate).

For operation at the thermodynamic limit $SEC_{norm} = SEC_{tr}^{norm}$, and the SEC_{tr}^{norm} (i.e., Eq. 4.2) increases with product water recovery as illustrated in **Figure 4-3** (the inset graph), for a target salt rejection of 99% and ideal pump and ERD (i.e., $\eta_p = \eta_E = 1$), with a more rapid rise in energy consumption as the recovery level surpasses about 60%. It is noted that the rate of pump work is dependent on the imposed pressure, pump and energy recovery efficiencies, feed flow rate, and for a given permeate product recovery it is independent of the membrane permeability. Also, the normalized energy consumption, SEC_{tr}^{norm} , is independent of the membrane hydraulic permeability when operating at the limit of the thermodynamic restriction (Eq. 4.2). In other words, if the membrane permeability is such that it enables operation, at the desired product water recovery, such that osmotic pressure of the exit brine stream approaches the feed-side pressure, using a

more permeable membrane would not reduce the required energy for desalting but may

have an impact on membrane and other operational costs as discussed in the next section.
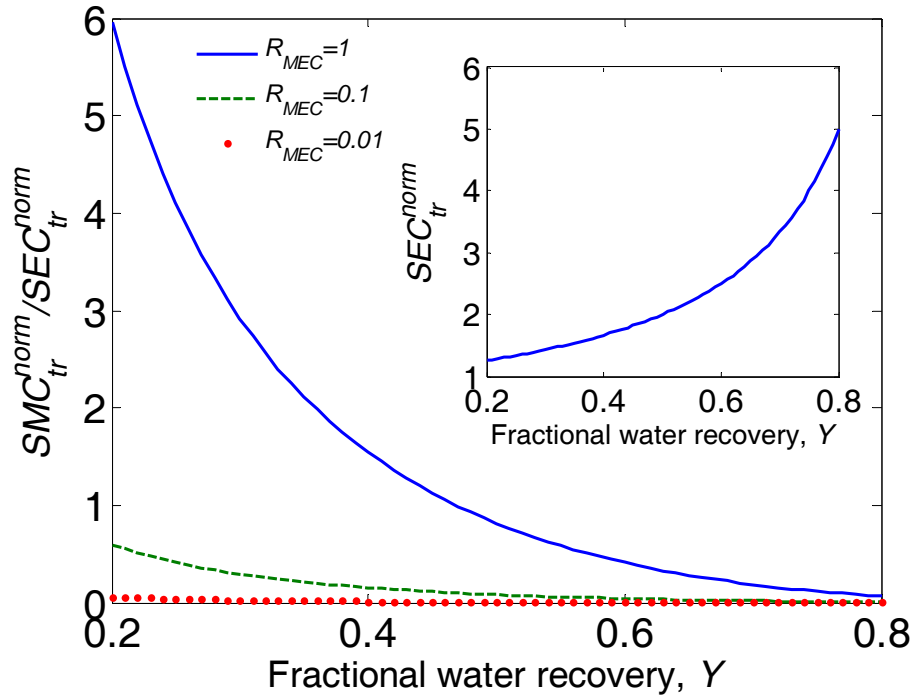
Figure 4-3. **Variation of the ratio of specific membrane (SMC_{tr}^{norm}) to specific energy (SEC_{tr}^{norm}) costs for operation up to the limit of thermodynamic restriction with respect to target water recovery. The inset graph is for the normalized specific energy consumption (SEC_{tr}^{norm}) for RO operation up to the limit imposed by the thermodynamic restriction.**

4.2.3. Specific membrane cost (SMC) for RO operation at the thermodynamic limit

In order to assess the water production membrane cost (i.e., amortized membrane cost per

produced permeate or hereinafter referred to as the "specific membrane cost") for a given

desalting process, it is convenient to compare the membrane and energy costs on the

same basis of energy units (i.e., $Pa \cdot m^3$). This conversion can be achieved [38], given an

energy price, e.g., $\varepsilon(\$/kWh)$ and the conversion factor of $\beta(Pa \cdot m^3 / kWh)$.

Accordingly, for a single-stage RO process, it was recently shown that the specific membrane cost in terms of energy units (SMC) is given by [38]:

$$SMC = \frac{m \times A_m}{Q_p} = \frac{m}{Q_p} \left[\frac{Q_p}{L_p \left(\Delta P - \sigma \overline{\Delta \pi} \right)} \right] \tag{4.3}$$

where m is the amortized membrane price in equivalent energy units per unit area, $m = m_A \beta / \varepsilon$, in which, for example, m is in units of $Pa \cdot m^3 / m^2 \cdot h$, where m_A is the amortized membrane unit price, $\$ / m^2 \cdot h$. As shown in Chapter 3, the specific membrane cost for RO desalting operation up to the thermodynamic limit (designated as SMC_{tr}), i.e. where $\Delta P = \Delta \pi_{exit}$, normalized with respect to the feed osmotic pressure SMC_{tr} / π_o is given by:

$$SMC_{tr}^{norm} = \frac{m}{R L_p \pi_0^2 \left[\frac{1}{1-Y} - \frac{1}{Y} ln \left(\frac{1}{1-Y} \right) \right]} \tag{4.4}$$

as derived from Eq. (4.3) making use of the log-mean average for the osmotic pressure ($\overline{\Delta \pi} = \pi_o R \ln\left(1 / \left(1 - Y \right) \right) / Y$). It is noted that for operation at the thermodynamic limit ΔP is just $\pi_o R / (1 - Y)$ and thus it can be shown that the SMC (Eq. 4.3) is inversely proportional to π_o and thus $SMC_{tr}^{norm} \propto (1 / \pi_o^2)$. Equation (4.4) indicates that, for the same product water recovery, the normalized specific membrane cost (SMC_{tr}^{norm}) will decrease with increasing membrane hydraulic permeability, salt rejection and feed osmotic pressure. The use of a more permeable membrane would reduce the required membrane

70

area (**Figure 4-4**) as well as the required size or number of pressure vessels. One could also argue that the cost of membrane cleaning and replacement would be reduced. However, operation at a higher permeate flux could result in greater degree of fouling which could counteract the above gain.
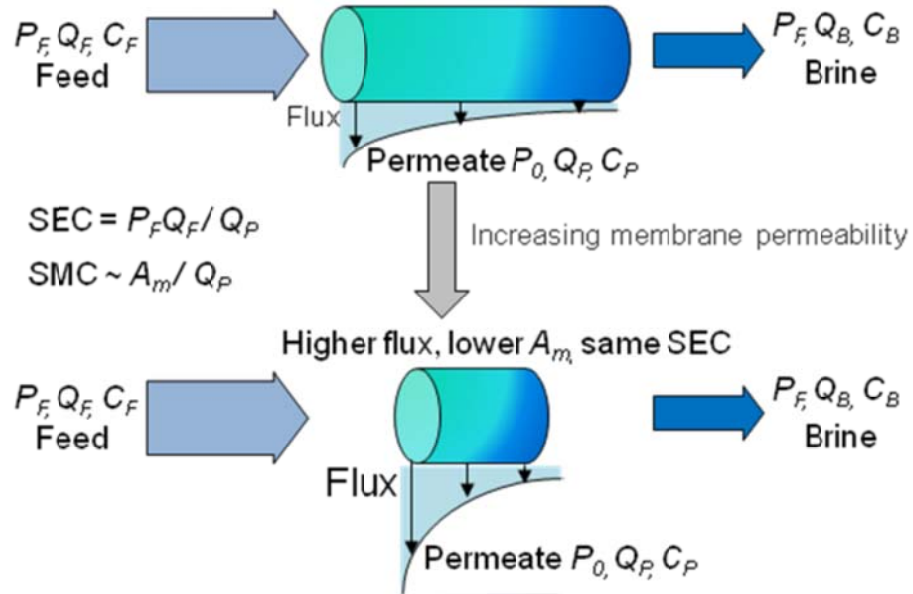
Figure 4-4. **Illustration of the effect of membrane permeability on the SEC and SMC for RO process operation at the thermodynamic limit.**

It is noted that the required membrane surface area (A_m), and hence the membrane cost (Eq. 3), for a given permeate productivity, is related to the average net driving pressure, NDP ($= \Delta P - \sigma \overline{\Delta \pi}$) whereby $A_m \propto Q_p / NDP$. The consequence of this dependence can be illustrated via the simple example of desalting at 50% recovery. For example, desalting sea water with feed osmotic pressure of 2533 kPa (25 atm) (~35,000 mg/L TDS) at water recovery of 50% would lead to a brine exit osmotic pressure of 5066 kPa (50 atm). Therefore, the average net driving pressure, NDP ($= \Delta P - \sigma \overline{\Delta \pi}$) for the

permeate flux would be 1554 kPa (15.3 atm) (assuming $\sigma = 1$). In comparison, desalting of brackish water of 3,500 mg/L TDS (osmotic pressure of 253.3 kPa (2.5 atm) at water recovery of 50% would result in an exit brine osmotic pressure of 506.6 kPa (5 atm) and thus an average NDP of 155.4 kPa (1.53 atm). Therefore, for the same water recovery a higher average NDP is obtained for the higher osmotic pressure feed, as long as the operation is up to the limit imposed by the thermodynamic restriction, and thus a lower membrane area is required for seawater desalting relative to brackish water at the same recovery level. The above may appear counterintuitive but it is a consequence of operating at the limit of the thermodynamic restriction.

4.2.4. Membrane cost relative to energy cost for RO operation at the limit of the thermodynamic restriction and its implication on the future research needs of RO desalination

The specific membrane cost relative to the specific energy consumption, for operation at the limit for the thermodynamic restriction is obtained by dividing Eq. 4.2 by Eq. 4.4:

$$MER = \frac{SMC_{tr}^{norm}}{SEC_{tr}^{norm}} = \frac{R_{EMC}\eta_p Y(1-Y)}{\left[\left(\frac{1}{1-Y} - \frac{1}{Y}ln\left(\frac{1}{1-Y}\right)\right)\left(1-\eta_E(1-Y)\right)\right]} \qquad (4.5)$$

in which R_{MEC} is a dimensionless cost factor defined as:

$$R_{MEC} = \frac{\beta m_A}{\varepsilon L_p (R\pi_0)^2} \qquad (4.6)$$

Equation (4.5) indicates that, for a given water recovery, the *MER* ratio increases with R_{MEC}. This lumped factor R_{MEC} reflects the impact of feed water osmotic pressure, salt

rejection requirement and purchase price of electrical energy, membrane module on the relative contribution of the membrane cost over the energy cost in the total water production cost. It is especially striking that this dimensionless factor is inversely proportional to the square of the feed osmotic pressure, due to the fact that energy cost and membrane cost are proportional (Eq. 4.2) and inversely proportional (Eq. 4.3) to the feed osmotic pressure, respectively. As a consequence of this dimensionless factor, the contribution of energy cost in the total water production cost will increase dramatically as feed water osmotic pressure increase as shown in the following paragraph. A reasonable quantitative assessment of the relative membrane to energy cost can be provided by considering the magnitude range of the factor R_{MEC}. For the purpose of the present analysis the estimated membrane price per unit area (m), of current low pressure RO membranes (i.e., $L_p = 0.39 - 2.2 \times 10^{-11} m^3 / m^2 \cdot s \cdot Pa$) is taken to be in the range of $10 - 20 \ \$/m^2$ [155] (thus $m_A = 0.63 - 1.3 \times 10^{-7} \ \$/m^2 \cdot s$, assuming membrane life of five years, and the U.S. electrical energy price is estimated in the range of $0.05 - 0.2 \ \$/kWh$. It is noted that with improvements in membrane technology, future membrane costs will be likely to be lower compared to current prices. Finally, the range of water salinity of typical interest is about $1,000 - 45,000 mg/L$ TDS (equivalent to osmotic pressure range of 72.4-3257 kPa). For the above range of parameters, the R_{MEC} ranges from ~0.001-1. For example, for seawater of ~ 35,000 mg/L TDS and for brackish water of 1000 mg/L TDS, R_{MEC} would range from about 0.01 to 1, respectively.

The dependence of the ratio (MER) of membrane to energy cost (in equivalent energy units) on product water recovery is illustrated in **Figure 4-3**, for different values of the dimensionless R_{MEC} number, for the case of ideal pump and ERD (i.e., $\eta_p = \eta_E = 1$). As expected, the membrane cost decreases relative to the energy cost with increased product water recovery and decreasing R_{MEC}. As an example, for R_{MEC}=0.04 (e.g., achieved for desalination of 35,000 mg/L TDS seawater with the Dow FilmTec SW30XLE-400i, $L_p = 0.39 \times 10^{-11} m^3 / m^2 \cdot s \cdot Pa$), the ratio of the specific membrane cost (SMC_{tr}) to the specific energy consumption (SEC_{tr}), for water recovery of ~30-50%, is in the range of 3~12%. For seawater desalination, the percentage of the energy cost (%EC) is usually ~40%-50% of the total water production cost [47]. For the above range, the contribution of specific membrane cost to the total water production cost, which can be estimated as the product of the above two factors (i.e., %EC x SMC_{tr}/ SEC_{tr}), is about 1.2%-6% of the total water production cost, which is within the range of membrane cost reported in the literature. This suggests that the maximum benefit one may expect from improving the membrane permeability is a decrease of the total water production cost by about the same percentage. It is noted, for example, that doubling of the membrane permeability will decrease the specific membrane cost (see Eq. 4.4) by half, and thus will decrease the total water production cost by ~0.6% - 3%. It is also acknowledged that the capital cost of pressure vessels is directly impacted by the membrane area (e.g., lower membrane area may require reduced number or size of pressure vessels). For the above range of membrane cost contribution to the total water production cost, inclusion of pressure vessels cost (amortized over 30 years; [155, 156] would result in a reduction of the total

water production cost by ~ 0.7% - 3.5%. Admittedly, despite the above modest percentage in water production savings, the absolute dollar savings may be significant for large RO plants. The decision of whether the above is achievable will depend on whether it will be possible to operate the RO process at a higher flux while avoiding the bio-fouling and mineral scaling problems that remain as obstacles to high flux RO operation. For desalination of mildly brackish water of ~ 3500 mg/L TDS, R_{MEC}=1 and the MER ranges from 6 to 0.07 as the water recovery increases from 20% to 80%, respectively. This behavior implies that at low water recovery, the use of higher permeability membranes will be beneficial in reducing the overall water production since the specific membrane cost is higher than the specific energy consumption. Indeed, it has been reported that membrane cost is an important factor for brackish water desalination [47] at moderate recoveries ($\lesssim 60\%$). However, for inland water desalting, feed pretreatment and brine management costs will both increase with decreasing water recovery, thus reducing the economic incentive for operating at low water recoveries. On the other hand, as product water recovery is increased the specific energy cost will rise while the SMC will decrease, thus providing diminished economic incentive for developing more permeable membranes for brackish water desalting at high recovery. While the above discussion focused on the use of ideal feed pump and ERD, it is important to state that operation with non-ideal pump and ERD (i.e., $\eta_p < 1$ and $\eta_E < 1$) will lower the MER (Eq. 4.5) and thus the present conclusions are valid for the entire range of pump and ERD efficiencies.

It should be recognized that the development of low pressure (high permeability) RO membranes has progressed rapidly starting in about the 1990's. The earlier higher pressure membranes were of lower permeability and thus the operating feed-pressures were typically much higher than the brine osmotic pressure at the targeted recovery and thus operation at the thermodynamic limit was not practical. The current generation of RO membranes are already of permeability levels that are sufficient (or nearly so) to enable operation approaching the thermodynamic restriction limit, while providing the practically desired permeate flux. Therefore, it is reasonable to conclude that significant reduction in the cost of RO water desalination is less likely to arise from the development of significantly more permeable membranes, but is more likely to arise from effective and lower cost of feed pretreatment and brine management, development of fouling and scale resistant membranes, optimization of process configuration and control schemes (e.g., to account for variability of feed salinity [44] and even temporal fluctuation of electrical energy costs), as well as utilization of low cost renewable energy sources.

4.3. Conclusions and recommendations for future research needs

A simple analysis of the specific membrane cost to specific energy cost, for RO desalination, was carried out to assess the range of water recovery over which improvements in membrane permeability would be beneficial to reducing RO water production cost. With the current generation of high permeability RO membranes it is now feasible to operate the RO desalting process up to the limit imposed by the

thermodynamic restriction. Therefore, as illustrated in the present analysis, given the present day electrical energy and membrane prices, there may be a benefit in developing membranes of even greater permeability at low water recoveries for inland brackish water desalting. However, at low water recovery there are typically an added costs associated with feed pretreatment and brine management for inland water desalting. On the other hand, for seawater RO desalting the energy cost is much higher than membrane cost (compared at equivalent energy units), and thus there is little economic incentive for developing higher permeability membranes if the objective is to lower the cost of seawater desalination. The ratio of membrane to energy costs is dependent on the water recovery level and a dimensionless cost factor (R_{MEC}) that includes the impact of feed water salinity, membrane permeability, salt rejection requirement and purchase costs of electrical energy and membrane area. The present analysis suggests that further significant improvements in RO membrane permeability are less likely to be the major driver to achieving further significant reduction in the cost of RO desalting. Future reduction in RO water production cost can arise from a variety of other process improvements including, but not limited to improved fouling-resistant membranes [157-160], lower cost of feed pretreatment and brine management, advanced control schemes, process optimization, as well as low cost renewable energy sources.

Chapter 5   Two-stage RO Optimization

5.1.   Overview

Simplified process models to optimize the structure of RO membrane desalination plants have been proposed in the literature [90, 120, 125, 126, 129, 144-146]. The "Christmas tree" configuration developed in the early 1970's was used for the early generation of RO spiral-wound membranes. However, with the emergence of higher permeability membranes, it is unclear if the above configuration of membrane modules is also optimal for ultra-low pressure RO modules [120]. It has been argued that the SEC can be lowered by utilizing a large number of RO membrane units in parallel so as to keep the flow and operating pressure low [145]. It has also been claimed that the SEC decreases upon increasing the number of membrane elements in a vessel [29]. In the mid 1990's researchers have suggested that a single-stage RO process would be more energy efficient [147]. However, it has been also claimed that a two-stage RO was more energy efficient than single-stage RO [145]. The above conflicting views suggest that there is a need to carefully compare the energy efficiency of RO desalination by appropriately comparing single and multi-stage RO processes on the basis of appropriately normalized feed flow rate and SEC taking into consideration the feed osmotic pressure, membrane permeability and membrane area. Motivated by the above considerations the problem of RO energy cost optimization is revisited when highly permeable membranes are used, via

a simple mathematical formalism, with respect to the energy efficiency of a two-stage RO relative to one-stage RO and its drawback in terms of extra membrane area requirement.

5.2. Two-stage RO optimization and comparison with single-stage RO

5.2.1. Specific energy consumption for a two-stage RO

The approach discussed previously for a single-stage RO in the previous chapter can be easily extended for multiple stage RO operation. An illustration of the approach is provided here for the simple two-stage RO configuration shown in Figure 5-1 where the overall product water recovery, Y, is the result of RO desalting at recoveries of Y_1 and Y_2 in the first and second RO stages, respectively.
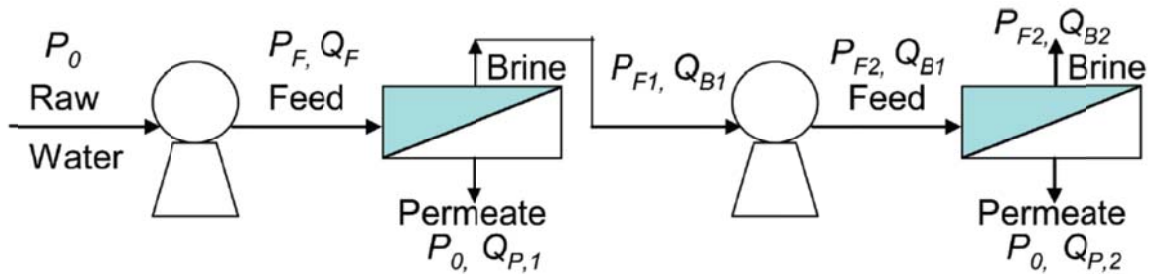
Figure 5-1. **Schematic of a simplified two-stage RO system. (Note: the inter-stage pump is optional and needed when the pressure to the second stage cannot be met using a single feed pump).**

The analysis of the above system is first presented assuming the efficiency of the feed and interstage to be 100% with the effect of pump efficiency considered in Section 9.4Also, it is noted that based on a simple mass balance, one can derive the following relationship between the overall and the individual stage recoveries:

$$Y = Y_1 + (1 - Y_1)Y_2 = Y_1 + Y_2 - Y_1Y_2 \tag{5.1}$$

The rate of work done by the first stage pump, $\dot{W}_{tr}^{1st}$, at the limit of thermodynamic restriction, is $\dot{W}_{tr}^{1st}$ given by:

$$\dot{W}_{tr}^{1st} = \frac{\pi_0}{1-Y_1}Q_f \tag{5.2}$$

Similarly, the rate of work done by the second stage pump at the limit of thermodynamic restriction, $\dot{W}_{tr}^{2nd}$, is given by:

$$\dot{W}_{tr}^{2nd} = (\frac{\pi_0}{1-Y} - \frac{\pi_0}{1-Y_1})Q_f(1-Y_1) \tag{5.3}$$

where the two terms in the first bracket show the difference between the first-stage brine pressure and second-stage feed pressure. In writing Eq. (5.3) it is assumed that the pressure of the brine stream from the first stage is fully available for use in the second RO stage. The normalized SEC of this two-stage RO process at the limit of thermodynamic restriction, ($SEC_{tr,norm}(2ROs)$), at a total water recovery Y is given by:

$$SEC_{tr,norm}(2ROs) = \frac{\dot{W}_{tr}^{1st} + \dot{W}_{tr}^{2nd}}{YQ_f\pi_0} = \frac{1}{Y}(\frac{1}{1-Y_1} + \frac{1-Y_1}{1-Y} - 1) \tag{5.4}$$

The difference of the normalized specific energy consumption between the two-stage and one-stage RO (*1RO*), at the limit of thermodynamic restriction (i.e., when the applied pressure is equal to the exit osmotic pressure difference) is given by:

$$SEC_{tr,norm}(2ROs) - SEC_{tr,norm}(1RO) = \frac{Y_1(Y_1 - Y)}{Y(1-Y_1)(1-Y)} < 0 \tag{5.5}$$

Eq. (5.5) implies that at the same overall water recovery, under the above stated assumptions (the pressure of the brine stream from the first stage is fully available for use in the second RO stage), the two-stage RO process will require less energy than a single-

stage RO process. The fractional energy cost savings, f_{ES}, for the two-stage relative to

the one-stage RO process is given by:

$$f_{ES} = \frac{SEC_{tr,norm}(1RO) - SEC_{tr,norm}(2ROs)}{SEC_{tr,norm}(1RO)} = \frac{Y_1(Y - Y_1)}{(1 - Y_1)} \qquad (5.6)$$

The optimal fractional energy savings depends on both the overall and stage product

water recoveries as depicted by plotting Eq. (5.6) in Figure 5-2.
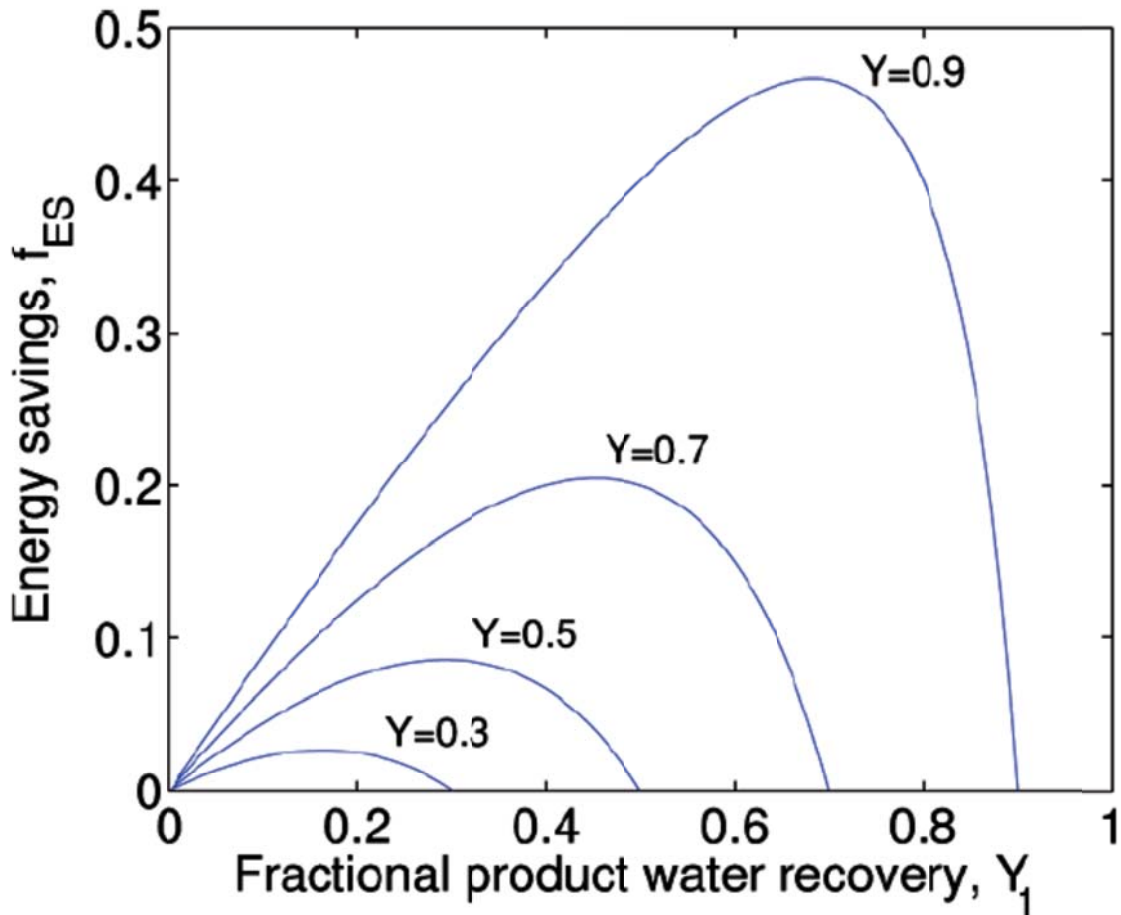
Figure 5-2. **Fractional energy savings achieved when using a two-stage relative to a single-stage RO process. (Note: Y is the total water recovery and Y_1 is the water recovery in the first-stage RO.).**

81

For a given target overall product water recovery, the maximum energy savings (or global minimum for energy consumption) for the two-stage RO relative to single-stage RO process), with respect to product water recovery in the first stage, can be obtained by setting $\partial f_{ES} / \partial Y_1 = 0$ and solving to obtain the optimal first stage recovery, $Y_{1,opt}$,

$$Y_{1,opt} = 1 - \sqrt{1-Y} \qquad (5.7)$$

with the corresponding optimal water recovery for the second stage RO system obtained from the combination of Eqs. (5.1) and (5.7):

$$Y_2 = \frac{Y - Y_{1,opt}}{1 - Y_{1,opt}} = \frac{Y - 1 + \sqrt{1-Y}}{\sqrt{1-Y}} = 1 - \sqrt{1-Y} = Y_{1,opt} \qquad (5.8)$$

The above results indicate that, for a two-stage RO system, operation of each stage at the same inherent water recovery level is the optimal strategy for reducing the SEC. Accordingly, the maximum fractional energy savings, when adopting a two-stage RO process relative to a single-stage RO process (at a given total water recovery), is obtained from Eqs. (5.6) and (5.7):

$$(f_{ES})_{max} = (1 - \sqrt{1-Y})^2 \qquad (5.9)$$

As expected, Eq. (5.9) predicts that the fractional energy savings increases with total water recovery.

The above analysis for the two-stage RO process can be repeated by adding stages in series to further reduce the energy consumption. It should be recognized, however, that in the limit of an infinite number of stages, all of equal water recovery, a reversible thermodynamic process is approached, at which the lowest possible energy consumption is achieved, albeit the flux would also vanish as a consequence of the diminishing net

pressure driving force. This optimum water recovery distribution is independent on whether or not an energy recovery device (ERD) is deployed and the ERD efficiency if it were to be deployed. This behavior is because the deployment of ERDs will decrease the SEC of both systems by the same absolute value.

5.2.2. Membrane area for a two-stage RO process optimized with respect to energy consumption

The two-stage RO process is more energy efficient relative to a single-stage RO process. However, one must consider the membrane area requirement when operating with two-stages. Considering a two-stage RO process, each stage utilizing membrane of the same permeability, the membrane areas of the first RO stage ($A_{mem,1}$) and the second RO stage ($A_{mem,2}$) are given by,

$$A_{mem,1} = \frac{Q_{p,1}}{L_p \pi_{0,1} [\frac{1}{1-Y_1} - \frac{1}{Y_1} ln(\frac{1}{1-Y_1})]} \tag{5.10}$$

$$A_{mem,2} = \frac{Q_{p,2}}{L_p \pi_{0,2} [\frac{1}{1-Y_2} - \frac{1}{Y_2} ln(\frac{1}{1-Y_2})]} \tag{5.11}$$

where $Q_{p,1}$ and $Q_{p,2}$ are the permeate flow rate for the first and second RO stages, respectively, and $\pi_{0,1}$ and $\pi_{0,2}$ are the corresponding feed osmotic pressure of the first and second stages. It is noted that, the osmotic pressure of the feed to the second RO stage is equal to that of the concentrate (or brine) stream from the first stage (i.e., $\pi_{0,2} = \frac{\pi_{0,1}}{1-Y_1}$). As discussed previously, the maximum energy savings is obtained when

$Y_1 = Y_2$. For this energy-optimal operating condition, the ratio of membrane area for the second stage RO relative to the first stage RO is given by:

$$\frac{A_{mem,2}}{A_{mem,1}} = (1-Y_1)\times(1-Y_2) = 1-(Y_1+Y_2-Y_1Y_2) = 1-Y \qquad (5.12)$$

where use was made of Eq. (5.1). As an example, for a two-stage RO desalting process (Figure 5-1) operating at a total recovery of 75%, each stage would be operated at water recovery of 50% (the minimum energy consumption), achieving an energy consumption savings of 25% relative to a single-stage RO (as shown in Chapter 3) operating at the same total water recovery. However, according to Eq. (5.12), the required membrane surface area for the second RO stage is one fourth that of the first RO stage (Figure 5-3).
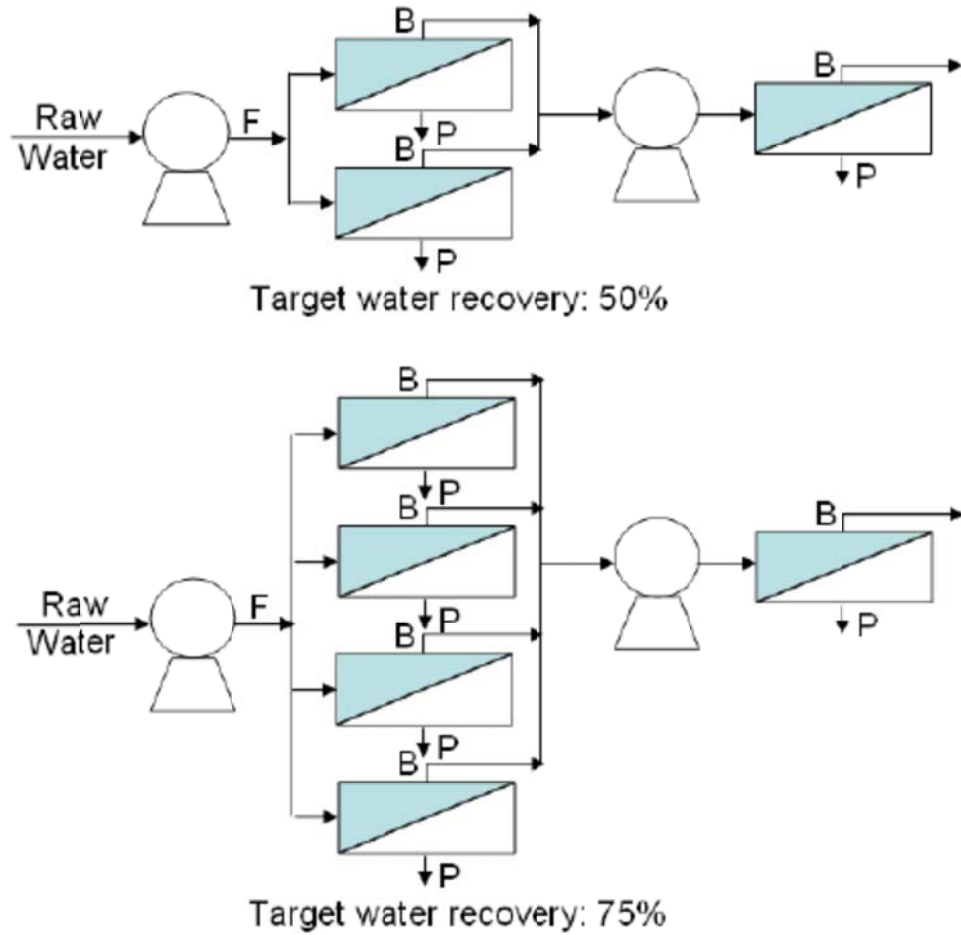
Figure 5-3. **Illustration of the membrane arrangement in a two-stage RO process for two different target water recoveries.**

The membrane area for a single-stage RO process, desalting a feed stream of the same salinity (i.e., $\pi_0 = \pi_{0,1}$) at the same overall recovery (Y) as a two-stage RO process, is given by:

$$A_{mem,SRO} = \frac{Q_{p,2} + Q_{p,1}}{L_p \pi_0 [\frac{1}{1-Y} - \frac{1}{Y} ln(\frac{1}{1-Y})]} \qquad (5.13)$$

and the fractional membrane area increase (f_{MAI}) for the two-stage RO process relative to the single-stage RO process (Eq. (5.13)), for operation at the optimal condition with respect to energy savings (i.e., when $Y_1 = Y_2$), is given by:

$$f_{MAI} = \frac{A_{mem,1} + A_{mem,2}}{A_{mem,SRO}} - 1 = \frac{(1 - \sqrt{1-Y})(2-Y)}{Y}$$

$$\times \frac{[\frac{1}{1-Y} - \frac{1}{Y}ln(\frac{1}{1-Y})]}{[\frac{1}{\sqrt{1-Y}} - \frac{1}{1-\sqrt{1-Y}}ln(\frac{1}{\sqrt{1-Y}})]} - 1$$

(5.14)

Eq. (5.14) indicates that the membrane area required for a two-stage RO process is higher, for any given overall permeate water recovery, relative to a single-stage RO (Figure 5-4) since the net transmembrane driving pressure ($\overline{NDP}$) is lower for the two-stage RO process. As the above analysis indicates, the energy savings obtained with the two-stage RO process is gained at the expense of a higher membrane surface area. Therefore, process optimization must consider the consumption of both energy and the membrane area.
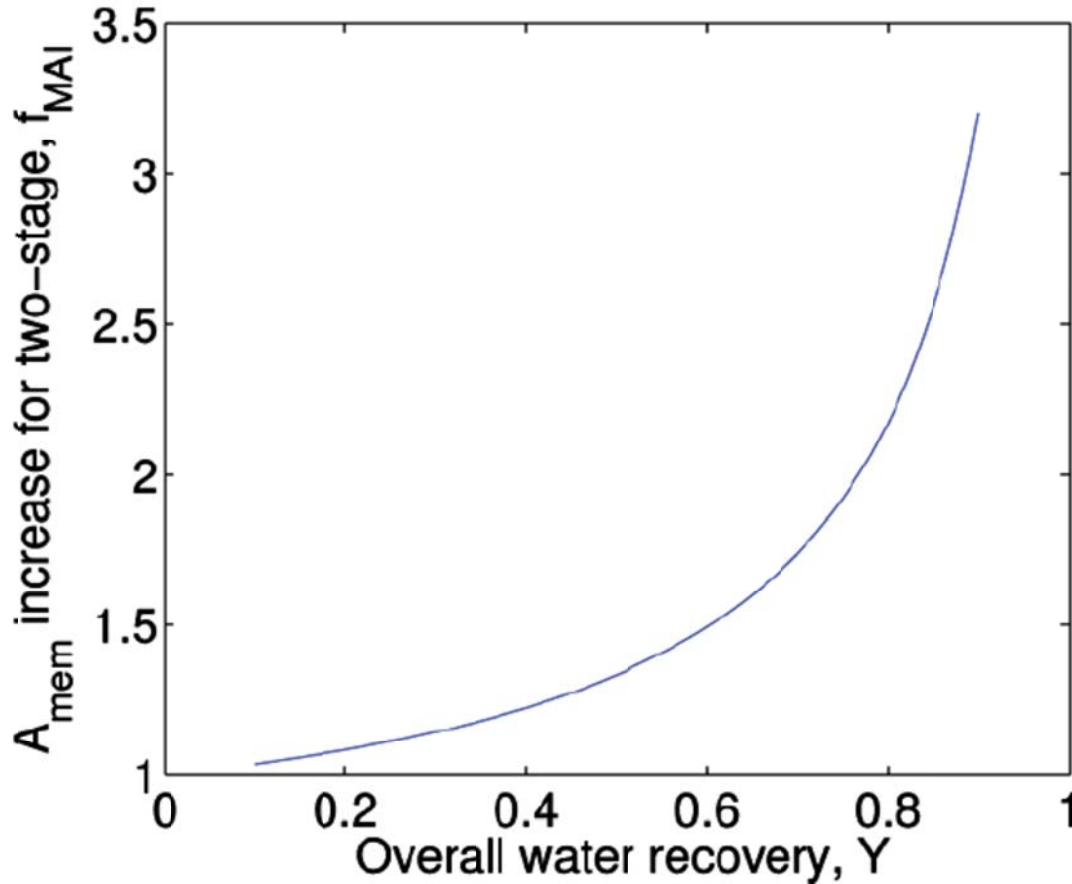
Figure 5-4. Fractional membrane area increase for a two-stage relative to a single-stage RO process (both stages of the two-stage RO and single-stage RO processes are operated at the thermodynamic limit. The two-stage RO process is operated at its minimum specific energy consumption.).

5.2.3. Overall cost optimization considering membrane and energy consumption for a two-stage versus a single-stage RO process

Optimal design of a two-stage RO process requires balancing of the energy savings and the increased membrane surface area required to achieve the target total recovery, relative to a single-stage RO process. An analysis of this tradeoff can be conveniently demonstrated for the simple special case for which the two-stage RO process will operate at its maximum energy savings, but as can be shown (using Eqs. (5.10), (5.11) and

(5.13)) this would require the greatest surface area increase relative to a single-stage RO process. It is convenient to compare the membrane and energy consumption on the same basis of energy consumption units. This conversion can be achieved, given an energy purchasing price, e.g., $\varepsilon(\$/kWh)$ and the conversion factor of $\beta(Pa \cdot m^3/kWh)$, such that, for a single-stage RO process, the specific amortized membrane expenditure per permeate produced (SMC) is given by:

$$SMC = \frac{m \times A_m}{Q_p} = \frac{m}{L_p\left(\Delta P - \frac{\pi_0}{Y} ln\left[\frac{1}{1-Y}\right]\right)} \tag{5.15}$$

where m is the amortized membrane price per unit area ($m = m_A \beta/\varepsilon$, in which, for example, m is in units of $Pa \cdot m^3/m^2 \cdot h$, where m_A is the amortized membrane unit cost, $\$/m^2 \cdot h$). At the point where the applied pressure is equal to the osmotic pressure difference at the exit region, SMC , normalized with respect to the feed osmotic pressure, can be obtained from Eq. (5.15) to yield:

$$SMC_{norm} = \frac{m}{L_p\pi_0^2\left(\frac{1}{1-Y} - \frac{1}{Y}ln\left[\frac{1}{1-Y}\right]\right)} \tag{5.16}$$

Inspection of Eq. (5.16), suggests that a convenient dimensionless membrane price, m_{norm}, which is independent of the RO operating conditions can be defined as

$m_{norm} = \frac{m}{L_p(\pi_0)^2}$.

The penalty due to the increased membrane expenditure for a two-stage relative to a single-stage RO process, P_{SMC} , at the optimal two-stage RO operation (i.e., $Y_1 = Y_2$), can be expressed as:

$$P_{SMC} = \frac{m_{norm}}{[\frac{1}{1-Y} - \frac{1}{Y}ln(\frac{1}{1-Y})]}$$
$$\times(\frac{(1-\sqrt{1-Y})(2-Y)}{Y} \times \frac{[\frac{1}{1-Y} - \frac{1}{Y}ln(\frac{1}{1-Y})]}{[\frac{1}{\sqrt{1-Y}} - \frac{1}{1-\sqrt{1-Y}}ln(\frac{1}{\sqrt{1-Y}})]} - 1)$$

(5.17)

The gain in energy savings for using a two-stage relative to a single-stage RO process, G_{SEC}, obtained from Eq. 5.9 (also for the optimal condition of $Y_1 = Y_2$) and the minimum SEC for a single-stage RO process (as shown in the Chapter 3), is given by:

$$G_{SEC} = \frac{1}{Y(1-Y)} \times (1 - \sqrt{1-Y})^2$$

(5.18)

Combining Eqs. (5.17) and (5.18), the overall cost savings for a two-stage RO process relative to a single-stage RO process, S_{ov}^{em}, considering both energy and membrane consumption, is given by:

$$S_{ov}^{em} = G_{SEC} - P_{SMC} = \frac{(1-\sqrt{1-Y})^2}{Y(1-Y)} - \frac{m_{norm}}{[\frac{1}{1-Y} - \frac{1}{Y}ln(\frac{1}{1-Y})]}$$
$$\times(\frac{(1-\sqrt{1-Y})(2-Y)}{Y} \times \frac{[\frac{1}{1-Y} - \frac{1}{Y}ln(\frac{1}{1-Y})]}{[\frac{1}{\sqrt{1-Y}} - \frac{1}{1-\sqrt{1-Y}}ln(\frac{1}{\sqrt{1-Y}})]} - 1)$$

(5.19)

In order to illustrate the overall fractional cost savings for a two-stage relative to a single-stage RO process, the estimated range of the dimensionless membrane price of m_{norm} can be derived given reasonable ranges for m_A, membrane price per unit area ($10\$/m^2$), L_p ($10^{-11} - 10^{-10} m/Pa \cdot s$) for RO membranes, osmotic pressure for salinity range of about $1,000 - 35,000 mg/L$ total dissolved solids, and current energy price range ($0.05 - 0.15\$/kWh$). ($0.05 - 0.15\$/kWh$) Assuming the membrane life of about 5 years, for seawater, given the high salinity (and thus osmotic pressure) $m_{norm} < 0.1$. Therefore,

as can be seen in Figure 5-5 and from Eq. (5.19), when the total water recovery is greater than about 30%, a two-stage RO process is more cost effective (i.e., $S_{ov}^{em} > 0$) than a single-stage RO process, even with the additional membrane expenditure for the two-stage RO process. In contrast, for brackish water of salinity in the range of $1,000-10,000 mg/L$, $m_{norm} > 1$, and thus for a water recovery of Y less than 80%, it is apparent that a single-stage RO process is more cost effective than a two-stage RO process (i.e., $S_{ov}^{em} < 0$).
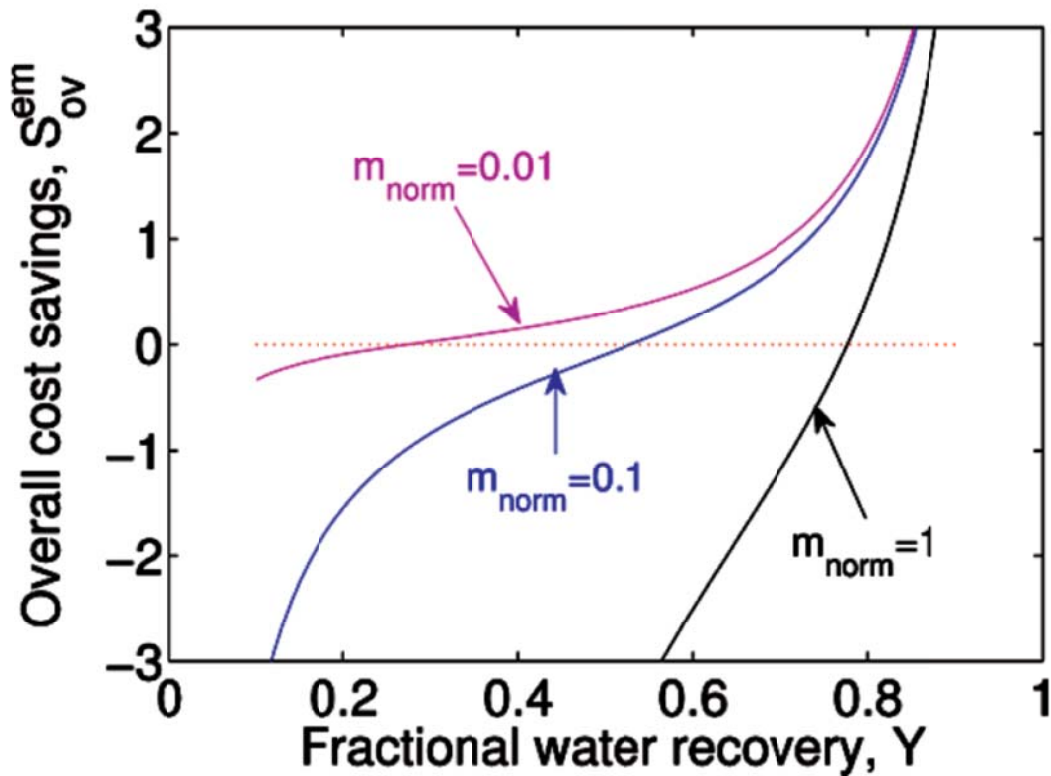
Figure 5-5. **Overall cost savings due to the adoption of two-stage RO considering both energy and membrane consumption.**

5.3. Effect of Pump efficiency on the SEC of a two-stage RO system

For the two-stage RO system shown in Figure 5-1, the rate of work by the first pump, $\dot{W}_{tr}^{1st}$, at the limit of thermodynamic restriction, is given by:

$$\dot{W}_{tr}^{1st}(\eta_{pump,1}) = \frac{\pi_0}{(1-Y_1)\eta_{pump,1}}Q_f \tag{5.20}$$

where $\eta_{pump,1}$ is the efficiency of the first pump. Similarly, the rate of work by the second pump at the limit of thermodynamic restriction, $\dot{W}_{tr}^{2nd}$, is given by:

$$\dot{W}_{tr}^{2nd}(\eta_{pump,2}) = \frac{(Y-Y_1)\pi_0}{(1-Y)\eta_{pump,2}}Q_f \tag{5.21}$$

where $\eta_{pump,2}$ is the efficiency of the second pump. Therefore, the SEC of this two-stage RO process, at the limit of thermodynamic restriction, accounting for pump efficiencies, is given by:

$$SEC_{tr}(2ROs) = \frac{\pi_0}{Y}[\frac{1}{(1-Y_1)\eta_{pump,1}} + \frac{Y_2}{(1-Y_2)\eta_{pump,2}}] \tag{5.22}$$

where $Y = Y_1 + Y_2 - Y_1 Y_2$. For this case, the optimal water recoveries in each stage are obtained by solving $\partial(SEC_{tr}(2ROs))/\partial Y_1 = 0$ at a given total water recovery Y and are given by:

$$Y_{1,opt} = 1 - \sqrt{\frac{\eta_{pump,2}}{\eta_{pump,1}}(1-Y)} \tag{5.23}$$

$$Y_{2,opt} = 1 - \sqrt{\frac{\eta_{pump,1}}{\eta_{pump,2}}(1-Y)} \tag{5.24}$$

and the corresponding normalized minimum SEC for this two-stage RO at a total water recovery Y is given by:

$$(SEC_{tr,norm}(2ROs))_{min} = \frac{1}{Y\sqrt{\eta_{pump,2}}}(\frac{2}{\sqrt{\eta_{pump,1}(1-Y)}} - \frac{1}{\sqrt{\eta_{pump,2}}}) \qquad (5.25)$$

From Eq. (5.22) we can conclude that as pump efficiencies $\eta_{pump,1}$, $\eta_{pump,2}$ increase, the SEC decreases, although the capital cost of the pump may increase with efficiency. It is important to determine which stage requires a pump of higher efficiency in order to minimize the overall SEC. For example, if the product of $\eta_{pump,1}$ and $\eta_{pump,2}$ is fixed, one can determine the optimal $\eta_{pump,2}$ by rewriting Eq. (5.25) as follows:

$$(SEC_{tr,norm}(2ROs))_{min} = \frac{1}{Y}(\frac{2}{\sqrt{\eta_{pump,1}\eta_{pump,2}(1-Y)}} - \frac{1}{\eta_{pump,2}}) \qquad (5.26)$$

which shows that as $\eta_{pump,2}$ increases, the overall SEC decreases. The conclusion is that, in a two-stage RO process, the higher efficiency pump should be used in the second-stage to minimize the overall SEC since the second-stage requires higher pressure than the first-stage. In practice, however, pump efficiency is typically higher at a higher flow rate which is the case for the first stage feed pump. Therefore, a more detailed analysis would have to consider the flow rate dependence of the pump efficiency for the specific pumps to be employed in the two-stage process.

5.4.   Conclusions

Considering the energy consumption and membrane area expenditure in the comparison of a single-stage and two-stage process: for seawater desalination $m_{norm} \sim 0.01$, a two-stage process is more cost effective than a single-stage RO process for water recoveries greater than 30%, but less cost effective for water recoveries less than 30%; while for mildly brackish water desalination $m_{norm} \sim 1$, a two-stage process would be more cost effective than a single-stage RO process for water recoveries greater than 80%, but less cost effective for water recoveries less than 80%. Clearly, if the membrane purchasing price is lower relative to the energy purchasing price, a two-stage process will be desirable for reducing the overall cost. It is important to note that the above conclusions are based on the use of a logarithmic average of the osmotic pressure in the membrane stages and also neglecting the dependence of pump flow rate and pressure delivery on pump efficiency. Considerations of the above are provided in Sections 3.4.3 and 9.4.

Chapter 6   Two-pass Optimization

6.1.   Overview

In previous chapters, the effect of the thermodynamic restriction on the optimization of the specific energy consumption (SEC) in single and multi-stage RO membrane desalting was studied following a theoretical formalism. It was shown that the optimum recovery level for attaining a minimum SEC operation, for single and multi-stage RO processes, was impacted by the deployment of energy recovery device, membrane and brine management costs. The present chapter the approach presented in Chapters 3-5 to include the effect of membrane salt rejection on the SEC and to evaluate the energy consumption and its optimization for a two-pass membrane desalination process. The two-pass membrane desalting configuration, which is a relatively new configuration for seawater desalting, has not been extensively studied [58, 148, 149] and in previous studies has been touted as an approach for reducing energy consumption in seawater desalination [161].

An earlier approach to optimizing the partial recoveries (i.e., for each pass) in a two-pass desalination process, without energy recovery for overall product water recovery in the range of 50%-70% was proposed by Noronha *et al.* [148]. The above study showed that an optimal solution, with respect to the recoveries of each pass, can be obtained via a numerical algorithm, for specific plant configuration and membranes, however, it did not provide a comparison of energy consumption relative to a single-stage

operation, but it was noted that energy consumption is higher for a two-pass process. In a later study, Cardona *et al.* [58] compared the SEC of a two-pass membrane desalination process, which they termed "double-stage", to a single-pass RO process, both without the use of an energy recovery device. Based on a specific case study using standard process model calculations based on bulk properties of the retentate stream, for a target salt rejection of 98.3% and 41.2% water recovery, it was concluded that the two-pass process has a potential for energy savings on the order of 13-15% for the specific case of less than 50% total water recovery. A recent report [149] on extensive pilot studies of a two-pass seawater NF desalination process by the Long Beach Water Department [161], suggested that the two-pass process would require about 20% less energy, when operating at 42% product water recovery, compared to a single pass RO membrane desalination process. The above two-pass NF desalination study did not report the use of energy recovery devices and did not present conclusive experimental data or theoretical reasoning for the claimed superiority of the two-pass process. Moreover, the relatively limited comparisons provided in the literature have not addressed the limitations imposed by the thermodynamic cross flow restriction on the minimum achievable specific energy consumption [38].

Previous studies on two-pass desalination have not considered the impact of energy recovery when comparing the SEC for the two-pass membrane desalting configuration relative to single or multi-stage RO process configurations. Moreover, the relatively limited comparisons provided in the literature have not addressed the limitations imposed by the thermodynamic cross flow restriction on the minimum achievable specific energy

consumption [38]. Accordingly, the current study presents a systematic comparison of the SEC optimization for a two-pass versus a single-stage membrane desalination process. The analysis considers the limits imposed by the thermodynamic cross-flow restriction, use of energy recovery devices, the constraint imposed by membrane rejection, and retentate recycling.

6.2.   Preliminary: Single-pass optimization

In order to illustrate the approach to optimizing (i.e., minimizing) energy consumption in reverse osmosis membrane desalination processes, it is instructive to first consider the simple example of a single-pass membrane desalination process (where the process is classified as RO or NF depends on the level of salt rejection [162]) without the use of an energy recovery device (ERD) as shown schematically in Figure 3-2.

6.2.1.   Optimization of the SEC for a single-pass membrane desalination at the limit of the thermodynamic restriction

In order to compare the SEC for a single-pass process versus a two-pass membrane desalting process, the SEC for a single-pass process is first presented as a function of the target recovery, with and without the use of an energy recovery device (ERD). Subsequently, SEC optimizations of a two-pass membrane process (RO or NF) with and without ERDs are presented and compared with the single-pass process (Section 6.3).

The specific energy consumption (SEC) for a single-pass RO/NF desalting process in the absence of energy recovery (Figure 3-2) is given by Eq. 3.33 with salt rejection included as follows:

$$SEC \geq \frac{\pi_0 R_t}{Y_t(1-Y_t)\eta_p} \tag{6.1}$$

where the SEC is expressed in pressure units (e.g., kPa). It is convenient to normalize the SEC at the limit of the thermodynamic restriction with respect to the feed osmotic pressure such that:

$$SEC_{tr,norm} = \frac{SEC_{tr}}{(\pi_0)} = \frac{R_t}{\eta_p Y_t(1-Y_t)} \tag{6.2}$$

An example of this dependence on the target water recovery (i.e., Eq. (6.2)) is plotted in Figure 6-1 for a target salt rejection of 99% showing that the global minimum $SEC_{tr,norm}$ increases with decreasing pump efficiency. The optimal water recovery is unaffected by pump efficiency provided that the efficiency is independent of the water recovery or generated feed pressure. The minimum $SEC_{tr,norm}$, for a specific target salt rejection, R_t, can be found by setting $\partial(SEC_{tr,norm})/\partial Y_t) = 0$ from which it can be shown that the global minimum occurs at $Y_t = 0.5$ (or 50% recovery) where $(SEC_{tr,norm})_{min} = 4R_t/\eta_p$ (or $(SEC_{tr})_{min} = 4R_t\pi_o/\eta_p$). This means that in order to operate at the global minimum SEC (whose value increases with decreasing pump efficiency), the desalting process should be operated at an applied pressure equivalent to $2R_t\pi_0$ and at 50% recovery. The operation below 50% wastes energy that is discharged in the high-pressure brine stream,

and operation above 50% recovery results in rapid increase in the brine osmotic pressure and correspondingly the required feed pressure.
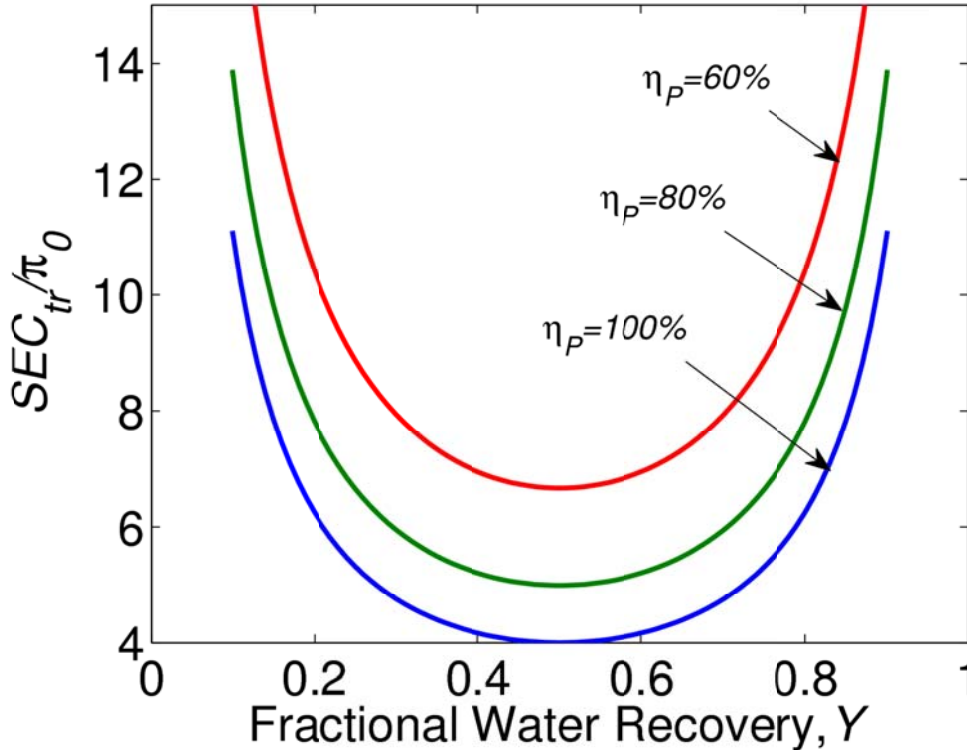
Figure 6-1. **Variation of the normalized SEC at the limit of the thermodynamic restriction with water recovery for a single-pass RO/NF at a target salt rejection of 99% without energy recovery (note:** η_p **represents the pump efficiency).**

It is instructive to illustrate the implications of the above analysis by considering the example of a single-pass seawater RO plant producing permeate of 500 mg/L total dissolved solids (TDS) from seawater feed of 35,000 mg/L TDS. Accordingly, $\pi_0 = 2,533 \ kPa$ (*or 25 atm*) and target salt rejection is $R_t = 99\%$, the global minimum energy consumption for the above case is $4R_t\pi_0 = 2.8kWh \ / \ m^3$. The average permeate

water flux, if one considers one of the available commercial RO membranes (e.g., Dow FilmTec SW30XLE-400i) with a permeability of $L_p = 0.78 \times 10^{-11} m^3 / m^2 \cdot s \cdot Pa$, at the above optimal condition, is computed from Eq. (6.16) as:

$$(FLUX)_{opt} = L_p \left[\frac{R_t \pi_0}{1 - Y_t} - R_t \pi_0 \frac{\ln[1/(1 - Y_t)]}{Y_t} \right] = 10.5 \ gallons / ft^2 \cdot day \qquad (6.3)$$

where $Y_{opt} = 0.5$, and $(\Delta P)_{opt} = 2R_t \pi_0$. It is important to note that, at the global energy-optimal operating point, the applied pressure and feed flow rate (input process variables), brine and product flow rate (output variables) are fixed for an RO plant with given A_m and L_p. It is noted that the global minimum energy consumption presented here is only for the case of single-pass process without energy recovery devices. As presented by the authors [38], the SEC can be further decreased by utilization of multi-stage configuration and energy recovery devices.

Effect of energy recovery

In order to reduce the required energy for RO/NF desalination, energy can be extracted from the high pressure concentrate (or brine) stream (Figure 3-14) using a variety of energy recovery schemes [137]. The rate of work done by the pump on the raw water, in the presence of an energy recovery device (ERD), is given by:

$$\dot{W}_{pump} = \Delta P \times (Q_f - \eta_E Q_b) \qquad (6.4)$$

where Q_b is the brine flow rates which is related to the permeate flow rate (Q_p) and product recovery (Eq. (6.4)), and η_p and η_E are the efficiencies of the feed pump and of

the energy recovery device (ERD), respectively. Thus, the specific energy cost for RO desalting, in the presence of an ERD, $SEC^{ERD}(Y, \Delta P, \eta)$, is given by:

$$SEC^{ERD}(Y, \Delta P, \eta_p, \eta_E) = \frac{\Delta P(Q_f - \eta_E Q_b)}{Q_p \eta_p} = \frac{\Delta P(1 - \eta_E(1 - Y_t))}{Y_t \eta_p} \qquad (6.5)$$

The normalized SEC for this configuration, $SEC^{ERD}_{tr,norm}$, at a given water recovery, Y_t, and salt rejection, R_t, in the limit of the thermodynamic restriction in the presence of an ERD, is obtained from Eq. (6.5) by using Eqs. (6.14) and (6.4) to yield:

$$SEC^{ERD}_{tr,norm} = \frac{(1 - \eta_E(1 - Y_t))R_t}{\eta_p Y_t(1 - Y_t)} \qquad (6.6)$$

The dependence of the normalized SEC (Eq. 6.6) on the total recovery and pump and ERD efficiencies is illustrated in Figure 6-2 for salt rejection of 99%. The deployment of an ERD shifts the optimal minimum energy location to lower recoveries. As the pump efficiency decreases the SEC increases. Note that the optimum recovery will be unaffected by the pump efficiency if it remains constant (e.g., invariant with recovery or feed pressure). However, it is apparent that with the use of an ERD, recoveries higher than 50% (i.e. the optimal recovery at the minimum SEC in the absence of an ERD) can be achieved at significantly lower specific energy cost, relative to desalting in the absence of energy recovery (i.e., $\eta_E = 0$, Eq. (6.2)), e.g., 40% and 50% lower SEC at Y_t=0.5 for ERD efficiencies of 80% and 100% (both for $\eta_p = 1$).
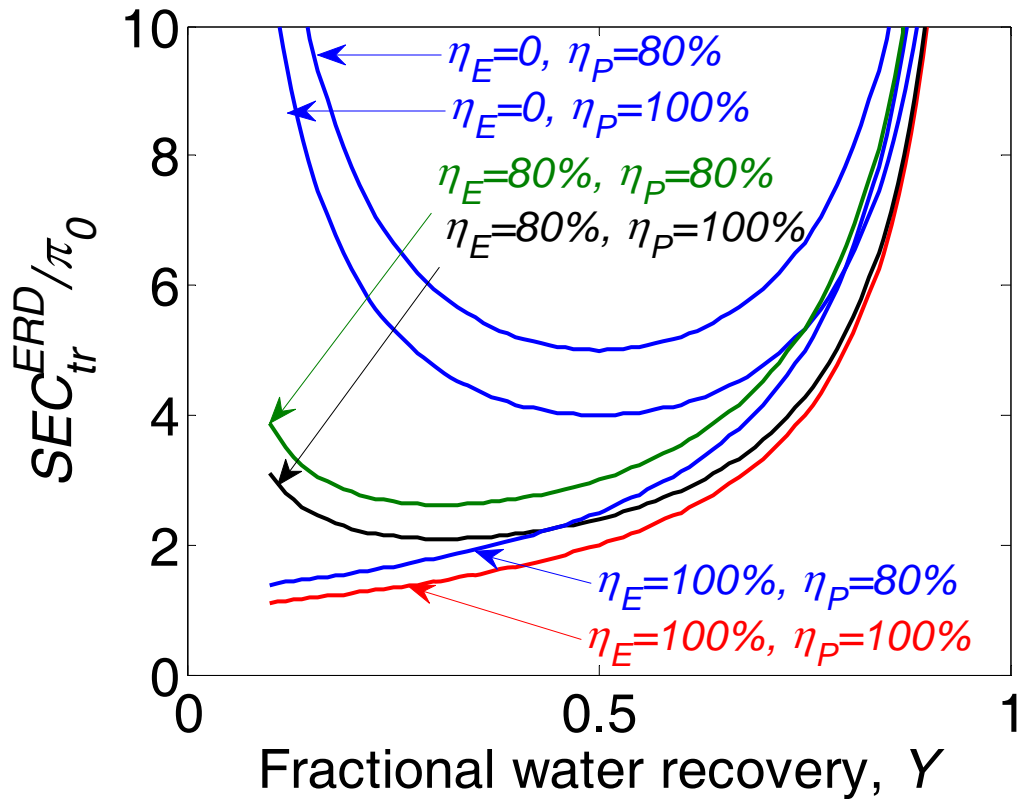
Figure 6-2. **Variation of the normalized SEC for a target salt rejection of 99% with fractional product water recovery using an ERD in a single-pass RO (note:** η_p **and** η_E **represent the pump and ERD efficiencies, respectively).**

The global minimum SEC for a target salt rejection (i.e., based on Eq. (6.6)), with respect to water recovery, can be derived by setting $\partial(SEC_{tr,norm}^{ERD})/(\partial Y) = 0$ and solving for the optimal recovery (Y_{opt}) at which $SEC_{tr,norm}^{ERD}$ is at its global minimum. When $\eta_P \neq f(Y_t, \Delta P)$, the following analytical solution is obtained,

$$Y_{opt} = \left(\sqrt{(1-\eta_E)}\right)/\left(1+\sqrt{(1-\eta_E)}\right) \tag{6.7a}$$

$$(SEC_{tr,norm}^{ERD})_{min} = R_t\left[1+\sqrt{(1-\eta_E)}\right]^2/\eta_P \tag{6.7b}$$

101

The above equations indicate that as the fractional ERD efficiency (i.e., η_E) increases, Y_{opt} decreases; thus, with increased ERD efficiency, the minimum SEC occurs at lower water recovery. Indeed, it is known in the practice of RO desalting that a higher benefit of energy recovery is attained when operating at lower recoveries.

6.3. Two-pass modeling results

Energy optimization for a two-pass RO/NF (Figure 6-3) can be explored similar to the analysis presented for a single-pass process (Section 6.2). In this process, the overall target product water recovery, Y_t, and the overall target salt rejection, R_t, are the results of RO/NF desalting at water recoveries and salt rejections of Y_1, R_1 and Y_2, R_2 in the first and second RO/NF passes, respectively. The general expressions for the SEC are first presented, followed by a discussion of the SEC, with and without energy recovery, relative to the performance of a single-pass process for the same total recovery and permeate quality.
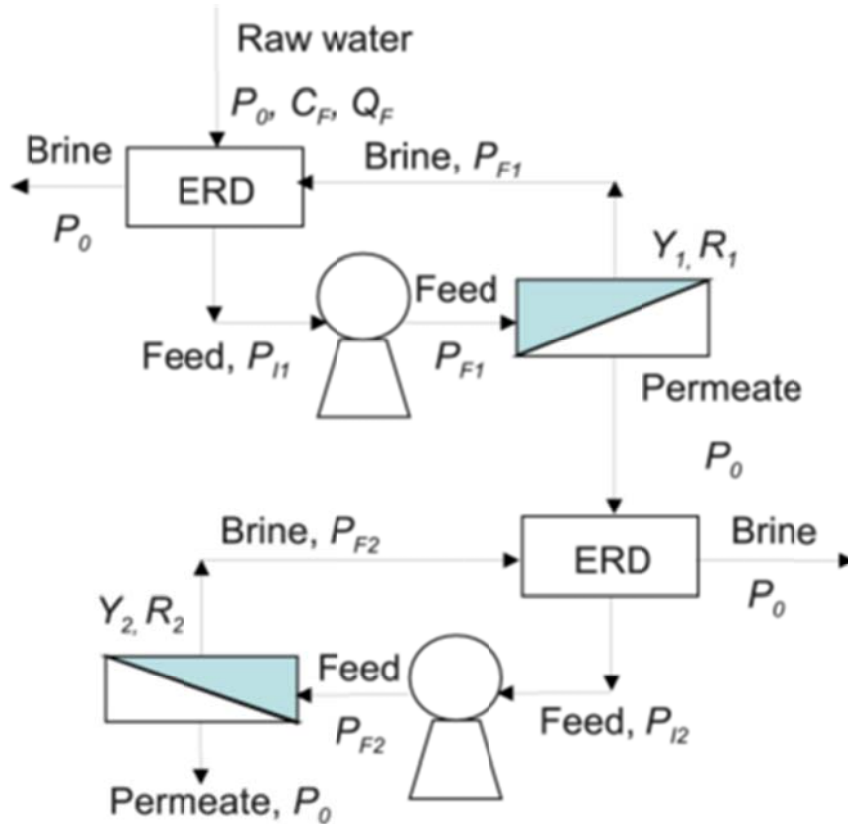
Figure 6-3. **Schematic of a two-pass RO/NF process with energy recovery devices (ERDs).**

Governing equations: SEC optimization for a two-pass RO/NF process at the thermodynamic limit

For a given feed flow rate, Q_f, the total permeate flow rate, Q_p, and total recovery, Y_t, are given by:

$$Q_p = Y_t Q_f = (Y_1 Q_f) Y_2 = Y_1 Y_2 Q_f \tag{6.8}$$

$$Y_t = Y_1 Y_2 \tag{6.9}$$

The permeate concentration from the first-pass RO/NF stage, $C_{p,1}$, i.e., the feed concentration for the second-pass RO/NF stage, and the permeate concentration from the

second-pass RO/NF stage, $C_{p,2}$, which characterizes the final product water quality, are given by:

$$C_{p,1} = (1 - R_1)C_f \qquad (6.10)$$

$$C_{p,2} = (1 - R_2)C_{p,1} \qquad (6.11)$$

where $C_{p,2}$ can also be expressed as(using Eqs. (6.10) and (6.11))

$$C_{p,2} = (1 - R_t)C_f = (1 - R_1)(1 - R_2)C_f \qquad (6.12)$$

with the overall salt rejection is given by

$$R_t = 1 - (1 - R_1)(1 - R_2) = R_1 + R_2 - R_1 R_2 \qquad (6.13)$$

The rates of work done by the first-pass pump, $\dot{W}_{tr,ERD}^{1st}$, and the second-pass pump, $\dot{W}_{tr,ERD}^{2nd}$, at the limit of the thermodynamic restriction, are given by (see Eq. 6.4):

$$\dot{W}_{tr,1st\,pass}^{ERD} = \left(\frac{R_1 \pi_0}{1 - Y_1}\right)\left(\frac{Q_f - \eta_{E1}(1 - Y_1)Q_f}{\eta_{P1}}\right) \qquad (6.14)$$

$$\dot{W}_{tr,2nd\,pass}^{ERD} = \left(\frac{R_2 \pi_{0,2}}{1 - Y_2}\right)\left(\frac{Y_1 Q_f - \eta_{E2}(1 - Y_2)Y_1 Q_f}{\eta_{P2}}\right) \qquad (6.15)$$

in which η_{P_1}, η_{P_2} and η_{E_1} and η_{E_2} are the pump and ERD efficiencies for the first and second passes, respectively, and $\pi_{0,2}$ is the osmotic pressure of the feed to the second-pass RO/NF, given by:

$$\pi_{0,2} = f_{os}C_{p,1} = f_{os}(1 - R_1)C_f = (1 - R_1)\pi_0 \qquad (6.16)$$

The SEC for the overall two-pass RO/NF process ($SEC_{tr,2\,passes}^{ERD}$), normalized with respect to the osmotic pressure of the process intake feed water (π_0), at the limit of the thermodynamic restriction, is obtained from the sum of Eqs. (6.13) and (6.14),

$$\frac{SEC_{tr,2\,passes}^{ERD}}{\pi_0} = SEC_{norm,2\,passes}^{tr,ERD} = \frac{\dot{W}_{tr,ERD}^{1st} + \dot{W}_{tr,ERD}^{2nd}}{Y_1 Y_2 Q_f \pi_0} =$$

$$= \left[\frac{R_1}{1-Y_1}\right]\left[\frac{1-\eta_{E_1}(1-Y_1)}{Y_1 Y_2 \eta_{P_1}}\right] + \left[\frac{R_2(1-R_1)}{1-Y_2}\right]\left[\frac{1-\eta_{E_2}(1-Y_2)}{Y_2 \eta_{P_2}}\right] \tag{6.17}$$

It is important to note that Eq. (6.17) is only valid for the range of $Y_t < Y_1 < 1$. When $Y_2 = 1$, there is complete salt passage through the membrane; therefore, the second-pass can be eliminated from the two-pass process, and thus the second term in Eq. (6.17) vanishes; this is equivalent to stating that only the first pass (or one-stage) exists requiring that $Y_1 = Y_t$ and $R_1 = R_t$. Similarly, when $Y_1 = 1$ this implies that $Y_2 = Y_t$ and $R_1 = 0$ indicating that there is no concentrate stream in the first-pass; thus, pump work is not required for the first-pass since only the second-pass exists (i.e., a configuration equivalent to a single-pass); therefore, the first term in Eq. (6.17) vanishes. Given the above arguments, the SEC for the overall two-pass RO/NF process is specified as follows:

$$
SEC_{norm,2\,passes}^{tr,ERD} = \begin{cases} \left(\dfrac{R_1}{1-Y_1}\right)\left(\dfrac{1-\eta_{E_1}(1-Y_1)}{Y_1Y_2\eta_{P_1}}\right) & Y_1 = Y_t \\[4ex] \left(\dfrac{R_1}{1-Y_1}\right)\left(\dfrac{1-\eta_{E_1}(1-Y_1)}{Y_1Y_2\eta_{P_1}}\right)+\left(\dfrac{R_2(1-R_1)}{1-Y_2}\right)\left(\dfrac{1-\eta_{E_2}(1-Y_2)}{Y_2\eta_{P_1}}\right) & Y_t < Y_1 < 1 \\[4ex] \left(\dfrac{R_2(1-R_1)}{1-Y_2}\right)\left(\dfrac{1-\eta_{E_2}(1-Y_2)}{Y_2\eta_{P_1}}\right) & Y_1 = 1 \end{cases}
\tag{6.18}
$$

The product (permeate) water recovery at which the minimum SEC for the overall two-pass RO/NF process is attained can be found, for a given target total recovery (Y_t) and salt rejection (R_t), based on Eq. (6.18) using a numerical search algorithm to locate a unique set of (R_1, Y_1) that will minimize the SEC subject to the following constraints:

$$
Y_t \le Y_1 \le 1
\tag{6.19a}
$$

and
$$
0 \le R_1 \le R_t, \; 0 \le R_1 \le R_t
\tag{6.19b}
$$

6.3.2. Effect of ERD efficiency on the SEC for a two-pass desalting process

For the special case of ERDs of 100% efficiency, the analysis revealed that with the use of energy recovery devices (i.e., ERDs), the global minimum energy, $\left(SEC_{norm,2\,passes}^{tr,ERD}\right)_{min}$, for the two-pass process always occurs (i.e., for any (Y_t, R_t) pair) when the salt rejection is zero in either the first or the second pass (i.e., the water recovery is 100% in either the first or the second pass). In other words, when $R_2=0$, the optimal $SEC_{norm,2\,passes}^{tr,ERD}$ is found at the condition of $R_1 = R_t$, $Y_1 = Y_t$, and thus the operating parameters for the second-pass are $R_2 = 0, Y_2 = 1$ (computed from Eqs. 6.9 and 6.13).

The above solution indicates that first-pass fulfills both the target water recovery and salt rejection. Therefore, the second-pass is not required and can be removed from the process. An equally valid optimal solution is when $R_1 = 0$ and $Y_1 = 1$ (i.e., $R_2 = R_t, Y_2 = Y_t$), which means that the first-pass is not required since the target recovery and salt rejection are accomplished in the second pass. The analysis suggests that, if a membrane of the appropriate rejection (and desired flux range) is available, then, at the global optimum, a single-pass RO/NF operation would be more energy favorable than a two-pass RO/NF process.

As an illustration of the above behavior and the impact of ERD efficiency, we consider the simple case of ERD efficiencies of 100% and 80% (the case of $\eta_E = 0$ is considered in Section 6.3.3) being identical for each pass and pump efficiency of 100%. The results for the $SEC_{norm,2\,passes}^{tr,ERD}$ are shown in Figure 6-4a and Figure 6-4b, for ERD efficiency of 100% and 80%, respectively, for a target total water recovery of 50% and 99% salt rejection, relative to the normalized SEC for a single-pass process for the same target recovery and salt rejection. As expected, the minimum normalized SEC of the two-pass process, is equivalent to the minimum normalized SEC for the single-pass (i.e., single stage) process (i.e., $SEC_{norm,1stage}^{tr,ERD} = 2$ for $\eta_E = 1$ and $SEC_{norm,1stage}^{tr,ERD} = 2.38$ for $\eta_E = 0.8$ at the target total recovery, Y_t, of 50%). At the lower ERD efficiency of 80% (assumed identical for both the two-pass and single-pass pumps), the $SEC_{norm,2\,passes}^{tr,ERD}$ achievable with the two-pass process increases but the $SEC_{norm,2\,passes}^{tr,ERD}$ trend with recovery and rejection is similar to the case of 100% ERD efficiency (Figure 6-4).
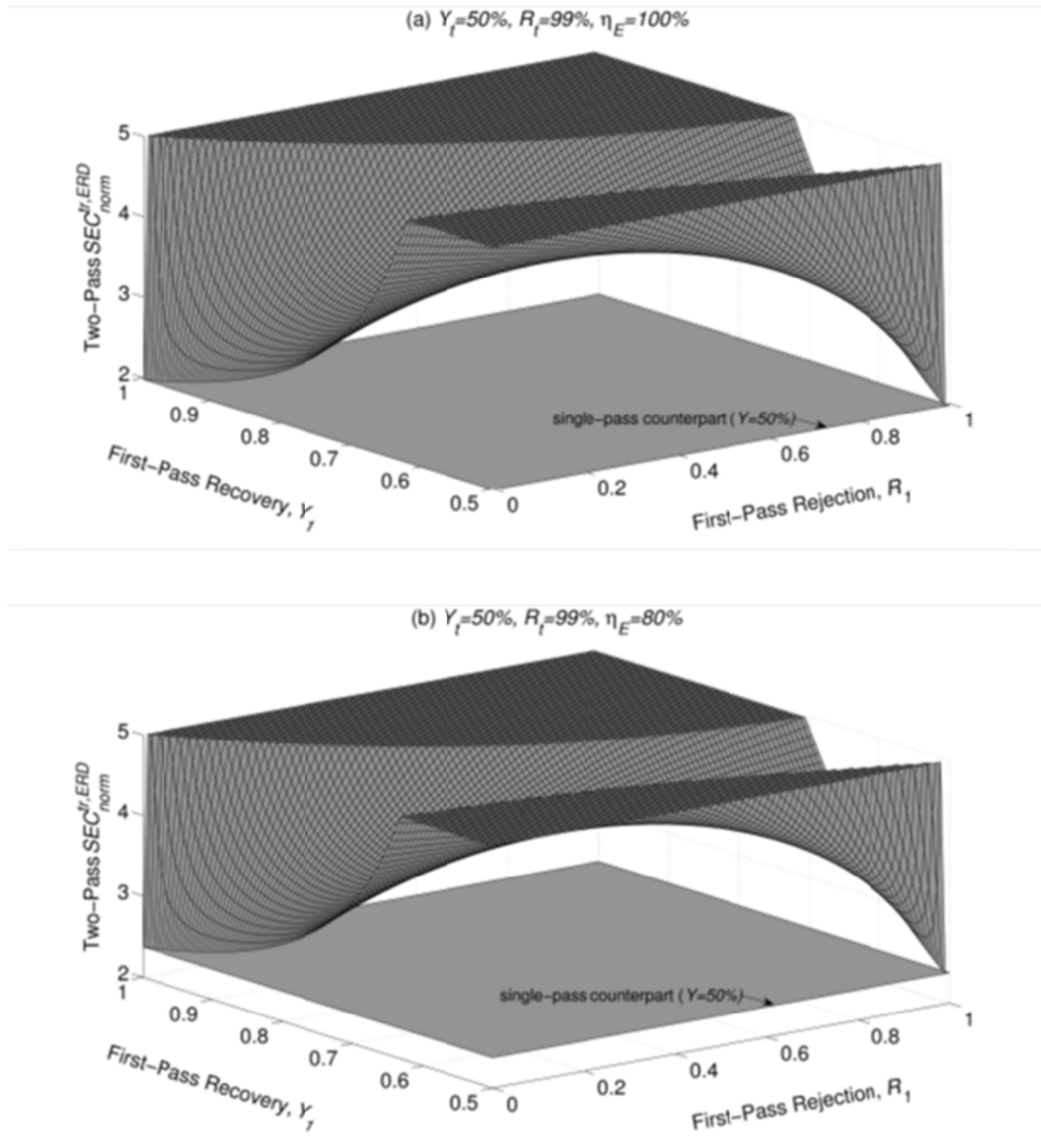
Figure 6-4. Variation of normalized SEC of a two-pass membrane desalination process at the limit of the thermodynamic restriction (with ERDs of 100% (Fig. a) and 80% (Fig. b) efficiency in each pass and $\eta_P = 1$ for all pumps) with respect to salt rejection and water recovery in the first-pass. The target water recovery and salt rejection are 50% and 99%, respectively. In both figures, the plots are truncated at a normalized SEC value of 5 in order to zoom in on the lower SEC region.

For the special case of 100% efficient pumps and ERDs of the same efficiency, for both the two-pass and single-pass processes, it is possible to arrive at an analytical solution for the $SEC_{norm,2\,passes}^{tr,ERD}$ for the overall two-pass process since the optimal solutions fall on the boundaries of $R_1=0$ and $R_2=0$. For example, when $R_1 = 0$, the optimum Y_2 value is obtained by setting $\left(\partial SEC_{norm,2\,passes}^{tr,ERD} / \partial Y_2\right) = 0$ and solving to obtain the following solution for the optimal recovery (for the second pass) at which the minimum SEC is obtained:

$$Y_{2,opt} = \frac{\sqrt{1-\eta_{erd}}}{1+\sqrt{1-\eta_{erd}}} \tag{6.20a}$$

$$\left(SEC_{norm,2\,passes}^{tr,ERD}\bigg|_{R_1=0}\right)_{min} = R_t\left(1+\sqrt{1-\eta_{erd}}\right)^2 \tag{6.20b}$$

Similarly, when $R_2 = 0$, the optimum Y_1 value is obtained from $\left(\partial SEC_{norm,2\,passes}^{tr,ERD} / \partial Y_1\right) = 0$, leading to the following solution

$$Y_{1,opt} = Y_t \tag{6.21a}$$

$$\left(SEC_{norm,2\,passes}^{tr,ERD}\bigg|_{R_2=0}\right)_{min} = \frac{(1-\eta_E(1-Y_t))R_t}{Y_t(1-Y_t)} \tag{6.21b}$$

It is noted that the global minimum *SEC* is the lower of the above two minima ((Eqs. 6.20b) and (6.21b)). The SEC of the single-pass (or single stage) counterpart is given by Eq. (22) and it is the same as Eq. (6.21b). Therefore, if $\left(SEC_{norm,2\,passes}^{tr,ERD}\bigg|_{R_1=0}\right)_{min} > \left(SEC_{norm,2\,passes}^{tr,ERD}\bigg|_{R_2=0}\right)_{min}$, a single-pass process will always be more energy efficient than its two-pass counterpart. However, if

$\left(SEC_{norm,2\,passes}^{tr,ERD} \Big|_{R_1=0} \right)_{min} < \left(SEC_{norm,2\,passes}^{tr,ERD} \Big|_{R_2=0} \right)_{min}$, there will be a sub-domain where a two-

pass process can be of greater energy efficiency relative to a single-pass process. Finally,

if $\left(SEC_{min}^{tr} \Big|_{R_1=0} \right)_{min} = \left(SEC_{norm,2\,passes|R_2=0}^{tr,ERD} \right)_{min}$, the optimized two-pass is as efficient as its

single-pass counterpart, but it will be less efficient if not optimized. The critical total

recovery, $Y_t^{critical}$, at which the transition occurs is determined by equation Eqs. (6.20a)

and (6.21a) to give

$$Y_t^{critical} = \frac{\sqrt{1-\eta_E}}{1+\sqrt{1-\eta_E}} \tag{6.21c}$$

Equation (6.21c), which is plotted in Figure 6-5, indicates that in the absence of energy

recovery (i.e., $\eta_E = 0$) $Y_t^{critical}$ reduces to the optimal recovery for a single-pass process as

presented in Section 6.2 (i.e., $Y_t^{critical} = Y_{opt} = 0.5$, Eq. (6.7a) and (6.21c)). On the other

hand, for an ideal ERD ($\eta_E = 1$) $Y_t^{critical} = 0$, indicating that a single–pass process is more

energy efficient than a two-pass process. For $Y_t \geq Y_t^{critical}$, a single-pass is always equally

or more energy efficient than a two-pass process, but for $Y_t < Y_t^{critical}$, there can be a sub-

domain in which a two-pass process will be more energy efficient; this would be the case

only when the single-stage process is not operating at its optimal recovery at which the

global minimum SEC is achieved. It should be recognized, however, that the optimized

two-pass process, for the configuration shown in Figure 6-3, will always reduce to a

single-stage process.
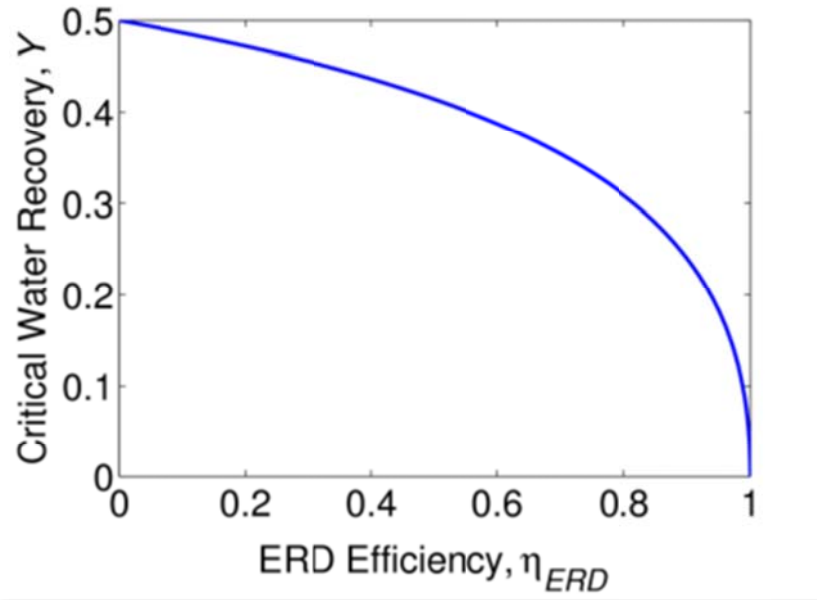
Figure 6-5. **The effect of ERD efficiency on the critical water recovery above which a single stage membrane desalting process is more efficient than a two-pass process (Eq. 6.21c).**

An additional example is presented below for a lower ERD efficiency of 80% (for both passes and for the single-pass operations with $\eta_P = 1$ for all pumps) for which $Y_t^{critical} = 0.309$ (see Eq. 6.21c). For $Y_t < 0.309$, there should be a sub-domain, in which a two-pass process will be more energy efficient than its single-pass counterpart. This behavior is illustrated in Figure 6-6a, for $Y_t = 0.3$ (i.e., $Y_t < Y_t^{critical}$) and $R_t = 0.99$, demonstrating a local region where $SEC_{norm,2\ passes}^{tr,ERD} < SEC_{norm,1\ pass}^{tr,ERD}$. At $Y_t = 0.31$ (i.e., $Y_t > Y_t^{critical}$) a single-pass is always more energy efficient as shown in Figure 6-6b. It is noted that, for the special case of an ideal ERD (i.e., $\eta_E = 1$), $Y_t^{critical} = 0$, a single-pass process will be more energy favorable than a two-pass process given that for all operations $Y_t > Y_t^{critical}$.
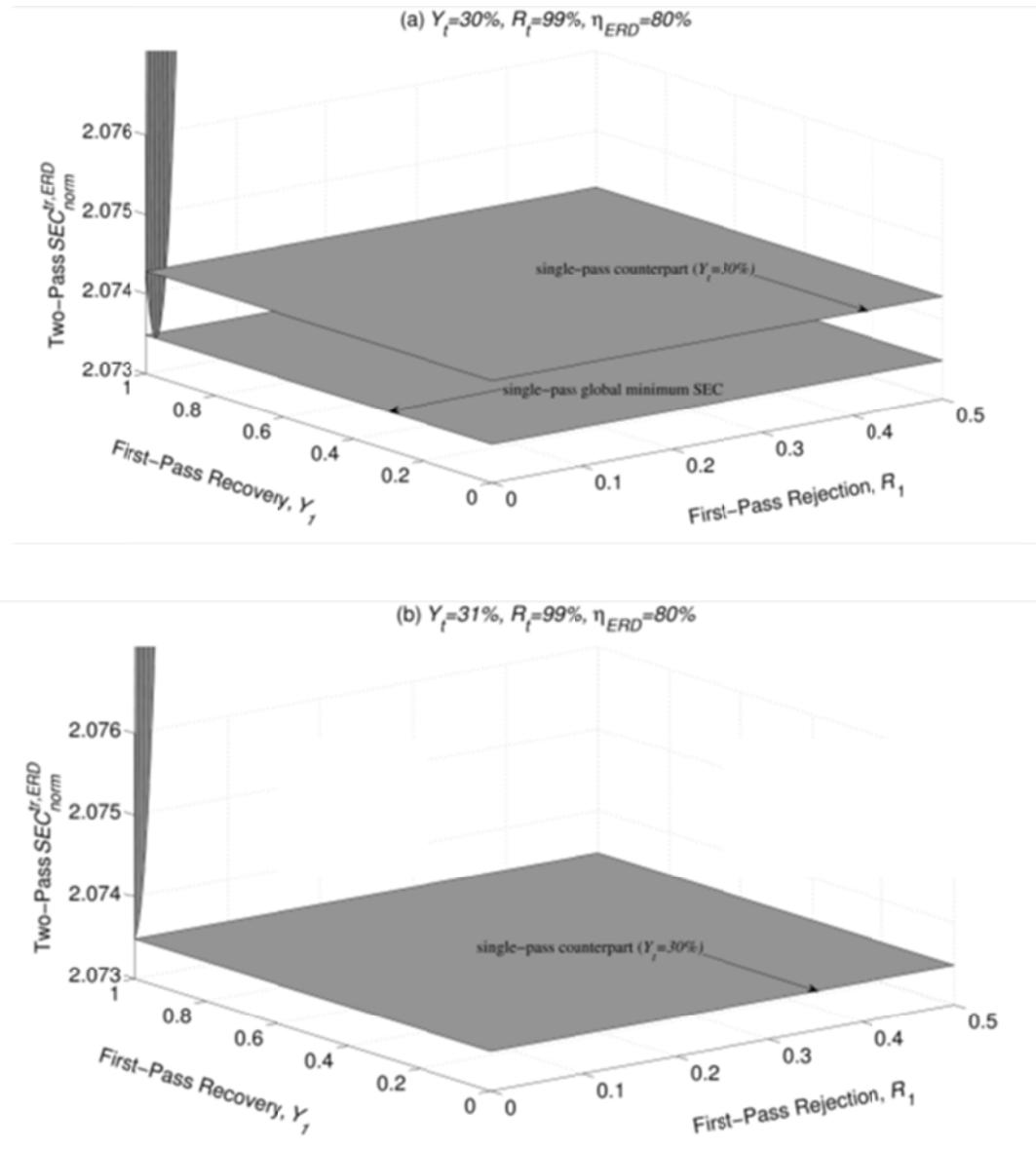
Figure 6-6. Variation of SEC of a two-pass RO/NF process and single-pass counterpart with respect to water recovery and salt rejection in the first-pass when the target water recovery is less than (Fig. a) and larger than (Fig. b) the critical value. (ERD and pump efficiencies are 80% and 100% for the two-pass and single-pass processes and the critical target water recovery is 30.9%). Both plots are set to zoom in on the lower normalized SEC region.

The above behavior can be understood by noting that in RO/NF desalting the required feed pressure (or energy, see Eq. (6.14)) is more sensitive to water recovery than salt rejection. When desalting is accomplished with a two-pass process, the water recovery in each of the two passes will be greater than the target total water recovery (provided that there is permeate production in both passes), as can be verified from Eq. (6.9) (i.e., $Y_t=Y_1Y_2$). For example, as can be seen in Figure 6-2, when using an ideal ERDs (i.e., $\eta_E=1$), the optimum water recovery approaches zero and the SEC increases with water recovery; therefore, regardless of the target water recovery, the SEC for a two-pass process will be higher SEC than a single-pass process, due to the fact that even when low rejection membranes are used in the two-pass process, the benefit of reducing the applied pressure (which varies linearly with rejection) is negated by the higher recovery which results in a much higher osmotic pressure and thus higher applied pressure. On the other hand, when the desired total water recovery is below the optimal recovery, the increase of water recovery, in each of the two passes, toward the optimal recovery will reduce the SEC of each pass. For example, in Figure 6-2, in the absence of energy recovery, i.e., $\eta_E=0$, the SEC will be lower when operating at 50% relative to 40% water recovery. Below the critical water recovery (i.e., the optimal recovery for a single pass process; see Figure 6-5), owing to the combined benefit of reducing the salt rejection requirement in each pass, there is a sub-domain in which a two-pass process can be more energy efficient than a single-pass (i.e., single stage) that operates at the same overall target water recovery. Further discussion of the existence of such a domain and comparison with single-pass operation is provided in Section 6.3.3.

113

6.3.3. Energy cost optimization of two-pass RO/NF without energy recovery

In the absence of energy recovery, the two-pass and single-pass desalting processes (Figure 6-7) are optimized as discussed in Section 6.3.2 by setting $\eta_E = \eta_{E_1} = \eta_{E_2} = 0$. For the condition of $\eta_{E_i} \neq f(Y_i, \Delta P_i)$, Eq. (6.21c) indicates that the critical water recovery, $Y_t^{critical}$, is 50%, above which the single-pass process will always be more energy efficient than the two-pass process. If $\eta_{E_i} = f(Y_i, \Delta P_i)$, the critical water recovery can only be obtained from a numerical solution of the optimization problem as represented by Eq. (6.18).
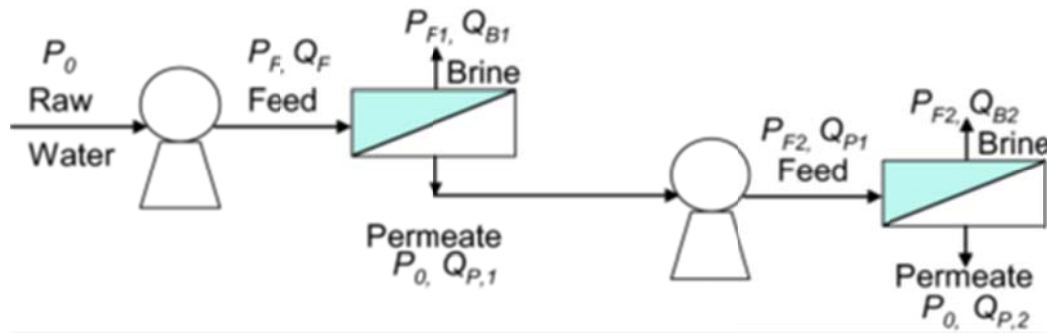
Figure 6-7. **Schematic of a two-pass RO/NF process without an energy recovery device (ERD).**

The implication of the above critical water recovery is that, in the absence of energy recovery, a single-pass process is more energy efficient than a two-pass process for $Y_t \geq 0.5$ as illustrated in Figure 6-8 for a process with ideal pumps (i.e., $\eta_p = 1$), target total recovery of 60% and salt rejection of 99%. Two solutions are found for the minimum SEC. The first is at $\left(SEC_{norm,2\,pass}^{tr,ERD} \right)_{min} = 4.13$ and $R_1 = 99\%, Y_1 = 60\%$. This solution implies that the first-pass fulfills both the water recovery and salt rejection requirements and the second-pass can be eliminated given that it would operate at

$R_2 = 0, Y_2 = 1$ The second solution which is at $\left(SEC_{norm,2\,pass}^{tr,ERD}\right)_{min} = 4.13$ and

$R_2 = 99\%, Y_2 = 60\%$, indicates that a second-pass can also fulfill both the water recovery

and salt rejection requirements; thus, for this solution the first-pass can be eliminated

given that it would operate at $R_1 = 0, Y_1 = 1$. In other words, for operation at the limit of

the thermodynamic restriction, the energy-optimized two-pass RO/NF process is a single-

pass RO/NF process.
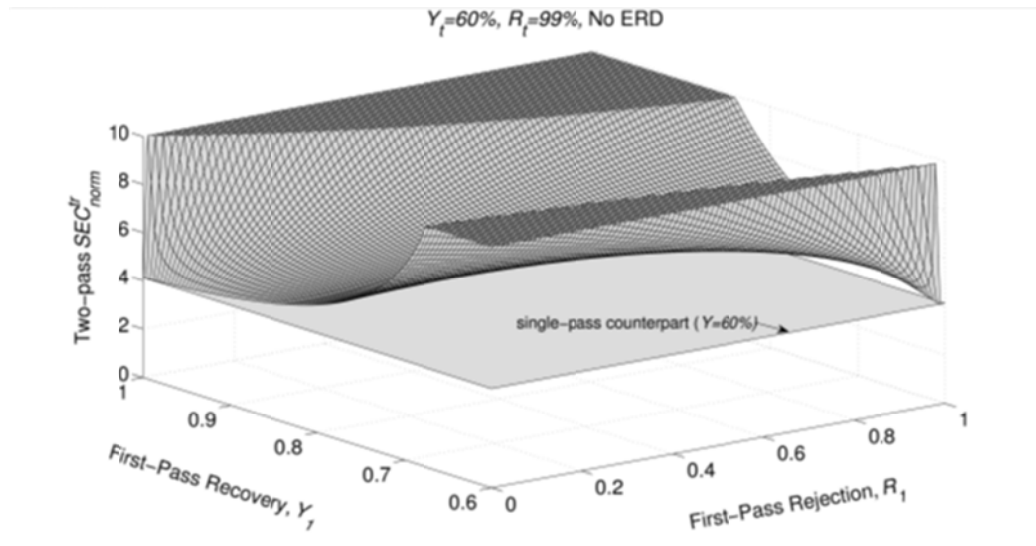
Figure 6-8. **Variation of normalized SEC of a two-pass membrane desalting process operating up to the thermodynamic restriction (without ERDs and 100% pump efficiency) with respect to salt rejection and water recovery in the first-pass. The target water recovery and salt rejection are 60% and 99%, respectively. The plot is truncated at a normalized SEC value of 10 in order to zoom in on the lower SEC region.**

On the other hand, below the critical total water recovery of 50%, there is an operational

sub-domain in which the two-pass process can be more energy efficient than its single-

pass counterpart as illustrated in Figure 6-9 for $Y_t = 0.3$ and $R_t = 0.99$. Specifically, for

115

the above overall water recovery and salt rejection, the operational points between

$(R_1 = 0, Y_1 = 60\%)$ and the intersection of the single-pass counterpart plane (

$SEC_{norm,1pass}^{tr} = 4.71$) with the two-pass surface are of lower normalized SEC relative to

the single-pass process, by as much as 16% when the first pass is operated at

$R_1 = 0$, $Y_1 = 60\%$. It is important to recognize that, when $Y_t < Y_t^{critical}$, although a two-

pass process can be more energy favorable, in the absence of energy recovery, than its

single-pass counterpart (operated at the same overall water recovery, i.e., 30%), this

would require operation at low water recovery. It is stressed that the optimized two-pass

is actually a pseudo-two-pass, i.e., a single-pass with an unpressurized bypass (since

$(R_1 = 0, Y_1 = 60\%)$, $(R_2 = 99\%, Y_2 = 50\%)$), which indicates that a two-pass process can

never be more energy efficient than a single-pass process.
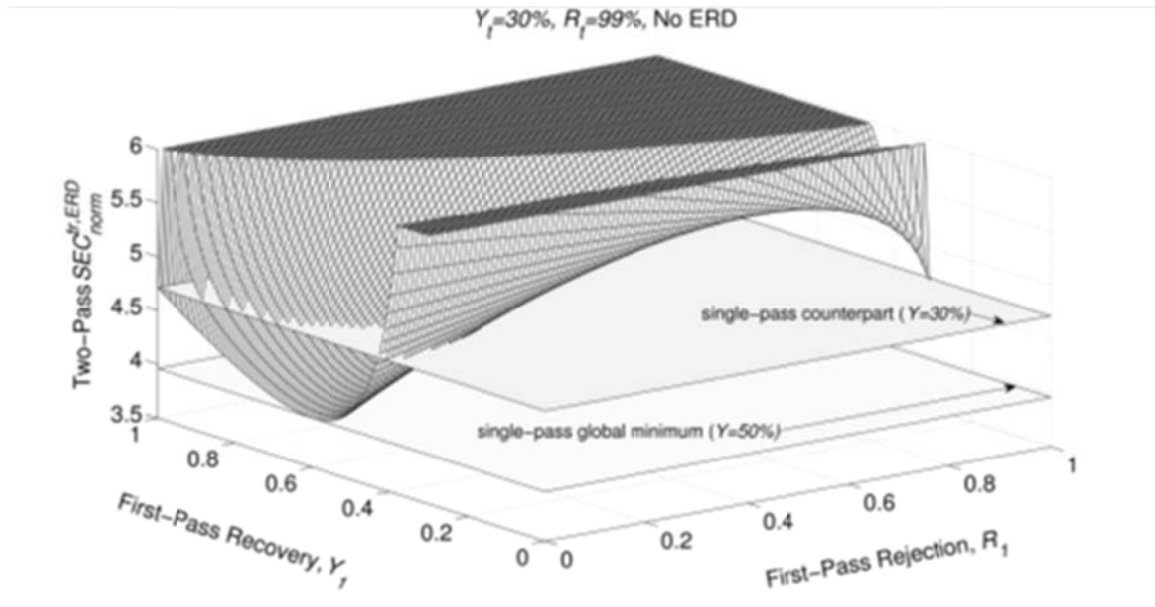
Figure 6-9. **Variation of the normalized SEC for a two-pass membrane desalting process operating up to the thermodynamic restriction (without ERDs and pumps of 100% efficiency) with respect to salt rejection and water recovery in the first-pass. The target water recovery and salt rejection are 30% and 99%, respectively. The plot is truncated at a normalized SEC value of 6 in order to zoom in on the lower SEC region.**

6.4. The constraint of membrane rejection

The previous optimization of the two-pass process with respect to energy consumption and the comparison with a single-pass process, assumed the availability of a membrane that can achieve the required salt rejection even with a single-pass process. However, if a membrane of the required overall desired rejection (i.e., R_t) in a single-pass is unavailable, then a two-pass is the only feasible approach, whereby the rejection of the available membrane (i.e., of the highest available rejection R_{max}) represents the constraint $R_{max} < R_t$ that has to be considered when optimizing the two-pass process. Accordingly,

in addition to the previous constraints ($Y_t \le Y_1 \le 1$ and $0 \le R_1 \le R_t$; Eq. (6.19b), the following two additional constraints are introduced in the optimization of Eq. (6.17):

$$0 \le R_1 \le R_{max} \text{ and } 0 \le R_2 \le R_{max} \tag{6.22}$$

For the purpose of illustrating the implications of the above constraints, it is convenient to consider the special case of a two-pass operation with ideal energy recovery (i.e., $\eta_E = 1$) and feed pumps (i.e., $\eta_p = 1$) for both passes. A numerical solution of the above optimization problem (a search for the minimum $SEC_{norm,2\,passes}^{tr,ERD}$ over the rejection range given by Eq. (6.22) and water recovery range of $Y_t \le Y_1 \le 1$), revealed that the optimal salt rejection for the first-pass is the maximum salt rejection that can be achieved by a membrane of the highest available rejection, i.e., $R_{1,opt} = R_{max}$. It is also important to note that, in order to achieve the target overall rejection R_t, R_{max} should be no less than $1 - \sqrt{1 - R_t}$ (determined by Eq. (6.13)). The specific energy consumption of the above two-pass desalination process, at the limit of the thermodynamic restriction, is obtained by substituting $R_1 = R_{1,opt} = R_{max}$, $R_t = R_1 + R_2 - R_1 R_2$, and $Y_t = Y_1 Y_2$ in Eq. (6.18), to yield:

$$SEC_{norm,2\,passes}^{tr,ERD} = \frac{R_{max}}{Y_2 - Y_t} + \frac{R_t - R_{max}}{1 - Y_2} \tag{6.23}$$

where all the efficiencies (pumps and ERDs) are taken to be ideal in this example. From Eq. (6.23), the second pass optimal recovery, $Y_{2,opt}$, is obtained by setting $\left(\partial SEC_{norm,2\,passes}^{tr,ERD} / \partial Y_2 \right) = 0$,

$$Y_{2,opt} = \frac{\sqrt{R_{max}} + Y_t\sqrt{R_t - R_{max}}}{\sqrt{R_{max}} + \sqrt{R_t - R_{max}}} \tag{6.24}$$

And the global normalized minimum energy consumption for the overall two-pass process is obtained by Eq. (6.24) in Eq. (6.23) yielding:

$$\left(SEC_{norm,2\,passes}^{tr,ERD}\right)_{min} = \frac{R_t + 2\sqrt{R_{max}(R_t - R_{max})}}{(1 - Y_t)} \tag{6.25}$$

An example of the variation of the salt rejection and water recovery for the two passes, at the optimal minimum energy point (Eq. (6.25)), as obtained from the above constrained optimization, is provided in Figure 6-10a-d, for a target overall salt rejection of 99% and total water recovery of 50%, with the corresponding $\left(SEC_{norm,2\,passes}^{tr,ERD}\right)_{min}$ shown in Figure 6-11. The analysis demonstrates the following behavior which is apparent in Figure 6-10: (a) the optimal rejection for the first pass is equal to that which is feasible by the available membrane of the highest rejection, with the second pass rejection decreasing with R_{max}, (b) the optimum first-pass water recovery decreases more rapidly with increasing R_{max}, while the second-pass water recovery increases at a somewhat faster rate with increasing R_{max}. Finally, it is noted that $\left(SEC_{norm,2\,passes}^{tr,ERD}\right)_{min}$ is a sensitive function of R_{max} showing, for example, about 58% decrease in the SEC as R_{max} increases from 0.9 to 0.99. The above analysis demonstrates that when operating a two-pass process it is desirable to operate the first-pass at the highest possible rejection.
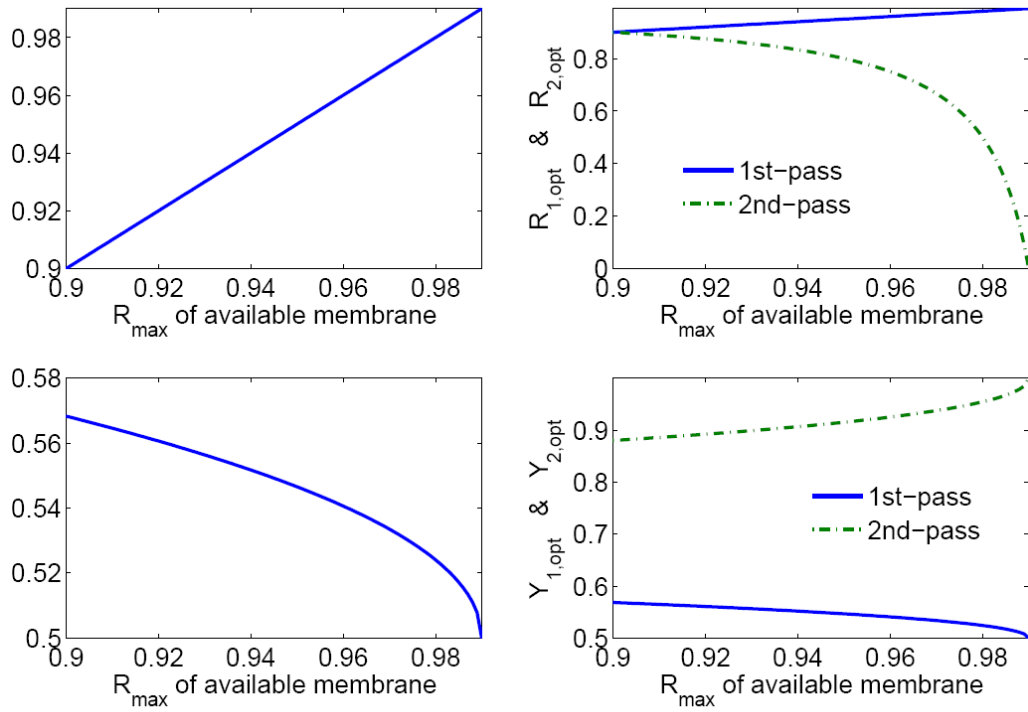
Figure 6-10. Optimization of a two-pass RO/NF process with ERDs and pumps of 100% efficiency under the constraint of membrane rejection. (The target water recovery and salt rejection are 50% and 99%, respectively.).
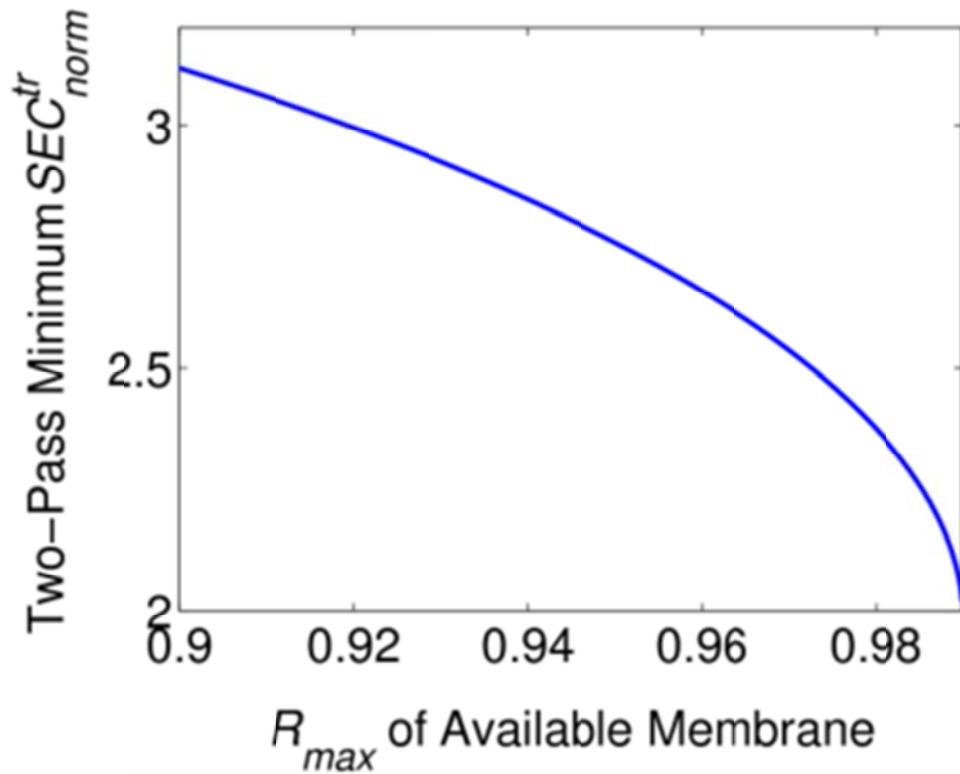
Figure 6-11. The variation of the minimum SEC for a two-pass membrane desalination process (Eq. 6.25), with ideal pumps and ERDs (i.e., $\eta_P = 1$ and $\eta_E = 1$) and target water recovery and salt rejection of 50% and 99%, respectively, operated up to the limit of the thermodynamic restriction, with the highest rejection of the available membrane (i.e., Rmax).

6.5. Conclusions and recommendations

. The present results indicate that if the desired overall salt rejection can be achieved in a single pass, then a single-pass configuration will be more energy favorable than a two-pass process configuration for the same level of total water recovery and salt rejection. However, if a membrane is not available to achieve the desired rejection in a single pass, then a two-pass configuration is the viable alternative, with the lowest energy consumption attained when the first-pass uses a membrane of the highest available salt

rejection. It is noted that for certain cases in which desalting is accomplished at recoveries below the critical water recovery (i.e., the optimal recovery for a single stage), there can be an operational sub-domain in which the two-pass process can be more energy efficient than a single-pass counterpart (which is not operating at its globally optimal state). Although retentate recycling from the second pass to the first pass feed can reduce the energy consumption for the two pass process, the optimal two-pass process is a single pass process.

It is important to recognize that additional energy will be consumed to pump the water from the sea, through the pretreatment devices and back to the sea depending on the site location. It is also noted that available membranes cannot work, currently, above 80 bars, which will limit the possible water recovery ratio. Finally, the ultimate target is always to minimize the final cost of the water produced. Therefore, optimization needs to be performed on the entire project, including the capital investment, pretreatment, post treatment, etc. However, inclusion of these issues will simply affect the optimal water recovery at which the RO desalination plant should operate. However, since the analysis presented in this Chapter covers the entire range of possible water recovery ([0 1]) and salt rejection ([0 1]), the conclusion that two-pass desalting will be less energy efficient than single-pass desalting will not be altered by including additional economic considerations. However, despite the lower energy efficiency of the two-pass process, there can be situations where a two-pass process is the preferred process, particularly in situations of difficult to achieve rejection of certain species as in the requirement for boron removal [163].

Chapter 7   Effect of Stream Mixing on RO Energy Cost Minimization

7.1.   Overview

Recent studies have demonstrated that when a membrane desalting process can be operated up to the limit imposed by the thermodynamic restriction, there is an optimal product water recovery at which the specific energy consumption (i.e., energy consumption per volume of permeate produced) is minimized **[38]**. It has been shown, via a formal optimization procedure, that the optimal operating condition shifts to higher recovery with increased membrane and brine management costs **[38]**. It has also been suggested that the energy consumption for membrane desalting would decrease with increased desalting stages where inter-stage pumps are utilized. The optimization model was successfully demonstrated in a recent study showing significant energy savings (up to 22%) under fluctuating feed salinity (up to 43%) **[44]**.

More recently, a two-pass membrane desalination process was evaluated and compared to a single-pass process when both processes operate at the limit of the thermodynamic restriction **[43]**. Considerations of energy recovery and pump efficiency and the limitations imposed by membrane rejection level have led to the conclusion that a single-pass process is more energy efficient relative to a two-pass process. However, in these works, the impact of various stream mixing and recycling configurations on the SEC of an RO plant was not fully studied.

Extending previous studies on RO optimization for operation at the thermodynamic limit, this work evaluates the effect of possible mixing/blending of various streams (feed, retentate, permeate) on the specific energy consumption (SEC) of RO desalination. To address this problem, the analysis begins with the simplest configuration: single-stage RO desalination, in which two possible recycling (partial retentate recycling and partial permeate recycling) operations are examined. Based on the results from the single-stage RO configuration, two-pass and two-stage desalting with recycling are then studied to determine the effect of various mixing/blending operations on the resulting SEC.

7.2. Effect of partial recycling operation on the SEC of single-stage RO desalting at the thermodynamic limit

7.2.1. Materials and reagents

For single-stage RO desalting, full recycling of either the retentate or permeate streams is not possible for a continuous process operation. Therefore, this chapter focuses on partial recycling. In partial retentate recycling operation, part of the retentate stream is diverted to the feed stream immediately before the RO module (Figure 7-1(a)), while in partial permeate recycling operation, part of the permeate stream is diverted to the raw feed (Figure 7-1 (b)).
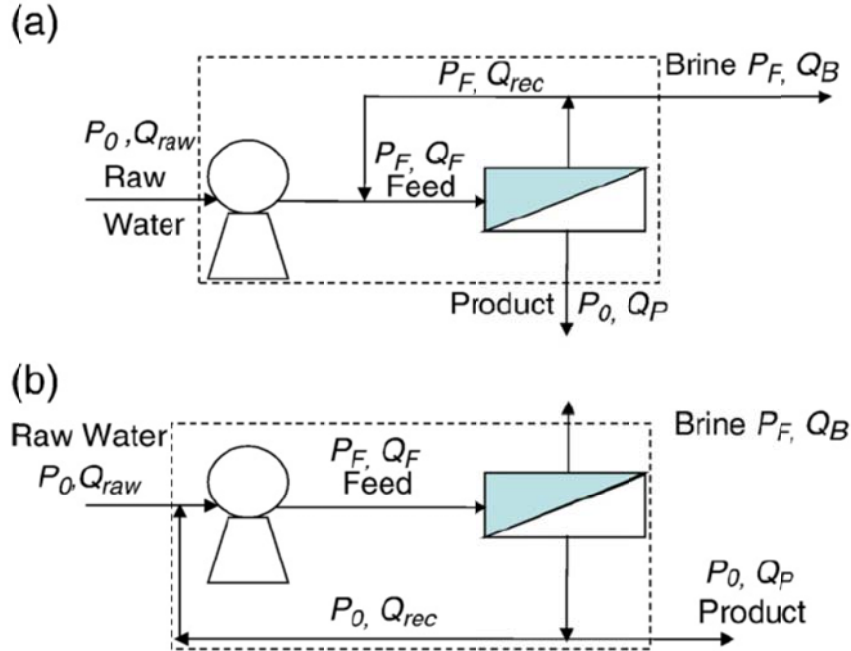
Figure 7-1. Schematics of a single-stage RO system with partial retentate recycling (a) and permeate recycling (b).

7.2.2. Partial retentate recycling in single-stage RO desalting

For single-stage RO desalting with partial retentate recycling as shown in Figure 7-1 (a), one can show, via a salt mass balance, that the brine-permeate osmotic pressure difference is $\Delta\pi_{brine} = \frac{\pi_0 R}{1-Y}$ (π_0: feed osmotic pressure, R: salt rejection, $Y(=\frac{Q_P}{Q_{raw}})$: overall water recovery where Q_P is the product water flow rate and Q_{raw} is the raw feed water flow rate), assuming linear relationship between the osmotic pressure and salt concentration [150].

When desalting at the limit of the thermodynamic restriction and neglecting the pressure drop in the system [38], the feed pressure is given by:

$$\Delta P = P_F - P_0 = \Delta\pi_{brine} = \frac{\pi_0 R}{1-Y} \tag{7.1}$$

Since the recycled retentate stream of a pressure P_F is fed directly into the inlet of the

RO unit, there is no additional pump work involved to pressurize it to P_F; thus, the rate

of pump work for the RO system in Figure 7-1 (a) is given by:

$$\dot{W} = \Delta P \times Q_{raw} = \frac{\pi_0 R}{1-Y} Q_{raw} \tag{7.2}$$

Therefore, the specific energy consumption (SEC) is given by:

$$SEC = \frac{\dot{W}}{Q_P} = \frac{\pi_0 R}{Y(1-Y)} \tag{7.3}$$

which is consistent with the SEC for a single-stage RO system (without recycling) that

operates at the limit of the thermodynamic restriction [38]. This means that partial

retentate recycling will not change the SEC of a single-stage RO desalting. The inclusion

of an energy recovery device (ERD) will not alter this conclusion since the brine stream

flow rate ($Q_B = Q_{raw} - Q_P$) and pressure (P_F), which determine the amount of energy that

can be recovered [38], are the same for operation with and without partial retentate

recycling.

7.2.3. Partial permeate recycling in single-stage desalting

For single-stage RO desalting with partial permeate recycling as shown in Figure 7-1 (b),

the brine-permeate stream osmotic pressure difference is also given by $\Delta\pi_{brine} = \frac{\pi_0 R}{1-Y}$

assuming linear relationship between osmotic pressure and salt concentration [150].

When desalting at the limit of the thermodynamic restriction, the feed pressure is also

given as in Eq. (7.1). Given a recycled stream flow rate of $Q_{rec} = \alpha Q_P$, where α is the

recycle-to-product ratio ($\alpha > 0$), the rate of pump work for a feed flow rate Q_F is given as

$$\dot{W} = \Delta P \times Q_F = \frac{\pi_0 R}{1-Y} \times (\alpha Q_P + Q_{raw}) \tag{7.4}$$

where

$$Q_F = Q_{rec} + Q_{raw} = \alpha Q_P + Q_{raw} \tag{7.5}$$

Therefore, the SEC for this system is given by

$$SEC = \frac{\Delta P \times Q_F}{Q_P} = \frac{\pi_0 R}{1-Y} \times \frac{(\alpha Q_P + Q_{raw})}{Q_P}$$

$$= \frac{\pi_0 R}{Y(1-Y)} + \frac{\alpha \pi_0 R}{1-Y} \tag{7.6}$$

In Eq. 7.6, the first term, $\frac{\pi_0 R}{Y(1-Y)}$), is the SEC for a single-stage RO desalting at a water recovery of Y (Section 2.1, if one replaces the configuration inside the dashed region of Figure 7-1 (b) by a single-stage RO system without recycling). Thus, the SEC of single-stage RO desalting with partial permeate recycling is less energy favorable than single-stage RO desalting without partial permeate recycling. If the pressure drop is taken into account, the SEC of partial permeate recycling operation will increase further. Likewise, the effect of an ERD will not change the above conclusion since the brine stream flow rate ($Q_B = Q_{raw} - Q_P$) and feed pressure (P_F) are the same for operation with and without partial permeate recycling [38].

The conclusion from the above simple analysis is that in a single-stage RO operation, permeate recycling increases the SEC, while retentate recycling does not change the SEC.

7.3. Effect of second-pass retentate recycling to the first-pass feed in a two-pass membrane desalting process

A two-pass RO/NF desalting has been proposed in the literature as a potential approach to lower energy consumption **[149]** or to achieve target salt rejection not feasible with a single pass **[163]**. As presented in Chapter 6, the two-pass process without recycling has no advantage with respect to energy savings and its optimized configuration defaults to a single-pass process **[43]**. Whether the two-pass with retentate recycling from the second-pass to the first pass feed could provide the means for reducing the energy consumption in the two-pass system is unknown. This approach is therefore investigated in this work and compared with a single-pass process at the same overall water recovery and salt rejection.

7.3.1. General Governing Equations

The case of full retentate recycling from the second-pass to the first pass is presented this section (Figure 7-2), in which the rates of work done by the first-pass pump, $\dot{W}_{tr,ERD}^{1st,recycle}$, and second-pass pump, $\dot{W}_{tr,ERD}^{2nd,recycle}$, at the limit of the thermodynamic restriction, are given by :
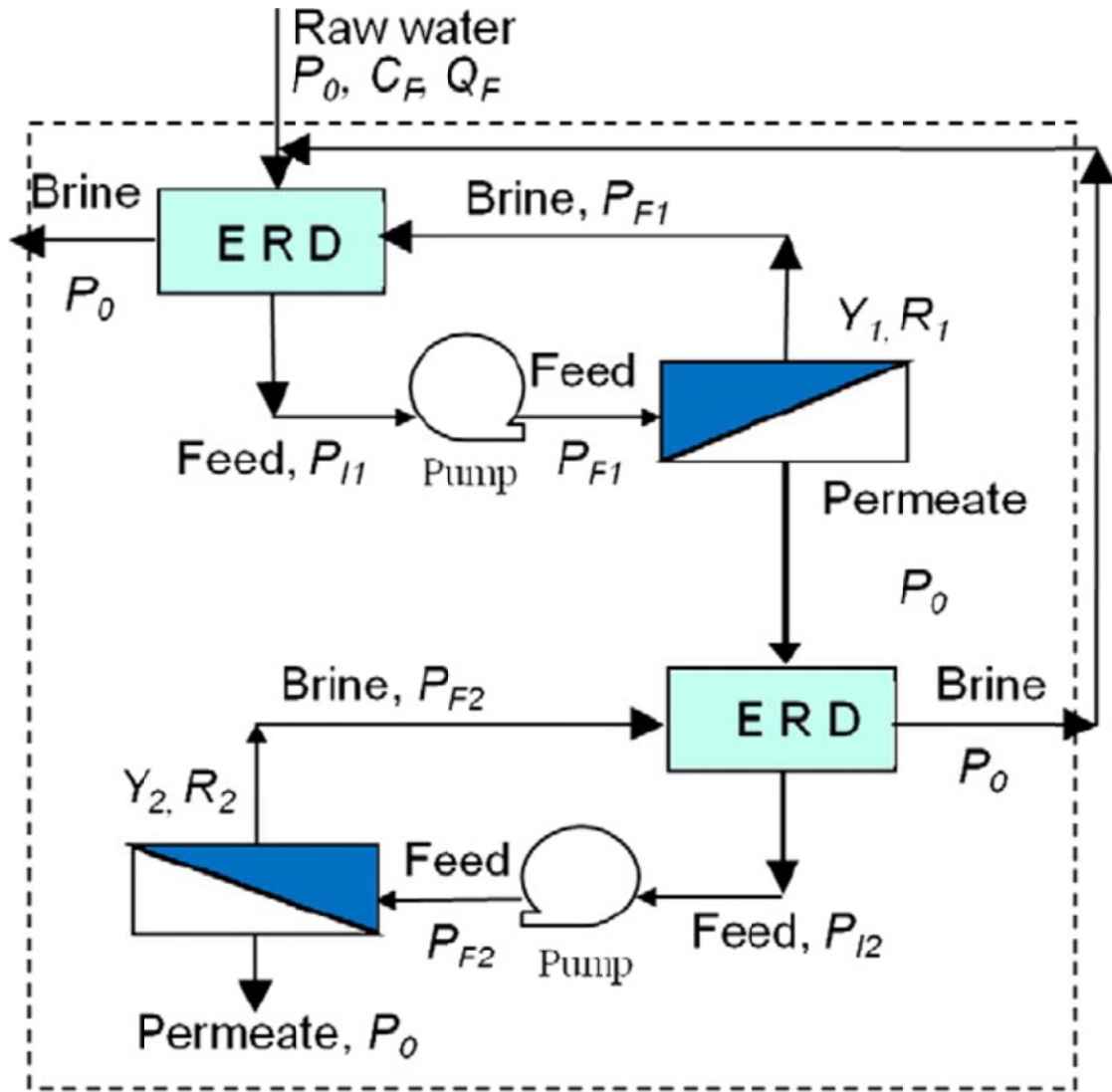
Figure 7-2. **Schematic of recycling the concentrate stream of the second-pass to the feed stream of the first-pass.**

$$\dot{W}_{tr,ERD}^{1st,recycle} = \left(\frac{R_1 \pi_{0,1}}{1-Y_1} \right) \left(\frac{Q_{f,1} - \eta_{E1}(1-Y_1)Q_{f,1}}{\eta_{P1}} \right) \tag{7.7a}$$

$$\dot{W}_{tr,ERD}^{2nd,recycle} = \left(\frac{R_2 \pi_{0,2}}{1-Y_2} \right) \left(\frac{Q_{f,2} - \eta_{E2}(1-Y_2)Q_{f,2}}{\eta_{P2}} \right) \tag{7.7b}$$

in which η_{P_1}, η_{P_2} η_{P_1} η_{P_2} and η_{E_1}, η_{E_1} η_{E_2} η_{E_2} are the pump and ERD efficiencies for the first and second passes, respectively, R_1, R_2 R_1, R_2 are salt rejections in the first and second-pass, respectively, Y_1, Y_2 Y_1, Y_2 are the water recoveries in the first and second-pass, respectively, $Q_{f,1}, Q_{f,2}$ $Q_{f,1}, Q_{f,2}$ are the feed flow rates to the first and second-pass, respectively, and $\pi_{0,1}, \pi_{0,2}$ $\pi_{0,1}, \pi_{0,2}$ are the osmotic pressures of the feed to the first and second-pass RO/NF, respectively, given by:

$$\pi_{0,2} = f_{os} C_{p,1} = f_{os} (1 - R_1) C_{f,1} = (1 - R_1)\pi_{0,1} \tag{7.7c}$$

The feed, brine and permeate flow rates of the second pass, $Q_{f,2}$ and $Q_{b,2}$, $Q_{p,2}$ respectively, calculated by simple mass balances, are given as :

$$Q_{f,2} = Q_{p,1} = Y_1 \times (Q_{raw} + Q_{b,2}) \tag{7.7d}$$

$$Q_{b,2} = (1 - Y_2) \times Q_{p,1} \tag{7.7e}$$

$$Q_{p,2} = Y_t \times Q_{raw} \tag{7.7f}$$

where Q_{raw} is the raw water flow rate, Y_t is the overall target water recovery, and Y_2 is defined by:

$$Y_2 = \frac{Q_{p,2}}{Q_{p,1}} \tag{7.7g}$$

The relationships among Y_1, Y_2 and Y_t are obtained by combining Eqs. (7.7d)–(7.7g):

$$Y_t = \frac{Y_1 Y_2}{1 - Y_1(1 - Y_2)}$$

$$Y_1 Y_2 = \frac{Y_t}{1 - Y_t}(1 - Y_1) \tag{7.7h}$$

130

The feed concentration to the first pass, $C_{f,1}$, which is the flow-rate-weighted average of the raw water stream concentration (C_{raw}) and second-pass brine stream concentration ($C_{b,2}$)), given by:

$$C_{f,1} = \frac{C_{raw}Q_{raw} + C_{b,2}Q_{b,2}}{Q_{raw} + Q_{b,2}} \qquad (7.7i)$$

where $C_{b,2}$ is given by:

$$C_{b,2} = \frac{1 - Y_2(1 - R_2)}{1 - Y_2}C_{p,1} \qquad (7.7j)$$

And R_2 is given by:

$$R_2 = 1 - \frac{C_{p,2}}{C_{p,1}} \qquad (7.7k)$$

where $C_{p,1}$ and $C_{p,2}$, the permeate concentration of the first and second passes, respectively, are given by:

$$C_{p,1} = (1 - R_1) \times C_{f,1} \qquad (7.7m)$$

$$C_{p,2} = (1 - R_t) \times C_{raw} \qquad (7.7n)$$

where R_t is the target water recovery. The relationship between $C_{f,1}$ and C_{raw} is derived by combining Eqs. (7.7c)–(7.7n):

$$\frac{C_{f,1}}{C_{raw}} = \frac{1 - Y_1(1 - Y_2)}{1 - Y_1(1 - R_1)[1 - Y_2(1 - R_2)]} \qquad (7.7p)$$

while the relationship among R_1, R_2 and R_t is given by:

$$R_t = 1 - \frac{C_{p,2}}{C_{raw}} = 1 - \frac{(1-R_2)(1-R_1)C_{f,1}}{C_{raw}}$$

$$= 1 - \frac{(1-R_1)(1-R_2)[1-Y_1(1-Y_2)]}{1-Y_1(1-R_1)[1-Y_2(1-R_2)]}$$

(7.7q)

The normalized two-pass SEC for a given total target water recovery, Y_t, and overall salt rejection, R_t, is then derived from the combination of Eqs. 7.7a-7.7q,

$$SEC_{norm,2\,passes}^{tr,ERD,recycle} = \frac{SEC_{tr,2\,passes}^{ERD,recycle}}{\pi_0} = \frac{\dot{W}_{tr,ERD}^{1st,recycle} + \dot{W}_{tr,ERD}^{2nd,recycle}}{Y_1 Y_2 Q_{f,1} f_{os} C_{raw}}$$

$$= \frac{[1-Y_1(1-Y_2)]}{1-Y_1(1-R_1)[1-Y_2(1-R_2)]} \times \frac{\left(\frac{R_1}{1-Y_1}\right)\left(\frac{1-\eta_{E1}(1-Y_1)}{\eta_{P1}}\right) + \left(\frac{R_2(1-R_1)Y_1}{1-Y_2}\right)\left(\frac{1-\eta_{E2}(1-Y_2)}{\eta_{P2}}\right)}{Y_1 Y_2}$$

(7.7r)

Equation (7r) which is applicable for operation at the limit of the thermodynamic restriction, is subject to the constraints of $0 \le R_1 < 1$, $0 \le R_2 < 1$, $0 < Y_1 \le 1$, $0 < Y_2 \le 1$, and Eqs. (7.7h) and (7.7q).

In summary, for this case, the SEC for permeate water production, normalized with respect to the feed osmotic pressure (i.e., π_0) at a target water recovery of Y_t and target salt rejection R_t for operation at the thermodynamic limit is given as [43]:

$$SEC_{norm,2\,passes}^{tr,ERD,recycle}$$

$$= \frac{[1-Y_1(1-Y_2)]}{1-Y_1(1-R_1)[1-Y_2(1-R_2)]} \times \frac{\left(\frac{R_1}{1-Y_1}\right)\left(\frac{1-\eta_{E1}(1-Y_1)}{\eta_{P1}}\right) + \left(\frac{R_2(1-R_1)Y_1}{1-Y_2}\right)\left(\frac{1-\eta_{E2}(1-Y_2)}{\eta_{P2}}\right)}{Y_1 Y_2}$$

(7.7r)

subject to the following constraints:

$$Y_t = \frac{Y_1 Y_2}{1 - Y_1(1-Y_2)}$$

(7.8)

132

$$R_t = 1 - \frac{(1-R_1)(1-R_2)[1-Y_1(1-Y_2)]}{1-Y_1(1-R_1)[1-Y_2(1-R_2)]} \qquad (7.9)$$

$$0 \le R_1 < 1, \, 0 \le R_2 < 1, \, Y_t \le Y_1 \le 1, \, 0 < Y_2 \le 1 \qquad (7.10)$$

7.3.2. Critical water recovery

In studying the impact of recycling the second-pass retentate stream to the first pass feed stream, the efficiencies of the feed pumps are taken to be independent of water recovery and feed pressure. This approach simplifies the analysis without a loss of generality regarding the overall conclusions pertaining to the comparison of the different operational models. It is noted that the feed flow rate to the second pass will be lower than the feed to the first pass. Therefore, the second pass feed pump is expected to operate at a lower efficiency relative to the first pass feed pump – a well-known characteristic pump behavior. However, a conservative analysis can be carried out by considering the efficiency of the first and second pass feed pumps to be identical. As a consequence, energy optimization is only affected within a pump efficiency factor which will drop out of the comparative analysis when considering the ratio of energy consumption for the two pass and single pass processes.

Following the above approach, extensive numerical optimizations have been carried out in this work with respect to different water recoveries, salt rejections and ERD efficiencies in the range [0 1] and results are summarized here. For the special case of the two-pass process with retentate recycling and ideal pumps (i.e., $\eta_P = 1$), it is possible to arrive at an analytical solution for the minimum $SEC_{norm,2\,passes}^{tr,ERD,recycle}$ since the optimal

133

solutions fall on the boundaries of $R_1 = 0$ or $R_2 = 0$ as shown in Chapter 6. When $R_1 = 0$,

R_2 is computed from Eq. 7.9 as follows:

$$R_2 = \frac{R_t(1 - Y_1 + Y_1 Y_2)}{(1 - Y_1 + Y_1 Y_2 R_t)} \tag{7.11}$$

Substituting Eqs. 7.9 and 7.11 into Eq. 7.7r, the normalized SEC of this two-pass process

with retentate recycling, is given by:

$$SEC^{tr,ERD,recycle}_{norm,2\,passes}\Big|_{R_1=0} = \frac{R_t(1 - Y_t)}{Y_t}[\frac{A(Y_1 + B)}{(1 - Y_1)(Y_1 - Y_t)} + C] \tag{7.12}$$

where $A = \frac{(1 - \eta_{E2} - Y_t^2)}{(1 - Y_t)}$, $B = \frac{Y_t(\eta_{E2} + Y_t - 1)}{(1 - \eta_{E2} - Y_t^2)}$ and $C = \frac{\eta_{E2} + Y_t - 1}{1 - Y_t}$. It is noted that A, B and C are

constants for each given target water recovery and second-pass ERD efficiency.

Determination of the minimum normalized SEC is equivalent to finding the minimum of

$\frac{A(Y_1 + B)}{(1 - Y_1)(Y_1 - Y_t)}$ since $SEC^{tr,ERD,recycle}_{norm,2\,passes}$ in Eq. (7.7r) is always greater than zero. It is also

equivalent to finding the maximum of $\frac{(1 - Y_1)(Y_1 - Y_t)}{A(Y_1 + B)}$ since $\frac{A(Y_1 + B)}{(1 - Y_1)(Y_1 - Y_t)}$ is always greater than

zero ($\frac{A(Y_1 + B)}{(1 - Y_1)(Y_1 - Y_t)} = \frac{1 - \eta_{E2}}{1 - Y_1} + \frac{Y_t^2}{Y_1 - Y_t} > 0$ under the constraint of Eq. (7.10)) and thus the optimum

Y_1 and corresponding minimum SEC are found to be:

$$Y_{1,opt} = \sqrt{Y_t + B(1 + Y_t + B)} - B \tag{7.13}$$

$$(SEC^{tr,ERD,recycle}_{norm,2\,passes}\Big|_{R_1=0})_{min} = \frac{R_t}{Y_t(1 - Y_t)}\left[\frac{(1 - \eta_{E2} - Y_t^2)^2}{(Y_t - \sqrt{1 - \eta_{E2}})^2} + (\eta_{E2} + Y_t - 1)(1 - Y_t)\right] \tag{7.14}$$

For Eqs. (7.13) and (7.14) to be valid, $Y_{1,opt} = \sqrt{Y_t + B(1 + Y_t + B)} - B$ has to be in the range

$[Y_t, 1]$. From Eq. (7.13), $(B + Y_{1,opt})^2 = Y_t + B(1 + Y_t + B) = Y_t + B + BY_t + B^2$, which is less

134

than $B^2 + 2B + 1 = (B+1)^2$ and larger than $Y_t^2 + BY_t + BY_t + B^2 = (Y_t + B)^2$, thus $Y_{1,opt}$ is in

the range $[Y_t, 1]$. Similarly, when $R_2 = 0$, R_1 is computed from Eq. (7.9) as follows:

$$R_1 = 1 - \frac{(1 - R_t)}{[1 - Y_1(1 - Y_2)] + Y_1(1 - Y_2)(1 - R_t)} \tag{7.15}$$

$$= 1 - \frac{(1 - R_t)}{1 - R_t Y_1(1 - Y_2)}$$

The normalized SEC of the two-pass process (Figure 7-2) with retentate recycling, is

obtained by substituting Eqs. 7.9 and 7.15 into Eq. 7.7r:

$$SEC_{norm,2\,passes}^{tr,ERD,recycle}\big|_{R_2=0} = \frac{R_t}{Y_t}\left(\frac{1}{1 - Y_1} - \eta_{E1}\right) \tag{7.16}$$

The optimum Y_1 value is obtained from $\left(\partial(SEC_{norm,2\,passes}^{tr,ERD,recycle}\big|_{R_2=0}) / \partial Y_1\right) = 0$, leading to

$$Y_{1,opt} = Y_t \tag{7.17}$$

$$\left(SEC_{norm,2\,passes}^{tr,ERD,recycle}\big|_{R_2=0}\right)_{min} = \frac{[1 - \eta_{E1}(1 - Y_t)]R_t}{Y_t(1 - Y_t)} \tag{7.18}$$

It is noted that, the global minimum SEC is the minimum of the above two minima (Eqs.

7.14 and 7.18). The SEC of the single-pass (or single stage) counterpart is given by

Eq. 7.15 and it is the same as Eq. 7.18. Therefore, if

$\left(SEC_{norm,2\,passes}^{tr,ERD,recycle}\big|_{R_1=0}\right)_{min} > \left(SEC_{norm,2\,passes}^{tr,ERD,recycle}\big|_{R_2=0}\right)_{min}$, a single-pass process will always be more

energy efficient than its two-pass counterpart. However, if

$\left(SEC_{norm,2\,passes}^{tr,ERD,recycle}\big|_{R_1=0}\right)_{min} < \left(SEC_{norm,2\,passes}^{tr,ERD,recycle}\big|_{R_2=0}\right)_{min}$ there will be a sub-domain where a two-

pass process can be of greater energy efficiency relative to a single-pass process. Finally,

if $\left(SEC_{norm,2\,passes}^{tr,ERD,recycle}\Big|_{R_1=0}\right)_{min} = \left(SEC_{norm,2\,passes}^{tr,ERD,recycle}\Big|_{R_2=0}\right)_{min}$, the optimized two-pass process is as efficient as its single-pass counterpart, but it will be less efficient if not optimized. The critical total recovery, $Y_t^{critical}$, at which the transition occurs is then determined by equating Eqs. 7.14 and 7.18 to give:

$$Y_t^{critical} = \frac{1-\eta_{E1}}{2\sqrt{1-\eta_{E2}} - (\eta_{E1}+\eta_{E2}-2)} \tag{7.19}$$

If $\eta_{E1} = \eta_{E2} = \eta_E$, the critical over water recovery is given by:

$$Y_t^{critical} = \frac{\sqrt{1-\eta_E}}{2[1+\sqrt{1-\eta_E}]} \tag{7.20}$$

Furthermore, if $\eta_{E1} = \eta_{E2} = 0$, $Y_t^{critical} = 0.25$, while if $\eta_{E1} = \eta_{E2} = 1$, $Y_t^{critical} = 0$. Eq. 7.20 (Figure 7-3) indicates that in the absence of energy recovery (i.e., $\eta_E = 0$) $Y_t^{critical}$ reduces to half the optimal recovery for a single-pass process [43] (i.e., $Y_t^{critical} = 0.5Y_{opt} = 0.25$, Eq. 7.19). On the other hand, for an ideal ERD ($\eta_E = 1$)$Y_t^{critical} = 0$, indicating that a single–pass process is more energy efficient than a two-pass process. For $Y_t \geq Y_t^{critical}$, a single-pass is always equally or more energy efficient than a two-pass process, but for $Y_t < Y_t^{critical}$, there can be a sub-domain in which a two-pass process will be more energy efficient; this would be the case only when the single-pass process is not operating at the optimal recovery at which the global minimum SEC is achieved. It should be recognized, however, that the globally optimized two-pass process, for the configuration shown in Figure 7-2, will always reduce to a single-pass process. Specific examples, that illustrate the process with second-pass retentate recycling are presented in Sections 7.3.3-7.3.5 for

desalting with energy recovery at 100% and 80% efficiency and without energy recovery to demonstrate the impact of ERD efficiency on the SEC optimization of a two-pass process with retentate recycling.
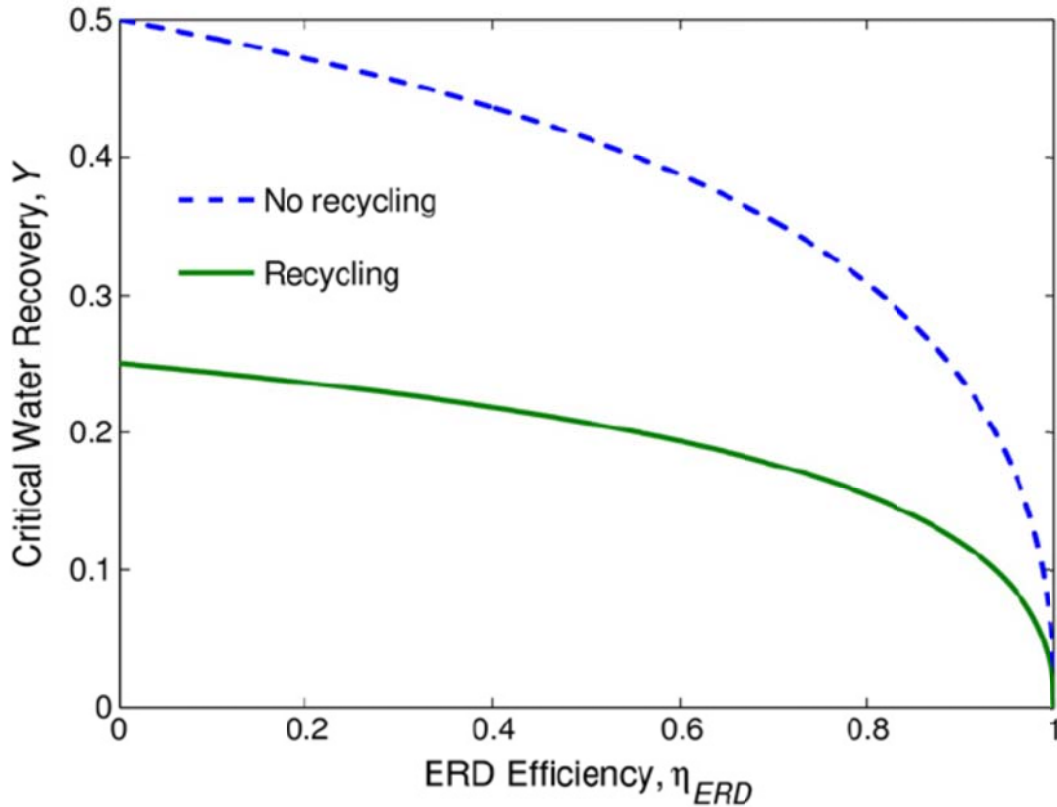
Figure 7-3. **Critical water recovery vs. ERD efficiency for the process depicted in Figure 7-2**.

7.3.3. Two-Pass Desalting with Complete Retentate Recycling and Ideal Energy Recovery

For the case of desalting with ideal energy recovery (i.e., 100%), the normalized two-pass SEC is obtained from Eq. 7.7r by setting η_{E1} and η_{E2} to unity. The critical water recovery as computed from Eq. (7.20) is zero and thus a single-pass process without recycling is always more energy efficient than a two-pass process with second-pass

137

retentate recycling. As an example, the normalized SEC, with the feed pumps taken to be ideal (i.e., $\eta_{P1} = \eta_{P2} = 1$) is plotted in Figure 7-4, for desalting operation up to the limit of the thermodynamic restriction, for a target overall water recovery (Y_t) and salt rejection (R_t) of 48% (typical water recovery in ADC pilot study [143]) and 99%, respectively. The bottom plane in Fig. 4 is the normalized SEC for a single-pass process without recycling, also operating up to the limit of the thermodynamic restriction, with the same target recovery and salt rejection as above. The results depicted in Figure 7-4 show that a single-pass process (without recycling the second-pass retentate stream to the first-pass feed stream) is more energy efficient than a two-pass process with retentate recycling, provided that both cases target the same overall water recovery and salt rejection. It is only when the two-pass process reduces to a single-pass process (the plane in Figure 7-4) that it can be as efficient as the single-pass process.
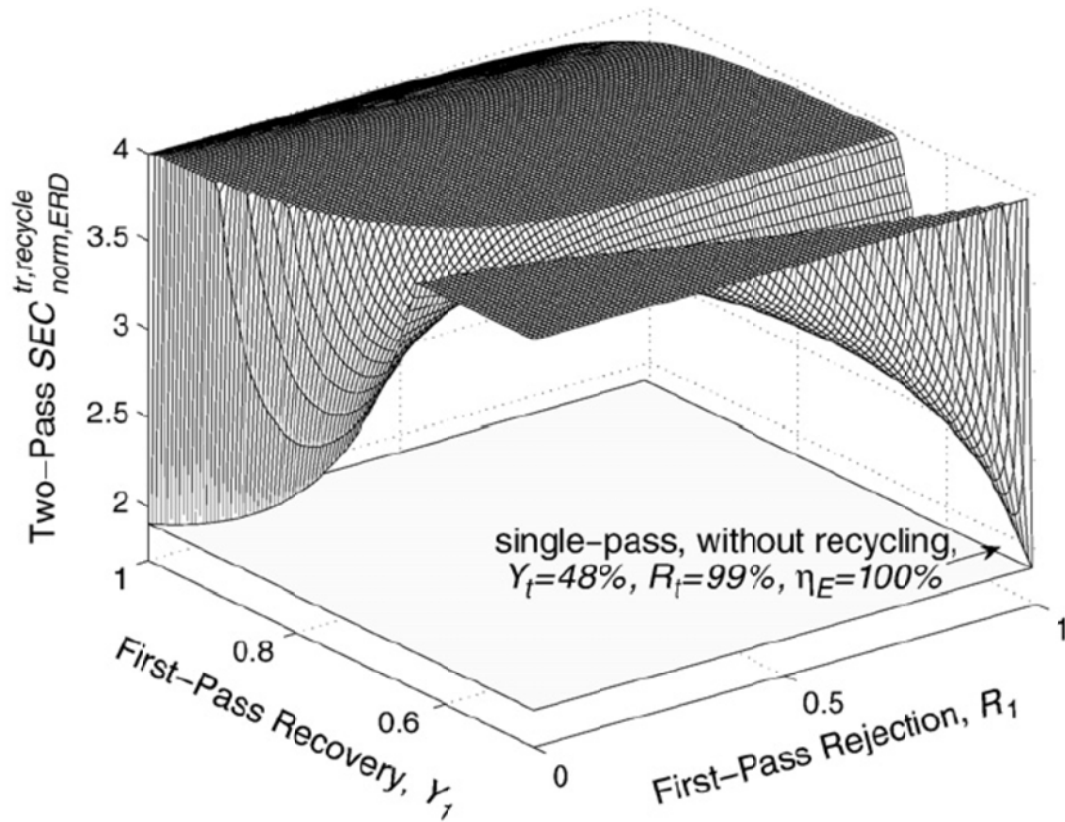
Figure 7-4. Variation of the normalized SEC of a two-pass membrane desalting process (with ERDs of 100% efficiency in each pass, therefore the critical target water recovery is zero according to Eq. 7.20), with respect to salt rejection and water recovery in the first-pass, operated up to the limit of the thermodynamic restriction, for operation with full recycling of the second-pass brine stream to the first-pass feed stream. The target water recovery and salt rejection are 48% and 99%, respectively. The plot is truncated at a normalized SEC of 4 in order to zoom in on the lower SEC region.

7.3.4. Two-Pass Desalting with Complete Retentate Recycling and Non-Ideal Energy Recovery

Illustration of the effect of non-ideal energy recovery on the normalized two-pass SEC is shown in Figure 7-5, for the case of 80% energy recovery (i.e., $\eta_{E1} = \eta_{E2} = 0.8$ in Eq. 7.7r) and ideal pumps (i.e., $\eta_{P1} = \eta_{P2} = 1$). According to Eq. 7.20, the critical overall

water recovery ($Y_t^{critical}$) is 15.45%. Figure 7-5a and b show the normalized SEC of a two-pass membrane desalting process operated up to the limit of the thermodynamic restriction, with recycling of the second-pass brine stream to the first-pass feed stream, with respect to salt rejection and water recovery in the first-pass. The target salt rejection is 99% in both Figure 7-5a and b. The target water recovery in Figure 7-5a is 15% (i.e., $< Y_t^{critical}$), while in Figure 7-5b it is 16% (i.e., $> Y_t^{critical}$). Both plots are truncated at a normalized SEC of 2.55 in order to zoom in on the lower SEC region. Figure 7-5a shows that at this specific condition ($Y_t < Y_t^{critical}$), there is a sub-domain in which the two-pass process has a lower SEC than a single-pass process operated at the same water recovery (the higher plane in Figure 7-5a). However, the optimized two-pass process has the same SEC as a single-pass process when operated at the critical water recovery. On the other hand as shown in Figure 7-5b, when the target water recovery (16%) is higher than $Y_t^{critical}$, the two-pass process would always be of a higher SEC than its single-pass counterpart operated at the same water recovery (16%, the lower plane in Figure 7-5b). It is only when the two-pass process reduces to a single-pass (the lower plane in Figure 7-5b) that it can be as efficient as the single-pass process.
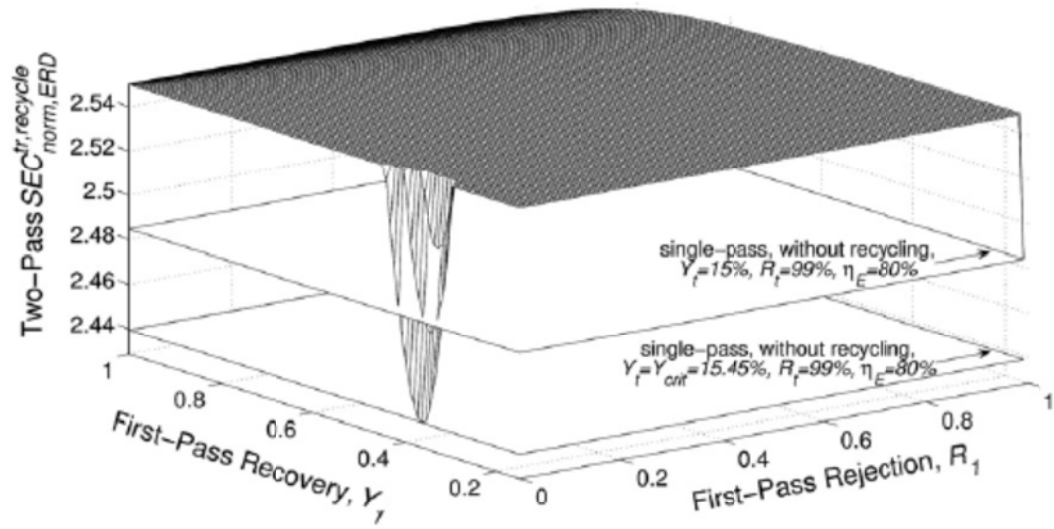
(b) $Y_t=16\%$, $R_t=99\%$, $\eta_E=80\%$
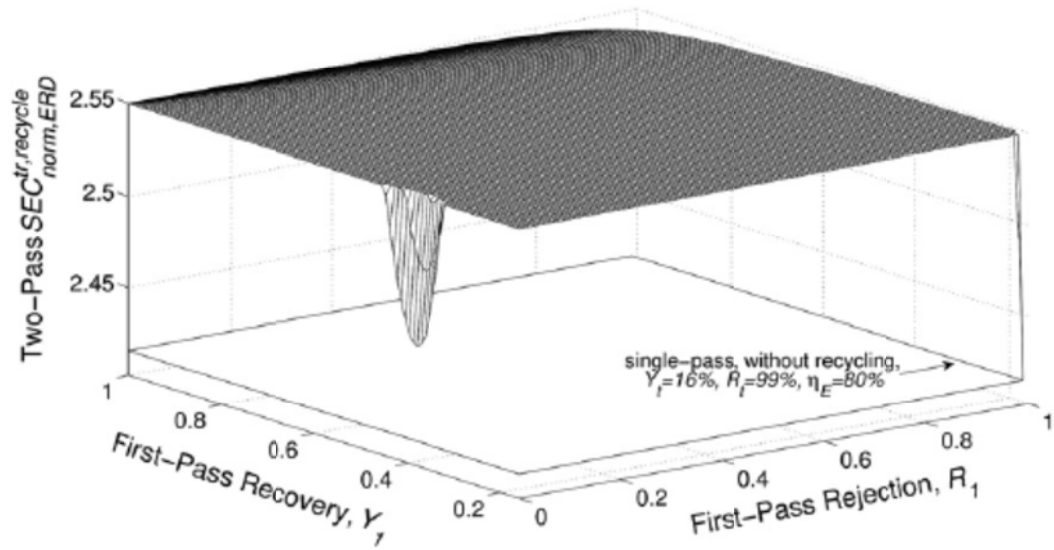
Figure 7-5. **Variation of the normalized SEC of a two-pass membrane desalting process (with ERDs of 80% efficiency in each pass, therefore the critical target water recovery is 15.45% according to Eq. 7.20) operated up to the limit of the thermodynamic restriction, with full recycling of the second-pass brine stream to the first-pass feed stream, with respect to salt rejection and water recovery in the first-pass. The target salt rejection is 99% with the target water recovery of (a) 15% (i.e., less than the critical target water recovery), and (b) 16% (i.e., greater than the critical water recovery). Both plots are truncated at a normalized SEC of 2.55 in order to zoom in on the lower SEC region.**

7.3.5. Two-Pass Desalting with Complete Retentate Recycling without Energy Recovery

The normalized SEC for two-pass desalting with ideal pumps, but without energy recovery devices (i.e., $\eta_{E1} = \eta_{E2} = 0$ and $\eta_{P1} = \eta_{P2} = 1$ in Eq. 7.7r), the normalized two-pass process SEC is illustrated in Figure 7-6a and b for recoveries above and below the critical recovery of 20% (Eq. 7.20). The two-pass membrane desalting process operated up to the limit of the thermodynamic restriction, with the recycling of the second-pass brine stream to the first-pass feed stream, with a total target salt rejection is 99%. The target water recovery in Figure 7-6a is 24% (i.e., $< Y_t^{critical}$), while in Figure 7-6b it is 26% (i.e., $> Y_t^{critical}$). Both plots are truncated at a normalized SEC of 5.6 in order to zoom in on the lower SEC region. When $Y_t < Y_t^{critical}$ (Figure 7-6a), there is a sub-domain in which the two-pass process has a lower SEC than a single-pass process when operated at the same water recovery (the higher plane in Figure 7-6a). However, the optimized two-pass process has the same SEC as a single-pass process when operated at the critical water recovery. When $Y_t > Y_t^{critical}$ (Figure 7-6b), the two-pass process always has a higher SEC than its single-pass process counterpart when operated at the same water recovery (26%, the plane in Figure 7-6b). At the optimal energy consumption state, the two-pass process reduces to a single-pass (or single-stage) process (the plane in Figure 7-6b).
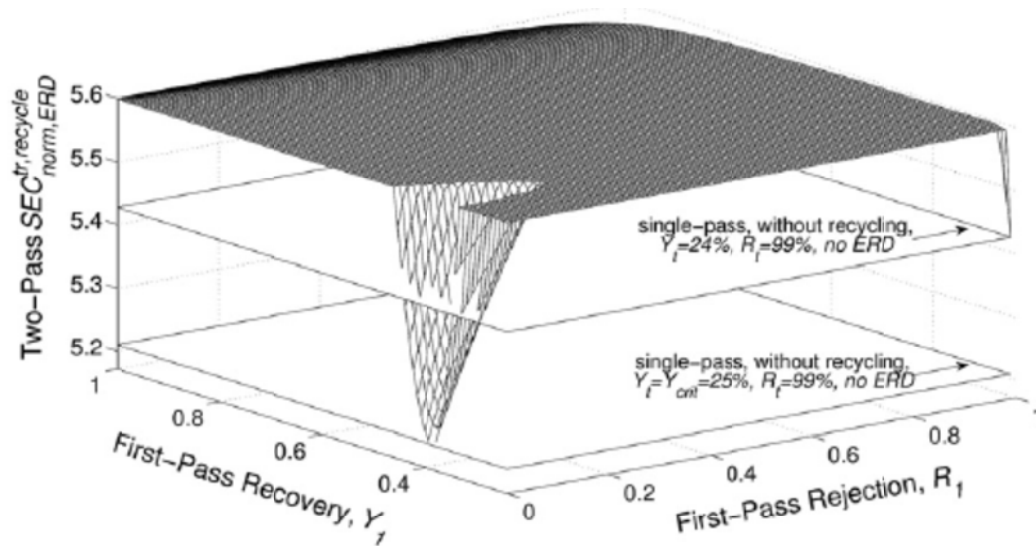
(b) $Y_t=26\%$, $R_t=99\%$, No ERD
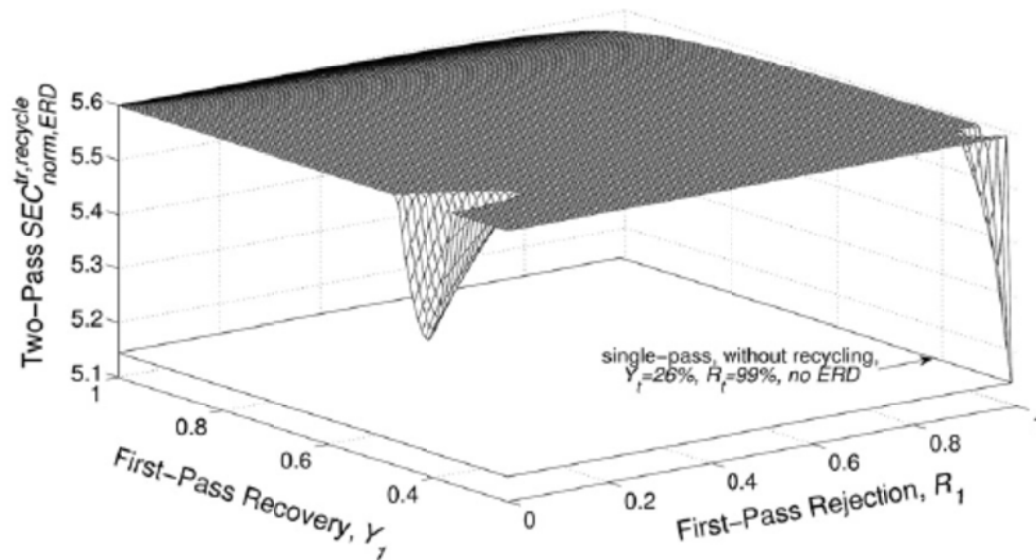
Figure 7-6. **Variation of the normalized SEC of a two-pass membrane desalting process (without ERDs, therefore the critical target water recovery is 25% according to Eq. 7.20) operated up to the limit of the thermodynamic restriction, with full recycling of the second-pass brine stream to the first-pass feed stream, with respect to salt rejection and water recovery in the first-pass. The target salt rejection is 99% with the target water recovery of (a) 24% (i.e., less than the critical target water recovery), and (b) 26% (i.e., greater than the critical water recovery). Both plots are truncated at a normalized SEC of 5.6 in order to zoom in on the lower SEC region.**

As stated in Sections 6.5 and 7.3, although membrane desalting via a two-pass process with or without recycling is less energy efficient than a single-pass (or single-stage) process, there can be situations where a two-pass process is preferred, particularly in situations of difficult to achieve rejection of certain species (boron removal [163]).

7.4. SEC optimization of two-stage RO Desalting with feed diversion to the second-stage

In considering the operation of a two-stage process, it is interesting to evaluate the potential impact of diverting part of the feed stream of the first-stage to the second-stage (in order to reduce the salinity of the feed to the second-stage RO, Figure 7-7) on the SEC optimization. Following recent analysis of the process [38], the rates of work done by the first-stage pump, $\dot{W}_{tr}^{1st}$, and second-stage pump, $\dot{W}_{tr}^{2nd}$, at the limit of the thermodynamic restriction, are given by:

$$\dot{W}_{tr}^{1st} = \frac{\pi_0}{1-Y_1} \times (Q_{f,1} + Q_{d,1}) \tag{7.21}$$

$$\dot{W}_{tr}^{2nd} = \frac{\pi_{0,2}}{1-Y_2} Q_{f,2}[1-\eta_{E_2}(1-Y_2)] - \frac{\pi_0}{1-Y_1} Q_{f,2} \tag{7.22}$$

where η_{E2} is the efficiency of the ERD in the second stage; Y_1 and Y_2 are the water recoveries in the first and second stage, respectively ($Y_1 = Q_{p,1}/Q_{f,1}$, $Y_2 = Q_{p,2}/Q_{f,2}$); $Q_{f,1}$, $Q_{p,1}$, $Q_{f,2}$ and $Q_{p,2}$ are the feed and permeate flow rates to the first and second stage, respectively ($Q_{f,2} = Q_{d,1} + (1-Y_1)Q_{f,1}$, where $Q_{d,1}$ is the raw water flow rate to the

second-stage); and π_0 and $\pi_{0,2}$ are the osmotic pressures of the feed to the first and second stage, respectively, and are related by the following (assuming 100% of salt rejection in each stage) expression:

$$\pi_{0,2} = \frac{Q_{d,1} + Q_{f,1}}{Q_{d,1} + (1 - Y_1)Q_{f,1}} \pi_0 \tag{7.23}$$
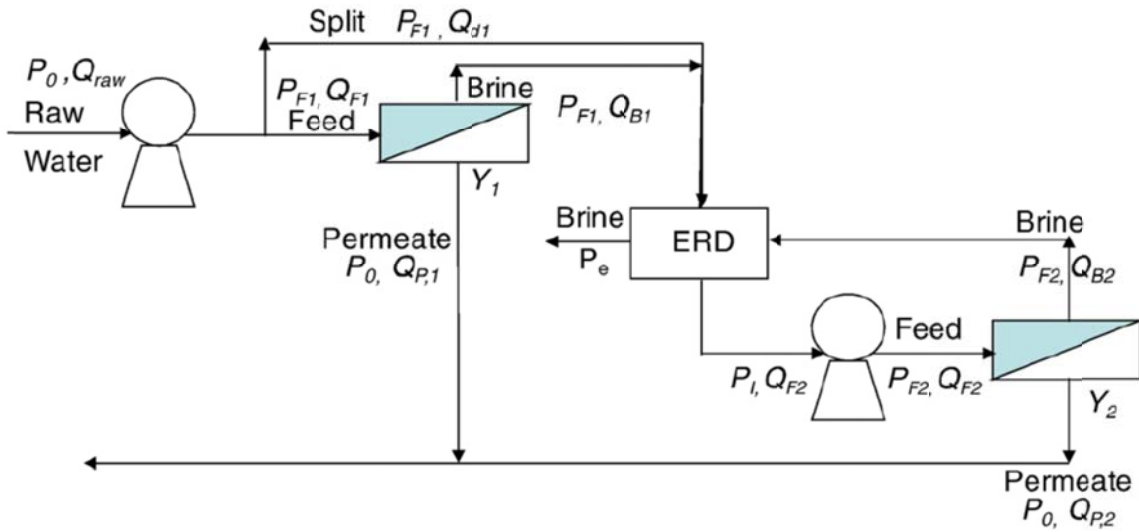
Figure 7-7. **Schematic of a two-stage RO process with part of the raw feed diverted to the second stage.**

Therefore, the average SEC of this two-stage process, normalized to the feed osmotic pressure, π_0, is given by

$$SEC_{tr,norm}^{2stgs} = \frac{\dot{W}_{tr}^{1st} + \dot{W}_{tr}^{2nd}}{(Q_{p,1} + Q_{p,2})\pi_0} \tag{7.24}$$

where

$$Q_{p,1} + Q_{p,2} = Y_t(Q_{f,1} + Q_{d,1}) \tag{7.25}$$

Combining Eqs. (7.21)-(7.25), the average SEC targeting a desired water recovery, Y_t, is dependent on the fractional water recovery in each stage and the diverted raw feed fraction, f_d, as follows:

$$SEC_{tr,norm}^{2stgs} = \frac{\frac{Y_1(1-f_d)}{1-Y_1} + \frac{1-Y_1+Y_1f_d}{1-Y_t} - \eta_{E_2}}{Y_t}$$ (7.26)

where the diverted raw feed fraction is $f_d = \frac{Q_{d,1}}{Q_{d,1}+Q_{f,1}}$. The objective is to minimize the function $SEC_{tr,norm}^{2stgs}$ in Eq. (7.26) in order to minimize the SEC, with respect to the following constraints:

$$0 \le f_d \le 1$$ (7.27)

$$0 < Y_1 < 1$$ (7.28)

$$0 < Y_2 < 1$$ (7.29)

The constraint $0 < Y_2 < 1$ requires $Y_1 < \frac{Y_t}{1-f_d}$ or $f_d > 1 - \frac{Y_t}{Y_1}$ based on the overall mass balance in Eq. (7.25).

The average SEC of a two-stage RO process without diverting the raw feed to the second stage , but targeting the same overall water recovery, Y_t, is determined by setting $f_d = 0$ in Eq. (7.26) leading to:

$$SEC_{tr,norm}^{2stgs,nd} = \frac{\frac{Y_1}{1-Y_1} + \frac{1-Y_1}{1-Y_t} - \eta_{E_2}}{Y_t}$$ (7.30)

where the superscript nd denotes "no diversion". In Eq. (7.30), $SEC_{tr,norm}^{2stgs,nd}$ is only a function of the water recovery in the first stage. Consistent with the optimization result

reported in Chapter 5, the optimum water recovery and minimum $SEC_{tr,norm}^{2stgs,nd}$ are given by:

$$Y_{1,opt} = 1 - \sqrt{1 - Y_t} \tag{7.31}$$

$$(SEC_{tr,norm}^{2stgs,nd})_{min} = \frac{\frac{2}{\sqrt{1-Y_t}} - \eta_{E_2} - 1}{Y_t} \tag{7.32}$$

The optimum (f_d, Y_1) set is obtained via a similar search algorithm used in Chapter 6. A typical result is shown in Figure 7-8, in which the bottom plane represents the minimum SEC of a two-stage RO process without diversion of the raw feed (Eq. 7.32). Figure 7-8 shows that the minimum SEC of a two-stage process with raw feed diversion occurs when $f_d = 0$, which is simply a two-stage process without feed diversion [38]. To help understand this point, one can take the diverting operation to its extreme situation, where all the feed to the first-stage is diverted to the second-stage: in this case, the two-stage RO process with diversion of the feed evolves into a single-stage RO process. As shown in Chapter 5, a single-stage RO process is less energy efficient than a two-stage RO process.
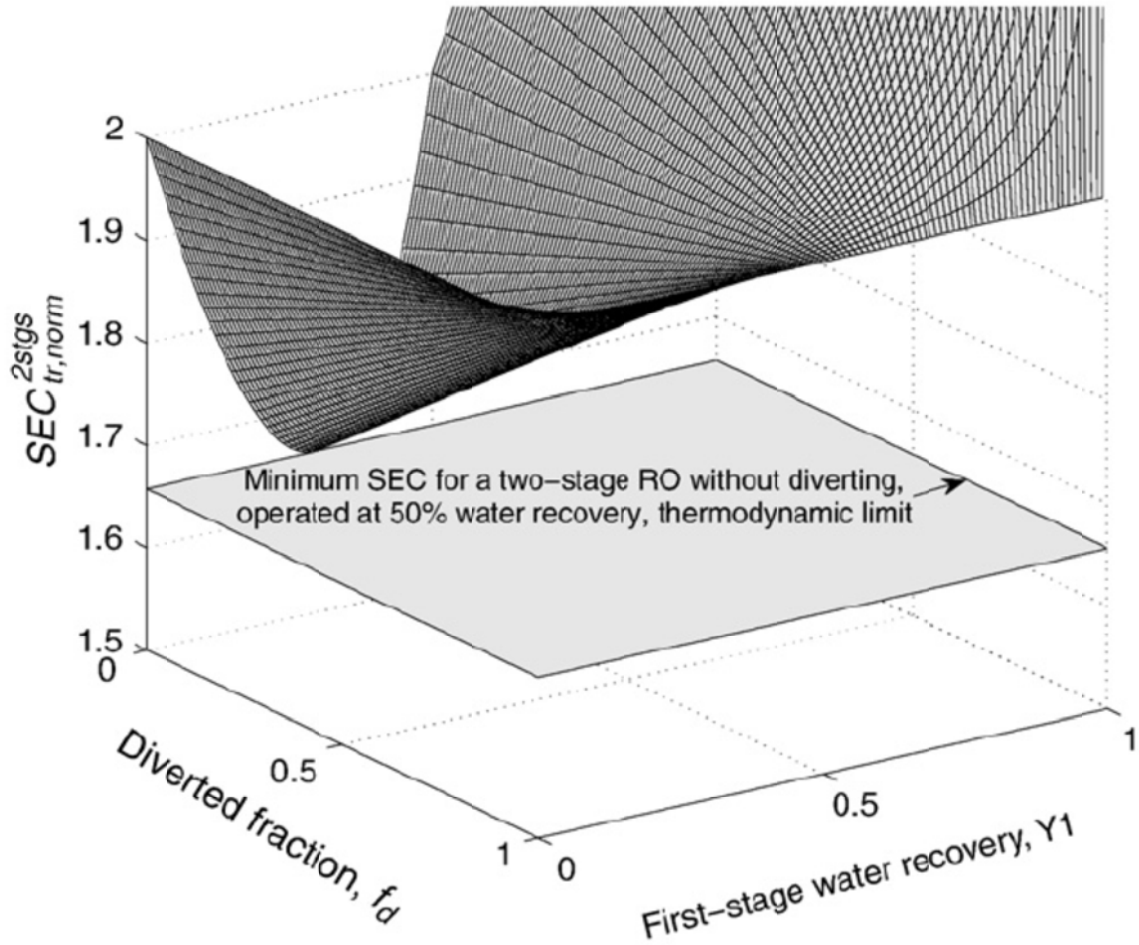
Figure 7-8. **Variation of SEC for a two-stage RO (targeting 50% of water recovery, ERD efficiency 100%) with respect to the diverted fraction and the first-stage water recovery.** f_d **is the fraction of the raw feed diverted from the first- to the second-stage RO.**

7.5.   Conclusions

The analysis clarifies that in a single-stage RO process, partial retentate recycling to the feed stream does not change the SEC, while partial permeate recycling to the feed stream increases the SEC when targeting the same overall water recovery. For a two-stage RO process, diverting part of the raw water feed from the first stage to the second-

148

stage RO does not decrease the minimum achievable SEC in the two-stage RO process. For a two-pass membrane desalination process, second-pass retentate recycling to the first-pass feed stream reduces the energy consumption relative to the case of no recycling. However, the optimal two-pass process always reduces to a single-pass (single-stage) process. In closure, the various mixing approaches considered in this chapter, while may be useful for various operational reasons, do not provide an advantage from the viewpoint of energy use reduction.

Chapter 8 Energy Consumption Optimization of Reverse Osmosis Membrane Water Desalination Subject to Feed Salinity Fluctuations

8.1. Overview

This chapter extends the analysis of Chapter 4 on energy consumption optimization to account for feed salinity fluctuations. Due to seasonal rainfalls, the feed water salinity will fluctuate both for seawater and brackish water. For example, at one location in the central San Joaquin Valley, the total dissolved solids (TDS) content deviated up to 52% from its annual average [39]. The specific objective is to determine the optimal time-varying operating policy for constant permeate productivity (i.e., constant permeate flow rate) in the presence of feed salinity fluctuations. A series of computational and experimental results are presented that demonstrate the applicability and potential in terms of energy savings of the proposed time-varying optimal operation policy. The approach of locating optimal operating points can be used as the set point for control purposes in reverse osmosis desalination systems [4, 164-167].

150

8.2. Preliminaries: RO Process Description and Modeling

In order to illustrate the proposed approach to energy cost optimization it is instructive to consider a membrane RO process without the deployment of an energy recovery device (ERD) as shown schematically in Figure 8-1.
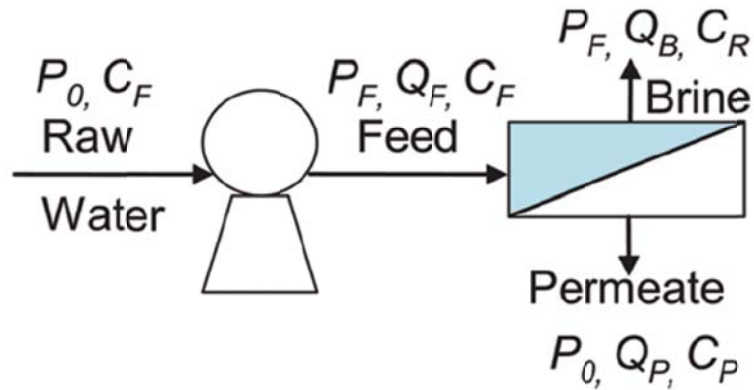
Figure 8-1.   **Schematic of simplified RO system**.

The energy cost associated with RO desalination is evaluated in the present analysis as the specific energy consumption (SEC) defined as the electrical energy needed to produce a cubic meter of permeate. Pump efficiency can be included in the following analysis in a straightforward fashion as presented in Chapter 3. As a first step, however, in order to simplify the presentation of the approach, the required electrical energy is taken to be equal to the pump work, (i.e., assuming a pump efficiency of 100%) where the more general approach is provided in Section 3.5.2. Accordingly, the SEC for the plant shown in Figure 8-1 is given by:

$$SEC = \frac{\dot{W}_{pump}}{Q_p} \tag{8.1}$$

8.3. Optimal Operation Policy for Energy Optimization

8.3.1. Feed Salinity Fluctuation and Operating Policies

For the purpose of illustration of the proposed optimal operation approach, we consider a simple feed salinity fluctuation profile shown in Figure 8-2. Specifically, consider a 20-hour time window in which the feed osmotic pressure in the first 10 hours is $500\,psi$, and it is then reduced to $200\ psi$ for the remaining 10 hours. For a single-stage RO system with constant feed flow rate Q_f, the average feed osmotic pressure is $350\ psi$. We will study the minimum specific energy consumption (SEC) of two difference cases. In case 1 (operating strategy A), the operating pressure is constant, while in case 2 (operating strategy B), it changes with the instantaneous feed osmotic pressure and will always be double that of the instantaneous feed osmotic pressure. In both cases the RO operation is at the limit of thermodynamic restriction.
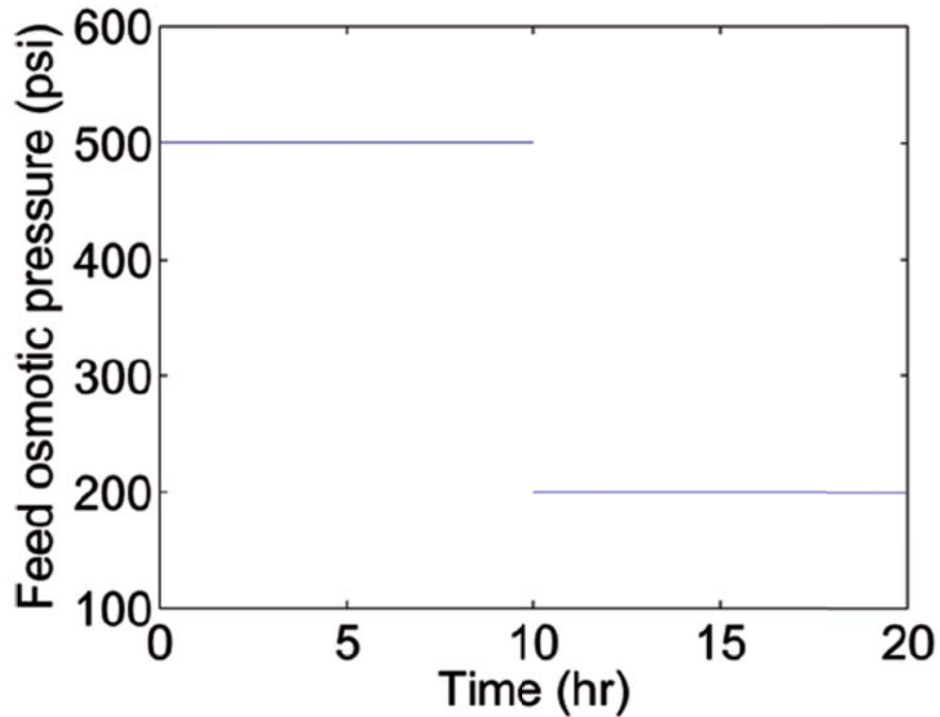
Figure 8-2.   **Feed osmotic pressure profile within 20 hours**.

In the presence of the feed salinity fluctuation of Figure 8-2, the following two operating

strategies may be considered.

- Operating strategy A: The transmembrane pressure is maintained at double that of the average (over the whole 20-hour time window) feed osmotic pressure, i.e. 700 psi.

- Operating strategy B: The transmembrane pressure is maintained at double that of the instantaneous feed osmotic pressure.

For a built plant to produce the same amount of permeate volume for both operating

strategy A and operating strategy B, the permeate flow rates in the first $10\,hrs$ and the

last $10\,hrs$ have to be the same. The specific energy consumption (SEC) comparison of

operating strategy A and operating strategy B is first considered e for an RO process

153

without an energy recovery device (see Figure 8-1) and the case of an RO process with an energy recovery device (see Figure 8-3) is subsequently addressed. In Figure 8-3, P_e and P_p are the brine discharge and permeate pressure, respectively, which are assumed here to be equal to P_0 (i.e., the atmospheric pressure) P_0.
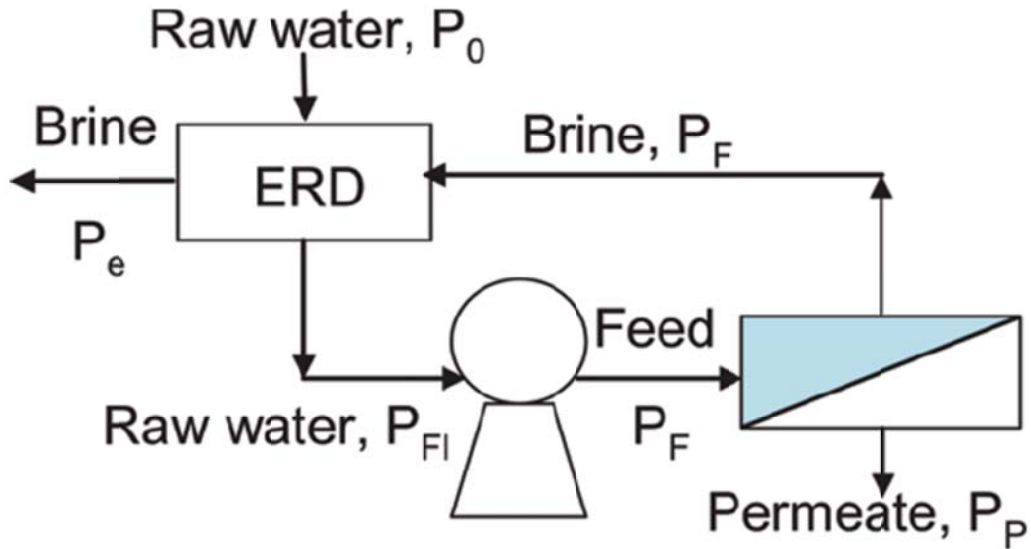
Figure 8-3.   **Simplified RO system with an energy recovery device (ERD).**

The rate of work done by the pump on the raw water, in the presence of an ERD, is given by:

$$\dot{W}_{pump} = \Delta P \times (Q_f - \eta Q_b) \tag{8.2}$$

where η is the efficiency of the energy recovery device.

8.4.   Optimal Operation Policy for an RO Process without ERD

8.4.1. Operating Strategy A

At the limit of thermodynamic restriction, the water recovery in the first 10 hrs,

$$Y_1 = 1 - \frac{500}{700} = \frac{2}{7} \tag{8.3}$$

and the water recovery in the last 10 hrs,

$$Y_2 = 1 - \frac{200}{700} = \frac{5}{7} \tag{8.4}$$

In order to produce the same amount of permeate volume, the feed flow rate in the first 10 hrs has to be 2.5 times that of the feed flow rate in the last 10 hrs ($Q_{f,2}$). Therefore, the permeate produced in the first 10 hrs computing from Eq. 8.2 is:

$$V_{p,1} = 2.5 \times Q_{f,2} \times \frac{2}{7} \times 10 \, hr = \frac{50}{7} Q_{f,2} \times hr \tag{8.5}$$

The energy consumption in the first 10 hrs is:

$$\begin{aligned} W_1 = \Delta P_1 \times V_{f,1} &= 700 \, psi \times \frac{7}{2} \times \frac{50}{7} Q_{f,2} \times hr \\ &= 17500 \, Q_{f,2} \cdot psi \cdot hr \end{aligned} \tag{8.6}$$

Similarly, the permeate produced in the last 10 hrs is:

$$V_{p,2} = Q_{f,2} \times \frac{5}{7} \times 10 \, hr = \frac{50}{7} Q_{f,2} \times hr \tag{8.7}$$

which is the same as the permeate volume in the first 10 hrs as required in this scenario. The energy consumption in the last 10 hrs is:

$$\begin{aligned} W_2 = \Delta P_2 \times V_{p,2} &= 700 \, psi \times \frac{7}{5} \times \frac{50}{7} Q_{f,2} \times hr \\ &= 7000 \, Q_{f,2} \cdot psi \cdot hr \end{aligned} \tag{8.8}$$

Therefore, the average SEC is:

$$\begin{aligned} \overline{SEC}^A = \frac{W_1 + W_2}{V_{p,1} + V_{p,2}} &= \frac{(17500 + 7000) \times Q_{f,2} \cdot psi \cdot hr}{(50/7 + 50/7) \times Q_{f,2} \times hr} \\ &= 1715 \, psi \end{aligned} \tag{8.9}$$

which can be converted into $11,824 \, kJ \, / \, m^3$, meaning that $11,824 \, kJ$ of energy is needed

to produce $1 \, m^3$ of permeate by adopting operating strategy A.

8.4.2. Operating Strategy B

The water recovery in the last 10 hrs is the same as the water recovery in the first 10 hrs

(both at 50%). In order to produce the same amount of permeate volume, the feed flow

rate in the first 10 hrs should be the same as the feed flow rate in the last 10 hrs ($Q_{f,2}'$).

The permeate produced in the first 10 hrs is:

$$V_{p,1}' = Q_{f,2}' \times \frac{1}{2} \times 10 \, hr = 5Q_{f,2}' \times hr \tag{8.10}$$

The energy consumption in the first 10 hrs is:

$$
\begin{aligned}
W_1' = \Delta P_1' \times V_{f,1}' &= 2 \times 500 \, psi \times 2 \times 5Q_{f,2}' \times hr \\
&= 10000 \, Q_{f,2}' \cdot psi \cdot hr
\end{aligned}
\tag{8.11}
$$

Similarly, the permeate produced in the last 10 hrs is:

$$V_{p,2}' = Q_{f,2}' \times \frac{1}{2} \times 10 \, hr = 5Q_{f,2}' \times hr \tag{8.12}$$

which is the same as the permeate volume in the first 10 hrs as required in this scenario.

The energy consumption in the last 10 hrs is:

$$
\begin{aligned}
W_2' = \Delta P_2' \times V_{f,2}' &= 2 \times 200 \, psi \times 2 \times 5Q_{f,2}' \times hr \\
&= 4000 \, Q_{f,2}' \cdot psi \cdot hr
\end{aligned}
\tag{8.13}
$$

Therefore, the average SEC is:

$$\overline{SEC}^B = \frac{W_1' + W_2'}{V_{p,1}' + V_{p,2}'} = \frac{(10000 + 4000) \times Q_{f,2}' \cdot psi \cdot hr}{(5+5) \times Q_{f,2}' \times hr} \tag{8.14}$$
$$= 1400 \, psi$$

which can be converted into $9,652 \, kJ/m^3$, meaning that $9,652 \, kJ$ of energy is needed to produce $1 m^3$ of permeate by adopting operating strategy B.

From Eq. 8.9 and Eq. 8.14, we see that the operating strategy A has a higher SEC than operating strategy B about 22.5% ($\frac{1715-1400}{1400} = 22.5\%$). Furthermore, in order to equate the total permeate volume in operating strategy A and operating strategy B, $Q_{f,2}' = \frac{10}{7} Q_{f,2}$. Thus, the total feed volume in operating strategy B is $2 \times \frac{10}{7} Q_{f,2} = \frac{20}{7} Q_{f,2}$, while the total feed volume in operating strategy A is $(2.5+1)Q_{f,2} = 3.5 Q_{f,2}$. Therefore, in order to obtain the same permeate volume, operating strategy A requires a higher volume of feed water, and thus, it has a lower overall water recovery.

8.5. Optimal Operation Policy for an RO Process with ERD of 100% Efficiency

8.5.1. Operating Strategy A

The water recovery in the last 10 hrs is 2.5 times that of the water recovery in the first 10 hrs. In order to produce the same amount of permeate volume, the feed flow rate in the first 10 hrs has to be 2.5 times that of the feed flow rate in the last 10 hrs ($Q_{f,2}$). The units of the flow rate in this chapter is volume per hour. Therefore, the permeate produced in the first 10 hrs is:

$$V_{p,1} = 2.5 \times Q_{f,2} \times \frac{2}{7} \times 10\,hr = \frac{50}{7} Q_{f,2} \times hr \qquad (8.15)$$

The energy consumption in the first 10 hrs is:

$$W_1^{ERD} = \Delta P_1 \times V_{p,1} = 700\,psi \times \frac{50}{7} Q_{f,2} \times hr$$
$$= 5000\,Q_{f,2} \cdot psi \cdot hr \qquad (8.16)$$

Similarly, the permeate produced in the last 10 hrs is:

$$V_{p,2} = Q_{f,2} \times \frac{5}{7} \times 10\,hr = \frac{50}{7} Q_{f,2} \times hr \qquad (8.17)$$

which is the same as the permeate volume in the first 10 hrs as required in this scenario.
The energy consumption in the last 10 hrs is:

$$W_2^{ERD} = \Delta P_2 \times V_{p,2} = 700\,psi \times \frac{50}{7} Q_{f,2} \times hr$$
$$= 5000\,Q_{f,2} \cdot psi \cdot hr \qquad (8.18)$$

Therefore, the average SEC is:

$$\overline{SEC}^A = \frac{W_1^{ERD} + W_2^{ERD}}{V_{p,1} + V_{p,2}} = \frac{(5000 + 5000) \times Q_{f,2} \cdot psi \cdot hr}{(50/7 + 50/7) \times Q_{f,2} \times hr}$$
$$= 700\,psi \qquad (8.19)$$

which can be converted into $4,826\,kJ/m^3$, meaning that $4,826\,kJ$ of energy is needed to produce $1m^3$ of permeate by adopting operating strategy A.

8.5.2. Operating Strategy B

In strategy B, the operating pressure will always be double that of the instantaneous feed osmotic pressure so that the water recovery in the last 10 hrs is the same as the water recovery in the first 10 hrs under the assumption that the system is

operated up to the limit of the thermodynamic restriction. In order to produce the permeate volume, the feed flow rate in the first 10 hrs has to be the same as that the feed flow rate in the last 10 hrs ($Q_{f,2}$'). The permeate volume produced in the first 10 hrs is:

$$V_{p,1}' = Q_{f,2}' \times \frac{1}{2} \times 10\,hr = 5Q_{f,2}' \times hr \tag{8.20}$$

The energy consumption in the first 10 hrs is:

$$\begin{aligned} W_1^{'ERD} = \Delta P_1' \times V_{p,1}' &= 2 \times 500\,psi \times 5Q_{f,2}' \times hr \\ &= 5000\,Q_{f,2}' \cdot psi \cdot hr \end{aligned} \tag{8.21}$$

Similarly, the permeate volume produced in the last 10 hrs is:

$$V_{p,2}' = Q_{f,2}' \times \frac{1}{2} \times 10\,hr = 5Q_{f,2}' \times hr \tag{8.22}$$

which is the same as the permeate volume produced in the first 10 hrs as required in this scenario. The energy consumption in the last 10 hrs is:

$$\begin{aligned} W_2^{'ERD} = \Delta P_2 \times V_{p,2}' &= 2 \times 200\,psi \times 5Q_{f,2}' \times hr \\ &= 2000\,Q_{f,2}' \cdot psi \cdot hr \end{aligned} \tag{8.23}$$

Therefore, the average SEC is:

$$\begin{aligned} \overline{SEC}^B = \frac{W_1^{'ERD} + W_2^{'ERD}}{V_{p,1}' + V_{p,2}'} &= \frac{(2000 + 5000) \times Q_{f,2}' \cdot psi \cdot hr}{(5+5) \times Q_{f,2}' \times hr} \\ &= 700\,psi \end{aligned} \tag{8.24}$$

which can be converted into $4,826\,kJ/m^3$, meaning that $4,826\,kJ$ of energy is needed to produce $1\,m^3$ of permeate by adopting operating strategy B.

From Eq. 8.19 and Eq. 8.24, it can be concluded that in the presence of an ERD of 100% efficiency, operating strategies A and B result in the same SEC. Furthermore, in order to

equate the total permeate volume in operating strategies A and B, $Q'_{f,2} = \frac{10}{7} Q_{f,2}$. Thus, the total feed volume in operating strategy B is $2 \times \frac{10}{7} Q_{f,2} \cdot hrs = \frac{20}{7} Q_{f,2} \cdot hrs$, $2 \times \frac{10}{7} Q_{f,2} = \frac{20}{7} Q_{f,2}$ while the total feed volume in operating strategy A is $(2.5+1)Q_{f,2} \cdot hrs = 3.5 Q_{f,2} \cdot hrs$. Therefore, in order to achieve the same permeate volume productivity, operating strategy A requires a higher feed water volume, and thus, it has a lower overall water recovery.

8.6. Effect of ERD Efficiency

In this subsection, the effect of ERD efficiency on the optimal operational policy subject to the feed salinity fluctuation. Similarly, two operating strategies A (constant pressure operation) and B (time-varying pressure operation) are compared.

8.6.1. Operating Strategy A

The water recovery in the last 10 hrs is 2.5 times that of the water recovery in the first 10 hrs (see Eq. 8.2 and 8.3). In order to produce the same permeate volume, the feed flow rate in the first 10 hrs has to be 2.5 times the feed flow rate in the last 10 hrs ($Q_{f,2}$). Therefore, the permeate volume produced in the first 10 hrs is:

$$V_{p,1} = 2.5 \times Q_{f,2} \times \frac{2}{7} \times 10\,hr = \frac{50}{7} Q_{f,2} \times hr \tag{8.25}$$

The energy consumption in the first 10 hrs is:

$$W_1^{ERD} = \Delta P_1 \times (V_{f,1} - \eta(V_{f,1} - V_{p,1}))$$
$$= 700\, psi \times (25 - \frac{125}{7}\eta)Q_{f,2} \times hr$$
$$= (17500 - 12500\eta)Q_{f,2} \cdot psi \cdot hr \qquad (8.26)$$

Similarly, the permeate volume produced in the last 10 hrs is:

$$V_{p,2} = Q_{f,2} \times \frac{5}{7} \times 10\, hr = \frac{50}{7}Q_{f,2} \times hr \qquad (8.27)$$

which is the same as the permeate volume in the first 10 hrs as required in this scenario.

The energy consumption in the last 10 hrs is:

$$W_2^{ERD} = \Delta P_2 \times (V_{f,2} - \eta(V_{f,2} - V_{p,2}))$$
$$= 700\, psi \times (10 - \frac{20}{7}\eta)Q_{f,2} \times hr \qquad (8.28)$$
$$= (7000 - 2000\eta)Q_{f,2} \cdot psi \cdot hr$$

Therefore, the average SEC is:

$$\overline{SEC}_{ERD}^A = \frac{W_1^{ERD} + W_2^{ERD}}{V_{p,1} + V_{p,2}}$$
$$= \frac{(17500 - 12500\eta) \cdot Q_{f,2} \cdot psi \cdot hr}{(50/7 + 50/7) \times Q_{f,2} \times hr} \qquad (8.29)$$
$$+ \frac{(7000 - 2000\eta) \cdot Q_{f,2} \cdot psi \cdot hr}{(50/7 + 50/7) \times Q_{f,2} \times hr}$$
$$= (1715 - 1015\eta)\, psi$$

which will reduce to $700\, psi$ (Eq. 8.19) when $\eta = 1$ (Section 8.5).

8.6.2. Operating Strategy B

The water recovery in the last 10 hrs is the same as the water recovery in the first 10 hrs. In order to produce the same amount of permeate volume the feed flow rate in the

first 10 hrs has to be the same as that the feed flow rate in the last 10 hrs ($Q'_{f,2}$).

Therefore, the permeate volume produced in the first 10 hrs is:

$$V'_{p,1} = Q'_{f,2} \times \frac{1}{2} \times 10\,hr = 5Q'_{f,2} \times hr \tag{8.30}$$

The energy consumption in the first 10 hrs is:

$$
\begin{aligned}
W_1^{'ERD} &= \Delta P'_1 \times (V'_{f,1} - \eta(V'_{f,1} - V'_{p,1})) \\
&= 2 \times 500\,psi \times (10 - 5\eta)Q'_{f,2} \times hr \\
&= 5000(2 - \eta)Q'_{f,2} \cdot psi \cdot hr
\end{aligned}
\tag{8.31}
$$

Similarly, the permeate volume produced in the last 10 hrs is:

$$V'_{p,2} = Q'_{f,2} \times \frac{1}{2} \times 10\,hr = 5Q'_{f,2} \times hr \tag{8.32}$$

which is the same as the permeate volume in the first 10 hrs as required in this scenario.

The energy consumption in the last 10 hrs is:

$$
\begin{aligned}
W_2^{'ERD} &= \Delta P'_2 \times (V'_{f,2} - \eta(V'_{f,2} - V'_{p,2})) \\
&= 2 \times 200\,psi \times (10 - 5\eta)Q'_{f,2} \times hr \\
&= 2000(2 - \eta)Q'_{f,2} \cdot psi \cdot hr
\end{aligned}
\tag{8.33}
$$

Therefore, the average SEC is:

$$
\begin{aligned}
\overline{SEC}_{ERD}^{B} &= \frac{W_1^{'ERD} + W_2^{'ERD}}{V'_{p,1} + V'_{p,2}} \\
&= \frac{(2000 + 5000)(2 - \eta) \times Q'_{f,2} \cdot psi \cdot hr}{(5 + 5) \times Q'_{f,2} \times hr} \\
&= 700(2 - \eta)\,psi
\end{aligned}
\tag{8.34}
$$

which will reduce to $700\,psi$ (Eq. 27) when $\eta = 1$ (Section 8.5).

The SEC difference between operational strategies A and B is $(1715 - 1015\eta) - 700(2 - \eta) \, psi = 315(1 - \eta) \, psi$. Thus, when $0 < \eta < 1$, the SEC of operating strategy A will be always greater than the SEC of operating strategy B, whereby the fractional SEC increase is,

$$\frac{\overline{SEC}_{ERD}^A - \overline{SEC}_{ERD}^B}{\overline{SEC}_{ERD}^B} = \frac{315(1-\eta)}{700(2-\eta)} = \frac{315}{700} \frac{(1-\eta)}{[1+(1-\eta)]} \qquad (8.35)$$

which is plotted in Figure 8-4. For example, when the ERD efficiency is 90%, the fractional SEC increase is 4.1%. Furthermore, in order to equate the total permeate volume in operating strategy A and operating strategy B, $Q_{f,2}' \cdot hrs = \frac{10}{7} Q_{f,2} \cdot hrs$. $Q_{f,2}' = \frac{10}{7} Q_{f,2}$. Thus, the total feed volume in operating strategy B is $2 \times \frac{10}{7} Q_{f,2} \cdot hrs = \frac{20}{7} Q_{f,2} \cdot hrs$ $2 \times \frac{10}{7} Q_{f,2} = \frac{20}{7} Q_{f,2}$, while the total feed volume in operating strategy A is $(2.5 + 1) Q_{f,2} \cdot hrs = 3.5 Q_{f,2} \cdot hrs$. $(2.5 + 1) Q_{f,2} = 3.5 Q_{f,2}$ Therefore, in order to get the same amount of permeate volume, operating strategy A requires greater volume of feed water, and thus, it has a lower overall water recovery.
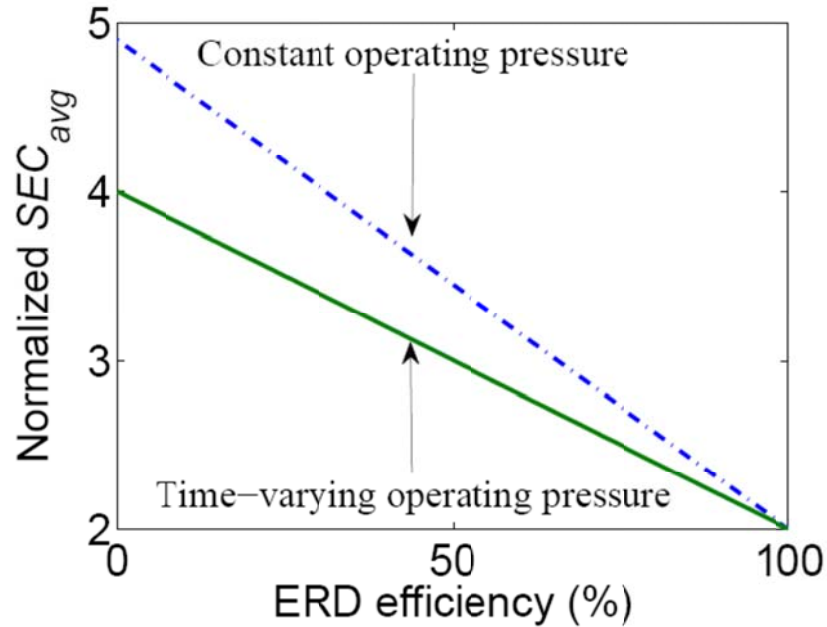
Figure 8-4.   **Variation of normalized SEC for operating strategy A (dash-dotted line) and B (solid line) with respect to ERD efficiency in the presence of 42.9% of feed fluctuation (Figure 8-2). The SEC is normalized with respect to the average feed osmotic pressure (i.e., 350 psi for the feed fluctuation profile in Figure 8-2).**

In summary, operating strategy A requires processing of larger volume of feed water relative to strategy B in order to obtain the same permeate volume and also has a higher SEC. In operating strategy B, adjusting the operating pressure to be at double that of the instantaneous feed osmotic pressure, enables the RO system to process less volume of feed water for producing an equivalent permeate volume and thus results in a lower SEC.

8.7.   Experimental Study

8.7.1. Experimental System

In order to test the proposed optimal operation policy, an experimental demonstration was conducted using the water desalination system shown in Figure 8-5. The

experimental system includes a feed tank, filters, pressure vessels, membrane modules, pumps, variable frequency drivers, valves, actuators, sensors (pH, temperature, conductivity, flow rate) and a data acquisition system. A detailed description of the system can be found elsewhere [164-166].
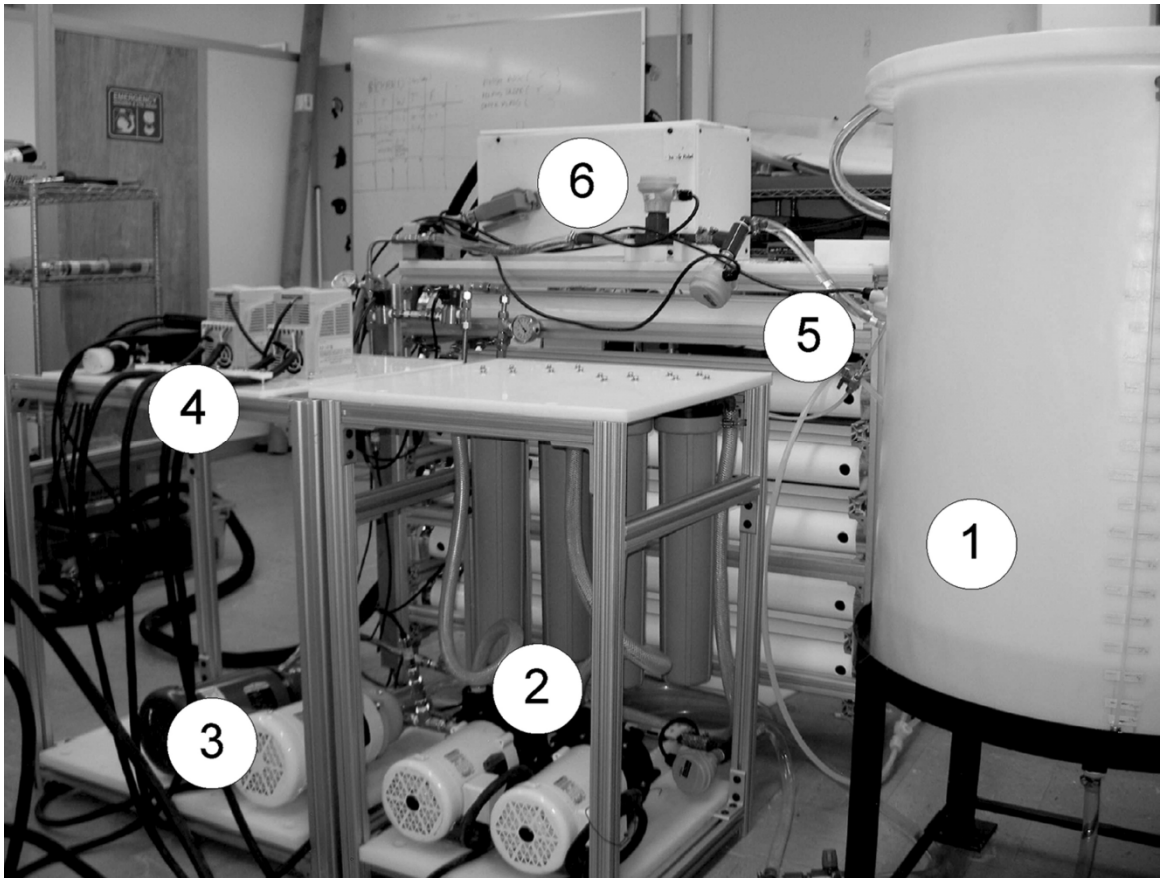
Figure 8-5. **UCLA experimental RO membrane water desalination system. Legend: (1) feed tank, (2) low-pressure pumps and prefiltration, (3) high-pressure positive displacement pumps, (4) variable frequency drives (VFDs), (5) pressure vessels containing spiral-wound membrane units (three sets of six membranes in series), and (6) National Instruments data acquisition hardware and various sensors**.

8.7.2. Experimental Design

Table 8-1.   Feed fluctuation experimental design.

	Strategy B		Strategy A	
	Experiment 1	Experiment 2	Experiment 3	Experiment 4
FC (mg/L)	$C_{f,1}$	$C_{f,2}$	$C_{f,1}$	$C_{f,2}$
PF (gpm)	Q_p	Q_p	Q_p	Q_p
FP (psi)	ΔP_1	ΔP_2	$\frac{1}{2}(\Delta P_1 + \Delta P_2)$	$\frac{1}{2}(\Delta P_1 + \Delta P_2)$
FF (gpm)	$Q_{f,1}$	$Q_{f,2}$	$Q_{f,3}$	$Q_{f,4}$
Y	50%	50%	Y_3	Y_4

(FC: feed concentration; FP: feed pressure; PF: permeate flow; Y: water recovery; RF: retentate flow; RC: retentate concentration; SEC: specific energy consumption.)

Based on the calculations of Section 8.4, a series of experiments were carried out to compare the SEC of the two different operating strategies, A and B, described in Section 8.3.. Strategy A constitutes an operation at a fixed pressure, while strategy B involves adjustment of the feed operating pressure to achieve 50% water recovery because 50% the optimal water recovery for RO without an ERD.. Specifically, the experimental procedure is as follows:

1.   Fix the feed concentration to be $C_{f,1}$;

2.   Adjust the RO feed flow rate $Q_{f,1}$ and RO feed pressure ΔP_1 to achieve 50% water recovery and record the resulting permeate flow rate $Q_{p,1}$;

3.   Adjust the RO feed concentration to $C_{f,2}$;

4.   Adjust the RO feed flow rate $Q_{f,2}$ and RO feed pressure ΔP_2 to achieve the same water recovery and permeate flow rate as those in step 2 (i.e., 50% water recovery and at the recorded $Q_{p,2} = Q_{p,1} = Q_p$);

5.   Maintain the feed concentration to $C_{f,2}$, tune the RO feed pressure to $\frac{1}{2}(\Delta P_1 + \Delta P_2)$ and the permeate flow rate to Q_p, and record the resulting feed flow rate $Q_{f,4}$ and water recovery Y_4;

6.   Adjust the feed concentration back to $C_{f,1}$;

7.   Adjust the RO feed pressure to $\frac{1}{2}(\Delta P_1 + \Delta P_2)$ and the permeate flow rate to Q_p, and record the resulting feed flow rate $Q_{f,3}$ and water recovery Y_3.

Two different feed solutions, i.e., $C_{f,1} = 9000\, mg\,/\,L$ (feed osmotic pressure is $104\, psi$) and $C_{f,2} = 5000\, mg\,/\,L$ (feed osmotic pressure is $60\, psi$) of feed water were desalinated at $25^{\circ}\mathrm{C}$ using Dow Filmtec XLE-2540 RO membranes. The feed, retentate and permeate pressure, flow rate and conductivity were measured in the experiments.

8.7.3. Experimental Results

The experimental results are listed in Table 8-2. The first column is the experimental set number as in Table 8-1. In experiments 1 and 2, the system was operated at 50% water recovery, producing 1 *gpm* of product permeate water, and the resulting feed pressures in the system were 230 *psi* (10% above the thermodynamic restriction in terms of applied pressure, see Eq. 8.6) and 149 *psi* (24% above the thermodynamic restriction in terms of applied pressure, see Eq. 8.6), respectively. According to the experimental procedure, experiments 3 and 4 are operated at the average pressure of experiments 1 and 2, i.e., 190 *psi*.

167

On the basis of the experimental results of Table 8-2, it is concluded that varying the feed pressure with time (strategy B) leads to substantial SEC savings. However, it is important to elaborate further on these experimental results and put them into perspective with respect to the type of experimental system used to carry them out. Specifically, referring to the results of Table 8-2, the water recovery decreases while the operating pressure increases from 149 *psi* to 190 *psi* for the same feed salinity when switching from experiment 2 to experiment 3. This is due to the physical limitations of the experimental system. In particular, the available settings of retentate valves and pump speed do not allow to regulate the feed pressure and feed flow rate independently.

Therefore, in order to increase the feed pressure and maintain the permeate flow to be 1 *gpm*, the high pressure pumps have to run faster, and thus, more water is discharged in the brine stream, thereby decreasing the water recovery. If the feed pressure and feed flow rate were possible to be adjusted independently (with an appropriate pump and valve choice), an estimate of the resulting SEC for such an operation can be computed as follows: specifically, instead of lower water recovery, the water recovery would increase as shown in Table 8-3. As limited by the thermodynamic restriction, the maximum water recovery in this case would be

$Y = 1 - \dfrac{\pi_0}{\Delta P} = 1 - \frac{60}{190} = 0.68 \ 1 - \frac{60}{190} = 0.68$ (see Eq. 8.6). If the system were to operate

(in terms of feed pressure) 10% above the thermodynamic limit pressure, the water recovery would be $1 - \frac{60}{190/(1+10\%)} = 0.65$ (see Eq. 8.6). If the system were to

operate 24% above the thermodynamic restriction, the water recovery would be $1 - \frac{60}{190/(1+24\%)} = 0.6$ (see Eq. 8.6 and the numbers shown in the parenthesis of Table 3). Similarly for experiment 4, the system cannot reach the permeate flow of 1 *gpm*, while operated at 190 *psi*, due to the physical limitations discussed above. However, a similar calculation to the one made for experiment 3 would lead to a water recovery of $1 - \frac{104}{190/(1+10\%)} = 0.4$ (if the system were to operate 10% above the thermodynamic restriction) and $1 - \frac{104}{190/(1+24\%)} = 0.32$ (if the system were to operate 24% above the thermodynamic restriction) as shown in Table 8-3.

Finally, another average case is to operate the RO process with feed pressures which are 17% (i.e., average of 24% and 10%) above the thermodynamic limit pressure for both experiments 3 and 4 as shown in Table 8-4; this would lead to water recoveries $Y = 1 - \frac{\pi_0}{\Delta P} = 1 - \frac{60}{190/(1+17\%)} = 0.63$ and

$Y = 1 - \frac{\pi_0}{\Delta P} = 1 - \frac{104}{190/(1+17\%)} = 0.36$, $1 - \frac{104}{190/(1+17\%)} = 0.36$ respectively. In this case, the average SEC is 415 *psi* for strategy A, which is about 9.5% higher than the average SEC of strategy B. In summary, in all of the cases (Tables Table 8-2– Table 8-4), the average SECs are $384 - 452$ *psi* and 379 *psi* for strategies A and B, respectively; therefore it can be concluded, both from the experimental results and the analysis, that it is better, from an energy optimization point-of-view, to adjust the feed pressure targeting 50% water recovery (strategy B) instead of adopting a constant operating pressure (strategy A).

Table 8-2.   Experimental results.

Set	FC (mg/L)	FP (psi)	PF (gpm)	Y	RF (gpm)	RC (mg/L)	SEC (psi)	SEC_{avg} (psi)
1	10400	230	1	0.50	1	35000	460	Strategy B
2	6000	149	1	0.50	1	19600	298	379
3	6000	190	1	0.19	4.25	12200	1000	Strategy A
4	10400	190	0.57	0.41	0.82	30000	463	805

(FC: feed concentration; FP: feed pressure; PF: permeate flow; Y: water recovery; RF: retentate flow; RC: retentate concentration; SEC: specific energy consumption.)

Table 8-3.   Experimental results and analysis.

Set	FC (mg / L)	FP (psi)	PF (gpm)	Y	SEC (psi)	SEC_{avg} (psi)
1	9000	230	1	0.50	460	Strategy B
2	5000	149	1	0.50	298	379
3*	5000	190	1	0.65(0.6)	292(316)	Strategy A
4*	9000	190	1	0.4(0.32)	475(594)	384(452)

(FC: feed concentration; FP: feed pressure; PF: permeate flow; Y: water recovery; RF: retentate flow; RC: retentate concentration; SEC: specific energy consumption. Data inside and before the parenthesis in strategy A are calculated based on the assumption that the RO processes are operated 24% and 10% above the corresponding thermodynamic limit pressures, respectively.)

Table 8-4.   Experimental results and analysis (2).

Set	FC(mg/L)	FP(psi)	PF(gpm)	Y	SEC(psi)	SEC_{avg} (psi)
1	9000	230	1	0.50	460	Strategy B
2	5000	149	1	0.50	298	379
3**	5000	190	1	0.63	302	Strategy A
4**	9000	190	1	0.36	528	415

(FC: feed concentration; FP: feed pressure; PF: permeate flow; Y: water recovery; RF: retentate flow; RC: retentate concentration; SEC: specific energy consumption. Data in sets 3** and 4** for strategy A are calculated based on the assumption that the feed pressures are 17% above the corresponding thermodynamic limit pressure, respectively.)

8.8.   Effect of the Feed Salinity Fluctuation Percentage on Energy Savings

The effect of the amplitude of feed salinity fluctuation on energy savings can be studied following the same procedure presented in Section 8.4, 8.5 and 8.6 Assuming the fractional feed fluctuation is σ (for example, the fractional feed flucturation in Figure 8-2 is 500/((500+200)/2)-1=3/7) and the average osmotic pressure is π_0 , π_0 then the osmotic pressure in the first 10 hrs is $(1+\sigma)\pi_0$ ($0<\sigma<1$), and the osmotic pressure in the last 10 hrs is $(1-\sigma)\pi_0$ . . σ Similarly, the following two operating strategies may be considered.

- Operating strategy A: The transmembrane pressure is maintained at double that of the average feed osmotic pressure, i.e. $2\pi_0$.

- Operating strategy B: The transmembrane pressure is maintained at double

that of the instantaneous feed osmotic pressure.

8.8.1. Operating strategy A

The water recovery in the last 10 hrs, $Y_1 = 1 - \frac{(1+\sigma)\pi_0}{2\pi_0} = \frac{1-\sigma}{2}$, and in the last 10 hrs,

$Y_2 = 1 - \frac{(1-\sigma)\pi_0}{2\pi_0} = \frac{1+\sigma}{2}$. In order to produce the same amount of permeate volume, the feed

flow rate in the first 10 hrs has to be $\frac{1+\sigma}{1-\sigma}$ times that of the feed flow rate in the last 10 hrs

$(Q_{f,2})$. The permeate produced in the first 10 hrs is:

$$V_{p,1} = \frac{1+\sigma}{1-\sigma} \times Q_{f,2} \times \frac{1-\sigma}{2} \times 10\,hr = 5(1+\sigma) \cdot Q_{f,2} \cdot hr \tag{8.36}$$

The energy consumption in the first 10 hrs is:

$$
\begin{aligned}
W_1^{ERD} &= \Delta P_1 \times (V_{f,1} - \eta(V_{f,1} - V_{p,1})) \\
&= 2\pi_0 \times [(1-\eta)(\frac{10(1+\sigma)}{(1-\sigma)} + 5\eta(1+\sigma))] \cdot Q_{f,2} \cdot hr \\
&= 10[\frac{2(1-\eta)(1+\sigma)}{1-\sigma} + \eta(1+\sigma)] \cdot \pi_0 \cdot Q_{f,2} \cdot hr
\end{aligned}
\tag{8.37}
$$

Similarly, the permeate produced in the last 10 hrs is:

$$V_{p,2} = Q_{f,2} \times \frac{1+\sigma}{2} \times 10\,hr = 5(1+\sigma) \cdot Q_{f,2} \cdot hr \tag{8.38}$$

which is the same as the permeate volume in the first 10 hrs as required in this scenario.

The energy consumption in the last 10 hrs is:

$$
\begin{aligned}
W_2^{ERD} &= \Delta P_2 \times (V_{f,2} - \eta(V_{f,2} - V_{p,2})) \\
&= 2\pi_0 \times [10 - \eta(10 - 5(1+\sigma))] \cdot Q_{f,2} \cdot hr \\
&= 10[2(1-\eta) + \eta(1+\sigma)] \cdot \pi_0 \cdot Q_{f,2} \cdot hr
\end{aligned}
\tag{8.39}
$$

Therefore, the average SEC is:

172

$$\overline{SEC}_{ERD}^{A} = \frac{W_1^{ERD} + W_2^{ERD}}{V_{p,1} + V_{p,2}}$$

$$= \frac{10[\frac{2(1-\eta)(1+\sigma)}{1-\sigma} + \eta(1+\sigma)]}{2 \times 5(1+\sigma) \cdot Q_{f,2} \cdot hr} \cdot \pi_0 \cdot Q_{f,2} \cdot hr$$

$$+ \frac{10[2(1-\eta) + \eta(1+\sigma)]}{2 \times 5(1+\sigma) \cdot Q_{f,2} \cdot hr} \cdot \pi_0 \cdot Q_{f,2} \cdot hr \qquad (8.40)$$

$$= \frac{\frac{2(1-\eta)(1+\sigma)}{1-\sigma} + 2\eta(1+\sigma) + 2(1-\eta)}{1+\sigma} \cdot \pi_0$$

$$= 2[\frac{(1-\eta)}{1-\sigma} + \frac{(1+\eta\sigma)}{1+\sigma}] \cdot \pi_0$$

8.8.2. Operating strategy B

The water recovery in the last 10 hrs is the same as the water recovery in the first 10 hrs. In order to produce the same amount of permeate volume, the feed flow rate in the first 10 hrs has to be the same as the feed flow rate in the last 10 hrs ($Q_{f,2}'$). The permeate produced in the first 10 hrs is:

$$V_{p,1}' = Q_{f,2}' \times \frac{1}{2} \times 10\, hr = 5Q_{f,2}' \times hr \qquad (8.41)$$

The energy consumption in the first 10 hrs is:

$$W_1^{'ERD} = \Delta P_1' \times (V_{f,1}' - \eta(V_{f,1}' - V_{p,1}'))$$
$$= 2 \times (1+\sigma) \cdot \pi_0 \times (10 - 5\eta)Q_{f,2}' \times hr \qquad (8.42)$$
$$= 10 \times (1+\sigma)(2-\eta) \cdot \pi_0 \cdot Q_{f,2}' \cdot hr$$

Similarly, the permeate produced in the last 10 hrs is:

$$V_{p,2}' = Q_{f,2}' \times \frac{1}{2} \times 10\, hr = 5Q_{f,2}' \times hr \qquad (8.43)$$

which is the same as the permeate volume in the first 10 hrs as required in this scenario. The energy consumption in the last 10 hrs is:

173

$$W_2^{'ERD} = \Delta P_2 \times (V_{f,2}' - \eta(V_{f,2}' - V_{p,2}'))$$
$$= 2 \times (1-\sigma) \cdot \pi_0 \times (10 - 5\eta)Q_{f,2}' \times hr \qquad (8.44)$$
$$= 10 \times (1-\sigma)(2-\eta) \cdot \pi_0 \cdot Q_{f,2}' \cdot hr$$

Therefore, the average SEC is:

$$\overline{SEC}_{ERD}^B = \frac{W_1^{'ERD} + W_2^{'ERD}}{V_{p,1}' + V_{p,2}'}$$
$$= \frac{10(1-\sigma+1+\sigma)(2-\eta) \cdot \pi_0 \cdot Q_{f,2}' \cdot hr}{(5+5) \times Q_{f,2}' \times hr} \qquad (8.45)$$
$$= 2(2-\eta) \cdot \pi_0$$

The SEC difference of operating strategy A from operating strategy B is $(2[\frac{(1-\eta)}{1-\sigma} + \frac{(1+\eta\sigma)}{1+\sigma}] - 2(2-\eta)) \cdot \pi_0$. When $0 < \eta < 1$, the SEC of operating strategy A will be always greater than the SEC of operating strategy B. The fractional SEC increase is:

$$\frac{\overline{SEC}_{ERD}^A - \overline{SEC}_{ERD}^B}{\overline{SEC}_{ERD}^B}$$
$$= \frac{2[\frac{(1-\eta)}{1-\sigma} + \frac{(1+\eta\sigma)}{1+\sigma}] - 2(2-\eta)}{2(2-\eta)} \qquad (8.46)$$
$$= \frac{1}{(2-\eta)}[\frac{(1-\eta)}{1-\sigma} + \frac{(1+\eta\sigma)}{1+\sigma}] - 1$$

which is plotted in Figure 8-6 when the efficiency of the ERD is set to be 90%. Figure 8-6 shows that as the feed salinity fluctuation percentage increases, the time-invariant operation increases the SEC more remarkably. Furthermore, while in some cases there is only marginal energy savings, it is still worthwhile to adopt the proposed time-varying operating strategy since future feed salinity fluctuation profiles are unknown. Finally, in order to equate the total permeate volume in operating strategy A and operating strategy B, $Q_{f,2}' = (1+\sigma)Q_{f,2}$. Thus, the total feed volume in operating strategy B is $2(1+\sigma) \cdot Q_{f,2}$,

while the total feed volume in operating strategy A is

$(\frac{1+\sigma}{1-\sigma}+1)Q_{f,2} = (1+\frac{2\sigma}{1-\sigma}+1)Q_{f,2} > (1+2\sigma+1)Q_{f,2}$. Therefore, in order to get the same

amount of permeate volume, operating strategy A requires a higher amount of feed water,

and thus, it has a lower overall water recovery.
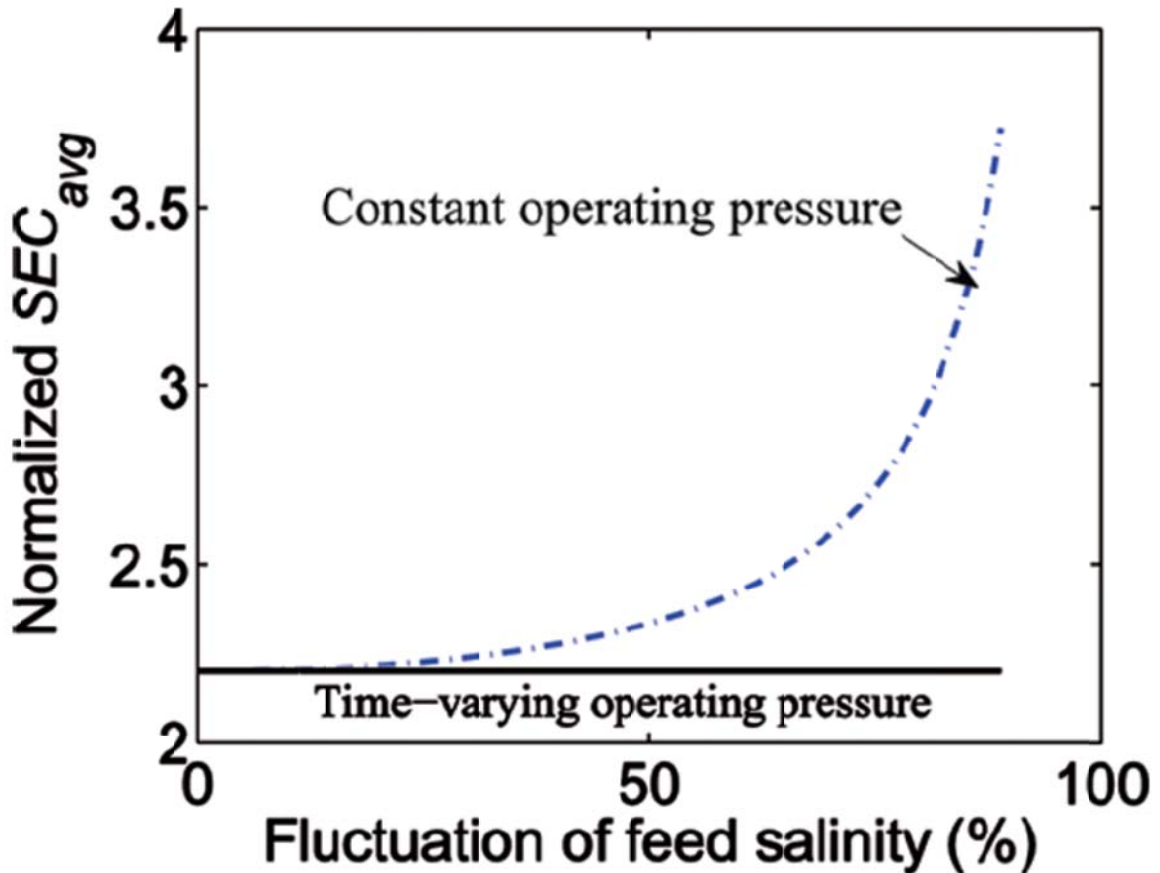
Figure 8-6.   **Variation of normalized SEC for operating strategy A (dash-dotted line) and B (solid line) with respect to feed salinity fluctuation in the presence of an ERD of 90% efficiency. The SEC is normalized with respect to the average feed osmotic pressure (i.e., 350 psi for the feed fluctuation profile in Figure 8-2).**

8.9. Conclusions

Based on a simple analysis for a reverse osmosis membrane desalination process given a specific feed concentration fluctuation profile, we found that the specific energy consumption can be substantially reduced, providing the same permeate flow. Even though in some cases there is only marginal energy savings, it is still worthwhile to adopt the proposed operating strategy given the lack of knowledge of future feed salinity profile. The other benefit of using the proposed approach is that it requires less amount of feed water since it has a higher overall water recovery than the time-invariant operating strategy. Higher overall water recovery will be more favorable especially when the concentrate stream disposal cost is high.

Chapter 9 Reducing Energy Consumption in Reverse Osmosis Desalination: Cyclic or Multi-Stage Operation?

9.1. Overview

Operating RO desalination as a thermodynamically reversible process would be most energy efficient. Therefore, one would argue that a dead-end RO desalting configuration with gradually increasing transmembrane pressure is the most energy optimal process approach to RO desalination. However, in a dead-end filtration process concentration polarization will be at a higher level and thus increased fouling propensity, relative to a crossflow filtration. In order to mimic dead-end filtration while retaining the advantage of crossflow filtration operation, a semi-continuous cross-flow RO operation can be deployed [42]. In such an approach, one employs total recycling of the retentate stream while continuously adding fresh feed at the same rate of permeate withdrawal. Once the threshold osmotic pressure is achieved, the system is drained of the concentrated holdup solution and the process is repeated. In this type of operation as in a multi-stage operation, the transmembrane pressure is raised gradually as the osmotic pressure of the retentate stream rises with increased recovery. However, the cyclic RO operation requires only one RO stage and thus less capital expenditure compared to a multi-stage process. However, a multi-stage process requires greater membrane area and additional expenditure of interstage pumps although it is more energy efficient than a single-stage RO process. Given the above considerations, in order to compare the energy consumption and overall process cost for the cyclic versus a single and multi-stage

177

processes it is necessary to first expand the analysis of the two-stage process presented in Chapter 5 to include the cost of interstage pumping and define the recovery in the cyclic process, taking into account the semi-batch nature of this operation, in a manner that allows direct comparison with the single or multi-stage processes. Subsequently, a detailed analysis is presented along with a comparison of the energy consumption relative to the single- and two-stage RO processes.

9.2. Modeling of single-stage and cyclic operation

In a continuous single-stage RO processes the retentate stream is discharged continuously, while the entire retentate stream in the cyclic RO process is recycled back to mix with the fresh feed which is then fed to the RO module. In the cyclic operation, the permeate flow rate is equal to the fresh feed flow rate Q_0 $(Q_0 = Q_p)$. Moreover, since the retentate stream is not continuously discharged in the cyclic RO process, the salts concentration in the holdup volume in the system increases with time since the salts introduced with the feed are rejected by the membrane while producing water at a permeate flow rate of Q_p. As a result, in a cyclic operation, the required feed pressure to produce permeate at the desired flow rate also increases with time. Therefore, the cyclic RO process is an inherently unsteady state process, irrespective of whether the permeate flow rate is time-varying or constant.
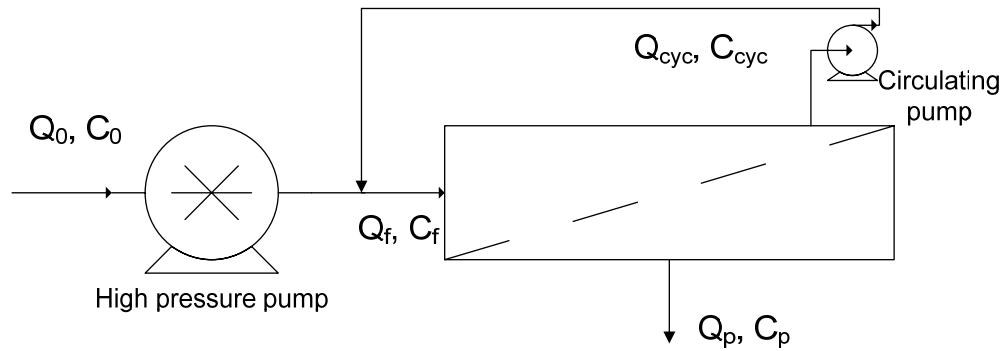
a. Schematic of cyclic operation
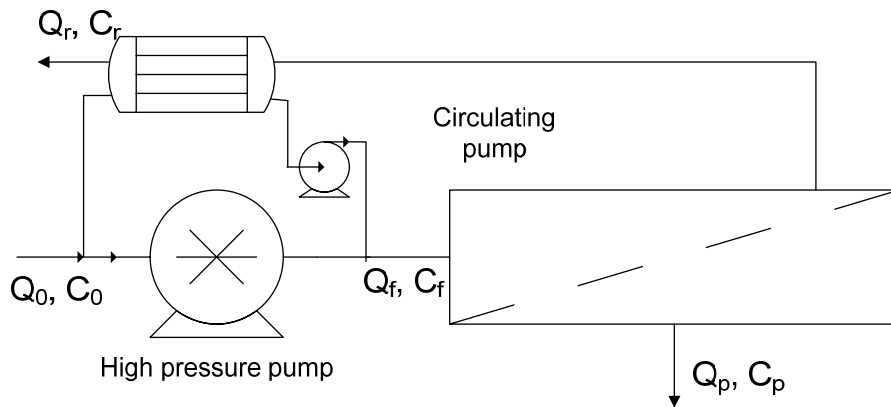
b. Schematic of continuous single-stage
operation with energy recovery

Figure 9-1. **Schematics of a cyclic RO system (a) and a continuous single-stage RO system with an ERD (b).**

Comparison of the energy efficiency of the cyclic and continuous single-stage RO process has to be done on the same basis, i.e., same water recovery and same permeate flow rate for the same membrane area (A_m). Accordingly, one needs to first recognize that overall water recovery of the cyclic system is not *100%* even though the permeate and feed flow rates are equal $(Q_0 = Q_p) \cdot (Q_0 = Q_p)$ Moreover, the cyclic operation is non-continuous with respect to time since it has to be stopped after running for a period of

time, say t_f, in order to drain/discard the t_f concentrate holdup in the membrane module once the designated pressure threshold is reached (e.g., maximum pressure rating for the RO vessel or in order to avoid mineral scaling and fouling) or as specified by the system operator. After the designated period of operation, the system has to be flushed with the fresh raw feed in order to restore the salt concentration in the RO system to its initial value (C_0). Therefore, within the time period from $t=0$ to t_f, the cumulative water recovery (Y) is the ratio of the total volume of permeate produced over the total feed volume (permeate volume plus the water hold-up capacity of the system, V_0), as quantified by the following relation:

$$Y = \frac{Q_p t_f}{Q_p t_f + V_0} \tag{9.1}$$

Since the cyclic operation is non-continuous with respect to time, there is also a down time, t_d, which includes time interval between two subsequent cycles in addition to the time for discharging the concentrate holdup in the system and restarting another cycle. Accordingly, it is convenient to define a down-time ratio, α_d given as:

$$\alpha_d = \frac{t_d}{t_f + t_d} \tag{9.2}$$

It is important to note that in principle it is possible for the cyclic RO process to continuously produce a permeate stream. In such an approach, during the discharging period (when $t = t_f$), t_f the cyclic operation can be switched to non-cyclic single-stage cross-flow operation mode by diverting the brine stream to discharge but without the energy recovery, to dilute the concentrate holdup in the system. During the diluting

operation, due to the concentration polarization inherent to permeate production, the salt concentration in the system cannot be restored to the fresh feed water concentration C_0. Therefore, in the subsequent cycle the system will start from an initial salt concentration that is higher than C_0, which would result in a higher SEC for the subsequent cycle. Following the same reasoning, each cycle will start from a higher initial concentration than its previous cycle, and therefore the system will eventually have to be shut down and flushed with the raw feed (without permeate production) or stored permeate. If permeate flushing is utilized, then this would amount to an equivalent downtime ratio with regards to permeate production as captured in the Eq. 9.2. In short, irrespective of the mode of cyclic operation (i.e., with or without permeate production during flushing with the raw feed or permeate), a hold-up volume of high salinity concentrate has to be eventually discharged, and thus the holdup volume is included in the definition of the overall recovery for the cyclic process (Eq. 9.1).

9.2.1. SEC of continuous single-stage RO process

The effective desalination (filtration) time is less than the operation time of the cyclic system. It then follows that when the down-time ratio is taken into account, the effective permeate flow rate in each cycle ($t_f + t_d$) has to be $t_f + t_d$ multiplied by a factor $[1-\alpha_d]$. Therefore, the equivalent permeate flow rate for a continuous single-stage RO system, $Q_{p,sseq}$, to produce the same permeate volume in the same operational period (t_f+t_f) is given by:

$$Q_{p,sseq} = [1-\alpha_d]Q_p \qquad (9.3)$$

and the normalized specific energy consumption $SEC_{ss,erd,norm}$ for the single-stage RO system with an ERD is given by Eq. 3.36 in Chapter 3 [38, 152], based on ether the log-mean or arithmetic osmotic pressure averages Eqs. 3.7a and 3.7b is given as:

$$SEC_{ss,erd,norm} = \left(\frac{Q_{p,sseq}}{A_m L_p \pi_0} + \frac{1}{Y} ln \left[\frac{1}{1-Y} \right] \right) \left(\frac{1 - \eta_{erd}[1-Y]}{Y} \right) \qquad (9.4a)$$

$$SEC_{ss,erd,norm} = \left(\frac{Q_{p,sseq}}{A_m L_p \pi_0} + \frac{1-Y/2}{1-Y} \right) \left(\frac{1 - \eta_{erd}[1-Y]}{Y} \right) \qquad (9.4b)$$

in which π_0 is the fresh feed osmotic pressure and η_{erd} is the ERD efficiency. The two SEC expressions based on the log-mean (Eq. 9.4a) and arithmetic (Eq. 9.4b) averages [146] provide alternate SEC estimates based on manner of averaging the osmotic pressure on feed-brine side for the purpose of computing the applied pressure. As shown in Figure 3-12 Chapter 3 the two averages are very close to each other and the difference resulting in the pressure calculation from the use of the two different osmotic pressure averaging methods (log-mean and arithmetic average) is within 4.5% for water recoveries less than 40%, but they deviate from each other for water recoveries higher than 40%. It is noted that linear averaging of the osmotic pressure is typically accepted in RO system design even at water recoveries higher than 40% [136, 167]. However, in order to evaluate the difference in the two averaging procedures (i.e., log-mean and arithmetic averages), a series of computer simulations were run in Chapter 10 for different feed pressures and flow rates and the permeate flow rate, concentration and retentate pressure simulated. For each simulation, the membrane surface osmotic pressure difference between the feed-brine and permeate side is obtained by subtracting the simulated frictional pressure drop

and net driving pressure from the transmembrane pressure. Afterwards, the simulated osmotic pressure difference at the membrane surface is compared with the arithmetic and log-mean averages in Figure 9-2, which suggests that the arithmetic averaging is more accurate for water recoveries higher than 40%. Therefore, in the presentation of this work, the arithmetical average is used to calculate the osmotic pressure at the feed-brine side. The details of the simulation are described in Chapter 10.
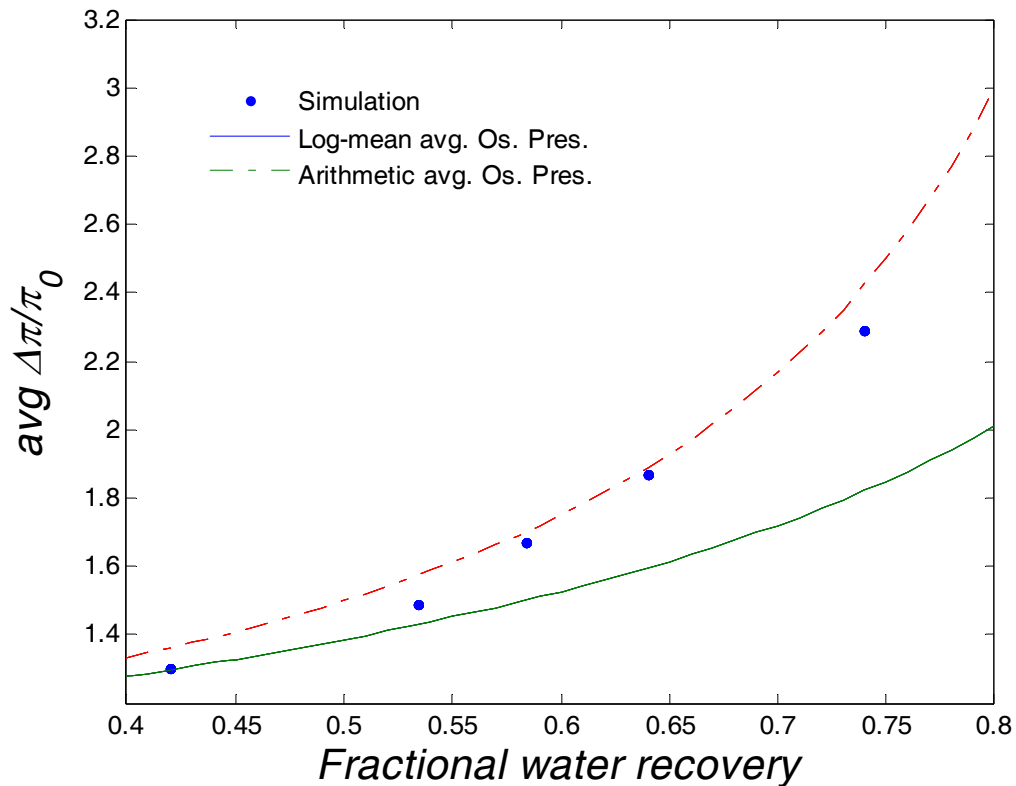
Figure 9-2. Simulated feed-brine side average osmotic pressure profile in comparison with log-mean and arithmetic average osmotic pressures computed (Eq. 3.27 from Chapter 3) from **Table 10-3** in Chapter 10 (simulation details are provided in Chapter 10 with simulation conditions listed in **Table 10-1**.).

The specific energy consumption (SEC) for the cyclic RO process is defined as the electrical energy consumed by the RO pump per product water volume produced (Chapter 3). In the cyclic RO process, the feed pressure profile increases with time as the osmotic pressure in the system rises due to the salt accumulation within the system holdup volume. Therefore, the change in mixed-cup osmotic pressure in the system is first quantified is first derived with a discussion of the effect of concentration polarization on the computed SEC subsequently provided in Section 10.2.

The SEC for the cyclic RO process is calculated as follows:

$$SEC_{cyc} = \frac{\int_0^{t_f} \frac{\dot{W}}{\eta_P} dt}{\int_0^{t_f} Q_p dt} \tag{9.5}$$

where η_P is the pump efficiency (a function of Q_0 and P_f) and Q_p is the permeate stream flow rate. The theoretical minimum required rate of pump work $\dot{W}$, at time t, is the product of pressure difference and flow rate, given as follows:

$$\dot{W} = (P_f - P_0)Q_0 \tag{9.6}$$

where Q_0 is the fresh feed water flow rate, P_0 is the atmospheric pressure and P_f is the feed pressure to the RO module. It is noted that Eq. 9.6 evolves from the mechanical energy equation or the extended Bernoulli equation and the velocity term and frictional pressure drop from the raw water source to the RO module inlet ($v^2/2 \sim 1$ (m/s)^2) is at least two orders of magnitude less than the pressure term ($\Delta P/\rho \sim 100,000/1,000$ (m/s)$^2 =$ 100 (m/s)^2) for RO water desalination and therefore they are neglected in Eq. 9.6. P_f in

Eq. 9.6 can be back-calculated from the classical dependence of the permeate flow rate Q_p on the pressure driving force in RO processes [150]:

$$Q_p = A_m L_p (P_f - P_p - \overline{\Delta\pi}) = A_m L_p (P_f - P_p - f_{cyc} f_{os} \overline{C} + f_{os} C_p) \tag{9.7}$$

where A_m is the active membrane surface area, L_p is the membrane permeability, $\overline{C}$ is the instantaneous mixed-cup average salt concentration at the feed-brine side, P_p is the permeate stream pressure. It is noted that the frictional pressure drop inside the membrane module is neglected in Eq. 9.7 as it only accounts for less than 1% of the applied pressure as shown in Chapter 3. Also, f_{os} is the osmotic pressure coefficient, and f_{cyc} is a correction factor to account for the concentration polarization effect. The linear dependence of the osmotic pressure on the salt concentration [150] is assumed in Eq. 9.7 since a linear dependence of osmotic pressure on concentration was validated in Chapter 3 (Figure 3-3) for a salinity range of 1,000 ppm - 70,000 ppm, which covers the salinity range encountered in seawater desalination.

The instantaneous location-averaged salt concentration, $\overline{C}$, in Eq. 9.7, which is used to calculate the average osmotic pressure inside the RO membrane module for the cyclic operation, is determined by the salt mass balance for the system:

$$Q_0 C_0 - Q_p C_p = V_o \frac{d\overline{C}}{dt} \tag{9.8}$$

with the following initial condition:

$$t = 0, \ \overline{C} = C_0 \tag{9.9}$$

185

where V_o is the water hold-up volume of the cyclic RO system, C_0 is the fresh feed water concentration (the system is initially assumed to be filled with the fresh feed water), and C_p is the permeate concentration of the permeate stream collected in a time interval from t to $t+dt$. The integration of Eq. (9.8) with its initial condition of Eq. 9.9.9 leads to:

$$\overline{C} = \frac{\int_0^t \left(Q_0 C_0 - Q_p C_p \right) dt}{V_0} + C_0 \tag{9.10}$$

Substituting Eq. 9.10 into Eq. 9.7 to solve for the feed pressure P_f,

$$P_f = \frac{Q_p}{A_m L_p} + P_p + f_{os} \left(f_{cyc} \left[\frac{\int_0^t \left(Q_0 C_0 - Q_p C_p \right) dt}{V_0} + C_0 \right] - C_p \right) \tag{9.11}$$

And upon substituting Eq. 9.11 into Eq. 9.10, the pump work from 0 to t_f can be computed as follows:

$$W = \int_0^{t_f} \left[\frac{Q_p}{A_m L_p} + P_p - P_0 + f_{os} \left(f_{cyc} \left[\frac{\int_0^T \left(Q_0 C_0 - Q_p C_p \right) dt}{V_0} + C_0 \right] - C_p \right) \right] \frac{Q_0}{\eta_P} dT \tag{9.12}$$

Thus, the specific energy consumption (SEC) of the cyclic operation from time 0 to t_f can be obtained by substituting Eq. 9.12 into Eq. 9.5,

$$SEC_{cyc} = \frac{\int_0^{t_f} \left[\frac{Q_p}{A_m L_p} + P_p - P_0 + f_{os} \left(f_{cyc} \left[\frac{\int_0^T \left(Q_0 C_0 - Q_p C_p \right) dt}{V_0} + C_0 \right] - C_p \right) \right] \frac{Q_0}{\eta_P} dT}{\int_0^{t_f} Q_p dT} \tag{9.13a}$$

186

In order to compare the cyclic process and the continuous single-stage RO process on the same basis, a number of assumptions are invoked when using Eq. 9.13a to simplify the analysis while retaining the essence of the quantitative comparison. First, it is noted that the electrical energy needed to discharge the concentrated water in the cyclic system during the down time period is negligible compared to the pressure energy for desalting and therefore it is neglected in computing the SEC of the cyclic RO system. Also, the additional electrical energy consumed by the circulating pump used in the cyclic RO process and the continuous single-stage RO process is not included in the comparison as it is reasonable to assume that these two pumps consume little energy. Generally the permeate-side concentration is much lower compared to the retentate-side concentration $\left(C_p << C_0 \right)$ due to the high rejection of the RO membranes (> 95%); therefore the C_p term can be neglected in Eq. 9.13a. Also, the permeate pressure is usually at the atmospheric pressure, therefore P_p and P_o cancel out in Eq. 9.13a; or the permeate pressure is sufficiently small compared to the feed pressure in Eq. 9.7 and can be neglected. The permeate flow rate Q_p can be assumed to be constant for the sake of comparing the cyclic system with a continuous single-stage RO process at the same productivity level. The pump efficiency η_p can be assumed to be 100% for the purpose of comparing the two processes as any other efficiency would have to be assumed to also be identical for the two processes in order to provide a fair comparison. Once the above assumptions, Eq. 9.13a can be simplified as:

$$ SEC_{cyc} = \frac{Q_p}{A_m L_p} + f_{os} C_0 \frac{\int_0^{t_f} f_{cyc} dt}{t_f} + \frac{f_{os} Q_0 C_0}{V_0} \frac{\int_0^{t_f} f_{cyc} t dt}{t_f} \qquad (9.13b) $$

where an equivalent correction factor, f_{cp}, is introduced f_{cp} to account for concentration polarization and match the following equation with Eq. (9.13b):

$$SEC_{cyc} = \frac{W}{t_f Q_p} = \frac{Q_p}{A_m L_p} + f_{cp} f_{os} C_0 + f_{cp} \frac{f_{os} C_0 Q_p}{2V_0} t_f \tag{9.13c}$$

For each infinitesimal time interval dt, the incremental water recovery is sufficiently small that it is reasonable to assume that f_{cp} approaches unity (equivalent to stating that concentration polarization is negligible for sufficiently small water recovery). Therefore Eq. 9.13c is rewritten as:

$$SEC_{cyc} = \frac{W}{t_f Q_p} = \frac{Q_p}{A_m L_p} + f_{os} C_0 + \frac{f_{os} C_f Q_p}{2V_0} t_f \tag{9.13d}$$

which indicates that the SEC_{cyc} increases with operation time t_f for a given Q_p, A_m, L_p, and C_0. The effect of this correction factor f_{cp} on the comparison of the cyclic and continuous single-stage is discussed in the following paragraphs.

Combining Eqs. 9.1 and 9.13d and eliminating the time variable t_f leads to the dependence of SEC on water recovery for the cyclic RO system:

$$SEC_{cyc} = \frac{Q_p}{A_m L_p} + f_{os} C_0 + \frac{f_{os} C_f}{2} \frac{Y}{1-Y} = \frac{Q_p}{A_m L_p} + \frac{\pi_0}{2} \frac{2-Y}{1-Y} \tag{9.14a}$$

Therefore, the SEC normalized with respect to feed osmotic pressure π_0 is given by:

$$SEC_{cyc,norm} = \frac{Q_p}{A_m L_p \pi_0} + \frac{1-Y/2}{1-Y} \tag{9.14b}$$

which enables comparison of the SECs for the cyclic and single-stage systems at the

same level of water recovery and normalized permeate flow rate ($\dfrac{Q_p}{A_m L_p \pi_0}$).

9.3.   SEC comparison between cyclic and continuous single-stage RO process

9.3.1. Comparison under 100% energy recovery in continuous single-stage RO process and zero downtime in cyclic RO process

When the downtime ratio approaches zero and the ERD efficiency is 100%, the SEC for

the cyclic RO process (Eq. 9.14b) is the same as the SEC for the continuous single-stage

RO process when the feed-brine side average osmotic pressure is evaluated by the

arithmetic average (Eq. 9.4b). However, the SEC for the cyclic RO process (Eq. 9.14b) is

greater than the SEC for the continuous single-stage RO process when the feed-brine side

average osmotic pressure is evaluated by log-mean average (Eq. 9.4a) since $\dfrac{1-Y/2}{1-Y} >$

$\dfrac{1}{Y}\ln\left[\dfrac{1}{1-Y}\right]$ for any Y in the range of [0 1] and any normalized permeate flow rate. As an

example, the solid line of $f_{cp}=1$ in Figure 9-3 shows the fractional increase of the

normalized SEC, as a function of target water recovery, when switching from a

continuous single-stage RO desalting (log-mean average of osmotic pressure is used) to a

cyclic operation while producing the normalized permeate flow rate, $\dfrac{Q_p}{A_m L_p \pi_0}=0.5$

(which is 10.5 GFD for a typical seawater desalination process when Dow FilmTec RO membrane SW30XLE-400i is used as shown in Chapter 3).

9.3.2. Impact of concentration polarization in the cyclic operation

When concentration polarization is considered, i.e., $f_{cp} > 1$ f_{cp} the SEC for the cyclic operation is underestimated as indicated by the bottom curve ($f_{cp} = 1$) in Figure 9-3. A simple evaluation of the sensitivity of the result on concentration polarization is shown in Figure # for $f_{cp} = 1$ (bottom curve and line), $f_{cp} = 1.1$ (middle curve and line) and $f_{cp} = 1.2$ (top curve and line). Consistent with Figure 9-2, the pressure difference results in a similar difference between the SECs computed using the two different averaging methods (Figure 9-3); as expected, this difference decreases as the normalized permeate flow rate increases (Figure 9-3). It is found that the inclusion of the concentration polarization effect does not change the conclusion that a cyclic operation is less energy efficient than a continuous single-stage RO process with 100% energy recovery operated at the same normalized permeate flow rate and water recovery. This conclusion is independent on which averaging is used for the feed-brine side osmotic pressure of the continuous single-stage RO system.
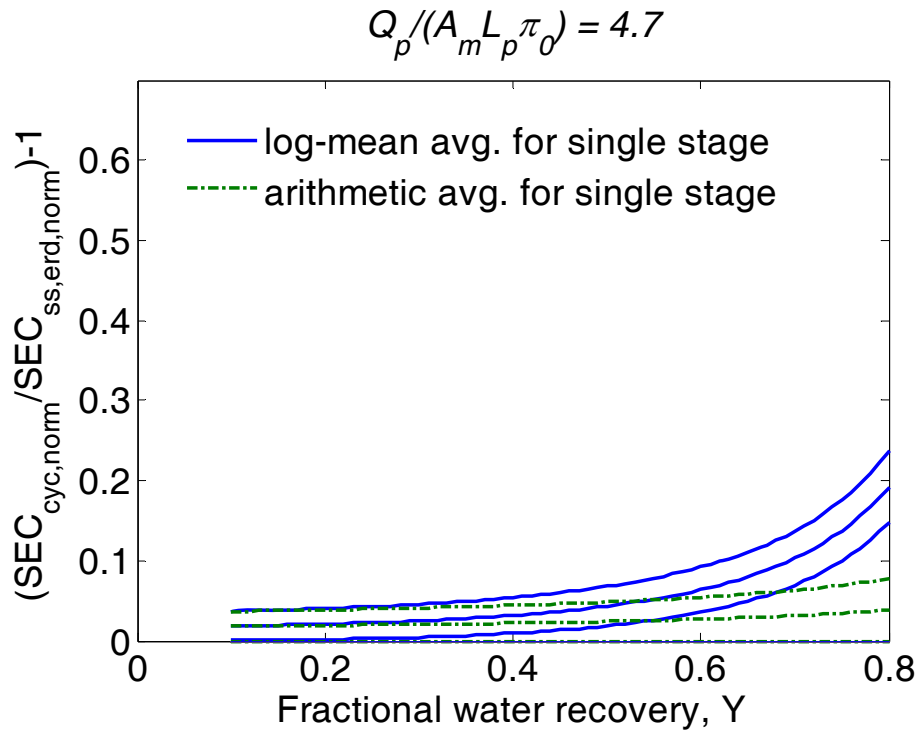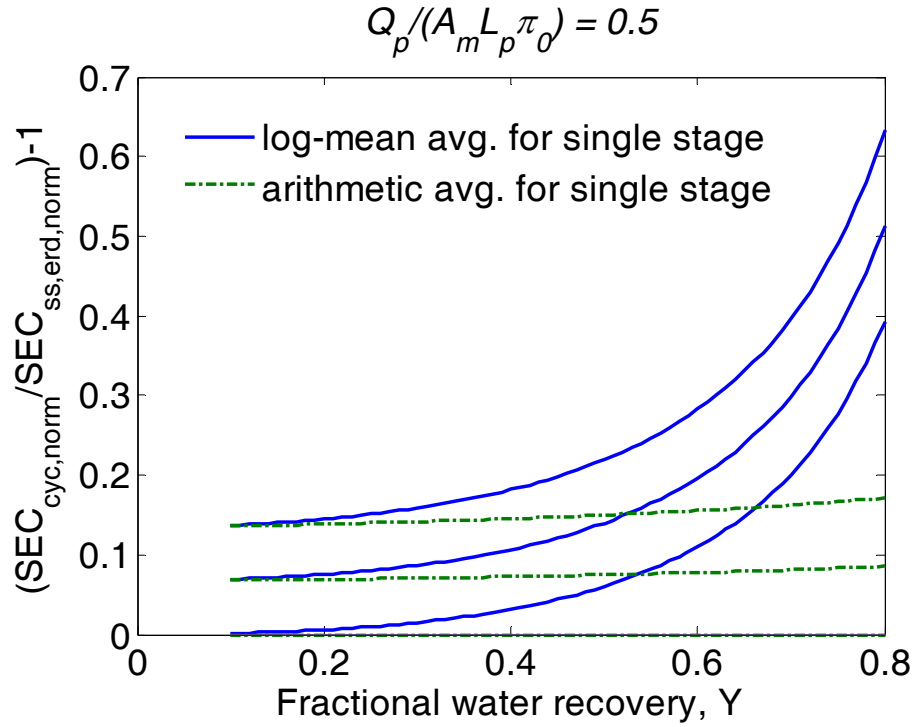
Figure 9-3. Fractional SEC increases for cyclic RO desalting relative to a continuous single-stage desalting with $\eta_{erd} = 1$. f_{cp} values in both graphs are 1, 1.1 and 1.2 for curves and lines from bottom to top, respectively.

The finding that a cyclic RO process is not more energy efficient than a continuous single-stage RO process may appear counter-intuitive given the fact that in the cyclic operation the operating pressure incrementally increases with time. The incremental increase in the operating pressure resembles the approach for the multi-stage process without the use of ERDs (analyzed in Chapter 3) in which the pressure is increased with successive RO stages. This equivalent operation is shown schematically in Figure 9-5 whereby the cyclic operation over a time period t_f can be conceptualized as a series of RO stages with injection of a portion of fresh raw feed into each stage, each accomplishing a portion of the recovery at an incrementally increasing feed pressure. . In the absence of dilution by raw feed to each stage, the multi-stage process as depicted in Fig. 9-4 would more closely approach the operation of a thermodynamically reversible process. Introduction of the raw water stream dilutes the inter-stage retentate stream; but on the other hand the feed splitting concentrates the raw water stream, and thus, more energy is required to desalt this concentrated raw water, which outweighs the energy savings in diluting the inter-stage retentate stream and results in a higher overall SEC of the whole system than the case of a two-stage process as proved in Chapter 5. In summary the energy efficiencies of cyclic, single-stage, two-stage and multi-stage RO operation can be ranked as: cyclic < single-stage with an ERD < two-stage with ERDs < multi-stage with ERDs.
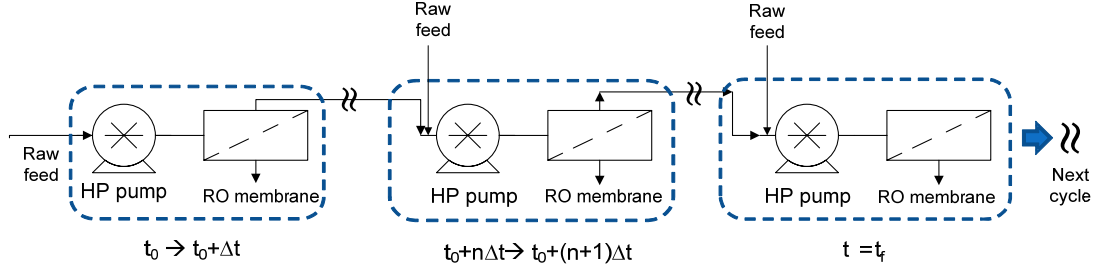
Figure 9-4. **Schematic of time evolution of cyclic operation.**

9.3.3. Effect of downtime and energy efficiency

For a given downtime ratio, the corresponding minimum ERD efficiency for the continuous single-stage operation to be as efficient as the cyclic operation, can be found by equating Eq. 9.4b and 9.14b to solve η_{erd}, and is as follows:

$$\eta_{erd,req} = \frac{1 - \dfrac{Y\left[\overline{NDP}_{norm} + \dfrac{1-Y/2}{1-Y}\right]}{\left[(1-\alpha_d)\overline{NDP}_{norm} + \dfrac{1}{Y}ln\left(\dfrac{1}{1-Y}\right)\right]}}{(1-Y)} \tag{9.15a}$$

$$\eta_{erd,req} = \frac{1 - \dfrac{Y\left[\overline{NDP}_{norm} + \dfrac{1-Y/2}{1-Y}\right]}{\left[(1-\alpha_d)\overline{NDP}_{norm} + \dfrac{1-Y/2}{1-Y}\right]}}{(1-Y)} \tag{9.15b}$$

where the log-mean and arithmetic osmotic pressure averages are used in Eqs. 15a and 9.15b, respectively, in computing the SEC for the continuous single-stage RO process. If the ERD efficiency is less than $\eta_{erd,req}$, the cyclic operation is more energy efficient; otherwise the continuous single-stage operation is more energy efficient (Figure 9-5). Consistently with Figure 9-2, Figure 9-5 also shows, as expected, that the discrepancy in the SEC computation resulting from the use of the two different osmotic pressure

averaging methods is within 5% for water recovery of 35% and within 30% for water recovery of 70%.

SEC at $Q_p/(A_m L_p \pi_0)$=0.5, α_d=0.1, and Y = 0.35

SEC at $Q_p/(A_m L_p \pi_0)$=0.5, α_d=0.1, and Y = 0.7
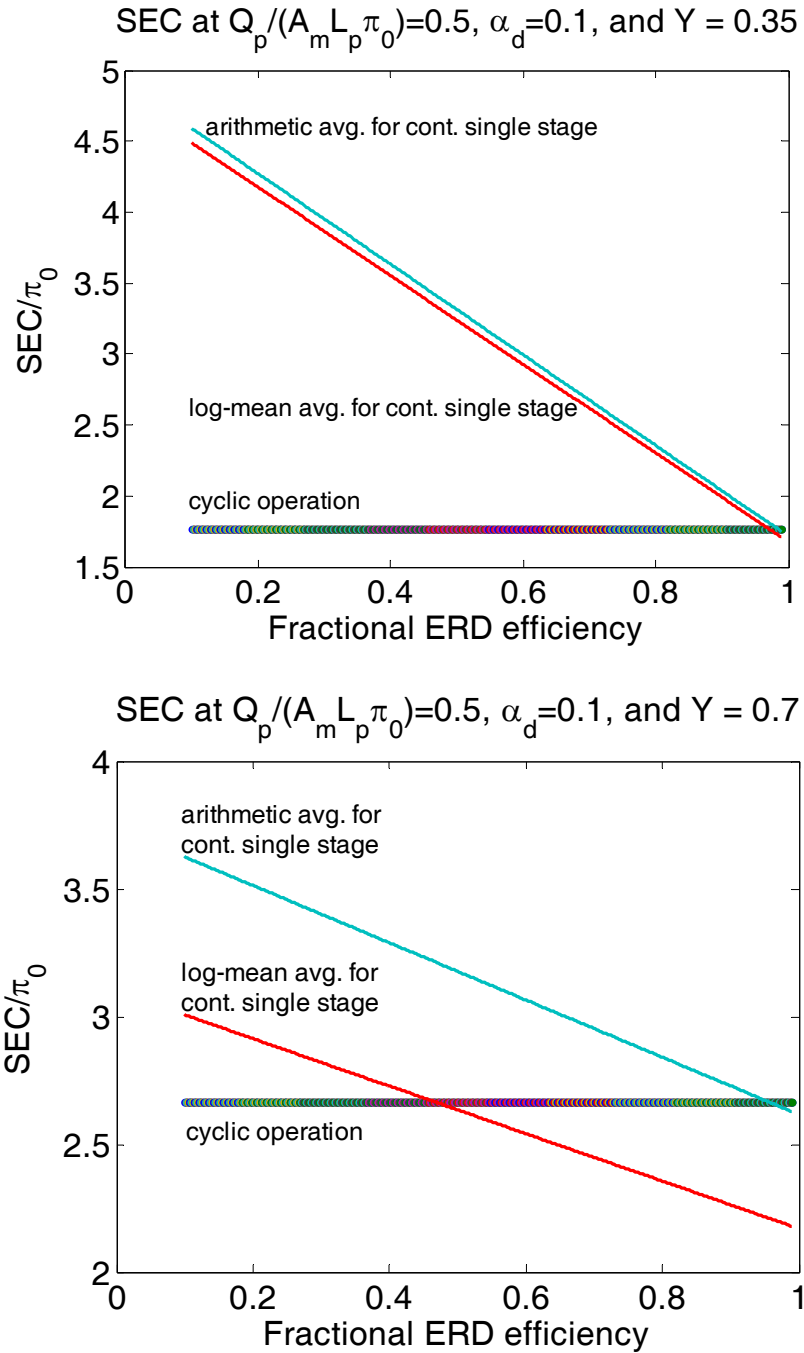
Figure 9-5.   Variation of normalized SEC for a cyclic operation and continuous single-stage desalting with respect to the ERD efficiency.

For example, when desalting seawater (osmotic pressure: 25 atm) with the Dow FilmTec SW30XLE-400i, ($L_p = 0.39 \times 10^{-11} m/s.Pa$), permeate flux at about 10.5 GFD,

$$\frac{Q_p}{A_m L_p \pi_0} = 0.5 ,$$ water recovery is 35% and the downtime ratio is 10%. If the ERD efficiency of a continuous single-stage operation is less than 97% (or 98% if the arithmetic average of the osmotic pressure is applied), the cyclic operation is more energy efficient. If the ERD efficiency of a continuous single-stage operation is larger than 97% (or 98% if the arithmetic average of the osmotic pressure is applied), the continuous single-stage RO operation is more energy efficient. The required minimum ERD efficiency (in this example is 97% or 98% if the arithmetic average of the osmotic pressure is applied), to allow a continuous single-stage operation as energy efficient as the cyclic operation, decreases with increasing normalized permeate flow rate and downtime ratio (Figure 9-6).
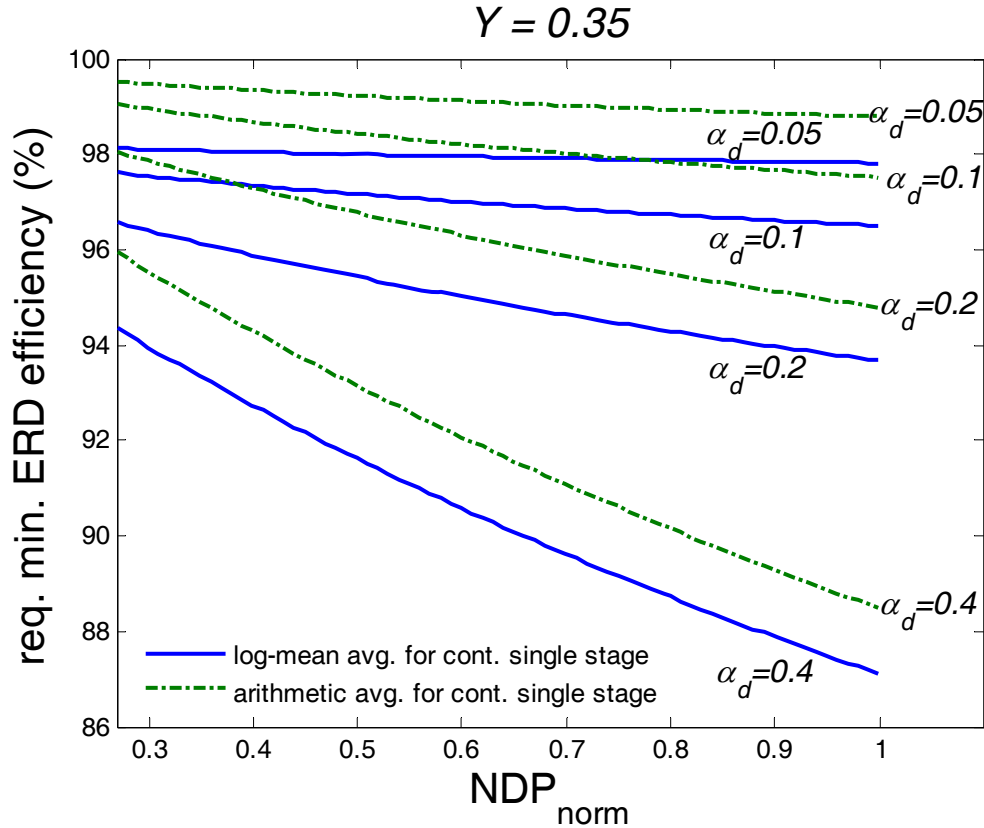
Figure 9-6. **Required minimum ERD efficiency of a single-stage RO vs. normalized permeate flow rate for a continuous single-stage RO system to be as efficient as a cyclic operation at the same water recovery and normalized permeate flow rate.**

As can be seen from Figure 9-6, if the log-mean average of the feed-brine osmotic pressure is applied, the minimum ERD efficiency is between 97% and 98% (the range will be 98-99.5% if the arithmetic average of the feed-brine osmotic pressure is applied) for downtime ratio in the range of 0.05 to 0.1, where the normalized permeate flow rate has very little impact on this required minimum ERD efficiency. It is important to note that the comparison set the membrane module to be identical in both systems. Therefore, Figure 9-6 implies that the cyclic operation is more cost-effective than the continuous single-stage RO process with an ERD since the cyclic operation works as energy efficient

as the continuous single-stage operation without the need of an ERD. This conclusion

holds for the target water recoveries less than 35% as shown in Figure 9-7 where the

required minimum ERD efficiency decreases with increasing target water recovery and

the conclusion is independent on which averaging method is used for the single-stage RO
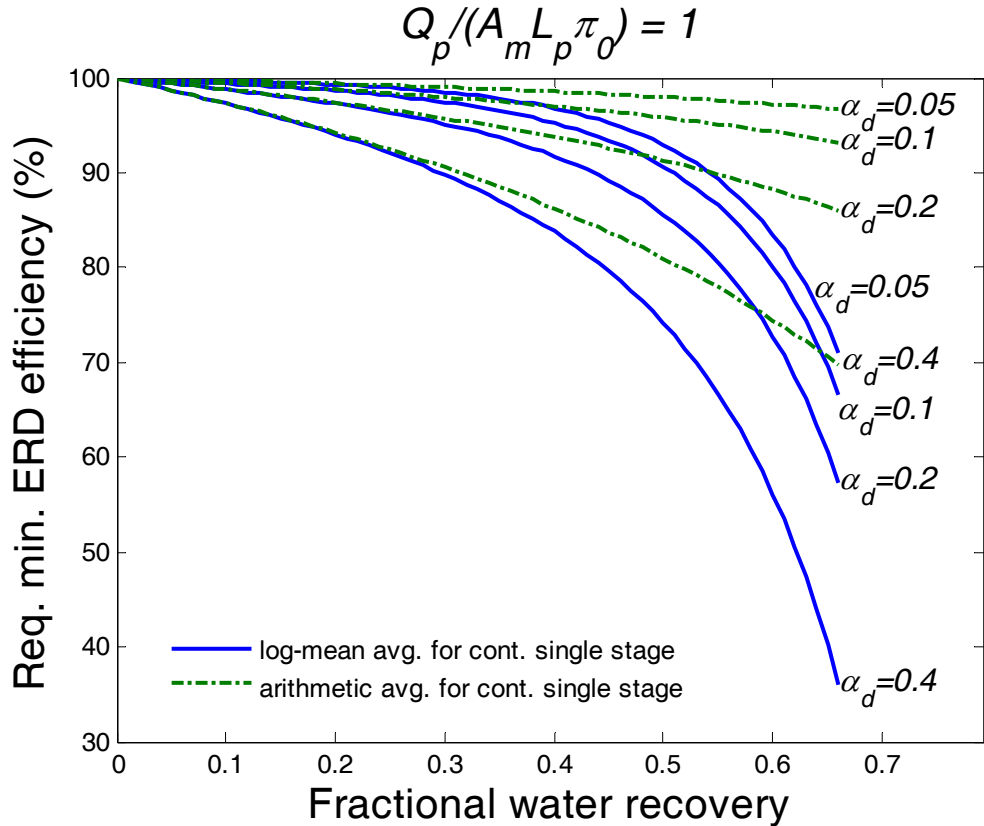
system.

Figure 9-7. Required minimum ERD efficiency of a single-stage RO vs. normalized permeate flow rate for a continuous single-stage RO system to be as efficient as a cyclic operation at the same water recovery and normalized permeate flow rate.

In summary, at low water recovery (<35%) and normalized permeate flow rate

(<1), for example, seawater desalination at less than 21 GFD of the permeate flux if Dow

FilmTec RO membrane SW30XLE-400i is used, the cyclic RO process with a downtime

ratio less than 10% is more cost effective than a continuous single-stage RO process with an ERD of energy recovery efficiency greater than 97%.

9.4. Two-stage vs. single-stage

From the previous section, it is concluded that a cyclic RO process with a downtime ratio less than 10% is more cost effective than a continuous single-stage RO process with an ERD of energy recovery efficiency greater than 97%, irrespective of which averaging is used. This section will compare the cost effectiveness of the cyclic RO process and a two-stage RO process with an ERD of energy recovery efficiency greater than 97%. The comparison is done indirectly by comparing the single-stage RO system and a two-stage RO system. As concluded in Chapter 5, a two-stage/multi-stage RO process is more energy efficient than a single-stage RO process. However, a two-stage process needs more pumps which may cost more than a single-stage RO process which requires only one pump. Therefore, in this section the cost of the pump will be studied for both a single-stage and two-stage RO systems. A pump's cost can be taken as proportional to the product of delivered feed flow rate (Q_F) and output (feed to RO) pressure (P_F), $k_p * Q_F * P_F$ [147], where k_p has the units of $/W (in the range of 0.5-1 $/W [155]). For the sake of adding this cost onto the energy cost, the pump cost is converted into the units of energy (Joule). The electricity price (ε in $/kWh), which is needed to make this conversion, is in the range of 0.05-0.1 $/kWh. Assuming the pump's life is t_p in hrs (usually in the range of 50,000-100,000 hrs, the specific capital cost on pumps (SPC^{1stg})

for a single-stage RO system is equal to the capital cost divided by the total permeate produced in the life span of the pump as follows:

$$SPC^{1stg} = \frac{k_p \left(Q_F * P_F \right)}{\varepsilon t_p Q_p} \tag{9.16}$$

where $\dfrac{k_p}{\varepsilon t_p}$ is a lumped unitless pump cost factor, which takes value in the range of 0.05 - 0.4 given the ranges of each variable t_p, k_p, and ε.

Following the approach in Chapter 5, for a single-stage RO system operated up to the limit of the thermodynamic restriction (i.e., $P_F = \pi_0/(1-Y_t)$), SPC^{1stg}_{norm}, the SPC normalized to the feed osmotic pressure (π_0) can be calculated as follows when the target water recovery (Q_p/Q_F, Q_p is the permeate flow rate) is set to be Y_t:

$$SPC^{1stg}_{norm} = \frac{k_p}{\varepsilon t_p} \frac{1}{Y_t(1-Y_t)} \tag{9.17}$$

For a two-stage RO system, the capital cost for the second pump is $k_p \left(Q_{F1} * P_{F1} + Q_{F2} * P_{F2} \right)$ where Q_{F1} and Q_{F2} are the feed flow rates to the first and second-stage respectively; P_{F1} and P_{F2} are the feed pressure to the first and second-stage. It is noted that the capital cost of the second pump is overestimated, or this can be viewed as the higher bound of the pump capital cost, while the lower bound of the pump capital cost will be discussed in the following paragraphs. Assuming each pump has a lifetime of t_p (in hrs) as in the single-stage RO system, the specific capital cost for this two-stage RO system on the pumps (SPC^{2stgs}) is equal to the capital cost divided by the total permeate produced in the life span of the pump as follows:

$$SPC^{2stgs} = \frac{k_p \left(Q_{F1} * P_{F1} + Q_{F2} * P_{F2} \right)}{\varepsilon t_p Q_p} \tag{9.18}$$

Following the approach in Chapter 5, one can assume that the two stages are operated up to the limit of the thermodynamic restriction and SPC^{2stgs}_{norm}, the SPC normalized to the feed osmotic pressure can be calculated as follows when the target water recovery is set to be Y_t:

$$SPC^{2stgs}_{norm} = \frac{SPC}{\pi_0} = \frac{k_p}{\varepsilon t_p} \frac{\left(1 - Y_1\right) + \left(1 - Y_2\right)}{Y_t \left(1 - Y_t\right)}$$

$$\text{where} \qquad Y_1 = \frac{Q_{P1}}{Q_{F1}} = \frac{\left(Q_{F1} - Q_{F2}\right)}{Q_{F1}}$$

$$Y_2 = \frac{Y_t - Y_1}{1 - Y_1} \qquad\qquad Y_t = \frac{Q_P}{Q_{F1}} \tag{9.19}$$

$$P_{F1} = \frac{\pi_0}{1 - Y_1} \qquad\qquad P_{F2} = \frac{\pi_0}{1 - Y_t}$$

Examining the first equation in the equation array (Eq. 9.19), one can find that

$\left(1 - Y_1\right) + \left(1 - Y_2\right) \geq 2\sqrt{\left(1 - Y_1\right)\left(1 - Y_2\right)} = 2\sqrt{\left(1 - Y_t\right)}$, where the equal sign is applied when

$Y_1 = Y_2 = 1 - \sqrt{\left(1 - Y_t\right)}$. Coincidently, the optimal water recovery in the first stage to minimize the normalized SPC is the same as the optimal recovery to minimize the energy consumption for the two-stage RO process. When the two-stage RO system is at its energy optimal water recovery distribution, the normalized specific pump cost difference between a single-stage and a two-stage RO system, or the penalty of specific pump cost increase for adopting a two-stage RO system over a single-stage RO system, P_{SPC}, can be obtained from subtracting Eq. 9.17 from the first equation in Eq. 9.19 and is as follows:

$$P_{SPC} = SPC_{norm}^{2stgs} - SPC_{norm}^{1stg} = \frac{k_p}{\varepsilon t_p} \frac{2\sqrt{(1-Y_t)}-1}{Y_t(1-Y_t)}$$

(9.20)

As an example to evaluate the effect of the pump (capital) cost on the overall cost savings of a continuous two-stage RO system relative to a continuous single-stage RO system, this pump cost difference has to be added to the overall cost savings as derived in Chapter 5 as follows:

$$S_{ov}^{emp} = G_{SEC} - P_{SMC} - P_{SPC}$$

$$= \frac{\left(1-\sqrt{1-Y_t}\right)^2}{Y_t(1-Y_t)} + \frac{k_p}{\varepsilon t_p} \frac{1-2\sqrt{(1-Y_t)}}{Y_t(1-Y_t)}$$

(9.21)

$$- \frac{m_{norm}}{\frac{1}{1-Y_t} - \frac{1}{Y_t}\ln\left(\frac{1}{1-Y_t}\right)} \times \left(\frac{\left(1-\sqrt{1-Y_t}\right)(2-Y_t)}{Y_t} \left(\frac{\frac{1}{1-Y_t} - \frac{1}{Y_t}\ln\left(\frac{1}{1-Y_t}\right)}{\frac{1}{\sqrt{1-Y_t}} - \frac{1}{1-\sqrt{1-Y_t}}\ln\left(\frac{1}{1-Y_t}\right)} \right) - 1 \right)$$

where S_{ov}^{emp} is overall cost savings (energy, membrane and pump) of a two-stage RO system relative to a single-stage RO system. If the overall cost savings is greater than zero, then the two-stage RO process is favorable; otherwise the single-stage is more favorable. An example of seawater desalination is plotted in Figure 9-8, with $m_{norm} = 0.01$ [168] and $\frac{k_p}{\varepsilon t_p} = 0.05$ (low), 0.1 (medium), and 0.2 (high). Due to its high osmotic pressure, seawater RO desalination is usually done at a water recovery lower than 50%. As can be seen in Figure 9-8, when the target water recovery is lower than 50%, the overall cost savings of the continuous two-stage RO system over the continuous single-stage RO system, decreases with increasing pump cost factor. The break-even point of

water recovery where the two-stage and single-stage RO systems are as efficient increases with increasing pump cost factor. When the target water recovery is higher than the break-even point of water recovery, the two-stage RO system is more favorable than a single-stage RO system. When the pump cost factor is lower (0.05), the two-stage RO system is more efficient than the single-stage RO when the target water recovery is greater than 35%. When the pump cost factor is medium (0.1), the two-stage RO system is more efficient than the single-stage RO when target water recovery is greater than 42%. When the pump cost factor is high (0.2), the two-stage RO system is more efficient than the single-stage RO when target water recovery is greater than 50%.

It is interesting to note from Eq. 9.20 that when the overall water recovery is 75% (It may not be practical due to the pressure limitation of current commercially available pressure vessels), P_{spc} (the penalty of specific pump cost increase for adopting a two-stage RO system over a single-stage RO system) is zero and the overall savings in unit production cost, normalized to the feed osmotic pressure, is independent on the pump cost factor. This conclusion holds irrespective of the feed salinity. When the target water recovery is lower than 75%, P_{spc} is positive, meaning adopting a two-stage RO system will increase the specific pump cost compared to a single-stage RO targeted at the same overall water recovery. However, if the target water recovery is higher than 75%, P_{spc} is negative, meaning adopting a two-stage RO system will decrease the specific pump cost compared to a single-stage RO targeted at the same overall water recovery.
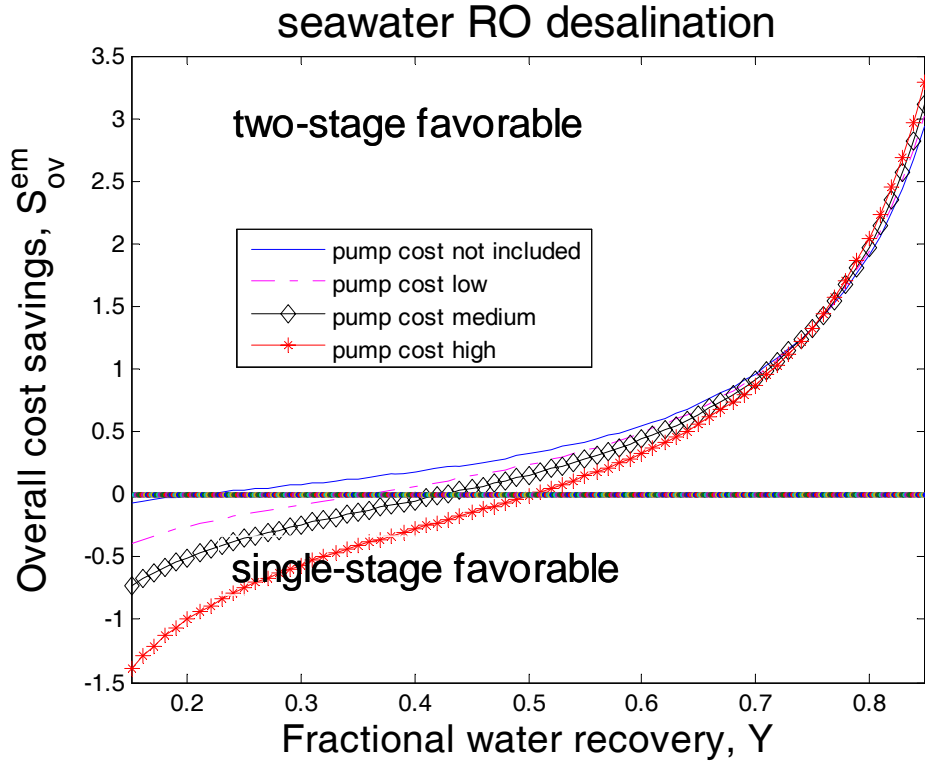
Figure 9-8. **Overall cost savings of continuous two-stage RO process over continuous single-stage, considering energy consumption, membrane cost, and pump cost (pump cost model by Eq. 9.18).**

The lower bound of the pump cost for the two-stage system will be $k_p \left[Q_{F1} * P_{F1} + Q_{F2} * \left(P_{F2} - P_{F1} \right) \right]$ and the corresponding normalized SPC will be as follows:

$$SPC_{lb}^{2stgs} = \frac{k_p}{\varepsilon t_p} \left[\frac{\left(1 - Y_1\right) + \left(1 - Y_2\right)}{Y_t \left(1 - Y_t\right)} - \frac{1}{Y_t} \right] \tag{9.22}$$

Following the same procedure, the overall cost savings of the two-stage over the single-stage RO system is plotted in Figure 9-9. The break-even water recovery decreases with increasing pump cost factor. It means that the two-stage system has a lower pump capital cost than a single-stage RO system. This may appear counterintuitive, but it is a

consequence of the model used here to quantify the pump cost for the two-stage RO system, $k_p \left[Q_{F1} * P_{F1} + Q_{F2} * \left(P_{F2} - P_{F1} \right) \right]$, which is exactly the energy consumption of the two-stage system. Recalling that the single-stage pump capital cost is proportional (the same proportionality constant) to the energy consumption of the single-stage RO system. As established in Chapter 5, the energy consumption in a two-stage system is lower than in a single-stage RO system, therefore, the pump capital cost is also lower for a two-stage system. As can be seen in Figure 9-9, a two-stage RO system is more efficient than a single-stage for water recoveries greater than 20%.
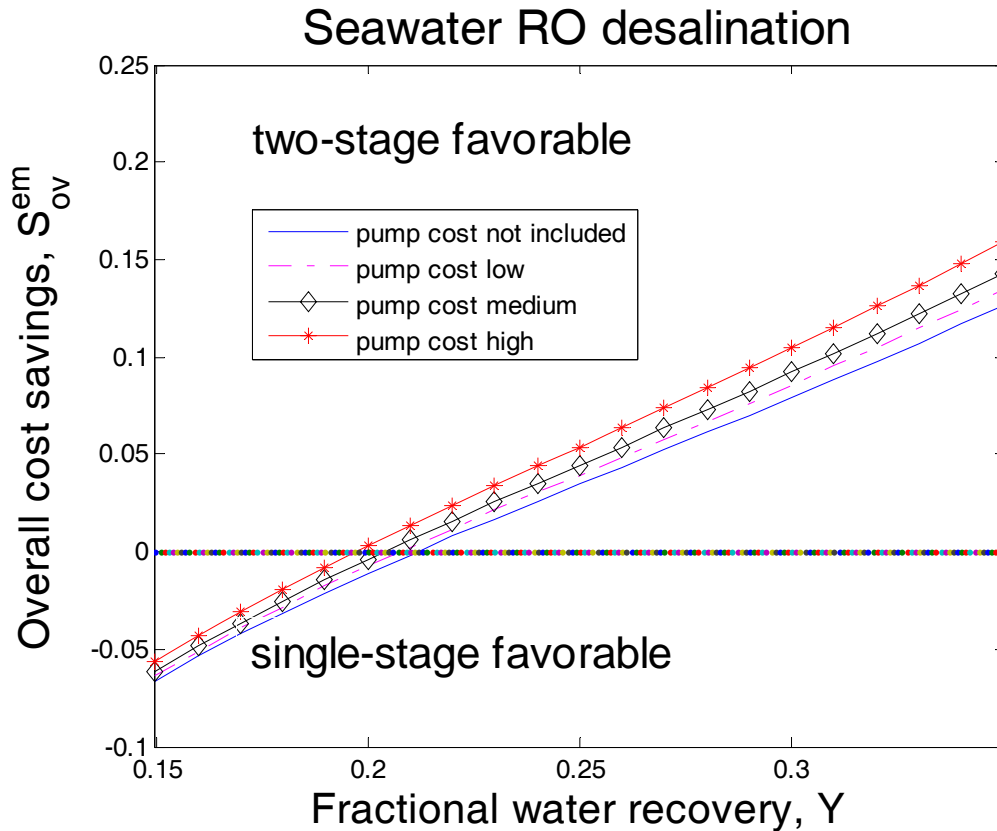
Figure 9-9.   Overall cost savings of continuous two-stage RO process over continuous single-stage, considering energy consumption, membrane cost, and pump cost (pump cost model by Eq. 9.22).

A good estimate will be obtained by taking the average of the these two cases and thus the pump cost for the two-stage system will be $k_p \left[Q_{F1} * P_{F1} + \left(Q_{F2} * \left(P_{F2} - P_{F1} \right) + Q_{F2} * P_{F2} \right) / 2 \right]$ and the corresponding normalized SPC will be as follows:

$$SPC_{avg}^{2stgs} = \frac{k_p}{\varepsilon t_p} \left[\frac{\left(1 - Y_1\right) + \left(1 - Y_2\right)}{Y_t \left(1 - Y_t\right)} - \frac{1}{2Y_t} \right] \tag{9.23}$$

Following the same procedure, the overall cost savings of the two-stage over the single-stage RO system is plotted in Figure 9-10. The break-even water recovery is between the above two extreme cases. When the pump cost factor is low, the two-stage RO process is more efficient than the single-stage RO process for water recoveries greater than 30%; when the pump cost factor is medium, the two-stage RO process is more cost effective than the single-stage RO process for water recoveries greater than 35%; when the pump cost factor is high, the two-stage RO process is more cost effective than the single-stage RO process for water recoveries greater than 42%.
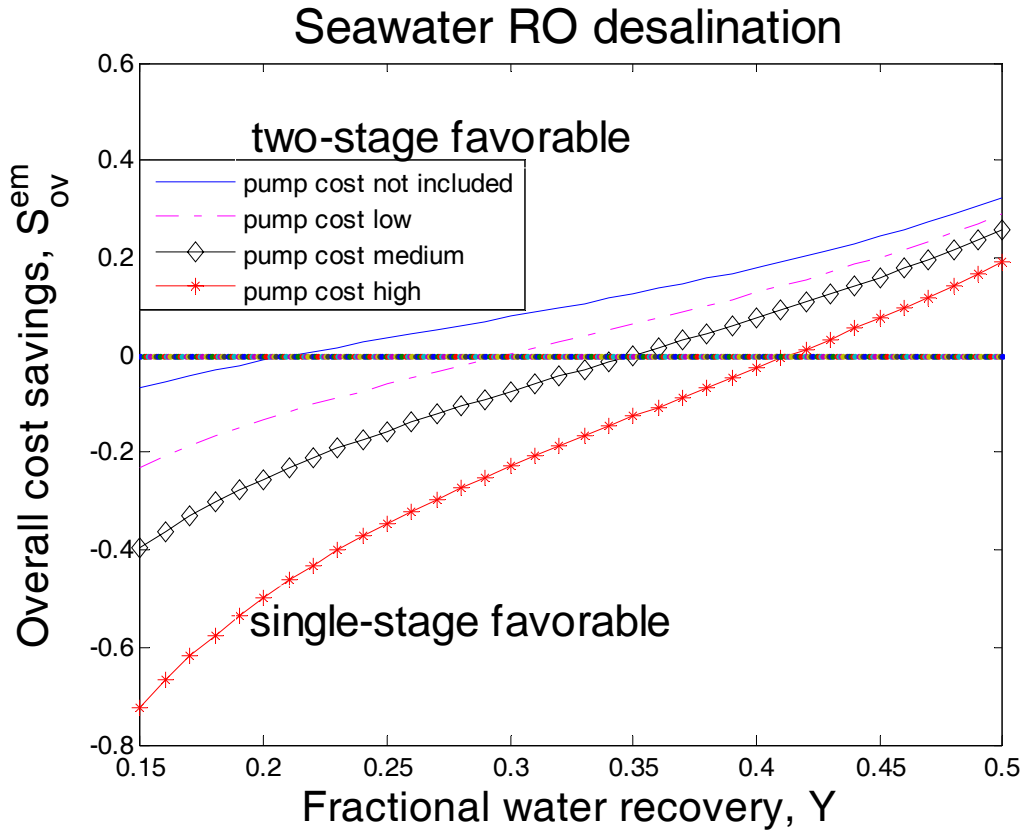
Figure 9-10. Overall cost savings of continuous two-stage RO process over continuous single-stage, considering energy consumption, membrane cost, and pump cost (pump cost model by Eq. 9.23).

The break-even water recoveries, above which the two-stage RO process will be more cost effective than the single-stage RO process, are summarized in Table 9-1.

Table 9-1.   Break-even water recovery for two-stage processes.

Pump cost factor	Break-even water recovery		
	Extreme Case 1	Extreme Case 2	Avg. Case
Low (0.05)	35%	19.7%	30%
Medium (0.1)	42%	20.4%	35%
High (0.2)	50%	20.8%	42%

In summary, the single-stage RO process is more cost effective than two-stage at lower recovery (<35%). If one were to split the first stage (its water recovery < total water recovery < 35%) in the two-stage RO process, the resulted three-stage RO process will be less efficient than the two-stage. One can keep splitting the first stage further, and it is reasonably argued that the single-stage RO process is more cost effective than the multi-stage RO desalting. Recall in the previous section, it is found that the cyclic RO process with a downtime ratio less than 10% is more cost effective than a continuous single-stage RO process for water desalination at low water recovery (<35%) and normalized permeate flow rate (<1); therefore, it can be concluded that for water desalination at low water recovery (<35%) and normalized permeate flow rate (<1), for example, seawater desalination at less than 21 GFD of the permeate flux if Dow FilmTec RO membrane SW30XLE-400i is used, the cyclic operation with a downtime ratio less than 10% is more cost effective than a continuous single-stage, two-stage and multi-stage RO desalting with an ERD of energy recovery efficiency greater than 97%.

9.5.   Conclusions

This chapter established a model to quantify the specific energy consumption (SEC) for a reverse osmosis (RO) process under cyclic operation, i.e., fully recycling retentate stream to mix with the fresh feed water stream and then feed into the RO module of the system. The normalized SEC for this cyclic operation, with respect to the water recovery, is derived and compared with a continuous single-stage RO operation without recycling. When the pressure drop is neglected for both cases, the SEC for cyclic operation is larger than the SEC for continuous cross-flow operation with 100% energy recovery of the retentate stream. In practice, the downtime ratio in the cyclic operation, the target water recovery and the normalized permeate flow rate determine the required minimum ERD efficiency for the continuous single-stage RO desalting to be as energy efficient as the cyclic desalting. Below this required minimum ERD efficiency, cyclic operation is more energy efficient than continuous single-stage RO operation with the ERD. This required minimum ERD efficiency decreases with increasing target water recovery and downtime ratio in the cyclic operation. At low water recovery (<35%) and normalized permeate flow rate (<1), for example, seawater desalination at less than 21 GFD of the permeate flux if Dow FilmTec RO membrane SW30XLE-400i is used, the cyclic operation with a downtime ratio less than 10% is more cost effective than continuous single-stage, two-stage and multi-stage RO desalting with an ERD of energy recovery efficiency greater than 97%.

Chapter 10   Effect of concentration polarization on RO desalination

10.1. Overview

Concentration polarization (CP) determines the osmotic pressure at the membrane surface on the feed-side of the flow channel. Therefore, this chapter evaluates the impact of CP on the thermodynamic restriction discussed in Chapter 3 and the conclusions reached in previous Chapters 3-9 regarding the specific energy consumption (based on the mixed-cup osmotic pressure).

10.2. Modeling the axial variation of permeate flux and salt passage in RO elements in series

The effect of concentration polarization and frictional pressure drop was explored for a single RO membrane element of length L, height H and width W as shown schematically in Figure 10-1. The above geometry was utilized as a surrogate of an unfolded spiral wound membrane module. The membrane length is divided into N compartments. It is noted that in the simulation N is set to be big enough, so that the concentration in each compartment can be taken as constant to enable the numerical simulation. The axial position is defined as $x_n = nL/N$. At the entrance $x_0 = 0$, at the exit, $x_N = L$, where L is the membrane length. n
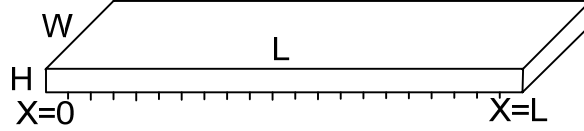
Figure 10-1. A rectangular RO membrane module.

For simplicity, concentration polarization is quantified by the film model (Eq. 9.24)

$$\frac{C_m(x) - C_p(x)}{C_f - C_p(x)} = exp\left[\frac{J_v(x)}{k(x)}\right] \tag{9.24}$$

In which the local feed-side mass transfer coefficient, $k(x)$, can be calculated from [169]:

$$k(x) = \frac{1}{1.475}\left[\frac{3Q_f}{H^2 W}\frac{D^2}{x}\right]^{1/3} \tag{9.28}$$

which is argued to be sufficiently accurate for RO modules with spacers [156]. The local permeate flux, , $J_v(x)$, is determined by membrane permeability and pressure driving force:

$$J_v(x) = L_p\left[P_f - \alpha\Delta P_{fric}(x) - \frac{\pi_0}{C_f}\left[1 - \beta f\left[C_m(x)\right]\right]C_m(x) + \frac{\pi_0}{C_f}\left[1 - \beta f\left[C_p(x)\right]\right]C_p(x)\right] \tag{9.25}$$

and the salt flux is governed by the combination of diffusional and convective transport mechanisms through the membrane as given below:

$$J_s(x) = C_p(x)J_v(x) = k_s\left[C_m(x) - C_p(x)\right] + (1-\sigma)J_v(x)(C_f + C_m(x))/2 \tag{9.26}$$

and where π_0, C_f, and P_f are the feed osmotic pressure, feed concentration and feed pressure respectively. It is noted that the coefficients, α, β are introduced in the permeate flux equation (Eq.9.25) to account for frictional pressure drop along the

membrane channel and non-linearity of the osmotic pressure (designated by the function $f(C_p(x))$ and $f(C_m(x))$ for the permeate and at the membrane surface, respectively) . When frictional pressure drop along the channel is neglected, ; $\alpha = 0$;and when frictional pressure drop is considered, $\alpha = 1$. When the osmotic pressure varies linearly concentration, $\beta = 0$, while $\beta = 1$ when the osmotic pressure is allowed to vary non-linearly with concentration.

The frictional pressure drop, ΔP_{fric} is, can be approximated by the following equation, which quantifies the pressure drop for laminar fluid flow through rectangular slit with two equally porous walls[153]:

$$\Delta P_{fric}(x) = (\frac{1}{2}\rho \bar{v}^{-2})(\frac{24}{Re} - \frac{648}{35}\frac{Re_W}{Re})(1 - \frac{2Re_W}{Re}\frac{x}{H})(\frac{x}{H})$$

(9.27)

where $\bar{v} = Q_f / H \bullet W$, $Re_W(x) = HJ_v(x)\rho / \mu$, H is the channel height and W is the W channel width.

In order to determine the optimal operating condition at which the SEC is at its minimum an analysis was carried out for a collection of RO elements in series.. The entire (P_f, Q_f) surface was searched with the constraint of P_f and Q_f values set by the membrane manufacturer. For each set of (P_f, Q_f) , a simulation based on Eqs. (9.24–9.28) as detailed in this section was performed to calculate the water recovery and the average permeate concentration in each of the six membrane elements, from which the overall water recovery and average permeate concentration were then obtained. The overall average permeate concentration as may be desired for the specific water use is

another constraint that is introduced in the optimization problem. For example, for drinking water production, the permeate concentration is not allowed to exceed $500\,mg/L$. In some cases, there may be a specific overall element water recovery constraint. For example, most membrane manufacturers set the upper water recovery limit for a given RO element at 15% in order to to reduce membrane fouling.

10.2.1. Simulation approach

In order to simulate the axial variation of the concentration along the membrane surface and the resulting permeate flux and salt concentration for a given pair of P_f and Q_f, the membrane length is divided into N compartments. At the entrance $x_0 = 0$, at the exit, $x_N = L$, where L is the membrane length. N is sufficiently large, such that $\frac{L}{N}$ is sufficiently small and thus the membrane surface concentration in a given membrane element can be assumed constant. In the present analysis a configuration of six membrane elements in series was considered as an example as shown in Figure 10-2.
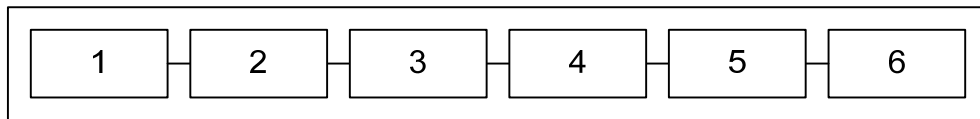
Figure 10-2.   Schematics of 6 pressure vessels series, each housing one membrane element.

The cumulative permeate flow rate at each axial position is calculated from:

$$Q_{p,A}(x) = W \int_0^x J(x')dx' \tag{9.29}$$

Then the cumulative water recovery (up to axial position x) is

$$Y(x) = \frac{Q_{p,A}(x)}{Q_f} \tag{9.30}$$

and the average permeate concentration for this membrane element is

$$\overline{C_p} = \frac{W \int_0^L J_s(x)dx}{YQ_f} \tag{9.31}$$

For the second membrane element, the feed stream is the fully mixed retentate stream from the previous element and the same protocol (described above) is used to calculate the recovery and permeate concentration. This same approach is repeated for the third, fourth, fifth and sixth element in order to obtain the final overall water recovery based on the raw feed flow rate and average permeate concentration for the six elements.

10.2.2. Simulation results

Simulations (See Appendix for the Matlab Code) were carried out for a collection of six membrane elements in series. The Dow FilmTec XLE-2540 RO membrane elements were selected for the simulations. The simulations were carried out for a 3500 mg/L NaCl feed solution for the conditions listed in Table 10-1. The pressure was set to be double that the feed osmotic pressure to test the water recovery and check its agreement with the prediction (50% water recovery at thermodynamic restriction) in Chapter 3. The overall recovery of the 6 pressure vessels in series is 51.2% and the normalized SEC is 3.91 and permeate concentration is within 467 ppm. The normalized SEC is lower than 4 because the salt rejection in this case is only required to be 86.7% (Rej = 1 − 467/3500 = 86.7%),

which is much less than 100%. The profiles of different variables in the first element and the last (6th element) are shown below.

Table 10-1.   Simulation conditions.

Membrane width (m)	2.9 [162]
Membrane length (m)	0.895 [162]
Half channel height (m)	$0.355*10^{-3}$ [162]
No. of pressure vessels	6
No. of membrane element per vessel	1
Solution density (kg/m^3)	$1*10^3$
Solution diffusivity (m^2/s)	$1.6*10^{-9}$(Nerst theory for diluted NaCl aqueous solution)
Water permeability (m/s/Pa)	$2.22*10^{-11}$[167]
NaCl permeability (m/s)	$2.15*10^{-7}$[167]
Feed salinity (ppm)	3500
α	1
β	0
σ	1
Cross-flow velocity (cm/s)	4-8 (Re =Hu / = 14-28, laminar flow)
Feed pressure (psi)	80
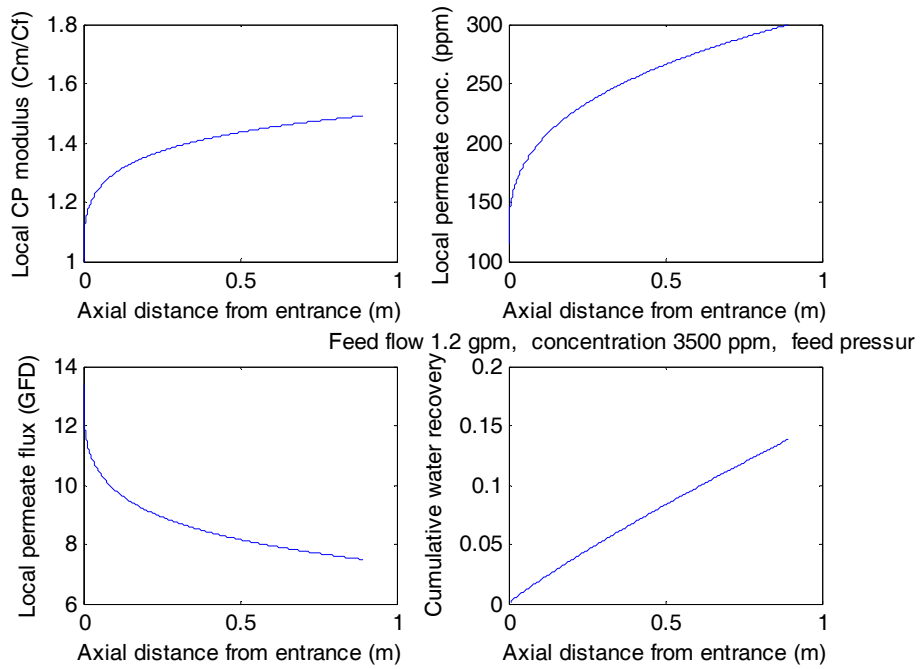
Figure 10-3. Simulation results for the first element.
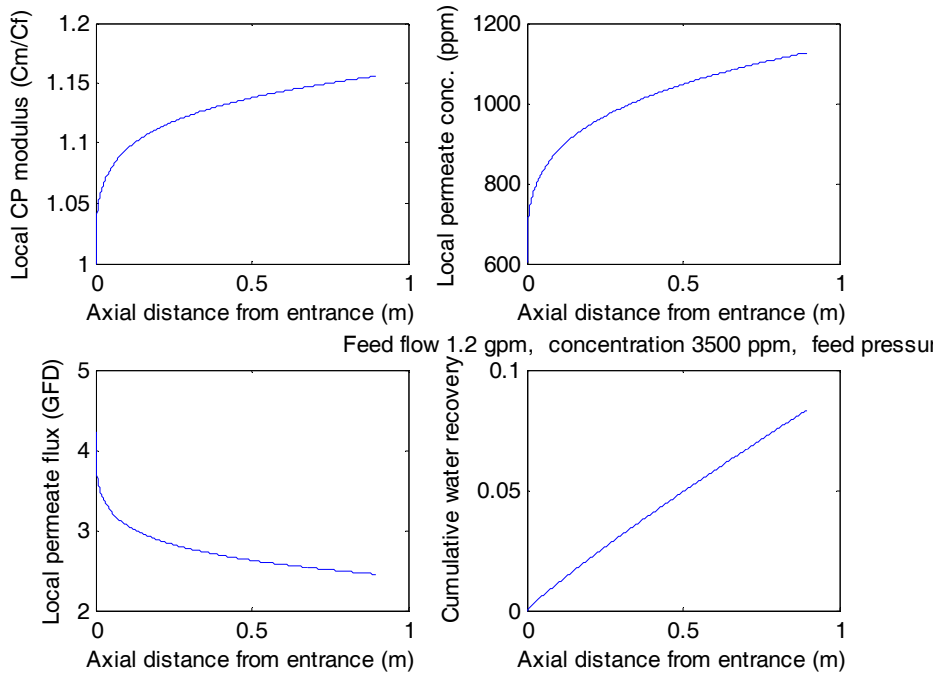
Figure 10-4. Simulation results for the last element.
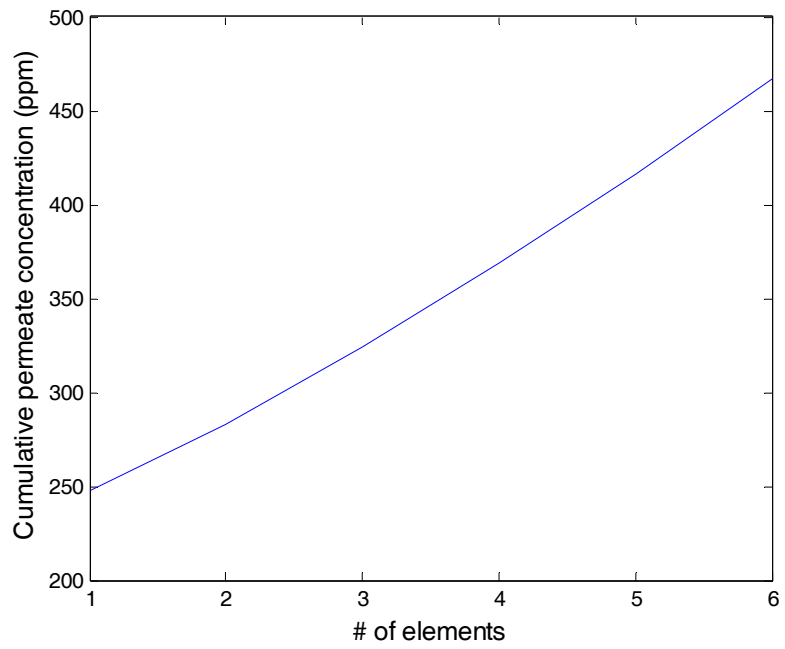
Figure 10-5.   Accumulative permeate concentration vs. number (#) of membrane elements.
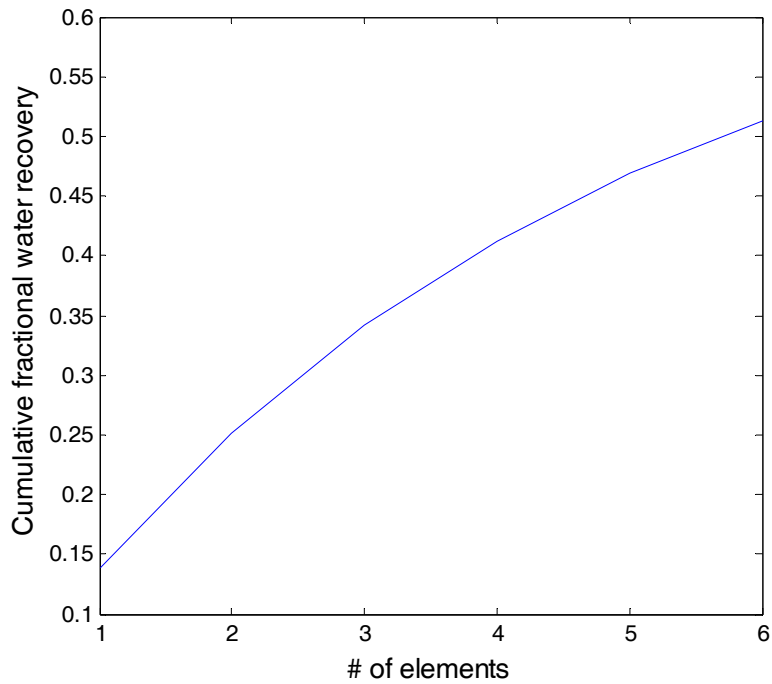
Figure 10-6.   Cumulative fractional water recovery vs. # of membrane elements.

217

Figure 10-5 and Figure 10-6 show that as the number (#) of elements increases, the system overall water recovery approaches the thermodynamic limit (50% water recovery in this case when the feed pressure is twice that of the feed osmotic pressure). However, as the number (#) of elements increases, the overall permeate water concentration increases.

10.2.3. Comparison of this work with the commercial Dow FilmTec RO simulator (ROSA)

In order to evaluate the accuracy of the current model in assessing the effect of the concentration polarization and frictional pressure drop on the membrane performance, showed the comparison between this work and ROSA [167] running at the same feed flow rate and feed pressure using Dow FilmTec XLE-2540 RO membranes in six pressure vessels and each vessel has one RO membrane in it. It is concluded that the simple film model predicts the water recovery within 10% deviation from ROSA, while the permeate concentration is within 20% of deviation. a similar membrane performance as the software package provided by the membrane manufacturer. It is noticed that: for constant feed pressure simulation, the water recovery and permeate concentration increases with the decreasing feed flow rate. The comparison between the normalized SEC with the SECtr/π_0 show that the system approaching the thermodynamic restriction as the feed flow rate is reduced. When the feed flow rate was reduced to 1.1 gpm, the permeate concentration is only 1% lower than the drinking water standard and the corresponding SEC is only 8% higher than the thermodynamic restriction (*R/Y(1-Y)*). The normalized SEC can be lower than 4 because the salt rejection in this case is only

required to be 86% since the feed water salinity is 3500 ppm ($R = 1 - 500/3500 = 86\%$), which is much less than 100%.

Table 10-2.   Comparison of this work with ROSA simulation (inputs: P_f and Q_f, outputs: C_p and Y).

psi	gpm	Cp		Y		SEC/π_0	Salt Rej.	SECtr/π_0	SEC/SEC$_{tr}$
		this work	ROSA	this work	ROSA				
80	3	301	236	0.271	0.293	7.38	0.91	4.63	1.60
80	2	351	288	0.375	0.381	5.33	0.90	3.84	1.39
80	1.6	393	326	0.435	0.433	4.60	0.89	3.61	1.27
80	1.2	467	386	0.512	0.506	3.91	0.87	3.47	1.13
80	1.1	495	407	0.536	0.529	3.73	0.86	3.45	1.08

(Simulation parameters see Table 10-1.)

10.2.4. Optimum water recovery and SEC

As shown previously, the RO operation for a given feed pressure will reach its minimum SEC when the water recovery reaches its maximum while satisfying the permeate product water quality (500 ppm). In other words, this pressure is the minimum pressure to achieve the recovery while satisfying the product quality requirement. This datum set of water recovery and SEC (computed from feed pressure divided by water recovery) will be one point of the locus of minimal SEC for producing drinking water at different water recovery levels. From this locus, one can find the optimum water recovery and corresponding minimum SEC. The detailed approach to find the optimum water recovery for this example is as follows: for the following values of feed pressures: 72, 76, 80, 84, 88, 92, 96, 100 and 104 psi, feed flow rate values were decreased from 2 gpm (these values were chosen because they are in the vicinity of the optimal operating pressure

predicted in Chapter 3) until the permeate concentration reaches within 1% of the drinking water standard, i.e., about 495 ppm. The operating conditions under which is the permeate concentration were 495 ppm were recorded in Table 10-3 from which it is can be deduced that the minimum SEC will occur at a water recovery between 56.8% and the corresponding normalized SEC is about 3.7 and it is about 6% away from the thermodynamic restriction. The deviation from the theoretically predicted water recovery (50%) and normalized SEC (4) is due to the fact that the salt rejection is much less than 100%.

Table 10-3.   Minimum SEC operation for different given feed pressure values.

P_f psi	Q_f gpm	C_P (ppm)	Fractional Y	SEC/π_0	Salt Rej.	SEC_{tr}/π_0	SEC/SEC_{tr}
72	1.15	495	0.458	3.930	0.86	3.46	1.14
76	1.12	494	0.5	3.800	0.86	3.44	1.11
80	1.1	495	0.536	3.731	0.86	3.45	1.08
82	1.1	494	0.551	3.721	0.86	3.47	1.07
84	1.09	496	0.568	3.697	0.86	3.50	1.06
86	1.1	496	0.581	3.701	0.86	3.53	1.05
88	1.1	494	0.594	3.704	0.86	3.56	1.04
96	1.11	495	0.639	3.756	0.86	3.72	1.01
100	1.13	494	0.657	3.805	0.86	3.81	1.00
104	1.14	495	0.67	3.881	0.86	3.88	1.00

10.3. Conclusions

The film model in this chapter is in good agreement with commercial software in predicting the membrane performance. Simulations presented in this chapter show that for constant feed pressure, the water recovery and permeate concentration increase with

decreasing feed flow rate. The local minimum SEC for a given feed pressure approaches the thermodynamic restriction with the salt rejection factor taken into account. The global minimum SEC and corresponding optimal water recovery were 3.7 and 56.8%, respectively. The deviation from the simplified model in Chapter 3 is due to the fact that the required salt rejection is only 86%, much less than 100%.

Appendix A

Comparison of Forward Osmosis and RO Desalination

A.1. Introduction

Forward osmosis (FO) is a membrane desalination process that utilizes a draw solution having a high osmotic pressure to extract water from a saline water source. The challenge in FO is to regenerate the draw solution while extracting the permeated water as a water source of sufficient use quality. This requires separation of the active ingredient of the draw solution for the purpose of both reusing the draw solution chemicals while also recovering the permeate product water at a sufficient level of purity. As an illustration, Figure A-1 depicts the FO process along a distillation process for regeneration of the draw solution chemicals and product water recovery. Effective FO process requires a draw solution that has a high osmotic pressure and with the active (draw solution) solute that is more volatile than water; the latter requirement is necessary if the active draw solution ingredient is to be recovered via a distillation process. Although the permeation of water from feed to the high osmotic draw solution requires little energy input, relative to the process of RO desalination, heat energy may be required for the draw solution regeneration. For example, when ammonium carbonate is used as the active draw solution ingredient, the separation of the ammonia and CO_2 from the spent draw solution requires heat energy which is also utilized for the accompanying process of evaporating large volumes of water.

In order to assess the relative energy consumption for FO relative to RO a demonstrative analysis was carried for a desalination of an aqueous NaCl solution with a target water recovery of 50%. This recovery level was selected since it is the optimal recovery level at which the specific energy consumption is at its minimum for RO desalting without energy recovery. Both FO and RO system were assumed to operate up to the thermodynamic restriction (at the exit region of the membrane modules) in order to have a common baseline for comparison of the two processes. For the above target recovery of 50%, the osmotic pressure of the draw solution needs to twice that in order to achieve 50% water recovery. In the present analysis aqueous NH_4CO_3 (2 mol% and 3 mol%) solution was selected as the draw solution given the recent literature claims of low regeneration cost for this draw solution [20].
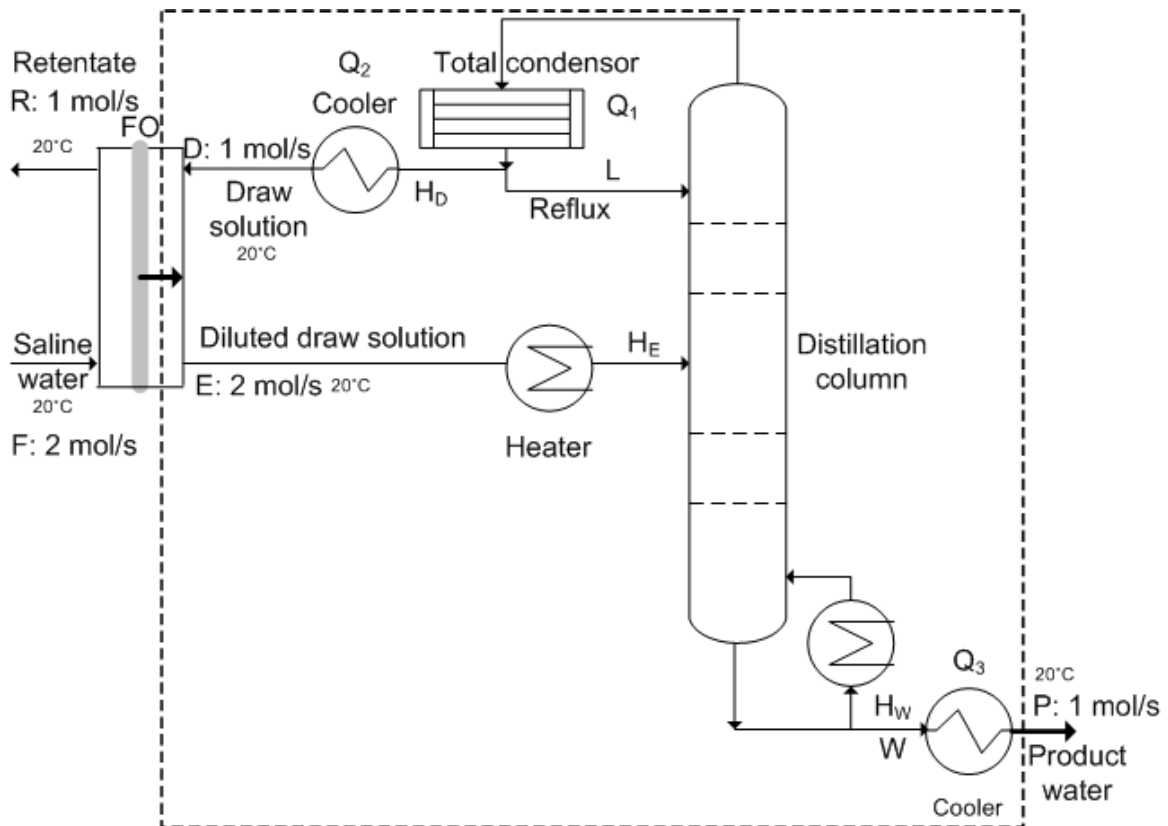
Figure A-1.   Water desalination: forward osmosis followed by distillation.

A.2.   Analysis

A schematic representation of the FO process along with the distillation regeneration scheme is shown in Figure A-1. For the system inside the dashed box of Figure A-1, the enthalpy change is zero if one assumes that only water molecules can pass through the FO membrane and the final product obtained (right corner of Figure A-1) is pure water. From a theoretical thermodynamic viewpoint, a process for which there is no enthalpy change does not require heat input. It means that if the heat released by the system to its surrounding and can be recovered at a 100% efficiency for reuse where heating is needed (i.e., the heater preceding the distillation column), then the heat

consumption for the distillation process after the FO process is zero. On the other hand, if all the above three elements cannot be reutilized the energy consumption of the FO-Distillation process will be $Q_1+Q_2+Q_3$. Therefore, in the present analysis a heat energy recovery efficiency, η_h, is defined such that the normalized specific heat consumption (SHC$_{norm}$) of the integrated FO-distillation system for producing pure water is given as follows:

$$SHC_{norm} = (1-\eta_h)*(Q_1 +Q_2+ Q_3)/\pi_0 \qquad (A.1)$$

where π_0 is the saline source water osmotic pressure. It is noted that if η_h is unity, SHC$_{norm}$ is zero. On the other hand if η_h is zero, SHC$_{norm} = (Q_1 +Q_2+ Q_3)/\pi_0$.

The heat flow terms Q_1, Q_2 and Q_3 (Figure A-1) are quantified by noting the following:

a) Heat released by condensation of the top stream in the distillation column (Q_1), is equal to the decrease in the enthalpy when the top stream (D+L, where D: distillate stream, L: reflux stream) in the distillation column is brought from its dew point to its bubble point. This heat value depends on the required draw solution concentration. In the current calculation, zero reflux is assumed (meaning there is no rectifying section of the distillation column), which results in an underestimation of the heat consumption in the distillation column.

b) Heat released by the distillate when its temperature is decreased from its bubble point to 20°C (Q_2), is equal to the enthalpy change due to the temperature decrease.

c) Heat released by the bottom pure water, when its temperature is decreased from 100°C to 20°C (Q_3), is equal to the enthalpy change due to the decrease in temperature.

Two different draw solution concentrations were evaluated in the analysis (Table A-1) in assessing Q_1 targeting a desalting operation of 50% water recovery.

    i.   Case 1: An aqueous draw solution consisting of 2 mol% $(NH_4)_2CO_3$ having osmotic pressure of 50 atm and feed saline water having osmotic pressure of 25 atm. When the FO system operates up to the thermodynamic limit, the feed saline water concentration can be doubled to match the osmotic pressure of the draw solution. It is noted that due to the counter-flow pattern in the FO membrane system (Figure A-1), the draw solution is diluted to match the osmotic pressure of feed saline water.

    ii.   Case 2: An aqueous draw solution consists of 3 mol% $(NH_4)_2CO_3$ having osmotic pressure of 80 atm with saline feed water of 40 atm osmotic pressure.

Table A-1.   Enthalpy values the streams in the FO-distillation process (generated from OLI simulation according to the condition specified in the table).

Case #	(NH4)2CO3 mole %	Temperature $^\circ C$	Enthalpy J/mol	Q1 J/mol	Q2 J/mol	Q3 J/mol	Q1+Q2+Q3 J/mol
1 and 2	0	20	-286,207				
1 and 2	0	100	-280,169				
1	1	20	-292,513				
1	2	20	-298,880	45,338	4,506	6,038	55,882
1	2	76.77 (b)	-294,374				
1	2	98.45 (d)	-249,036				
2	1.5	20	-295,692				
2	3	20	-305,273	46,999	4,428	6,038	57,465
2	3	74.9 (b)	-300,845				
2	3	97.7 (d)	-253,846				
(b: bubble point, d: dew point)							

From Table A-1, the SHC for the two cases: 1 and 2 can be calculated as follows:

Case 1: $SHC_{norm} = (1- \eta_h)*(Q_1 + Q_2 + Q_3)/\pi_0 = (1- \eta_h)*1242$

Case 2: $SHC_{norm} = (1- \eta_h)*(Q_1 + Q_2 + Q_3)/\pi_0 = (1- \eta_h)*798$

In which π_0 is the saline feed osmotic pressure. For the equivalent product water recovery, the normalized specific energy consumption while for RO desalination (see Chapter 3) is given as $SEC_{norm} = 4$ (without an ERD) and $SEC_{norm} = 2$ (with 100% efficient ERD). Accordingly, the comparison between FO-Distillation and RO desalination is depicted in Figure A-2 for the two case studies.
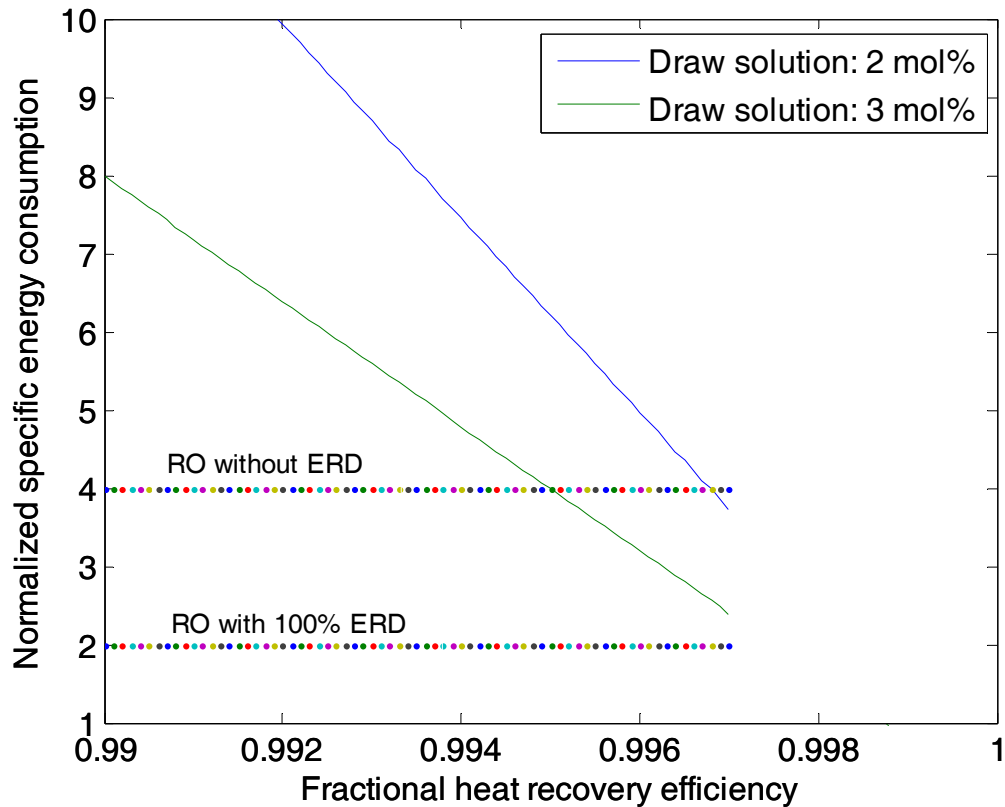
Figure A-2. Comparison of the specific energy consumption for FO-distillation and RO process.

The comparison shown in Figure A-2 clearly indicates that FO-distillation is less energy efficient than RO process at 50% water recovery even for high salinity feed water of 40 atm osmotic pressure, since it is unlikely that heat recovery efficiency (for FO) would reach 99%. It is also noted that the SEC for RO with energy recovery is significantly lower than FO. FO may be more efficient than RO provided that near complete heat recovery can be attained, but this is clearly a challenge that even if could be attained would be accompanied with significant capital cost.

Appendix B

Matlab Code for Concentration Polarization Simulation

Main Code File for Simulating Concentration Polarization

```matlab
clear all;
clc;

% constants (M3 system size)
Am = 2.6;
W = Am/0.895/2; %Dow FilmTec XLE 2540. length is 0.895 m. only simulate
the half channel height
Lp = 2.22E-11; % water permeability
alpha = 1; %correction factor for frictional pressure drop
rho = 1.0E3; %solution density
H = 3.55E-4; %half channel height
mu = 1E-3; %solution viscosity
D = 1.6E-9; %solution diffusivity
ks = 2.15E-7; % salt permeability
fos = 7.87E7;% osmotic pressure coefficient


Qf0 = 1.2*6.165E-5;   % m^3/s. feed flow rate (1 gpm = 6.165e-5 m^3/s).
Qf0 = Qf0/2; %flow rate for the half channel height and half width
Qf = Qf0;
Cf0 = 3.5E-3;% kg salt/kg solution
Cf = Cf0;
Pf0 = Cf0*fos*2; % ** 3 <- 10 points from [2, 10] in Pa
Pf = Pf0;
pz0 = Cf0*fos; %feed osmotic pressure
%%%%%%%%%%%%%%%%%%%%%%%%%%%%%%%%%%%
t_min = 0;
t_max = 0.895; %t is length. t_max = 0.895 m. for Dow FilmTec XLE-2540
ns = 0.001;
t = t_min : ns : t_max;
nn = length(t);
nm = 6;
%%%%%%%%%%%%%%%%%%%%%%%%%%%%%%%%%%%%%


%fval = zeros(3, nn);
options = optimset('Display','off');


%%%%%%%%%%%%%%%%%%%%%%%%%%%%%%%%%%%%%
yt = 1;
ys = ones(nm, 1);

xs = zeros(3, nn);
```

```matlab
xp = [Cf, 1E-3 * Cf, 1E-3];

ocsm=0;
for kk=1:nm  %nm # of element in a stage
    % depending paramaters
    pz = Cf*fos;
    v = Qf / (H * W)
    Re = H * v * rho / mu;
    Qf0_norm(kk) = 2.*Qf0/Am/Lp/pz0/kk    %Qf0_norm up to kk element.
normalized Qf value for Paper_1.
    for ii=1:nn
        f = @(x)myFun(x, t(ii), Pf, Qf, Cf, W, Lp, alpha, pz, D, rho, H,
mu, v, Re, ks);    % pass paramters into the function
        [xs(:, ii)] = fsolve(f, xp, options); %xs is the array of
x(1):Cm, x(2):Cp, x(3):Jv.
        xp = xs(:, ii);

%        display(t(ii));
    end

    dPf = 0.5 * rho * v^2 * (24 / Re - 648 / 35 *  H * xs(3, nn) * rho
/ mu / Re) * (1 - 2 * H * xs(3, nn) * rho / mu / Re * t_max / H) *
t_max / H;

    y = zeros(1, nn);
    sf = 0;
    for ii=2:nn
        y(ii) = y(ii-1) + 0.5 * (xs(3, ii-1) + xs(3, ii)) * ns; %local
permeate flux Jv(x)
        sf = sf + 0.5 * (xs(2, ii-1) * xs(3, ii-1) + xs(2, ii) * xs(3,
ii)) * ns;
    end

    y = y .* ( W / Qf);
    sf = sf * W;  %salt flux
    mcp = sf / y(nn) / Qf;  %cumulative average permeate concentration
for each membrane element
    ocsm = ocsm + sf; %overall accumulated salt mass.


    %%%%%%%%%%%%%%%%%%%%%%%%%%%%%%%%%%%%%%%%%%%%%%%%%
    %for a single module, plot the Cm Cp permeate flux profile.
    Qf_gpm = 2*round(Qf0/(3.785E-3/60)*10)/10; %use both upper and
bottom half channel to run ROSA simulation
    Cf_ppm = round(Cf0*1E6);
    Pf_psi = round(Pf0/6894.75729);

    figure
    title({['Feed flow ' num2str(Qf_gpm) ' gpm, ' ' concentration '
num2str(Cf_ppm) ' ppm, ' ' feed pressure ' num2str(Pf_psi) ' psi.']})
    subplot(2,2,1)
    plot(t, xs(1,:)/Cf);
```

```matlab
    xlabel('Axial distance from entrance (m)')
    ylabel('Local CP modulus (Cm/Cf)')
    %title({['Feed flow ' num2str(Qf_gpm) ' gpm, ' ' concentration '
num2str(Cf_ppm) ' ppm, ' ' feed pressure ' num2str(Pf_psi) ' psi.']})

    subplot(2,2,2)
    plot(t, xs(2,:)*1E6);
    xlabel('Axial distance from entrance (m)')
    ylabel('Local permeate conc. (ppm)')
    %title({['Feed flow ' num2str(Qf_gpm) ' gpm, ' ' concentration '
num2str(Cf_ppm) ' ppm, ' ' feed pressure ' num2str(Pf_psi) ' psi.']})

    subplot(2,2,3)
    plot(t, xs(3,:)/4.71543992E-7);
    xlabel('Axial distance from entrance (m)')
    ylabel('Local permeate flux (GFD)')


    subplot(2,2,4)
    plot(t,y)
    xlabel('Axial distance from entrance (m)')
    ylabel('Cumulative water recovery')
    title({['Feed flow ' num2str(Qf_gpm) ' gpm, ' ' concentration '
num2str(Cf_ppm) ' ppm, ' ' feed pressure ' num2str(Pf_psi) ' psi.']})
    %%%%%%%%%%%%%%%%%%%%%%%%%%%%%%%%%%%%%%%%%%%%%%%%%%%%%%%%%%%%

    %%
    Cf = (Cf - y(nn) * mcp) / (1 - y(nn));
    Qf = Qf * (1 - y(nn));
    Pf = Pf - dPf;
    PresDp(kk) = Pf0 - Pf %cumulative pres drop
    yt = yt * (1 - y(nn));
    ys(kk) = ys(kk) - yt;
    ocp_ppm(kk) = ocsm/ys(kk)/Qf0*1E6;

%     kk
    ys.*Qf0.*2/6.165E-5 %cum. perm. flow
%     ys
%     (Pf0-2.*ys.*Qf0./kk./Am./Lp)./pz0 %-(Pf0-Pf)./2
%     Pf

end

figure
title({['Feed flow ' num2str(Qf_gpm) ' gpm, ' ' concentration '
num2str(Cf_ppm) ' ppm, ' ' feed pressure ' num2str(Pf_psi) ' psi, 6
element.']})
%subplot(2,1,1)
plot(1:nm, ys);
xlabel('# of elements','fontsize',12)
ylabel('Cumulative fractional water recovery','fontsize',12)
```

```matlab
% %%%%
% figure
% title({['Feed flow ' num2str(Qf_gpm) ' gpm, ' ' concentration '
num2str(Cf_ppm) ' ppm, ' ' feed pressure ' num2str(Pf_psi) ' psi, 6
element.']})
% %subplot(2,1,1)
% plot(ys, (Pf0./pz0-Qf0_norm.*ys'-PresDp.*2/pz0),'d',ys,-log(1-
ys)./ys,'+',ys,(1-ys/2)./(1-ys),'>');
% legend('This simulation','Log-mean avg.','Arithmetic avg.')
% xlabel('Cumulative fractional water recovery','fontsize',12)
% ylabel('Normalized average osmotic pressure','fontsize',12)
%%%%
figure
title({['Feed flow ' num2str(Qf_gpm) ' gpm, ' ' concentration '
num2str(Cf_ppm) ' ppm, ' ' feed pressure ' num2str(Pf_psi) ' psi, 6
element.']})
%subplot(2,1,2)
plot(1:nm, ocp_ppm);
xlabel('# of elements','fontsize',12)
ylabel('Cumulative permeate concentration (ppm)','fontsize',12)

ys
ocp_ppm
```

Function myFun

```matlab
function F = myFun(x, t, Pf, Qf, Cf, W, Lp, alpha, pz, D, rho, H, mu, v,
Re, ks)


F = [x(1) - x(2) - (Cf - x(2)) * exp(x(3) * 1.475 * (H^2 * W * t / (3 *
Qf * D^2))^(1/3));
     x(3) - Lp * (Pf - alpha * 0.5 * rho * v^2 * (24 / Re - 648 / 35 *
H * x(3) * rho / mu / Re) * (1 - 2 * H * x(3) * rho / mu / Re * t / H)
* t / H - pz / Cf * (x(1)-x(2)));
     x(1) - x(2) - x(2) * x(3) / ks;
    ];
```

Bibliography

1. Butt, F.H., F. Rahman, and U. Baduruthamal, *Identification of Scale Deposits through Membrane Autopsy.* Desalination, 1995. **101**(3): p. 219-230.

2. Butt, F.H., F. Rahman, and U. Baduruthamal, *Hollow fine fiber vs. spiral-wound reverse osmosis desalination membranes .2. Membrane autopsy.* Desalination, 1997. **109**(1): p. 83-94.

3. Shannon, M.A., et al., *Science and technology for water purification in the coming decades.* Nature, 2008. **452**(7185): p. 301-310.

4. Gray S, S.R., Duke M, Rahardianto A and Cohen Y *Seawater Use and Desalination Technology. In: Peter Wilderer (ed.) Treatise on Water Science, .* Oxford: Academic Press., 2011. **vol. 4, pp. 73–109**

5. Kaghazchi, T., et al., *A mathematical modeling of two industrial seawater desalination plants in the Persian Gulf region.* Desalination, 2010. **252**(1-3): p. 135-142.

6. Jamal, K., M.A. Khan, and M. Kamil, *Mathematical modeling of reverse osmosis systems.* Desalination, 2004. **160**(1): p. 29-42.

7. Ghobeity, A. and A. Mitsos, *Optimal time-dependent operation of seawater reverse osmosis.* Desalination, 2010. **263**(1-3): p. 76-88.

8. Li, M., *Minimization of Energy in Reverse Osmosis Water Desalination Using Constrained Nonlinear Optimization.* Industrial & Engineering Chemistry Research, 2010. **49**(4): p. 1822-1831.

9.   Avlonitis, S.A., D.A. Avlonitis, and T. Panagiotidis, *Experimental study of the specific energy consumption for brackish water desalination by reverse osmosis.* International Journal of Energy Research, 2010: p. n/a-n/a.

10.   Raluy, G., L. Serra, and J. Uche, *Life cycle assessment of MSF, MED and RO desalination technologies.* Energy, 2006. **31**(13): p. 2361-2372.

11.   Khayet, M., et al., *Optimization of solar-powered reverse osmosis desalination pilot plant using response surface methodology.* Desalination, 2010. **261**(3): p. 284-292.

12.   Bourouni, K., T. Ben M'Barek, and A. Al Taee, *Design and optimization of desalination reverse osmosis plants driven by renewable energies using genetic algorithms.* Renewable Energy, 2011. **36**(3): p. 936-950.

13.   Sassi, K.M. and I.M. Mujtaba, *Optimal design and operation of reverse osmosis desalination process with membrane fouling.* Chemical Engineering Journal, 2011. **171**(2): p. 582-593.

14.   Peñate, B. and L. García-Rodríguez, *Current trends and future prospects in the design of seawater reverse osmosis desalination technology.* Desalination, 2012. **284**(0): p. 1-8.

15.   Khayet, M., C. Cojocaru, and M. Essalhi, *Artificial neural network modeling and response surface methodology of desalination by reverse osmosis.* Journal Of Membrane Science, 2011. **368**(1-2): p. 202-214.

16. Lu, Y.-y., et al., *Optimum design of reverse osmosis seawater desalination system considering membrane cleaning and replacing.* Journal Of Membrane Science, 2006. **282**(1-2): p. 7-13.

17. Lu, Y.-Y., et al., *Optimum design of reverse osmosis system under different feed concentration and product specification.* Journal Of Membrane Science, 2007. **287**(2): p. 219-229.

18. Rahardianto, A., et al., *Diagnostic characterization of gypsum scale formation and control in RO membrane desalination of brackish water.* Journal Of Membrane Science, 2006. **279**(1-2): p. 655-668.

19. Oh, H.-J., T.-M. Hwang, and S. Lee, *A simplified simulation model of RO systems for seawater desalination.* Desalination, 2009. **238**(1-3): p. 128-139.

20. McCutcheon, J.R., R.L. McGinnis, and M. Elimelech, *Desalination by ammonia–carbon dioxide forward osmosis: Influence of draw and feed solution concentrations on process performance.* Journal Of Membrane Science, 2006. **278**(1-2): p. 114-123.

21. Semiat, R., *Energy Issues in Desalination Processes.* Environmental Science \& Technology, 2008. **42**(22): p. 8193--8201.

22. Nanomagnetics, *a UK based company.* http://www.nanomagnetics.com/.

23. Wilf, M., *Design consequences of recent improvements in membrane performance.* Desalination, 1997. **113**(2-3): p. 157--163.

24. Nemeth, J.E., *Innovative system designs to optimize performance of ultra-low pressure reverse osmosis membranes.* Desalination, 1998. **118**(1-3): p. 63--71.

25.   Fethi, K., *Optimization of energy consumption in the 3300 m(3)/d RO Kerkennah plant.* Desalination, 2003. **157**(1-3): p. 145--149.

26.   Beca, J., *Pharmaceutical discharge: Zero discharge for pharma plant.* Filtration \& Separation, 2007. **44**(6): p. 40--41.

27.   Manth, T., M. Gabor, and E. Oklejas, *Minimizing RO energy consumption under variable conditions of operation.* Desalination, 2003. **157**(1-3): p. 9--21.

28.   Busch, M. and W.E. Mickols, *Reducing energy consumption in seawater desalination.* Desalination, 2004. **165**: p. 299--312.

29.   Wilf, M. and C. Bartels, *Optimization of seawater RO systems design.* Desalination, 2005. **173**(1): p. 1--12.

30.   R05-, A.R.N., *Overview of Treatment Processes for the Production of Fit for Purpose Water: Desalination and Membrane Technologies.* 2005, Australian Sustainable Industry Research Centre Ltd.

31.   Lachish, U., *Optimizing the Efficiency of Reverse Osmosis Seawater Desalination.* urila.tripod.com/Seawater.htm, 2002.

32.   95, D., W.P.R. \, and D.P.R. No., *Desalination and Water Purification Technology Roadmap.* 2003, Sandia National Laboratories and the U.S. Department of Interior, Bureau of Reclamation.

33.   Brady, P.V., et al., *Inland Desalination: Challenges and Research Needs.* Journal of Contemporary Water Research & Education, 2005. **132**: p. 46-51.

34.   Water Science and Technology Board, *Review of the Desalination and Water Purification Technology Roadmap.* 2004: National Academies Press.

35.   Mickley, M.C., *Membrane Concentrate Disposal: Practices and Regulation*, in *Desalination and Water Purification Research and Development Program Report No. 123*. 2006, U.S. Department of the Interior, Bureau of Reclamation: Denver, CO.

36.   Bond, R. and S. Veerapaneni, *Zero Liquid Discharge for Inland Desalination*. 2007, Denver, CO: AWWA Research Foundation, AWWA, & IWA Publishing.

37.   Rahardianto, A., et al., *High recovery membrane desalting of low-salinity brackish water: Integration of accelerated precipitation softening with membrane RO*. Journal of Membrane Science, 2007. **289**(1-2): p. 123--137.

38.   Zhu, A., P.D. Christofides, and Y. Cohen, *Effect of Thermodynamic Restriction on Energy Cost Optimization of RO Membrane Water Desalination*. Ind. Eng. Chem. Res., 2009. **48**: p. 6010-6021.

39.   Mingheng, L., *Reducing specific energy consumption in Reverse Osmosis (RO) water desalination: An analysis from first principles*. Desalination, 2011. **276**(1-3): p. 128-135.

40.   Lee, K.P., T.C. Arnot, and D. Mattia, *A review of reverse osmosis membrane materials for desalination—Development to date and future potential*. Journal Of Membrane Science, 2011. **370**(1-2): p. 1-22.

41.   P. Poovanaesvaran, M.A.A., K. Sopian, N. Amin, M.I. Fadhel, M. Yahya, *Design aspects of small-scale photovoltaic brackish water reverse osmosis (PV-BWRO) system*. Desalination and Water Treatment, 2011. **27** p. 210–223.

42.   Efraty, A., *U.S. Patent 7,695,614 B2*. 2010.

43.   Zhu, A., P.D. Christofides, and Y. Cohen, *Minimization of energy consumption for a two-pass membrane desalination: Effect of energy recovery, membrane rejection and retentate recycling.* Journal of Membrane Science, 2009. **339**(1-2): p. 126--137.

44.   Zhu, A., P.D. Christofides, and Y. Cohen, *Energy Consumption Optimization of Reverse Osmosis Membrane Water Desalination Subject to Feed Salinity Fluctuation.* Industrial \& Engineering Chemistry Research, 2009. **48**: p. 9581--9589.

45.   Zhu, A., P.D. Christofides, and Y. Cohen, *On RO Membrane and Energy Costs and Associated Incentives for Future Enhancements of Membrane Permeability.* Journal of membrane science, 2009. **344**: p. 1--5.

46.   Zhu, A., Rahardianto A. Christofides P. D. and Y. Cohen, *Reverse Osmosis Desalination with High Permeability Membranes - Cost Optimization and Research Needs.* Desalination and Water Treatment.

47.   Bartman, A.R., et al., *Minimizing energy consumption in reverse osmosis membrane desalination using optimization-based control.* Journal of Process Control, 2010. **20**(10): p. 1261-1269.

48.   Abbas, A. and N. Al-Bastaki, *Modeling of an RO water desalination unit using neural networks.* Chemical Engineering Journal, 2005. **114**(1-3): p. 139--143.

49.   Abufayed, A.A., *Performance characteristics of a cyclically operated seawater desalination plant in Tajoura, Libya.* Desalination, 2003. **156**(1-3): p. 59--65.

50.   ALARRAYEDH, M., K. BURASHID, and K. ALMANSOOR, *Rajj Ro Plant Operational Costs Optimization.* Desalination, 1994. **97**(1-3): p. 235--251.

51.   Al-Otaibi, M.B., et al., *A computational intelligence based approach for the analysis and optimization of a crude oil desalting and dehydration process.* Energy \& Fuels, 2005. **19**(6): p. 2526--2534.

52.   ALRQOBAH, H., et al., *Optimization Of Chemical Pretreatment For Reverse-Osmosis (Ro) Seawater Desalination.* Desalination, 1987. **66**: p. 423--430.

53.   Al-Shayji, K.A., S. Al-Wadyei, and A. Elkamel, *Modelling and optimization of a multistage flash desalination process.* Engineering Optimization, 2005. **37**(6): p. 591--607.

54.   Al-Sofi, M.A., et al., *Optimization of hybridized seawater desalination process.* Desalination, 2000. **131**(1-3): p. 147--156.

55.   Areiqat, A. and K.A. Mohamed, *Optimization of the negative impact of power and desalination plants on the ecosystem.* Desalination, 2005. **185**(1-3): p. 95--103.

56.   Avlonitis, S.A., *Optimization of the design and operation of seawater RO desalination plants.* Separation Science And Technology, 2005. **40**(13): p. 2663--2678.

57.   BAKER, E.C., M.D. MOOSEMILLER, and G.C. MUSTAKAS, *Computer Optimization Of Reverse-Osmosis Processing Of Soy Whey With Cellulose-Acetate Modules.* Journal Of Applied Polymer Science, 1979. **24**(3): p. 749--762.

58.   Cardona, E., A. Piacentino, and F. Marchese, *Energy saving in two-stage reverse osmosis systems coupled with ultrafiltration processes.* Desalination, 2005. **184**(1-3): p. 125--137.

59.   Chao, P.F. and P. Westerhoff, *Assessment and optimization of chemical and physicochemical softening processes.* Journal American Water Works Association, 2002. **94**(3): p. 109-119.

60.   Dewani, P.P. and H.M. Jayaprakasha, *Process optimization for production of Peda from pre-concentrated milk by reverse osmosis and vacuum evaporation.* Journal Of Food Science And Technology-Mysore, 2004. **41**(4): p. 386--390.

61.   Duarte, A.P., J.C. Bordado, and M.T. Cidade, *Cellulose acetate reverse osmosis membranes: Optimization of preparation parameters.* Journal Of Applied Polymer Science, 2007. **103**(1): p. 134--139.

62.   Duarte, A.P., M.T. Cidade, and J.C. Bordado, *Cellulose acetate reverse osmosis membranes: Optimization of the composition.* Journal Of Applied Polymer Science, 2006. **100**(5): p. 4052--4058.

63.   ELNASHAR, A.M., *System-Design Optimization Of A Solar Desalination Plant Using A Multieffect Stack Type Distillation Unit.* Desalination, 1994. **97**(1-3): p. 587--618.

64.   ERICSSON, B., B. HALLMANS, and P. VINBERG, *Optimization For Design Of Large Ro Seawater Desalination Plants.* Desalination, 1987. **64**: p. 459--489.

65.   Fan, L.T., et al., *The optimal design of desalination systems.* Desalination, 1967. **3**(2): p. 225--236.

240

66. Fan, L.T., et al., *Analysis and Optimization Of A Reverse Osmosis Water Purification System--part I. Process Analysis and Simulation.* Desalination, 1968. **5**(3): p. 237--265.

67. Fan, L.T., et al., *Analysis and optimization of a reverse osmosis water purification system--part II. Optimization.* Desalination, 1969. **6**(2): p. 131--152.

68. FAN, L.T., et al., *Systems-Analysis Of Dual-Purpose Nuclear-Power And Desalting Plants .1. Optimization.* Desalination, 1972. **11**(2): p. 217--\&.

69. FANG, H.H.P. and E.S.K. CHIAN, *Optimization Of Ns-100 Membrane For Reverse-Osmosis.* Journal Of Applied Polymer Science, 1976. **20**(2): p. 303--314.

70. Fethi, K., *Optimization of Energy Consumption in the 3300 m3/d RO Kerkennah Plant.* Desalination, 2003. **157**: p. 145.

71. FOUAD, H.Y., *Optimization Of Natural Uranium Heavy-Water Moderated Reactors For Desalination .1. Light Water Cooled Reactors.* Atomkernenergie, 1974. **23**(3): p. 208--211.

72. Geisler, P., W. Krumm, and T. Peters, *Optimization of the energy demand of reverse osmosis with a pressure-exchange system.* Desalination, 1999. **125**(1-3): p. 167--172.

73. Geraldes, V., N.E. Pereira, and M.N. de Pinho, *Simulation and optimization of medium-sized seawater reverse osmosis processes with spiral-wound modules.* Industrial \& Engineering Chemistry Research, 2005. **44**(6): p. 1897--1905.

74. GIANNUZZI, L.F., O.E. HORN, and M. NAKHAMKIN, *Optimization Of Integrated Co-Generation Power-Plant And Desalination Plant-Systems For A*

Range Of Power And Water-Supply Requirements. Desalination, 1981. **39**(1-3): p. 437--446.

75.   Gilau, A.M. and M.J. Small, *Designing cost-effective seawater reverse osmosis system under optimal energy options.* Renewable Energy, 2007. **In Press, Corrected Proof**: p. --.

76.   Gotor, A., I.D. Pestana, and C.A. Espinoza, *Optimization of RO desalination systems powered by renewable energies.* Desalination, 2003. **156**(1-3): p. 351--351.

77.   Guria, C., P.K. Bhattacharya, and S.K. Gupta, *Multi-objective optimization of reverse osmosis desalination units using different adaptations of the non-dominated sorting genetic algorithm (NSGA).* Computers \& Chemical Engineering, 2005. **29**(9): p. 1977--1995.

78.   Hafsi, M.M.M. and A. Boughriba, *Five years experience in reverse osmosis plant optimization performances in Morocco.* Desalination, 2003. **153**(1-3): p. 227--227.

79.   Hamad, A. and M. Abdul-Karim, *Desalination using ambient air: simulation and energy optimization.* Desalination, 2005. **175**(3): p. 247--257.

80.   Hatfield, G.B. and G.W. Graves, *Optimization of a reverse osmosis system using nonlinear programming.* Desalination, 1970. **7**(2): p. 147--177.

81.   Idris, A., et al., *Optimization of cellulose acetate hollow fiber reverse osmosis membrane production using Taguchi method.* Journal Of Membrane Science, 2002. **205**(1-2): p. 223--237.

82. JACOBS, E.P., M.J. HURNDALL, and R.D. SANDERSON, *Optimization Of The Fabrication Variables Of Poly-2-Vinylimidazoline Tubular Reverse-Osmosis Membranes.* Separation Science And Technology, 1994. **29**(17): p. 2277--2297.

83. Jawad, M.A., *Future for desalination by reverse osmosis.* Desalination, 1989. **72**(1-2): p. 23--28.

84. Kamal, I. and G.V. Sims, *Thermal cycle and financial modeling for the optimization of dual-purpose power-cum-desalination plants.* Desalination, 1997. **109**(1): p. 1--13.

85. KORNEICH.AI, A.V. IZVEKOV, and A.A. MYAGKOV, *Optimization Of Basic Parameters Of Thermal Desalting Plants With Adiabatic Evaporation.* Desalination, 1970. **7**(2): p. 179--\&.

86. KOSAREK, L.J., *Purifying Water By Reverse-Osmosis .1. Operating Principles, Membranes, And Optimization Factors.* Plant Engineering, 1979. **33**(16): p. 103--106.

87. KUENSTLE, K. and V. JANISCH, *Optimization Of A Dual Purpose Plant For Seawater Desalination And Electricity Production.* Desalination, 1979. **30**(1-3): p. 555--569.

88. Laborde, H.M., et al., *Optimization strategy for a small-scale reverse osmosis water desalination system based on solar energy.* Desalination, 2001. **133**(1): p. 1--12.

243

89. Liang, S., C. Liu, and L. Song, *Two-Step Optimization of Pressure and Recovery of Reverse Osmosis Desalination Process.* Environmental Science \& Technology. **0**(0): p. --.

90. Lu, Y., et al., *Optimum design of reverse osmosis system under different feed concentration and product specification.* Journal of Membrane Science, 2007. **287**(2): p. 219--229.

91. Madaeni, S.S. and S. Koocheki, *Application of taguchi method in the optimization of wastewater treatment using spiral-wound reverse osmosis element.* Chemical Engineering Journal, 2006. **119**(1): p. 37--44.

92. Mahmoud Hafsi, M.M. and A. Boughriba, *Five years experience in reverse osmosis plant optimization performances in Morocco.* Desalination, 2003. **153**(1-3): p. 227--13.

93. Marcovecchio, M.G., P.A. Aguirre, and N.J. Scenna, *Global optimal design of reverse osmosis networks for seawater desalination: modeling and algorithm.* Desalination, 2005. **184**(1-3): p. 259--271.

94. Marcovecchio, M.G., et al., *Optimization of hybrid desalination processes including multi stage flash and reverse osmosis systems.* Desalination, 2005. **182**(1-3): p. 111--122.

95. Mendez, A. and G. Gasco, *Optimization of water desalination using carbon-based adsorbents.* Desalination, 2005. **183**(1-3): p. 249--255.

96. Mesa, A.A., C.M. Gomez, and R.U. Azpitarte, *Design of the maximum energy efficiency desalination plant (PAME).* Desalination, 1997. **108**(1-3): p. 111--116.

97.   Metaiche, M. and A. Kettab, *Mathematical modeling of desalination parameters: mono-stage reverse osmosis.* Desalination, 2004. **165**: p. 153--59.

98.   MULLER, H.U., *Optimization Problems In Obtaining Fresh Water By Reverse-Osmosis.* Chemie Ingenieur Technik, 1973. **45**(6): p. 431--431.

99.   Muller-Holst, H., M. Engelhardt, and W. Scholkopf, *Small-scale thermal seawater desalination simulation and optimization of system design.* Desalination, 1999. **122**(2-3): p. 255--262.

100.   Murthy, Z.V.P. and J.C. Vengal, *Optimization of a reverse osmosis system using genetic algorithm.* Separation Science And Technology, 2006. **41**(4): p. 647--663.

101.   Mussati, S.F., P.A. Aguirre, and N.J. Scenna, *A hybrid methodology for optimization of multi-stage flash-mixer desalination systems.* Latin American Applied Research, 2003. **33**(2): p. 141--147.

102.   Mussati, S.F., et al., *A new global optimization algorithm for process design: its application to thermal desalination processes.* Desalination, 2004. **166**(1-3): p. 129--140.

103.   Ning, R.Y. and J.P. Netwig, *Complete elimination of acid injection in reverse osmosis plants.* Desalination, 2002. **143**(1): p. 29-34.

104.   Ning, R.Y., et al., *Recovery optimization of RO concentrate from desert wells.* Desalination, 2006. **201**(1-3): p. 315-322.

105.   Ning, R.Y., et al., *Recovery optimization of RO concentrate from desert wells.* Desalination, 2006. **201**(1-3): p. 315--322.

106. NORDIN, S., B. ERICSSON, and B. WALLEN, *Optimization Of High-Pressure Piping In Reverse-Osmosis Plants.* Desalination, 1985. **55**(1-3): p. 247--259.

107. PAL, D. and M. CHERYAN, *Application Of Reverse-Osmosis In The Manufacture Of Khoa - Process Optimization And Product Quality.* Journal Of Food Science And Technology-Mysore, 1987. **24**(5): p. 233--238.

108. PARRINI, G., *Optimization Method For Processes, Derived From Non-Equilibrium Thermodynamics And Application To Vapour Compression Desalination.* Quaderni Dell Ingegnere Chimico Italiano, 1971. **7**(7-8): p. 99--\&.

109. PERONA, J.J., T.W. PICKEL, and K.A. KRAUS, *Hyperfiltration Studies .18. Optimization Of 2-Stage Plants For Desalination Of Brackish Waters.* Desalination, 1970. **8**(1): p. 73--\&.

110. Pestana, I.D., et al., *Optimization of RO desalination systems powered by renewable energies. Part I: Wind energy.* Desalination, 2004. **160**(3): p. 293--299.

111. Poullikkas, A., *Optimization algorithm for reverse osmosis desalination economics.* Desalination, 2001. **133**(1): p. 75--81.

112. RAUTENBA.R and P. PENNINGS, *Development And Optimization Of A Hydrate Process For Desalination Of Seawater.* Chemie Ingenieur Technik, 1973. **45**(5): p. 259--264.

113. RAUTENBACH, R. and W. DAHM, *Approximation Equations For Design And Optimization Of Wound Modules For Reverse-Osmosis.* Chemie Ingenieur Technik, 1986. **58**(5): p. 424--425.

114. Rautenbach, R. and W. Dahm, *Design And Optimization Of Spiral-Wound And Hollow Fiber RO-Modules.* Desalination, 1987. **65**(1-3): p. 259--275.

115. Seidel, A. and M. Elimelech, *Coupling between chemical and physical interactions in natural organic matter (NOM) fouling of nanofiltration membranes: implications for fouling control.* Journal of Membrane Science, 2002. **203**(1-2): p. 245-255.

116. Smart, J., V.M. Starov, and D.R. Lloyd, *Performance optimization of hollow fiber reverse osmosis membranes .2. Comparative study of flow configurations.* Journal Of Membrane Science, 1996. **119**(1): p. 117--128.

117. STAROV, V.M., J. SMART, and D.R. LLOYD, *Performance Optimization Of Hollow-Fiber Reverse-Osmosis Membranes .1. Development Of Theory.* Journal Of Membrane Science, 1995. **103**(3): p. 257--270.

118. Tlili, M.M., A.S. Manzola, and M. Ben Amor, *Optimization of the preliminary treatment in a desalination plant by reverse osmosis.* Desalination, 2003. **156**(1-3): p. 69--78.

119. Uche, J., L. Serra, and A. Valero, *Thermoeconomic optimization of a dual-purpose power and desalination plant.* Desalination, 2001. **136**(1-3): p. 147--158.

120. van der Meer, W.G.J., M. Riemersma, and J.C. van Dijk, *Only two membrane modules per pressure vessel? Hydraulic optimization of spiral-wound membrane filtration plants.* Desalination, 1998. **119**(1-3): p. 57--64.

121. van der Meer, W.G.J. and J.C. van Dijk, *Theoretical optimization of spiral-wound and capillary nanofiltration modules.* Desalination, 1997. **113**(2-3): p. 129--146.

122. VANBOXTEL, A.J.B., Z.E.H. OTTEN, and H.J.L.J. VANDERLINDEN, *Dynamic Optimization Of A One-Stage Reverse-Osmosis Installation With Respect To Membrane Fouling.* Journal Of Membrane Science, 1992. **65**(3): p. 277--293.

123. VORMS, G.A., et al., *Optimization Of Process For Concentration Of Electric Desalting Unit Wastes Under Pressure.* Chemistry And Technology Of Fuels And Oils, 1980. **16**(5-6): p. 418--420.

124. Voros, N., Z.B. Maroulis, and D. MarinosKouris, *Optimization of reverse osmosis networks for seawater desalination.* Computers \& Chemical Engineering, 1996. **20**: p. S345--S350.

125. Voros, N., Z.B. Maroulis, and D. Marinos-Kouris, *Optimization of reverse osmosis networks for seawater desalination.* Computers \& Chemical Engineering, 1996. **20**(Supplement 1): p. S345--S350.

126. Voros, N.G., Z.B. Maroulis, and D. Marinos-Kouris, *Short-cut structural design of reverse osmosis desalination plants.* Journal of Membrane Science, 1997. **127**(1): p. 47--68.

127. WADE, N.M., *Ro Design Optimization.* Desalination, 1987. **64**: p. 3--16.

128. WALCH, A., *Optimization Of Membranes For Use In Reverse-Osmosis.* Chemie Ingenieur Technik, 1974. **46**(4): p. 168--168.

129. Wessels, L.P., et al., *Innovative design of nano- and ultrafiltration plants.* Desalination, 1998. **119**(1-3): p. 341--345.

130. WILEY, D.E., C.J.D. FELL, and A.G. FANE, *Optimization Of Membrane Module Design For Brackish Water Desalination.* Desalination, 1985. **52**(3): p. 249--265.

131. Wilf, M. and K. Klinko, *Optimization of seawater RO systems design.* Desalination, 2001. **138**(1-3): p. 299--306.

132. Avlonitis, S., W.T. Hanbury, and M.B. Boudinar, *Spiral wound modules performance. An analytical solution, part I.* Desalination, 1991. **81**(1-3): p. 191--208.

133. Boudinar, M.B., W.T. Hanbury, and S. Avlonitis, *Numerical simulation and optimisation of spiral-wound modules.* Desalination, 1992. **86**(3): p. 273--290.

134. Avlonitis, S., W.T. Hanbury, and M.B. Boudinar, *Spiral wound modules performance an analytical solution: Part II.* Desalination, 1993. **89**(3): p. 227--246.

135. Villafafila, A. and I.M. Mujtaba, *Fresh water by reverse osmosis based desalination: simulation and optimisation.* Desalination, 2003. **155**(1): p. 1--13.

136. Avlonitis, S.A., M. Pappas, and K. Moutesidis, *A unified model for the detailed investigation of membrane modules and RO plants performance.* Desalination, 2007. **203**(1-3): p. 218--228.

137. Avlonitis, S.A., K. Kouroumbas, and N. Vlachakis, *Energy consumption and membrane replacement cost for seawater RO desalination plants.* Desalination, 2003. **157**(1-3): p. 151--158.

138. Spiegler, K.S. and Y.M. El-Sayed, *The energetics of desalination processes.* Desalination, 2001. **134**(1-3): p. 109--128.

139. Lachish, U., *Optimizing the Efficiency of Reverse Osmosis Seawater Desalination.* urila.tripod.com/Seawater.htm, 2002.

140. Song, L., et al., *Performance limitation of the full-scale reverse osmosis process.* Journal of Membrane Science, 2003. **214**(2): p. 239--244.

141. Song, L., et al., *Emergence of thermodynamic restriction and its implications for full-scale reverse osmosis processes.* Desalination, 2003. **155**(3): p. 213--228.

142. Song, L. and K.G. Tay, *Performance prediction of a long crossflow reverse osmosis membrane channel.* Journal of Membrane Science, 2006. **281**(1-2): p. 163--169.

143. Abderrahim, A., *Simulation and analysis of an industrial water desalination plant.* Chemical Engineering and Processing: Process Intensification, 2005. **44**(9): p. 999-1004.

144. van der Meer, W.G.J., C.W. A. Averink, and J.C. van Dijk, *Mathematical model of nanofiltration systems.* Desalination, 1996. **105**(1-2): p. 25--31.

145. Maskan, F., et al., *Optimal design of reverse osmosis module networks.* AIChE Journal, 2000. **46**(5): p. 946--954.

146. See, H.J., V.S. Vassiliadis, and D.I. Wilson, *Optimisation of membrane regeneration scheduling in reverse osmosis networks for seawater desalination.* Desalination, 1999. **125**(1-3): p. 37--54.

147. Malek, A., M.N.A. Hawlader, and J.C. Ho, *Design and economics of RO seawater desalination.* Desalination, 1996. **105**(3): p. 245--261.

148. Noronha, M., V. Mavrov, and H. Chmiel, *Simulation model for optimisation of two-stage membrane filtration plants--minimising the specific costs of power consumption.* Journal of Membrane Science, 2002. **202**(1-2): p. 217--232.

149. SHARIF, et al., *A new theoretical approach to estimate the specific energy consumption of reverse osmosis and other pressure-driven liquid-phase membrane processes.* Vol. 3. 2009, L'Aquila, ITALIE: Desalination Publications. 9.

150. Mulder, M., *Basic Principles of Membrane Technology.* 1997: Kluwer Academic Publishers (Boston).

151. 2.0, O.A., *OLI systems*, Morris Plains, NJ.

152. Manual, A., *Standard Practice for Standardizing Reverse Osmosis Performance Data.* ASTM international, 2000.

153. Karode, S.K., *Laminar flow in channels with porous walls, revisited.* Journal of Membrane Science, 2001. **191**(1-2): p. 237--241.

154. Zydney, A.L., *Stagnant film model for concentration polarization in membrane systems.* Journal of Membrane Science, 1997. **130**(1-2): p. 275--281.

155. Bartman, A., *Control and Monitoring of Reverse Osmosis Water Desalination.* PhD Dissertation, University of California, Los Angeles, 2011.

156. Shrivastava, A., S. Kumar, and E.L. Cussler, *Predicting the effect of membrane spacers on mass transfer.* Journal Of Membrane Science, 2008. **323**(2): p. 247-256.

157. Lin, N.H., et al., *Crystallization of calcium sulfate on polymeric surfaces.* Journal of Colloid and Interface Science, 2011. **356**(2): p. 790-797.

158. Lin, N.H., et al., *Polymer surface nano-structuring of reverse osmosis membranes for fouling resistance and improved flux performance.* Journal of Materials Chemistry, 2010. **20**(22): p. 4642-4652.

159. Kim, M.-m., et al., *Surface nano-structuring of reverse osmosis membranes via atmospheric pressure plasma-induced graft polymerization for reduction of mineral scaling propensity.* Journal Of Membrane Science, 2010. **354**(1-2): p. 142-149.

160. M. M. Kim, G.T.L., N. H. Lin and Y. Cohen, *Fouling and scaling resistant surface nano-structured membrane.* Provisional Patent Application USA, 2008. **No. 61/060,715**.

161. Vuong, D., *Two stage nanofiltration seawater desalination system.* US Patent 20030205526, 2003.

162. Gu, H., *Demonstration of Rapid Membrane Characterization and Real-Time Membrane Module Performance Analysis Using an Automated Reverse Osmosis Desalination Pilot Plant.* Master's Thesis, University of California Los Angeles, 2010.

163. Faigon, M. and D. Hefer, *Boron rejection in SWRO at high pH conditions versus cascade design.* Desalination, 2008. **223**(1-3): p. 10--16.

164. McFall, C.W., et al., *Control and Monitoring of a High Recovery Reverse Osmosis Desalination Process.* Industrial \& Engineering Chemistry Research, 2008. **47**(17): p. 6698-6710.

165. Bartman, A., et al., *Model-predictive control of feed flow reversal in a reverse osmosis desalination process.* Journal of Process Control, 2009.

166. Bartman, A.R., P.D. Christofides, and Y. Cohen, *Nonlinear Model-Based Control of an Experimental Reverse-Osmosis Water Desalination System.* Industrial \& Engineering Chemistry Research, 2009. **48**(13): p. 6126--6136.

167. Filmtec, D., *ROSA72 RO Simulator.* http://www.dowwaterandprocess.com/support_training/design_tools/rosa.htm, 2011.

168. Zhu, A.H., et al., *Reverse osmosis desalination with high permeability membranes - Cost optimization and research needs.* Desalination and Water Treatment, 2010. **15**(1-3): p. 256-266.

169. Kim, S. and E.M.V. Hoek, *Modeling concentration polarization in reverse osmosis processes.* Desalination, 2005. **186**(1-3): p. 111--128.